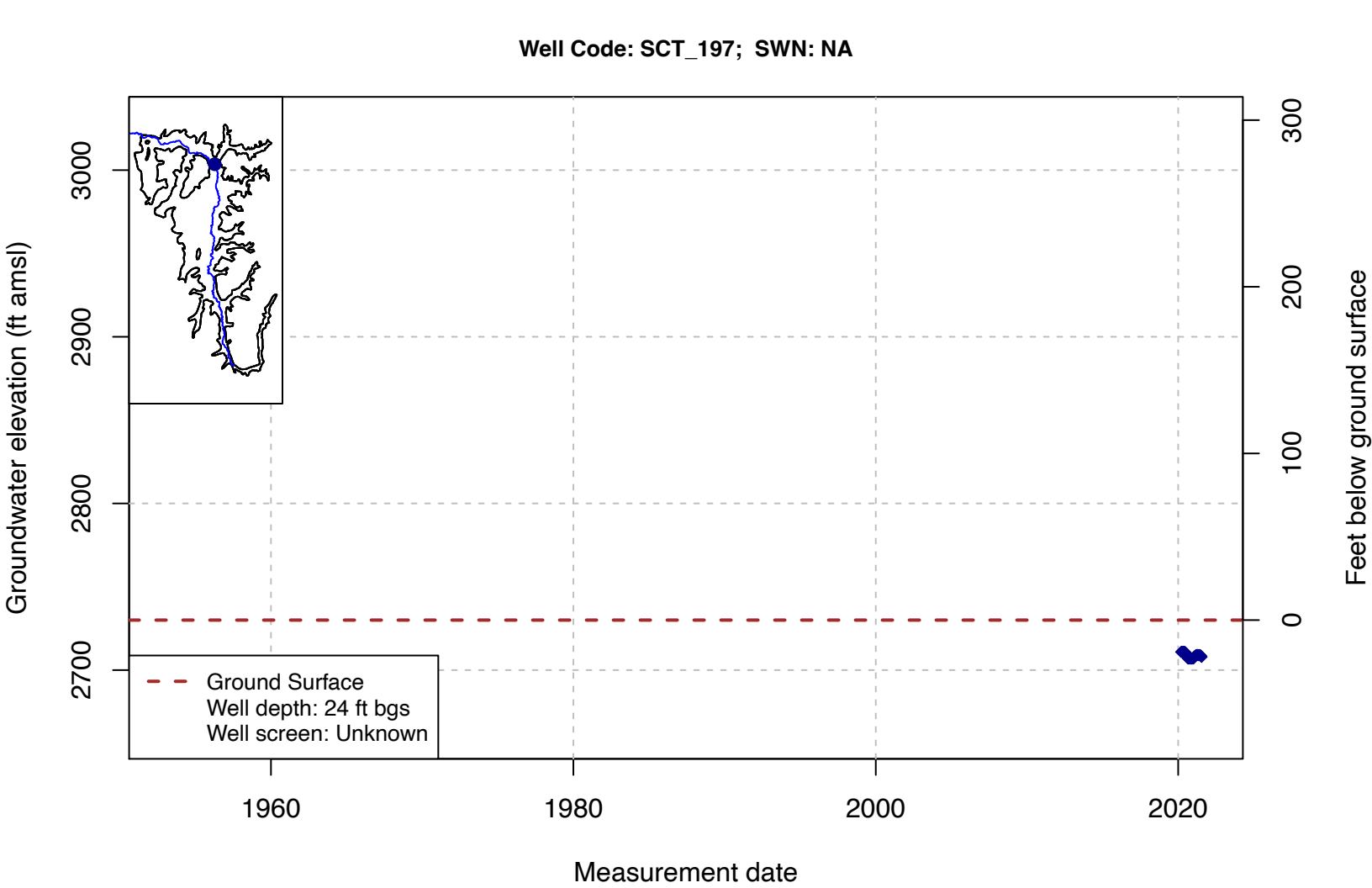
Well Code: SCT_197; SWN: NA
Groundwater elevation (ft amsl)
3000
2900
2800
2700
Feet below ground surface
300
200
100
0
1960
1980
2000
2020
Measurement date
Ground Surface
Well depth: 24 ft bgs
Well screen: Unknown

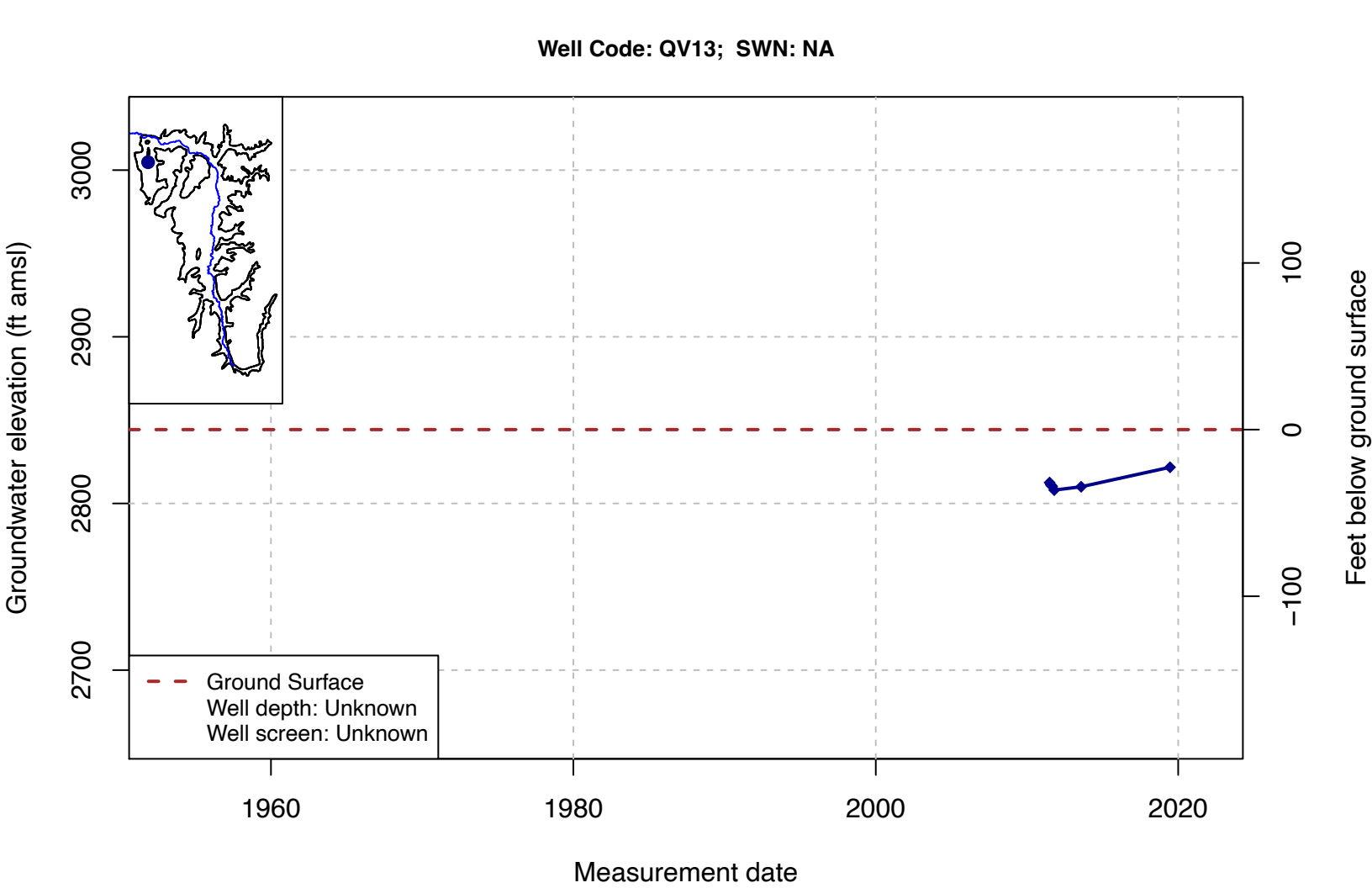
Well Code: QV13; SWN: NA
Groundwater elevation (ft amsl)
3000
2900
2800
2700
100
0
−100
Feet below ground surface
Ground Surface
Well depth: Unknown
Well screen: Unknown
1960
1980
2000
2020
Measurement date

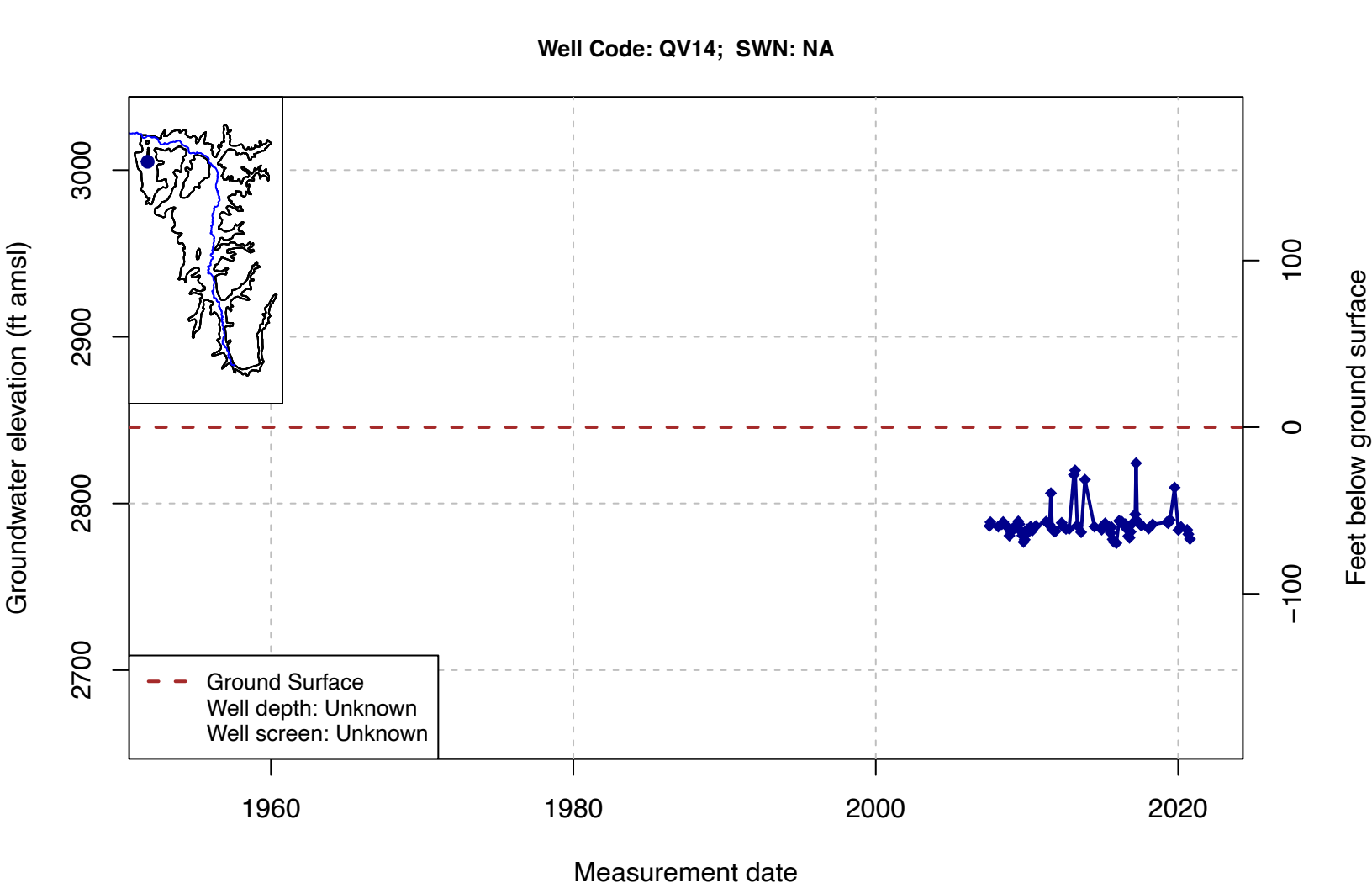
Well Code: QV14; SWN: NA
Groundwater elevation (ft amsl)
3000
2900
2800
2700
Feet below ground surface
100
0
−100
1960
1980
2000
2020
Measurement date
Ground Surface
Well depth: Unknown
Well screen: Unknown

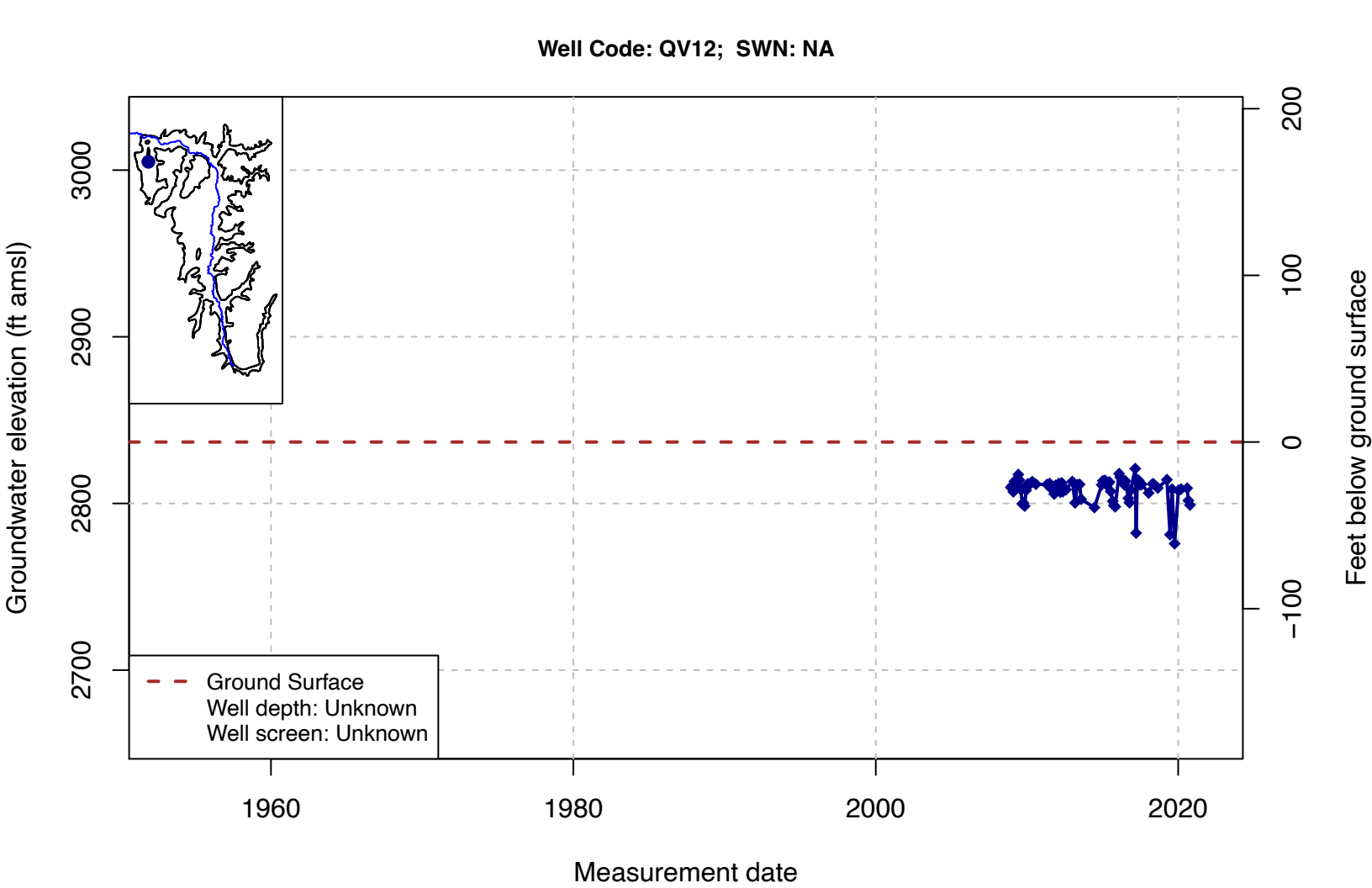
Well Code: QV12; SWN: NA
Groundwater elevation (ft amsl)
3000
2900
2800
2700
200
100
0
−100
Feet below ground surface
1960
1980
2000
2020
Measurement date
Ground Surface
Well depth: Unknown
Well screen: Unknown

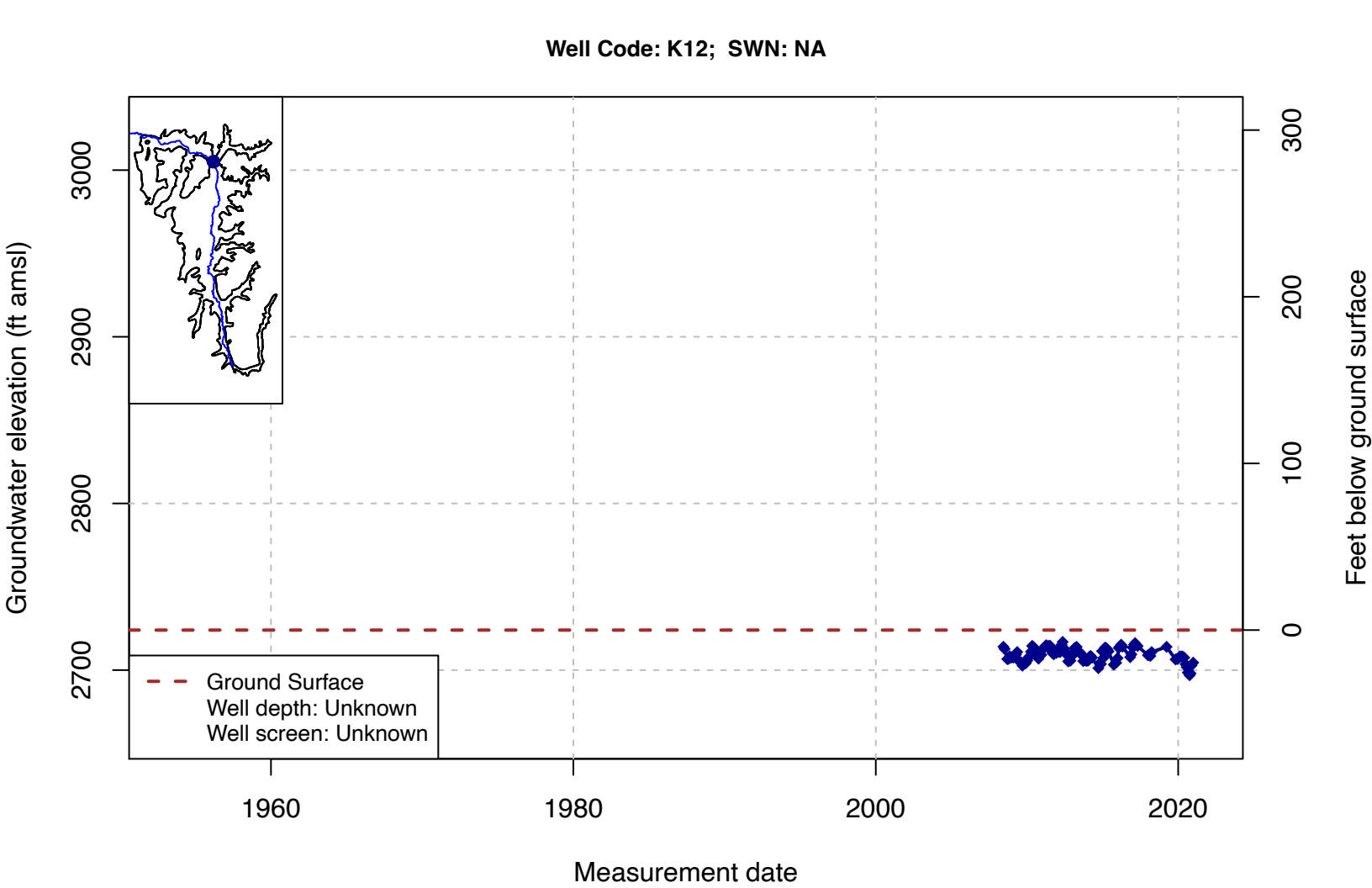
Well Code: K12; SWN: NA
Groundwater elevation (ft amsl)
3000
2900
2800
2700
Feet below ground surface
300
200
100
0
1960
1980
2000
2020
Measurement date
Ground Surface
Well depth: Unknown
Well screen: Unknown

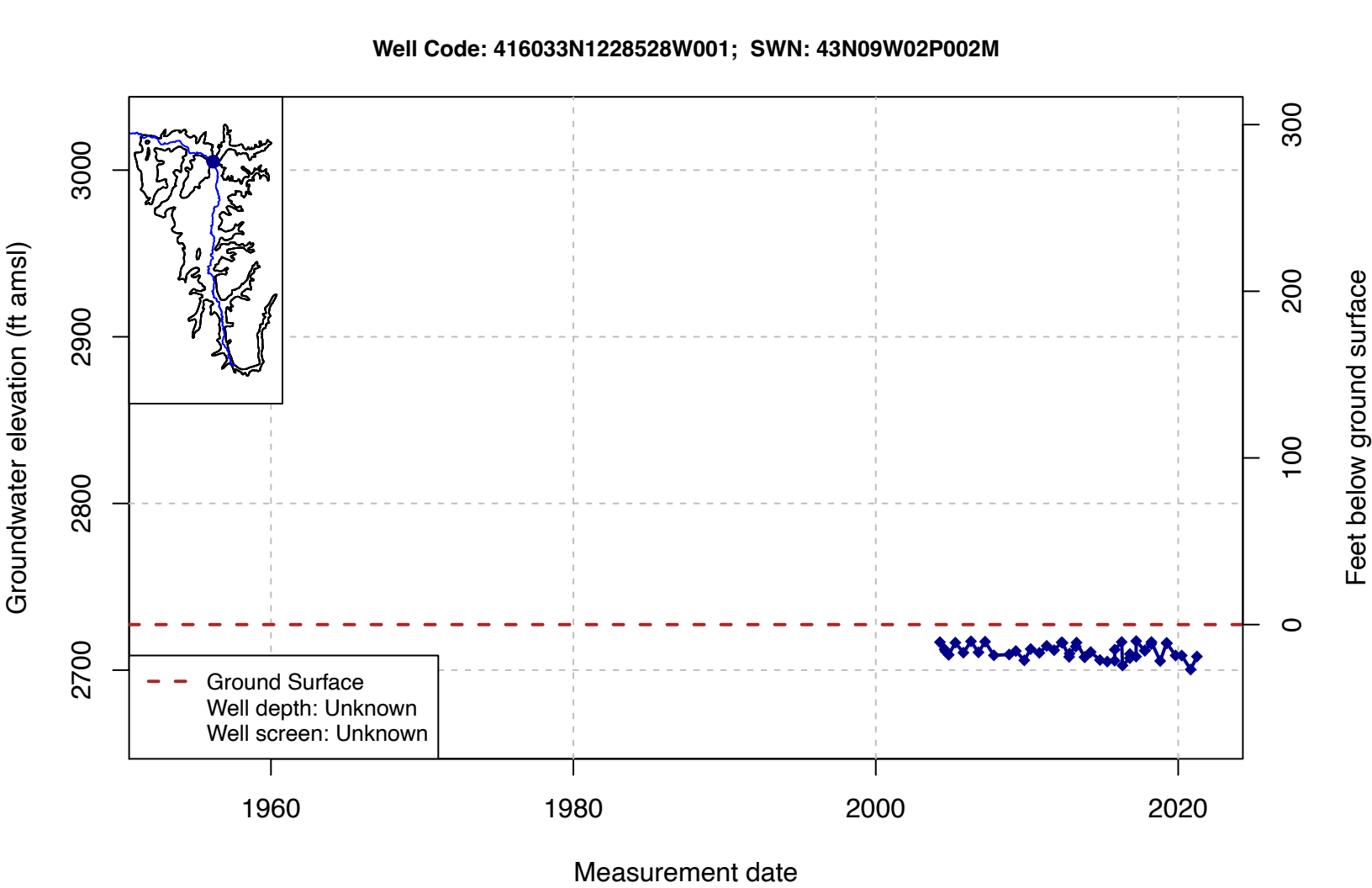
Well Code: 416033N1228528W001; SWN: 43N09W02P002M
Groundwater elevation (ft amsl)
3000
2900
2800
2700
Feet below ground surface
300
200
100
0
1960
1980
2000
2020
Measurement date
Ground Surface
Well depth: Unknown
Well screen: Unknown

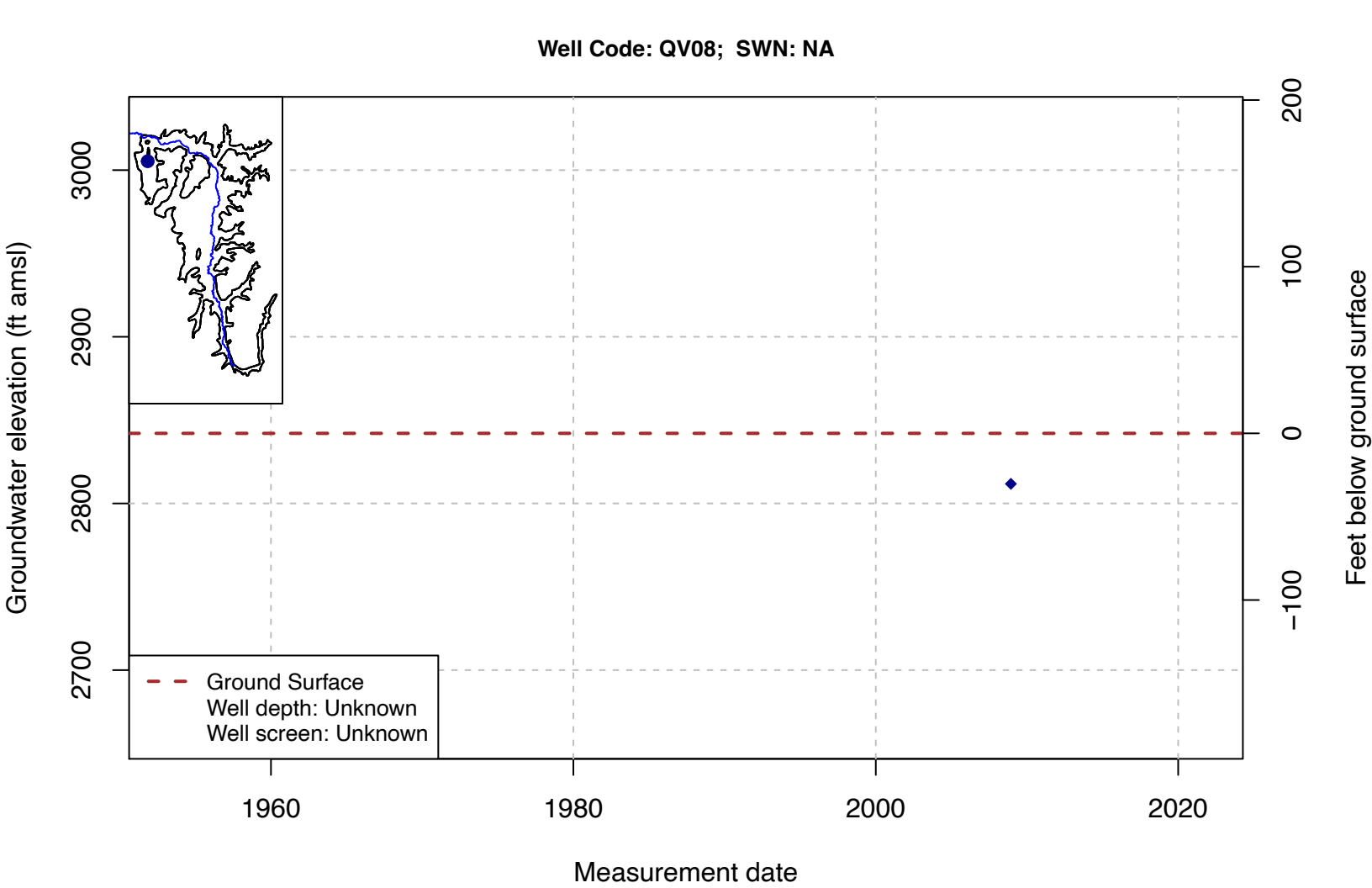
Well Code: QV08; SWN: NA
Groundwater elevation (ft amsl)
3000
2900
2800
2700
Feet below ground surface
200
100
0
−100
1960
1980
2000
2020
Measurement date
Ground Surface
Well depth: Unknown
Well screen: Unknown

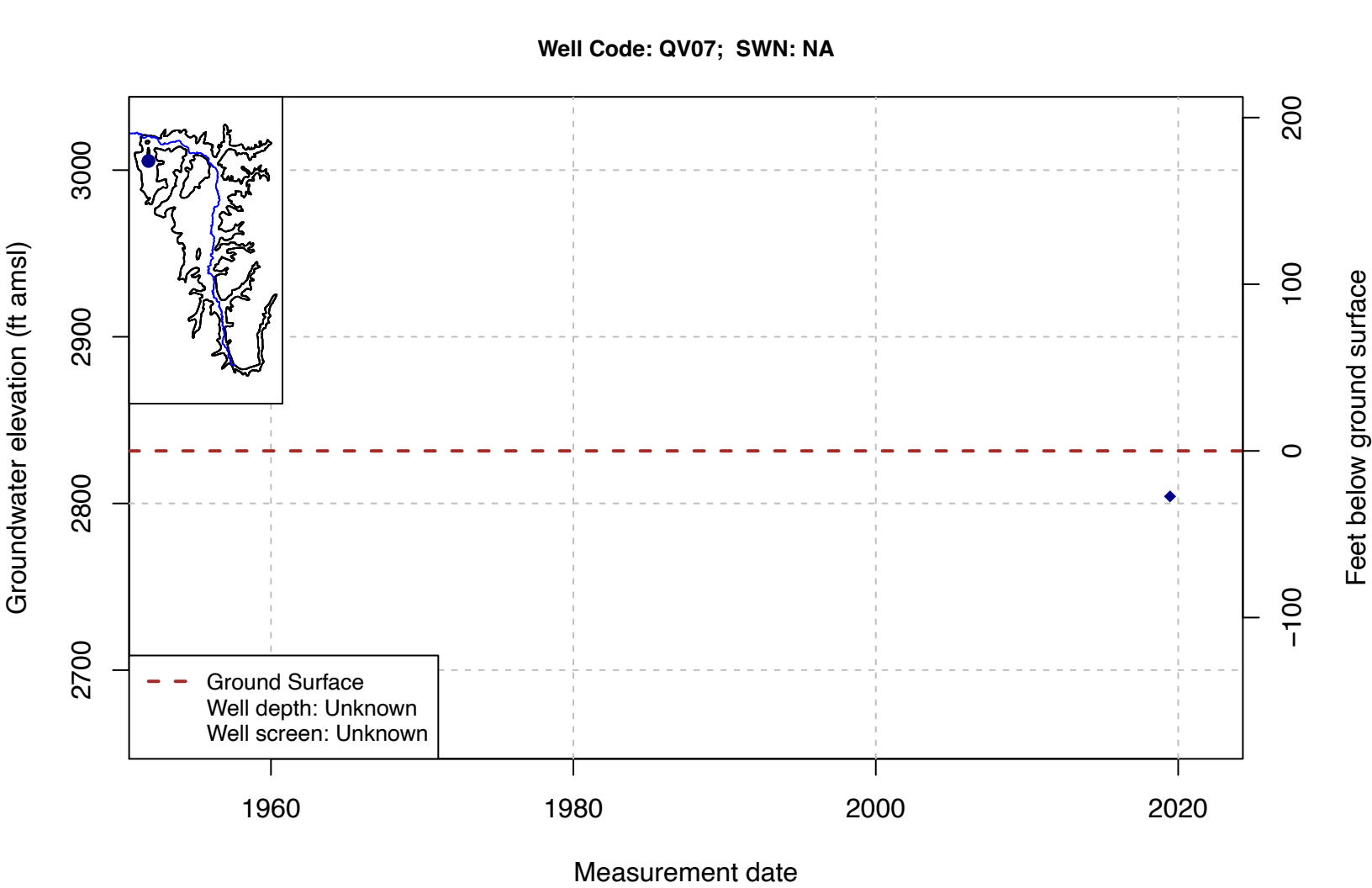
Well Code: QV07; SWN: NA
Groundwater elevation (ft amsl)
3000
2900
2800
2700
200
100
0
−100
Feet below ground surface
1960
1980
2000
2020
Measurement date
Ground Surface
Well depth: Unknown
Well screen: Unknown

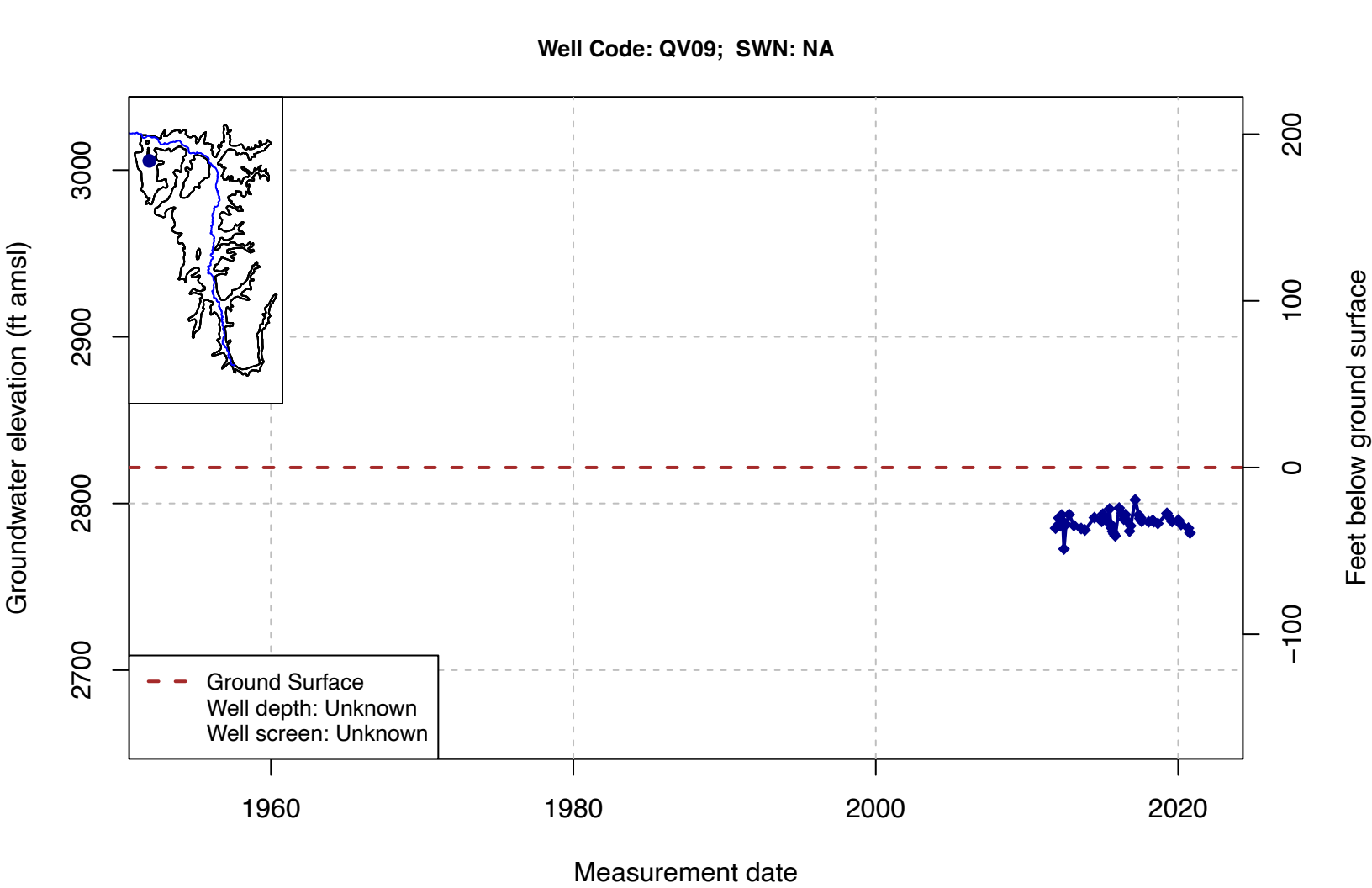
Well Code: QV09; SWN: NA
Groundwater elevation (ft amsl)
3000
2900
2800
2700
Feet below ground surface
200
100
0
−100
1960
1980
2000
2020
Measurement date
Ground Surface
Well depth: Unknown
Well screen: Unknown

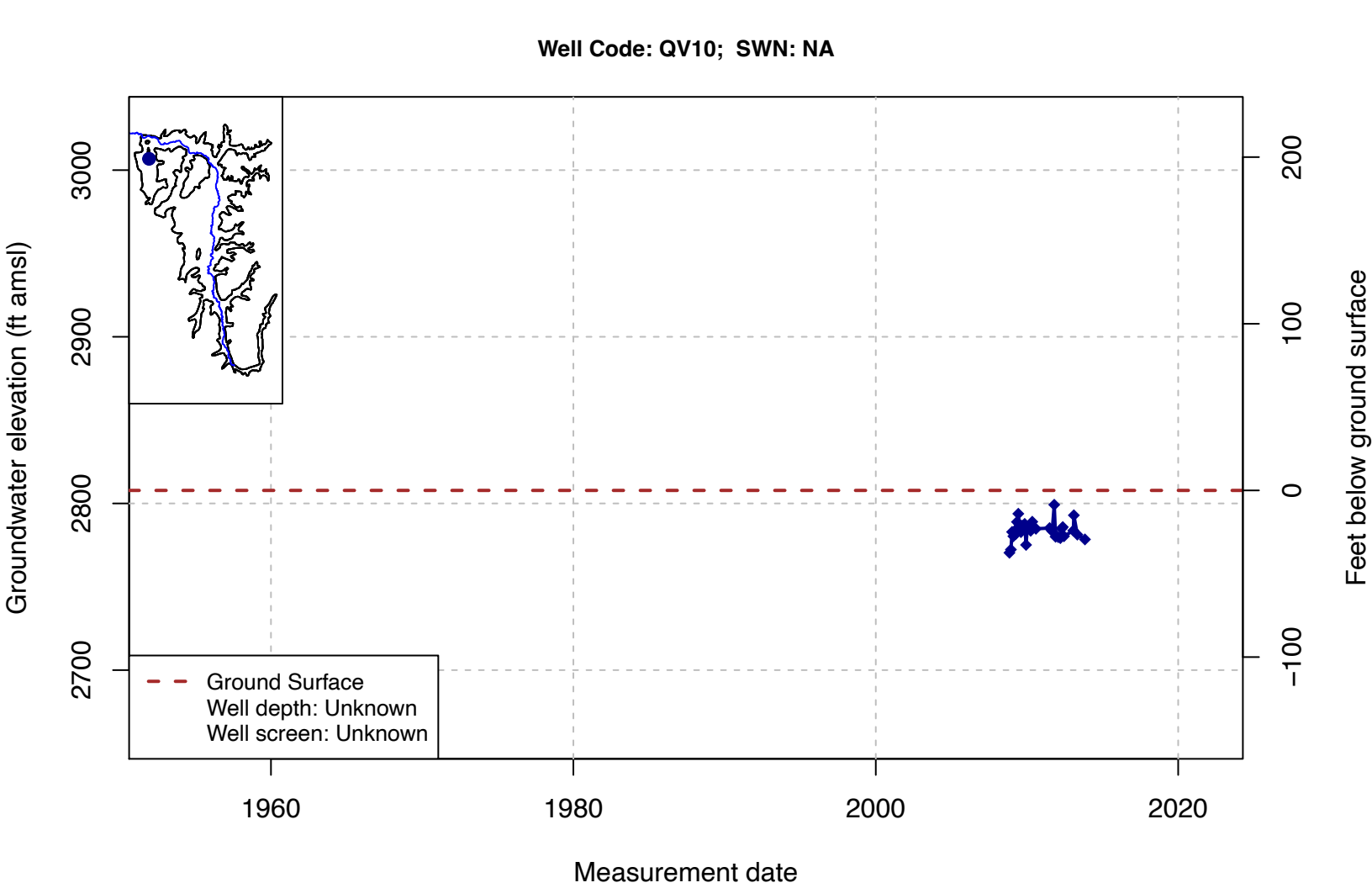
Well Code: QV10; SWN: NA
Groundwater elevation (ft amsl)
3000
2900
2800
2700
Feet below ground surface
200
100
0
−100
1960
1980
2000
2020
Measurement date
Ground Surface
Well depth: Unknown
Well screen: Unknown

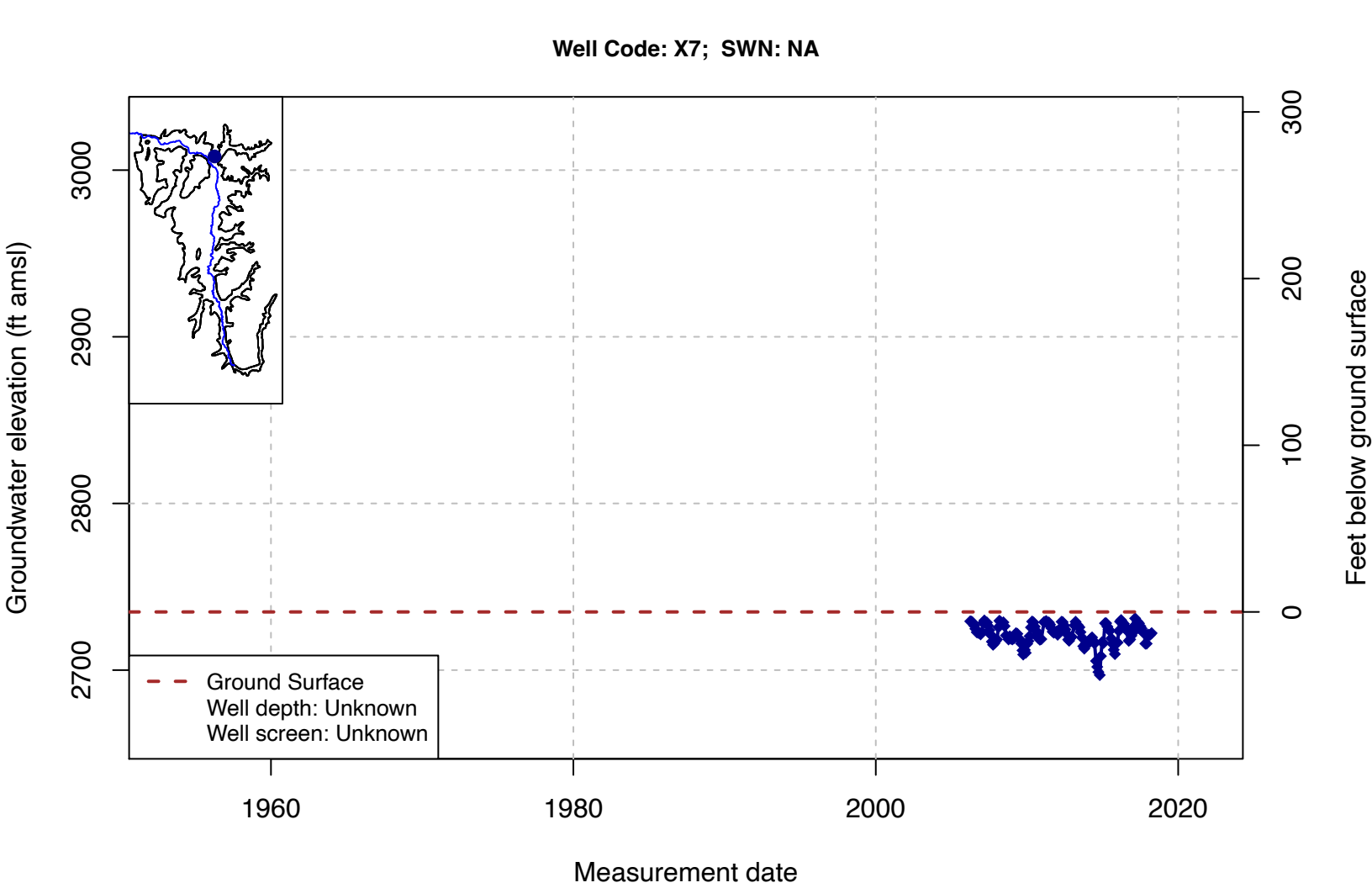
Well Code: X7; SWN: NA
Groundwater elevation (ft amsl)
3000
2900
2800
2700
Feet below ground surface
300
200
100
0
1960
1980
2000
2020
Measurement date
Ground Surface
Well depth: Unknown
Well screen: Unknown

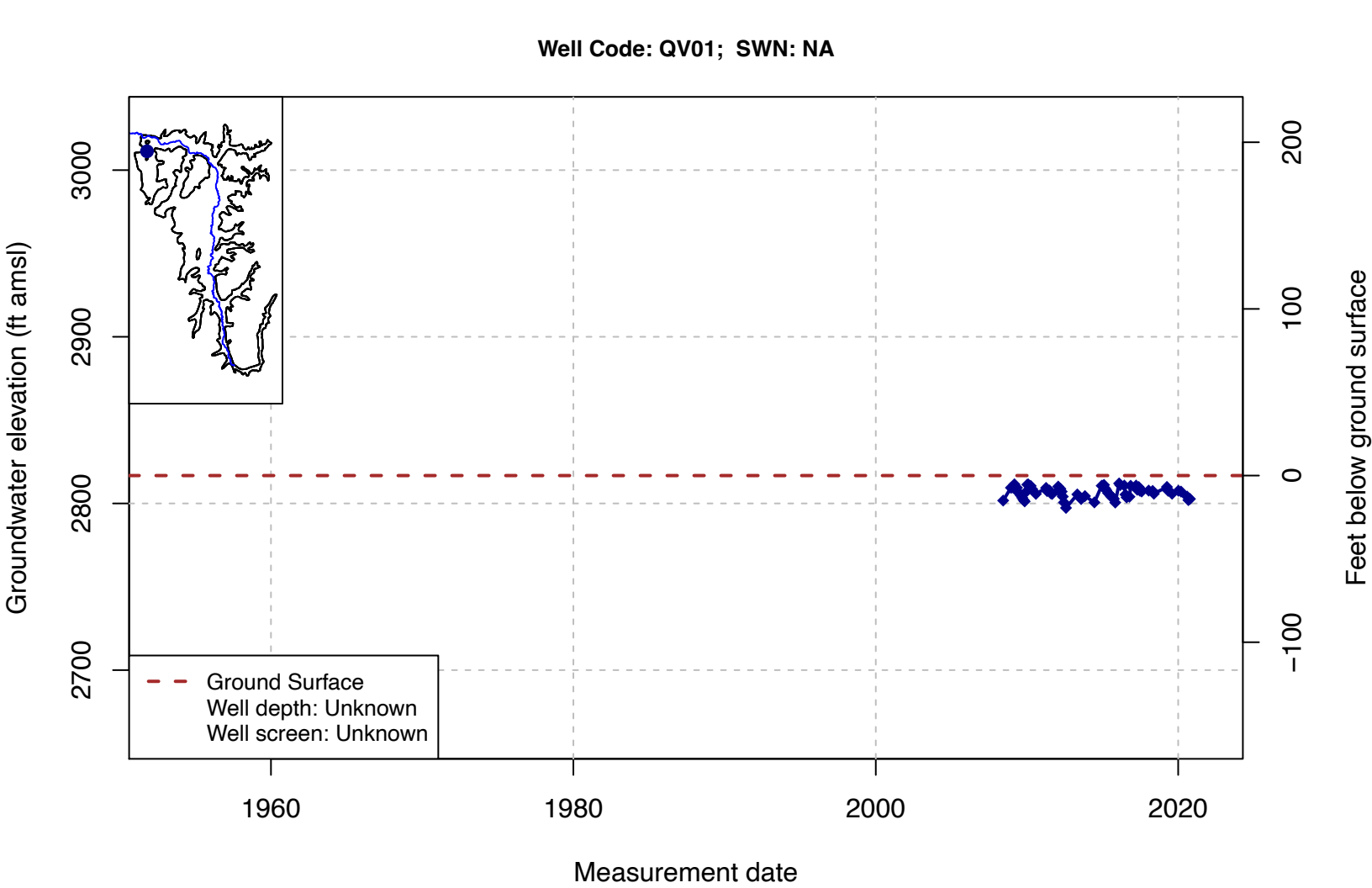
Well Code: QV01; SWN: NA
Groundwater elevation (ft amsl)
3000
2900
2800
2700
200
100
0
−100
Feet below ground surface
1960
1980
2000
2020
Measurement date
Ground Surface
Well depth: Unknown
Well screen: Unknown

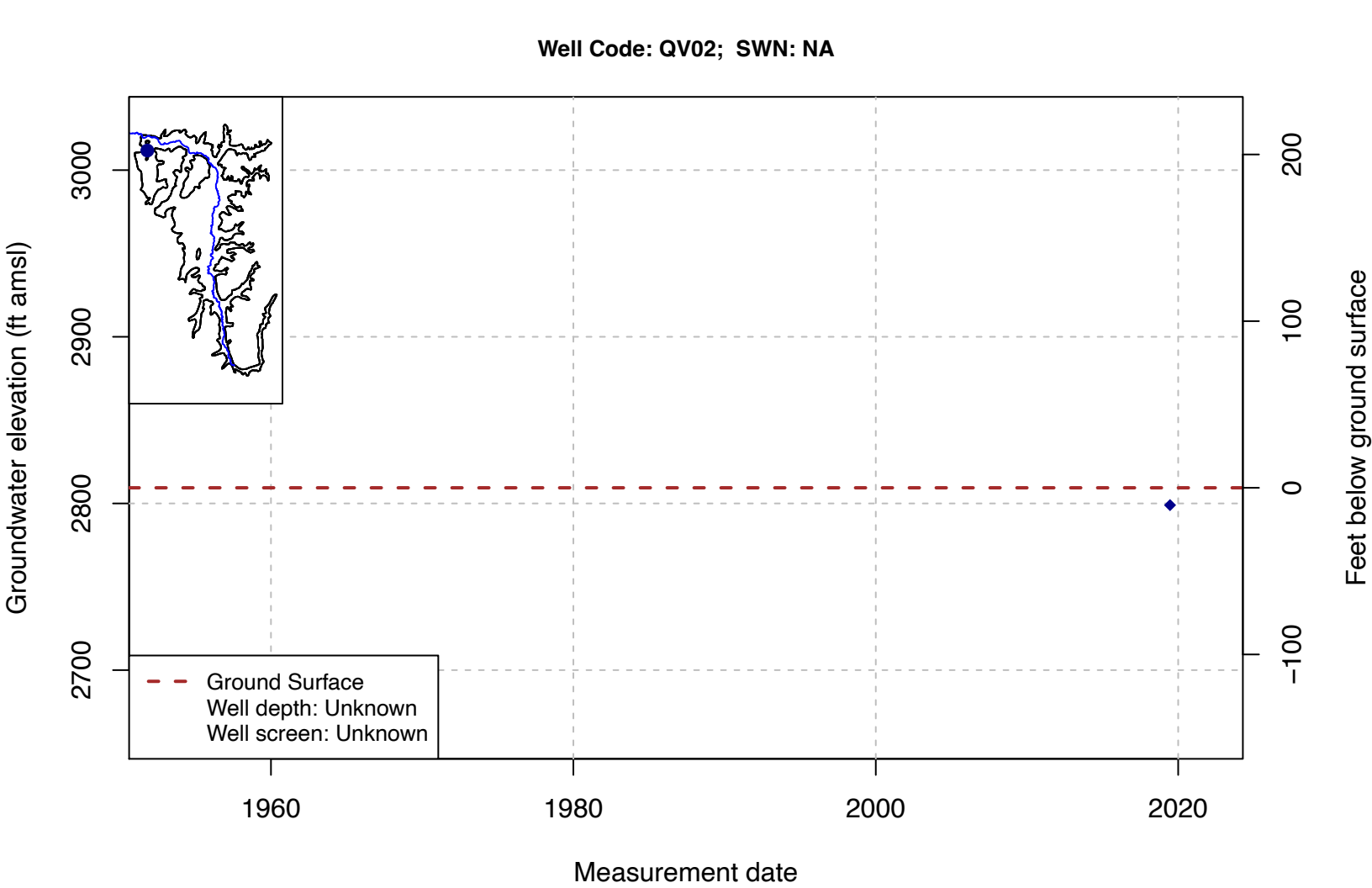
Well Code: QV02; SWN: NA
Groundwater elevation (ft amsl)
3000
2900
2800
2700
200
100
0
−100
Feet below ground surface
1960
1980
2000
2020
Measurement date
Ground Surface
Well depth: Unknown
Well screen: Unknown

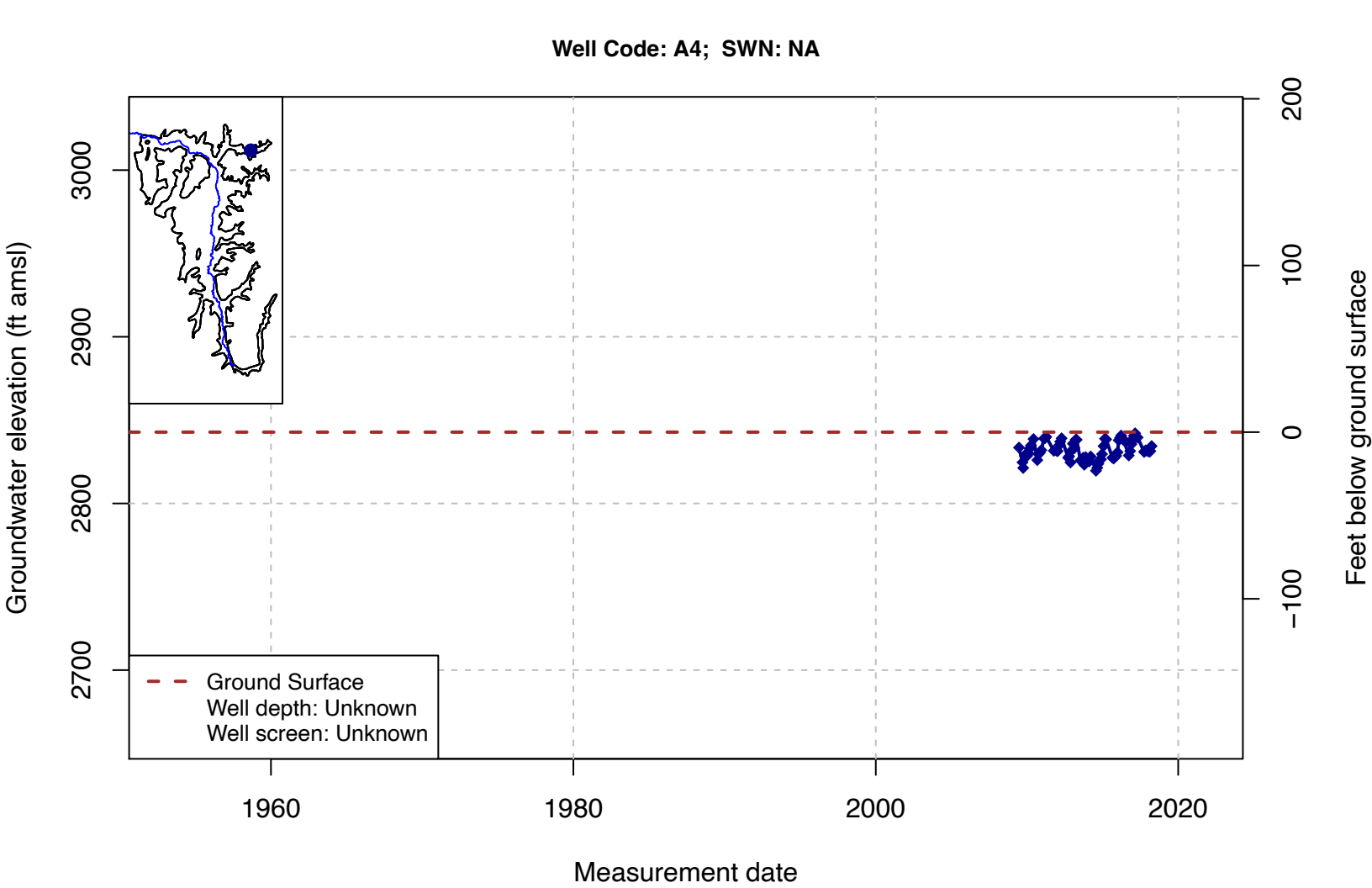
Well Code: A4; SWN: NA
Groundwater elevation (ft amsl)
3000
2900
2800
2700
200
100
0
−100
Feet below ground surface
1960
1980
2000
2020
Measurement date
Ground Surface
Well depth: Unknown
Well screen: Unknown

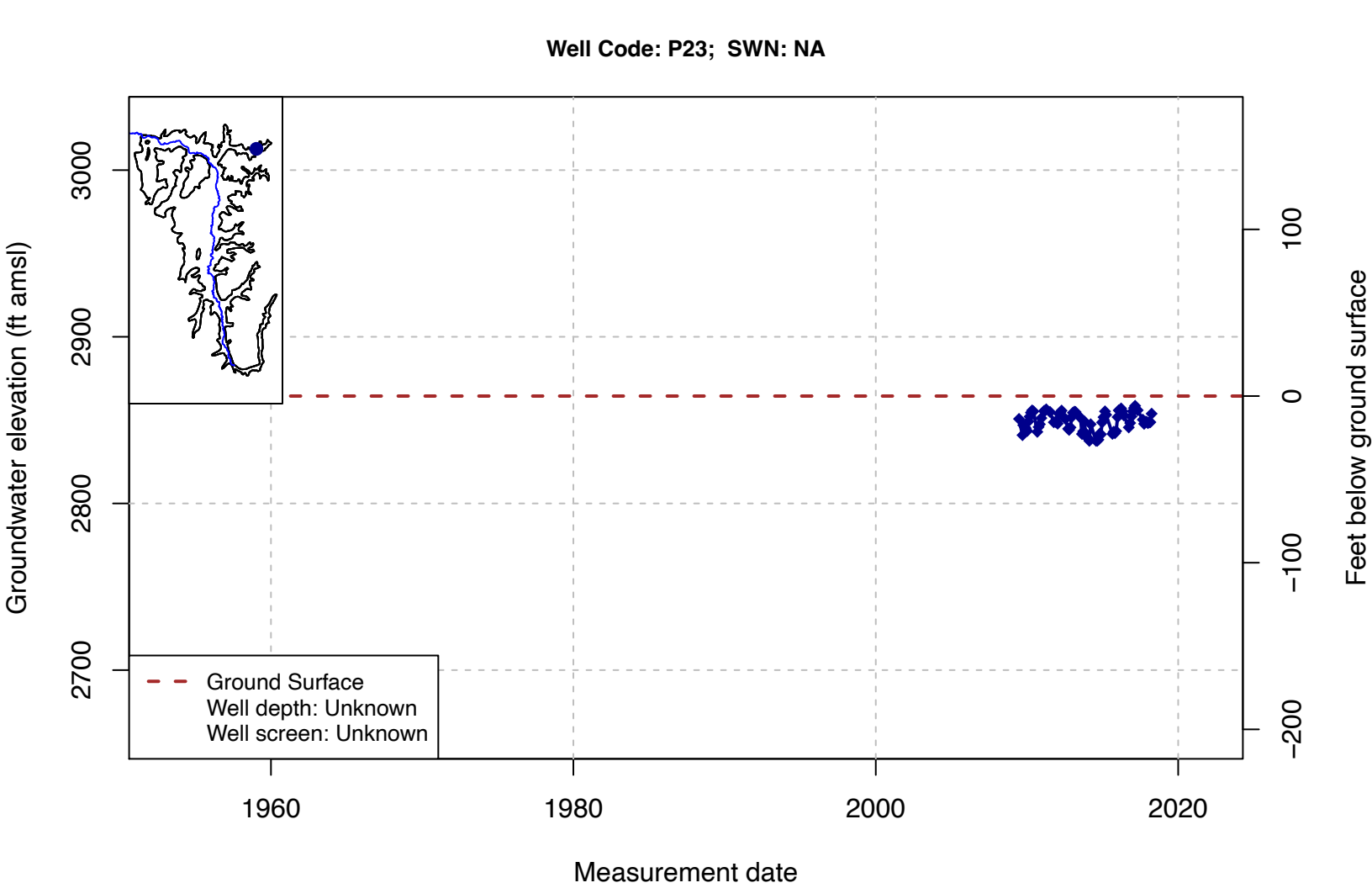
Well Code: P23; SWN: NA
Groundwater elevation (ft amsl)
3000
2900
2800
2700
Feet below ground surface
100
0
−100
−200
1960
1980
2000
2020
Measurement date
Ground Surface
Well depth: Unknown
Well screen: Unknown

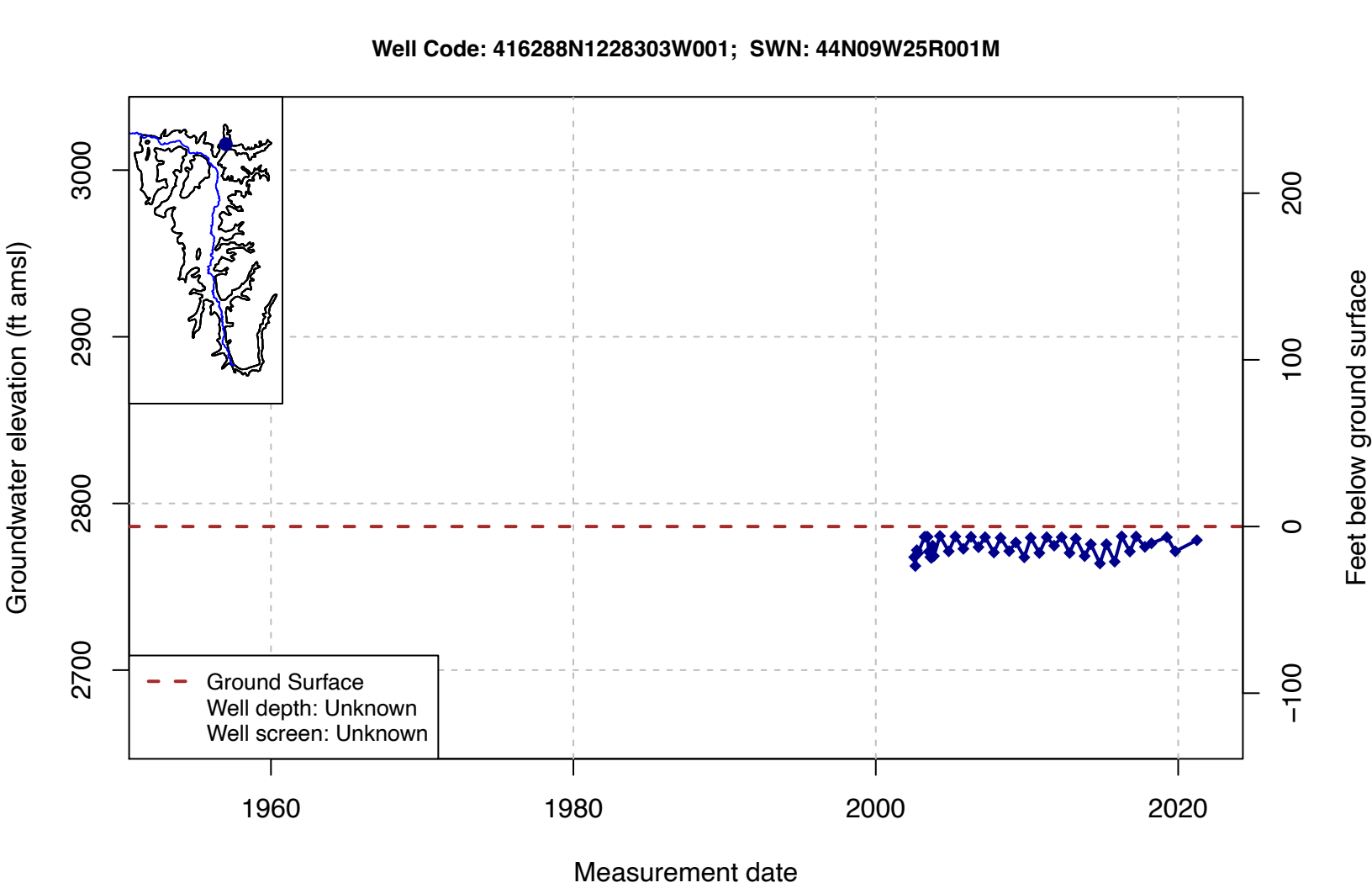
Well Code: 416288N1228303W001; SWN: 44N09W25R001M
Groundwater elevation (ft amsl)
3000
2900
2800
2700
Feet below ground surface
200
100
0
−100
1960
1980
2000
2020
Measurement date
Ground Surface
Well depth: Unknown
Well screen: Unknown

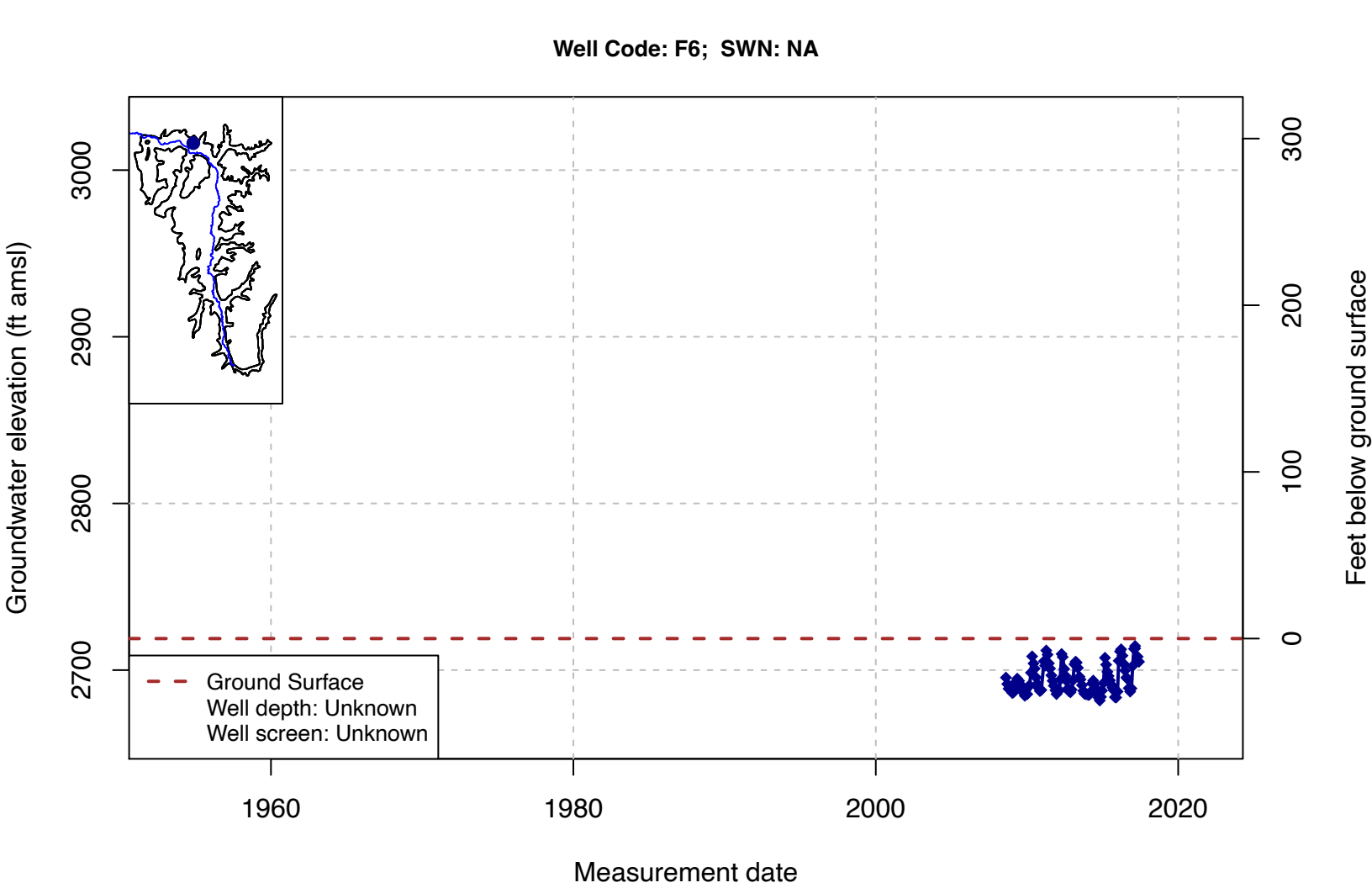
Well Code: F6; SWN: NA
Groundwater elevation (ft amsl)
3000
2900
2800
2700
Feet below ground surface
300
200
100
0
1960
1980
2000
2020
Measurement date
Ground Surface
Well depth: Unknown
Well screen: Unknown

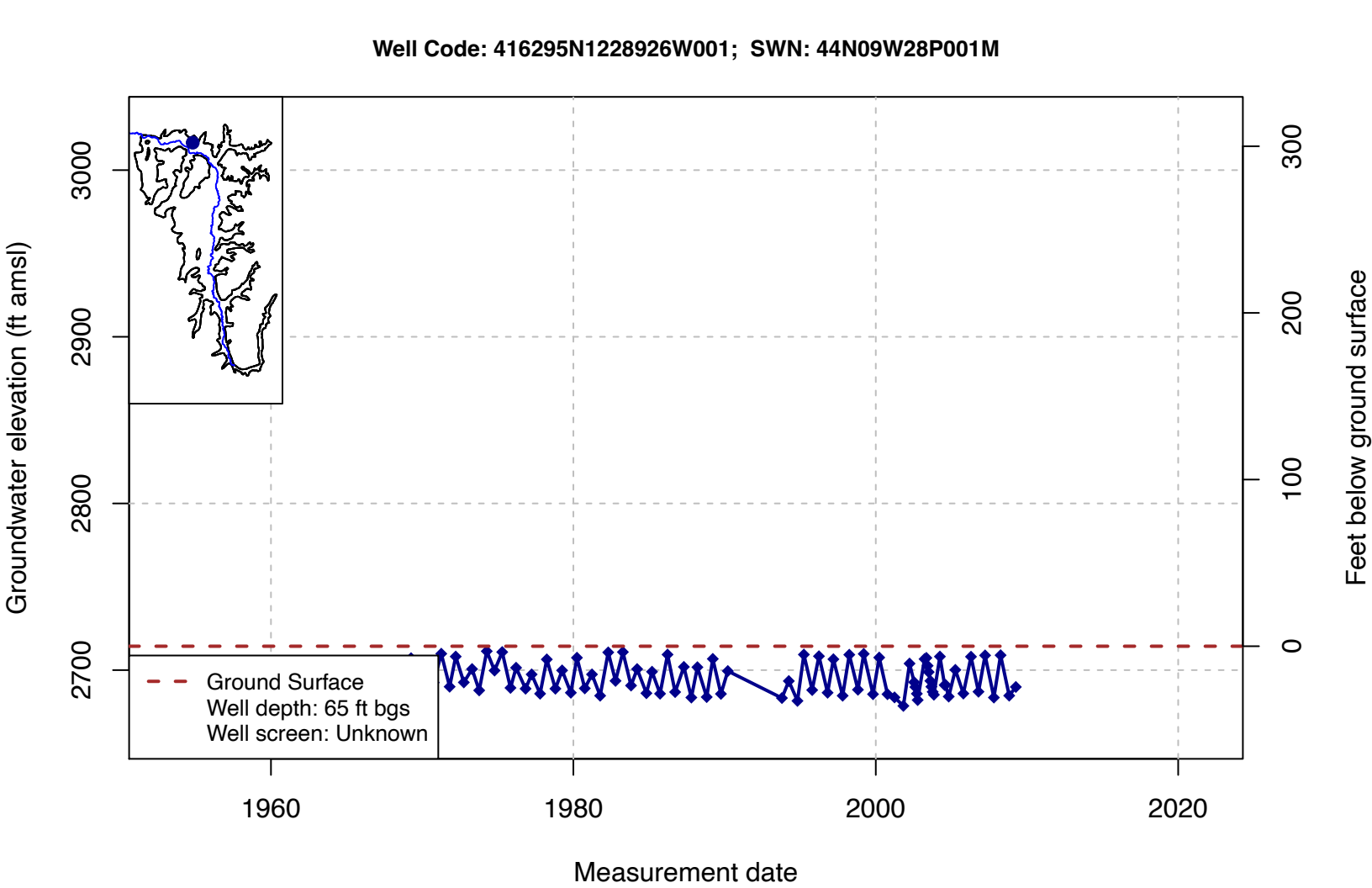
Well Code: 416295N1228926W001; SWN: 44N09W28P001M
Groundwater elevation (ft amsl)
3000
2900
2800
2700
Feet below ground surface
300
200
100
0
1960
1980
2000
2020
Measurement date
Ground Surface
Well depth: 65 ft bgs
Well screen: Unknown

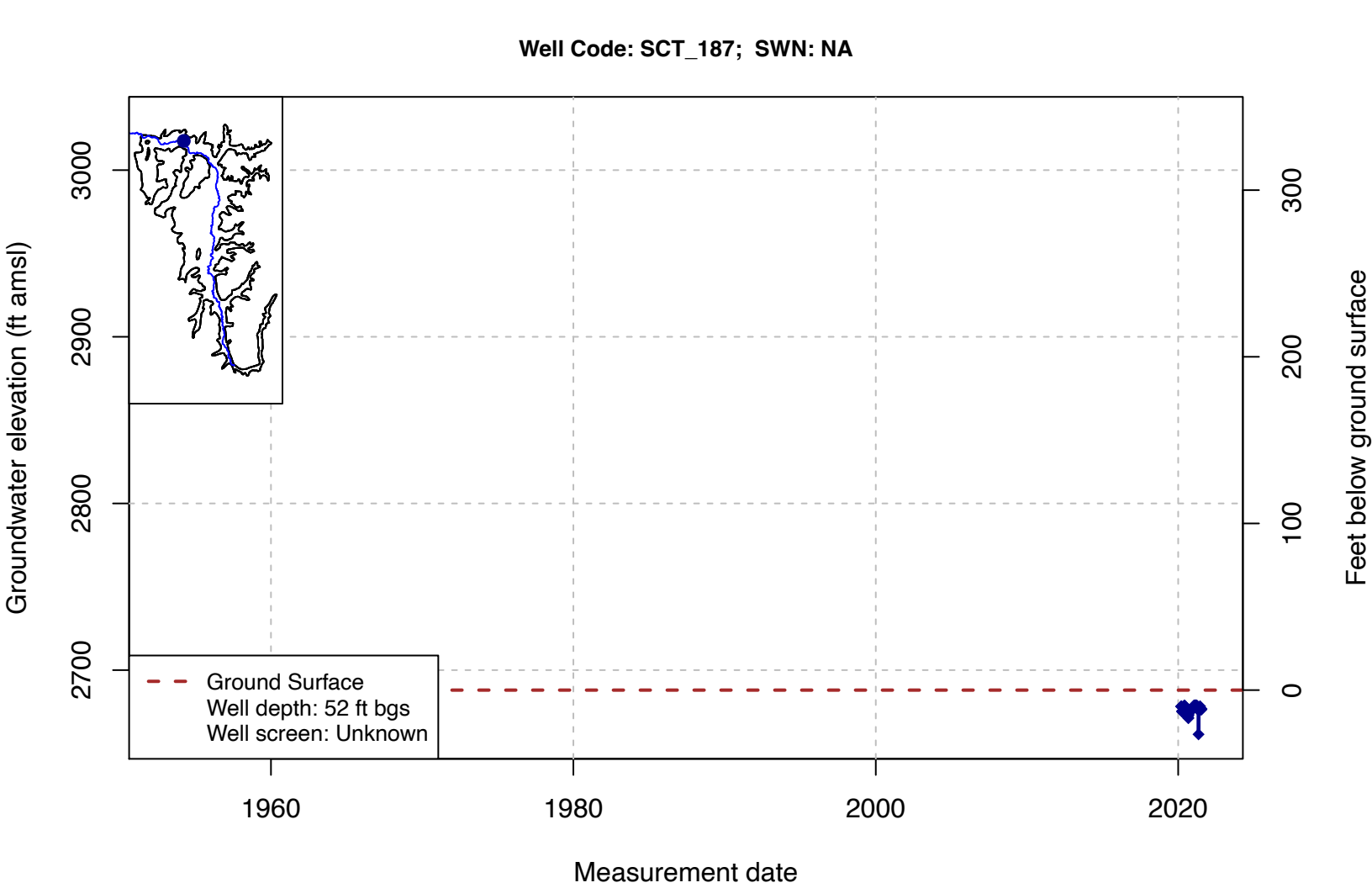
Well Code: SCT_187; SWN: NA
Groundwater elevation (ft amsl)
3000
2900
2800
2700
Feet below ground surface
300
200
100
0
Ground Surface
Well depth: 52 ft bgs
Well screen: Unknown
1960
1980
2000
2020
Measurement date

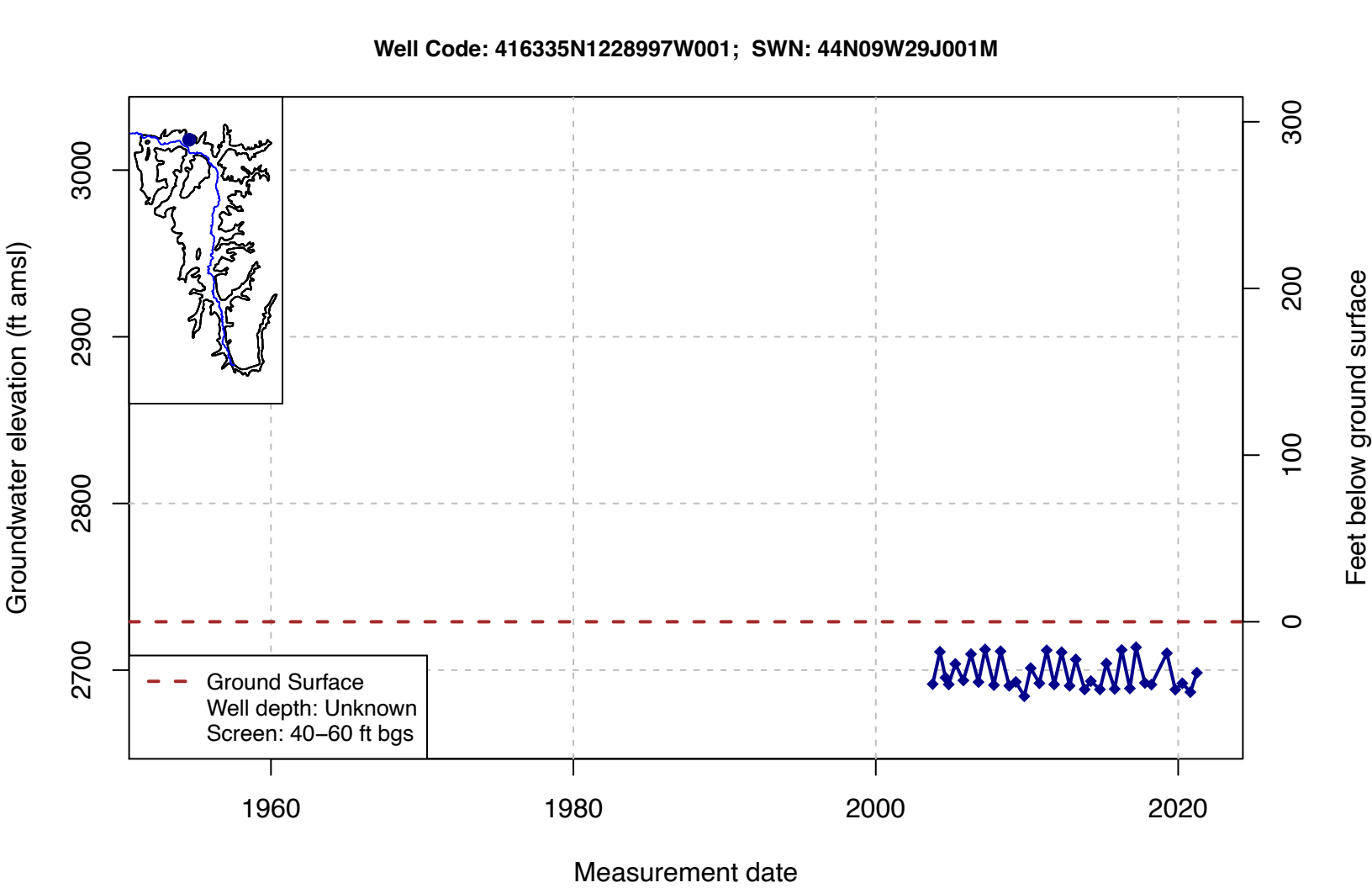
Well Code: 416335N1228997W001; SWN: 44N09W29J001M
Groundwater elevation (ft amsl)
3000
2900
2800
2700
Feet below ground surface
300
200
100
0
Ground Surface
Well depth: Unknown
Screen: 40–60 ft bgs
1960
1980
2000
2020
Measurement date

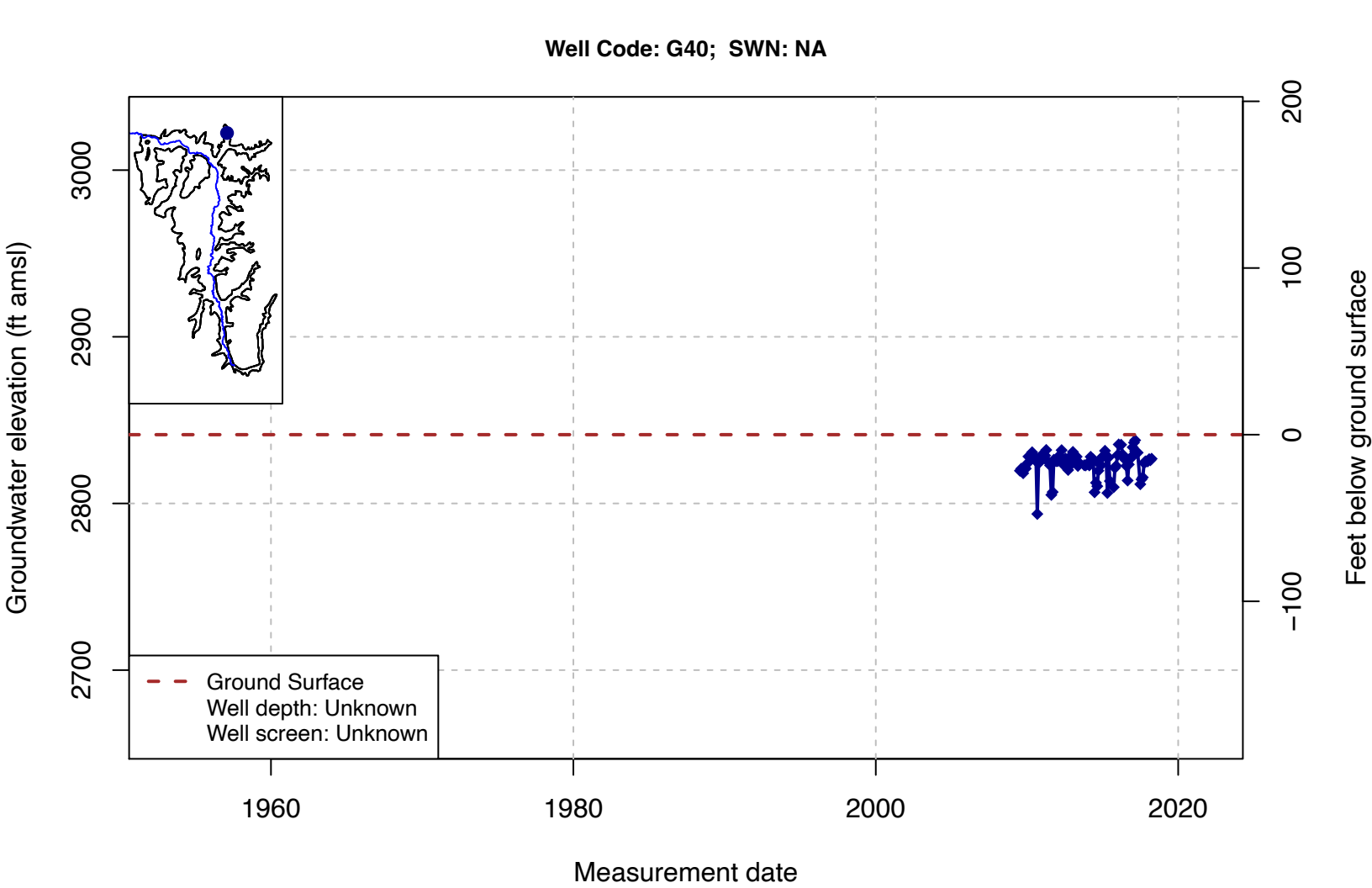
Well Code: G40; SWN: NA
Groundwater elevation (ft amsl)
3000
2900
2800
2700
200
100
0
−100
Feet below ground surface
1960
1980
2000
2020
Measurement date
Ground Surface
Well depth: Unknown
Well screen: Unknown

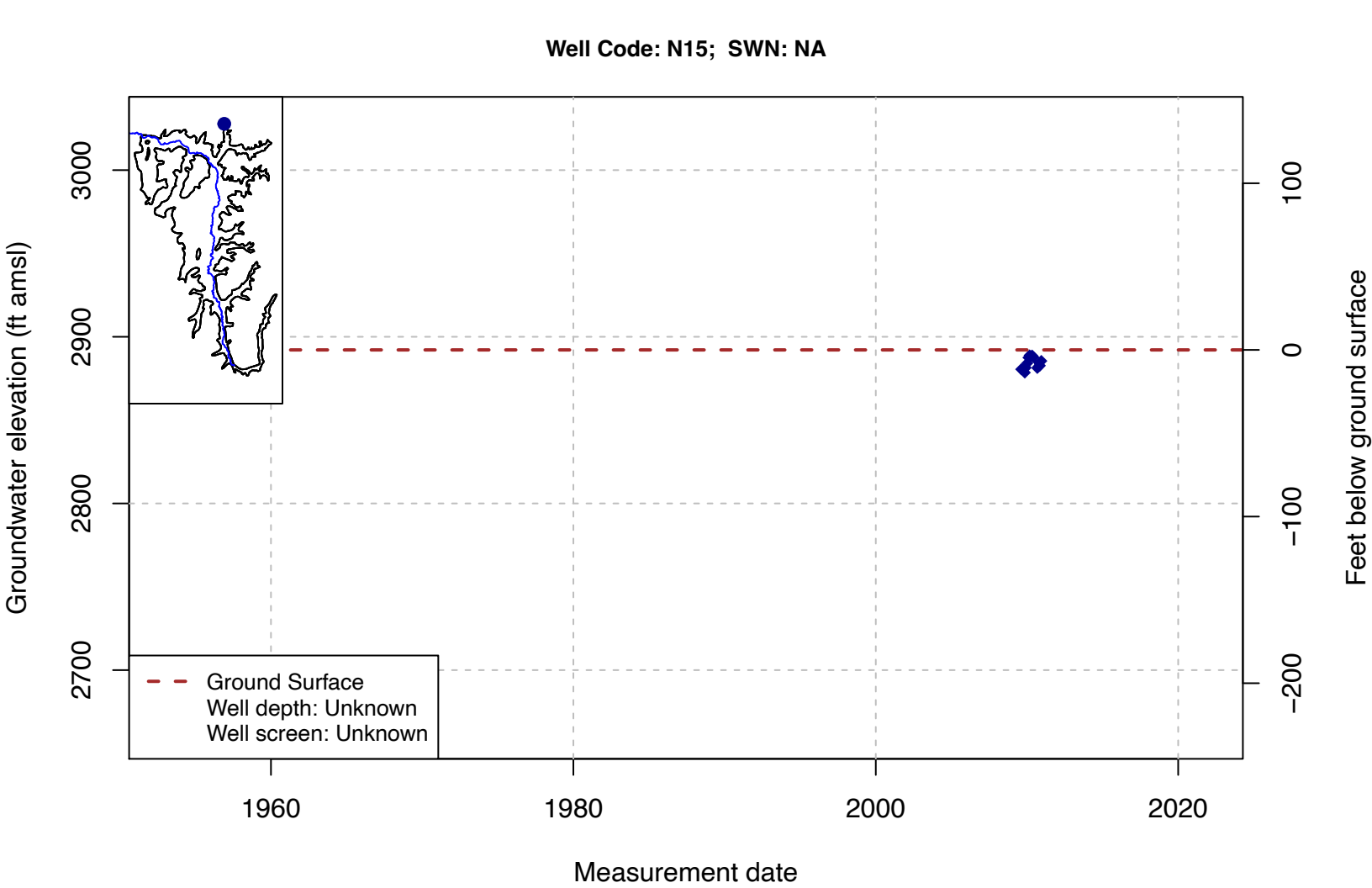
Well Code: N15; SWN: NA
Groundwater elevation (ft amsl)
3000
2900
2800
2700
Feet below ground surface
100
0
−100
−200
1960
1980
2000
2020
Measurement date
Ground Surface
Well depth: Unknown
Well screen: Unknown

Appendix 2-B Water Quality Assessment

Regulatory Background

Federal and State Regulations

The overarching federal law concerning groundwater quality is the Clean Water Act, passed in 1972, and applicable to surface waters and wetlands. In contrast, the federal Safe Drinking Water Act (SDWA) applies to both surface and groundwater, providing protection to drinking water supplies. Under the SDWA, federal standards were established through the United States Environmental Protection Agency (USEPA), in the form of maximum concentration levels (MCLs). Secondary maximum contaminant levels (SMCLs) have also been established at the federal level; these address esthetics of drinking water sources and are not enforceable. The state of California has its own Safe Drinking Water Act that includes MCLs and SMCLs which are, for select constituents, stricter than those set at the federal level. The California MCLs and SMCLs are codified in Title 22 of the California Code of Regulations (CCR). The standards established under the federal and state Safe Drinking Water Acts are enforced through the State Water Resource Control Board's (SWRCB's) Division of Drinking Water (DDW).

The California Porter-Cologne Water Quality Act, contained in California Water Code Division 7, applies to groundwater and surface waters, designating responsibility for water quality and safe drinking water to the SWRCB and the nine Regional Water Quality Control Boards (RWQCB) in California. The Act requires RWQCBs to develop water quality control plans for the region with defined water quality objectives. These water quality objectives, defined for specific hydrologic regions, protect the quality of surface waters, groundwaters, and associated beneficial uses. The water quality control plan must be approved by both the SWRCB and the USEPA. The Scott Valley Basin is in the North Coast Region and is regulated under the North Coast Regional Water Quality Control Board (Regional Water Board), with water quality objectives detailed in the Water Quality Control Plan for the North Coast Region (Basin Plan)[1] .

The SWRCB's Policy for Water Quality Control For Recycled Water (Recycled Water Policy)[2] , most recently amended in 2018, includes additional requirements to address salt and nutrients. Under this policy, Regional Water Boards are required to assess basins or subbasins within the region where water quality is threatened by salt and nutrients, and where management is required. In basins or subbasins where salt and nutrients are identified as a threat, a salt and nutrient management plan (SNMP) or equivalent management plan is required; this plan can address other constituents in addition to salt and nutrients.

Water Quality Control Plan for the North Coast Region

The Water Quality Control Plan for the North Coast Region (Basin Plan) is a regulatory tool used by the North Coast Regional Water Quality Control Board (Regional Water Board) to protect water quality within the North Coast Region. The Basin Plan is adopted by the NCRWQCB and approved by the State Water Resources Control Board; the water quality standards are approved by the United States Environmental Protection Agency (USEPA). Within the Basin Plan, beneficial uses of water, water quality objectives, including an antidegradation policy and plans for implementing protections are included. Table 2-1 of the Basin Plan designates all groundwaters with the beneficial uses of: Municipal and Domestic Supply (MUN), Agricultural Supply (AGR), Industrial Service Supply (IND), and Native American Culture (CUL) with potential beneficial of Industrial Process Supply (PRO) and Aquaculture (AQUA) (California North Coast Regional Water Quality Control Board 2018). For chemical constituents

---

[1] North Coast Regional Water Quality Control Board. 2018. "Water Quality Control Plan for the North Coast Region". Available: https://www.waterboards.ca.gov/northcoast/water_issues/programs/basin_plan/}

[2] SWRCB Resolution No. 2018-0057 and "Amendment to the Policy for Water Quality Control For Recycled Water". Available: https://www.waterboards.ca.gov/board_decisions/adopted_orders/resolutions/2018/121118_7_final_amendment_oal.pdf

in waters with MUN beneficial uses, the Basin Plan specifies that no waters are to exceed the maximum contaminant levels (MCL) in Title 22 of the California Code of Regulations (CCR). The Basin Plan also includes numeric water quality constituents, specifically for groundwaters in the Scott Valley hydrologic area. A complete list of constituents, comparison concentrations and sources are listed in Table 2.

Table 2: Comparison concentrations and data sources for constituents used in the water quality assessment

Full Name	MCL	Units	Source
2,4-Dichlorophenoxyacetic acid (2,4 D)	70	ug/L	Title 22 - Table 64444-A
Acetone	6300	ug/L	RfD
Silver	100	ug/L	Title 22 - Table 64449-A
Aluminum	200	ug/L	Title 22 - Table 64449-A
Alachlor	2	ug/L	Title 22 - Table 64444-A
Aldicarb	7	ug/L	HBSL
Aldicarb Sulfone	7	ug/L	HBSL
Aldicarb sulfoxide	7	ug/L	HBSL
Gross Alpha radioactivity	15	pCi/L	Title 22 - Table 64442
Arsenic	10	ug/L	Title 22 - Table 64431-A
Asbestos	7	MFL	Title 22 - Table 64431-A
Atrazine	1	ug/L	Title 22 - Table 64444-A
Azinphos Ethyl	10	ug/L	HBSL
Guthion (Azinphos Methyl)	10	ug/L	HBSL
Boron	0.1 (50% and 90% UL),	mg/L	Basin Plan - Table 3-1
Barium	1	mg/L	Title 22 - Table 64431-A
Bromodichloromethane (THM)	80	ug/L	MCL
Beryllium	4	ug/L	Title 22 - Table 64431-A
Bensulfuron Methyl	1000	ug/L	HBSL
Gross beta	50	pCi/L	MCL-US
Alpha-Benzene Hexachloride (Alpha-BHC)	0.15	ug/L	CA-Prop65
Beta-Benzene Hexachloride (Beta-BHC)	0.25	ug/L	CA-Prop65
Lindane (Gamma-BHC)	0.2	ug/L	Title 22 - Table 64444-A
Di(2-ethylhexyl)phthalate (DEHP)	4	ug/L	Title 22 - Table 64444-A
Methyl Bromide (Bromomethane)	10	ug/L	US-HAL
Bromate	10	ug/L	MCL-US
Bromacil	70	ug/L	US-HAL
n-Butylbenzene	260	ug/L	NL
sec-Butylbenzene	260	ug/L	NL
tert-Butylbenzene	260	ug/L	NL
Bentazon	18	ug/L	Title 22 - Table 64444-A
Benzene	1	ug/L	Title 22 - Table 64444-A
Benzo(a)pyrene	0.2	ug/L	Title 22 - Table 64444-A
Toluene	150	ug/L	Title 22 - Table 64444-A
Cadmium	5	ug/L	Title 22 - Table 64431-A
Carbon Disulfide	160	ug/L	HBSL
Chlorate	800	ug/L	NAS-HAL
Chlordane	0.1	ug/L	Title 22 - Table 64444-A
Chlorite	1	mg/L	MCL-US
Chloride	500	mg/L	Title 22 - Table 64449-B

Full Name	MCL	Units	Source
Chlorobenzene	70	ug/L	Title 22 - Table 64444-A
2 Chlorotoluene	140	ug/L	US-HAL
4 Chlorotoluene	140	ug/L	HBSL
Chloropicrin	12	ug/L	NAS-HAL
Cyanide (CN)	150	ug/L	Title 22 - Table 64431-A
Total Coliform Bacteria	0.99	Count	MCL
Chromium	50	ug/L	Title 22 - Table 64431-A
Chromium, Hexavalent (Cr6)	20	ug/L	HBSL
Carbofuran	18	ug/L	Title 22 - Table 64444-A
Carbon Tetrachloride	0.5	ug/L	Title 22 - Table 64444-A
Copper	1	mg/L	Title 22 - Table 64449-A
Cyanazine	0.3	ug/L	HBSL
Cypermethrin	40	ug/L	HBSL
Dacthal	70	ug/L	HBSL
Dalapon	200	ug/L	Title 22 - Table 64444-A
Dibromochloromethane (THM)	80	ug/L	MCL
1,2-Dibromo-3-chloropropane (DBCP)	0.2	ug/L	Title 22 - Table 64444-A
1,1-Dichloroethane (1,1 DCA)	5	ug/L	Title 22 - Table 64444-A
1,2 Dichloroethane (1,2 DCA)	0.5	ug/L	Title 22 - Table 64444-A
1,2 Dichlorobenzene (1,2-DCB)	600	ug/L	Title 22 - Table 64444-A
1,3-Dichlorobenzene	600	ug/L	US-HAL
1,4-Dichlorobenzene (p-DCB)	5	ug/L	Title 22 - Table 64444-A
1,1 Dichloroethylene (1,1 DCE)	6	ug/L	Title 22 - Table 64444-A
cis-1,2 Dichloroethylene	6	ug/L	Title 22 - Table 64444-A
trans-1,2, Dichloroethylene	10	ug/L	Title 22 - Table 64444-A
Dichloromethane (Methylene Chloride)	5	ug/L	Title 22 - Table 64444-A
1,3 Dichloropropene	0.5	ug/L	Title 22 - Table 64444-A
1,2 Dichloropropane (1,2 DCP)	5	ug/L	Title 22 - Table 64444-A
Dichlorprop	300	ug/L	HBSL
4,4’-DDD	0.1	ug/L	CA-CPF
4,4’-DDE	0.1	ug/L	CA-CPF
4,4’-DDT	0.1	ug/L	CA-CPF
Deethylatrazine	50	ug/L	CA-Prop65
Diazinon	1.2	ug/L	HBSL
Dicamba	210	ug/L	RfD
Dichlorvos (DDVP)	0.4	ug/L	HBSL
Dieldrin	0.002	ug/L	HBSL
Diesel	100	ug/L	US-HAL
Dimethoate	2	ug/L	HBSL
Dinoseb	7	ug/L	Title 22 - Table 64444-A
1,4-Dioxane	1	ug/L	HBSL
Diquat	20	ug/L	Title 22 - Table 64444-A
Diuron	2	ug/L	HBSL

Continued on next page

Full Name	MCL	Units	Source
Di(2-ethylhexyl)adipate	0.4	mg/L	Title 22 - Table 64444-A
Ethylbenzene	300	ug/L	Title 22 - Table 64444-A
1,2 Dibromoethane (EDB)	0.05	ug/L	Title 22 - Table 64444-A
Endosulfan I	42	ug/L	RfD
Endosulfan II	42	ug/L	RfD
Endosulfan Sulfate	42	ug/L	RfD
Endothall	100	ug/L	Title 22 - Table 64444-A
Endrin	2	ug/L	Title 22 - Table 64444-A
EPTC	200	ug/L	HBSL
Ethylene glycol	14	mg/L	US-HAL
Fluoride	2	mg/L	Title 22 - Table 64431-A
Trichlorofluoromethane (Freon 11)	150	ug/L	Title 22 - Table 64444-A
1,1,2-Trichloro-1,2,2-Trifluoroethane (Freon 113)	1.2	mg/L	Title 22 - Table 64444-A
Dichlorodifluoromethane	1	mg/L	HBSL
Fecal Coliform (bacteria)	0.99	Count	MCL
Iron	300	ug/L	Title 22 - Table 64449-A
Fenamiphos	0.7	ug/L	HBSL
Foaming Agents (MBAS)	0.5	mg/L	Title 22 - Table 64449-A
Fonofos	10	ug/L	HBSL
Formaldehyde	100	ug/L	US-HAL
Gasoline	5	ug/L	US-HAL
Glyphosate (Round-up)	700	ug/L	MCL-US
Tritium	20000	pCi/L	Title 22 - Table 64443
Hexachlorobutadiene	0.9	ug/L	HBSL
Hexachlorocyclopentadiene	50	ug/L	Title 22 - Table 64444-A
Hexachlorobenzene (HCB)	1	ug/L	MCL-US
Heptachlor	0.01	ug/L	Title 22 - Table 64444-A
Heptachlor Epoxide	0.01	ug/L	Title 22 - Table 64444-A
Hexazinone	400	ug/L	HBSL
Mercury	2	ug/L	Title 22 - Table 64431-A
Octogen (HMX)	0.35	mg/L	US-HAL
Iodide	1190	ug/L	NAS-HAL
Isopropylbenzene (Cumene)	770	ug/L	HBSL
Iprodione	0.8	ug/L	HBSL
Kerosene	100	ug/L	US-HAL
Linuron	5	ug/L	HBSL
Malathion	500	ug/L	HBSL
Metalaxyl	500	ug/L	HBSL
Methomyl	200	ug/L	HBSL
Metolachlor	700	ug/L	HBSL
Metribuzin	90	ug/L	HBSL
Methyl Isobutyl Ketone (MIBK)	120	ug/L	NL

Continued on next page

Full Name	MCL	Units	Source
Manganese	50	ug/L	Title 22 - Table 64449-A
Molybdenum	40	ug/L	US-HAL
Molinate	20	ug/L	Title 22 - Table 64444-A
MTBE (Methyl-tert-butyl ether)	5	ug/L	Title 22 - Table 64449-A
Methoxychlor	30	ug/L	Title 22 - Table 64444-A
Sodium	50	mg/L	AL
Naled	10	ug/L	HBSL
Naphthalene	17	ug/L	HBSL
Napropamide	800	ug/L	HBSL
Ammonia	30	mg/L	US-HAL
Nickel	100	ug/L	Title 22 - Table 64431-A
N-Nitrosodiethylamine (NDEA)	0.01	ug/L	CA-CPF
N-Nitrosodimethylamine (NDMA)	0.01	ug/L	CA-CPF
N-Nitrosodi-N-Propylamine (NDPA)	0.01	ug/L	CA-CPF
Nitrite as N	1	mg/L	Title 22 - Table 64431-A
Nitrate as N	10	mg/L	Title 22 - Table 64431-A
Nitrate+Nitrite	10	mg/L	Title 22 - Table 64431-A
Norflurazon	10	ug/L	HBSL
Oxamyl	50	ug/L	Title 22 - Table 64444-A
Oxyfluorfen	20	ug/L	HBSL
Parathion	0.02	ug/L	HBSL
Lead	15	ug/L	AL
n-Propylbenzene (Isocumene)	260	ug/L	NL
1,1,2,2 Tetrachloroethane (PCA)	1	ug/L	Title 22 - Table 64444-A
Perchlorate	6	ug/L	Title 22 - Table 64431-A
Polychlorinated Biphenyls (PCBs)	0.5	ug/L	MCL-US
Tetrachloroethene (PCE)	5	ug/L	Title 22 - Table 64444-A
PCNB	21	ug/L	RfD
Pentachlorophenol (PCP)	1	ug/L	MCL-US
Permethrin	4	ug/L	HBSL
Perfluorooctanoic acid	5.1	ng/L	US-HAL
Perfluorooctanoic sulfonate	6.5	ng/L	NL
pH	7.0-8.0	-log[H+]	Basin Plan - Table 3-1
Phorate	4	ug/L	HBSL
Picloram	0.5	mg/L	Title 22 - Table 64444-A
Prometon	400	ug/L	HBSL
Prometryn	300	ug/L	HBSL
Propachlor (2-Chloro-N-isopropylacetanilide)	90	ug/L	HBSL
Propanil	6	ug/L	HBSL
Propargite	1	ug/L	HBSL
Radium 226	5	pCi/L	Title 22 - Table 64442
Radium 228	5	pCi/L	Title 22 - Table 64442

Continued on next page

Full Name	MCL	Units	Source
RDX (hexahydro-1,3,5-trinitro-1,3,5-triazine)	0.3	mg/L	US-HAL
Radon 222	4000	pCi/L	MCL-US
Antimony	6	ug/L	Title 22 - Table 64431-A
Specific Conductivity	250 (50% UL), 500 (90% UL)	micromhos	Basin Plan - Table 3-1
Selenium	50	ug/L	Title 22 - Table 64431-A
Carbaryl (1-naphthyl methylcarbamate)	40	ug/L	HBSL
2,4,5-TP (Silvex)	50	ug/L	Title 22 - Table 64444-A
Simazine	4	ug/L	Title 22 - Table 64444-A
Sulfate	500	mg/L	Title 22 - Table 64449-B
Strontium	4000	ug/L	US-HAL
Strontium 90	8	pCi/L	Title 22 - Table 64443
Styrene	100	ug/L	Title 22 - Table 64444-A
tert-Butyl alcohol (TBA)	12	ug/L	NL
Bromoform (THM)	80	ug/L	MCL
1,1,1-Trichloroethane	200	ug/L	Title 22 - Table 64444-A
1,1,2-Trichloroethane	5	ug/L	Title 22 - Table 64444-A
1,2,4- Trichlorobenzene (1,2,4 TCB)	5	ug/L	Title 22 - Table 64444-A
2,3,7,8-TCDD	0.00003	ug/L	MCL-US
Trichloroethene (TCE)	5	ug/L	Title 22 - Table 64444-A
Chloroform (THM)	80	ug/L	MCL
1,2,3-Trichloropropane (1,2,3 TCP)	0.005	ug/L	Title 22 - Table 64444-A
Total Dissolved Solids	1000	mg/L	Title 22 - Table 64449-B
tebuthiuron	1000	ug/L	HBSL
Thiabendazole	231	ug/L	HHBP
Thiobencarb	1	ug/L	Title 22 - Table 64449-A
Total Trihalomethanes	80	ug/L	MCL-US
Thallium	2	ug/L	Title 22 - Table 64431-A
1,2,4-Trimethylbenzene	330	ug/L	NL
1,3,5-Trimethylbenzene	330	ug/L	NL
2,4,6-Trinitrotoluene (TNT)	1	ug/L	US-HAL
Toxaphene	3	ug/L	Title 22 - Table 64444-A
Trichlopyr	400	ug/L	HBSL
Trifluralin	20	ug/L	HBSL
Uranium	20	pCi/L	Title 22 - Table 64442
Vanadium	50	ug/L	RfD
Vinyl Chloride	0.5	ug/L	Title 22 - Table 64444-A
Warfarin	2	ug/L	HBSL
Xylenes (total)	1750	ug/L	Title 22 - Table 64444-A
Xylene, Isomers m & p	1750	ug/L	Title 22 - Table 64444-A
Zinc	5	mg/L	Title 22 - Table 64449-A

Water Quality Assessment

Data Sources

Water quality data was obtained from several databases and supplemented with data provided by local organizations and community members. The majority of the water quality data used in the assessment was sourced from the SWRCB's Groundwater Ambient Monitoring and Assessment Program (GAMA), a database containing datasets from agencies including the Department of Pesticide Regulation (DPR), Department of Water Resources (DWR), the State Water Board, Lawrence Livermore National Laboratory (LLNL) and the United States Geological Survey (USGS).

The datasets in GAMA with information in Scott Valley Groundwater Basin are:

- **The Public Water System Wells** dataset includes wells regulated by the State Water Board's Division of Drinking Water (DDW). This dataset includes information for active and inactive drinking water sources with 15 or more connections or more than 25 people per day.
- **National Water Information System (NWIS)**, a dataset provided by USGS with samples from water supply wells and reported quarterly to the State Water Board's data management system, GeoTracker.
- **Monitoring wells** regulated by the State Water Board includes wells under different regulatory programs, with data available for download through GeoTracker. There are monitoring wells in Scott Valley Basin for the following programs:
- Leaking Underground Storage Tank (LUST) Cleanup sites
- Department of Toxic Substances Control (DTSC) Cleanup Sites
- **DWR's Water Data Library**, a dataset including groundwater quality and depth data with samples from multiple well types including irrigation, stock, domestic and public supply.

In addition, information was obtained from USEPA Storage and Retrieval Data Warehouse (STORET), accessed through the National Water Quality Monitoring Council's (NWQMC) Water Quality Portal.

Selection of Numeric Thresholds

Numeric thresholds are used with well data to evaluate groundwater quality. These numeric standards are selected to satisfy all relevant groundwater quality standards and objectives; the general selection approach used is consistent with recommendations by the State Water Board for determination of assessment thresholds for groundwater [Reference]. More than one water quality objective or standard may apply to a constituent and a prioritization process is used to select the numeric threshold value. Where available, the strictest value, of the federal and state regulated water quality standards, and water quality objectives specified in the Basin Plan, is used.

The following sources were used in establishing the numeric thresholds:

i) Basin Plan numeric water quality objectives

Specific groundwater quality objectives are defined in the Basin Plan for specific conductance, nitrate and benzene. These limits are listed in Table 1 below.

ii) State and Federal Maximum Contaminant Levels (MCLs)

MCL-CA: State of California MCLs

MCL-US: Federal MCLs

Per the Basin Plan, groundwaters in the Scott Valley hydrologic area have a designated beneficial use as domestic or municipal water supply (MUN) beneficial use and must not exceed the maximum contaminant levels (MCLs) and secondary maximum contaminant levels (SMCLs) defined in Title 22 of the California Code of Regulations (CCR). The strictest value of the state and federal MCLs and SMCLs is used.

Table 1: Constituents of interest and associated regulatory thresholds for Scott River Valley Groundwater Basin

Constituent	Regulatory Source	Value
Benzene (ug/L)	Title 22	1 ug/L
Nitrate as Nitrogen (mg/L)	Title 22	10 mg/L
Specific Conductivity (mmhos)	Title 22	900 mmhos
Specific Conductivity (mmhos)	Basin Plan 90% Upper Limit	500 mmhos
Specific Conductivity (mmhos)	Basin Plan 50% Upper Limit	250 mmhos

Calculations

Specific water quality objectives for the Scott Valley hydrologic area groundwaters, as defined in the Basin Plan have specific limits and calculation requirements associated with specific conductance, hardness and boron. Per the Basin Plan, the 50% upper limit and 90% upper limit are defined as follows:

- 50% upper limits represent “the 50 percentile values of the monthly means for a calendar year. 50% or more of the monthly means must be less than or equal to an upper limit and greater”
- 90% upper limits represent “the 90 percentile values for a calendar year. 90% or more of the values must be equal to an upper limit and greater than or equal to a lower limit”.

Measurements of specific conductance and boron were organized to enable comparison to the 50% and 90% limits through calculation of monthly means for comparison to the 50% upper limits and organization by calendar year for comparison to the 50% and 90% upper limits.

Filtering Process

To analyze groundwater quality, several filters were applied for relevance and quality. Though groundwater quality data for the Basin is available from 1952, data was limited to only include information collected in the past 30 years. Restricting the timespan from which data was collected increases confidence in data collection methods and quality of the data and focuses on information that is reflective of current groundwater quality conditions.

Groundwater quality was analyzed through comparison, for each constituent, of well data to the corresponding comparison concentration. Maps were generated for each constituent showing well locations and number of samples and categorizing and displaying data into the following groups:

a) Not detected
b) Detected but below half of the comparison concentration
c) Detected and above half of the comparison concentration
d) Above the comparison concentration

Two iterations of of map generation was conducted with the following scenarios:

1. Data is limited to those collected in the past 30 years only (1990-2020)
2. Data is limited to wells that have more than one data point in the past 30 years (1990-2020)

For the second scenario, where data is limited to wells that have more than one data point in the past 30 years, timeseries are generated for each constituent and well to identify changes over time in groundwater quality at a location.

The following sections contain the maps produced from these analyses.

Results

Constituents of Concern (COCs)

Constituents of Concern (COCs) were identified based on visual identification of potential groundwater quality issues using the maps generated in this assessment, identification of common constituents of concern and through discussion with stakeholders. Resulting from this analysis and discussion with stakeholders, the full list of constituents of concern (COCs) were:

1. Nitrate as N
2. Specific Conductivity
3. Benzene

A series of maps for each COC, with water quality data from the past 30 years (1990-2020), show the location of tested wells and whether the maximum concentration ever recorded in that well has violated the MCL. In SCott River Valley, the water quality source database categorized some wells as either municipal or monitoring. Municipal wells are a public supply well related to a city or town. Monitoring wells are used for monitoring groundwater, such as for site cleanup programs or irrigated lands regulatory program.

The maps and associated timeseries for nitrate data in the Basin over the past 30 years are shown below.

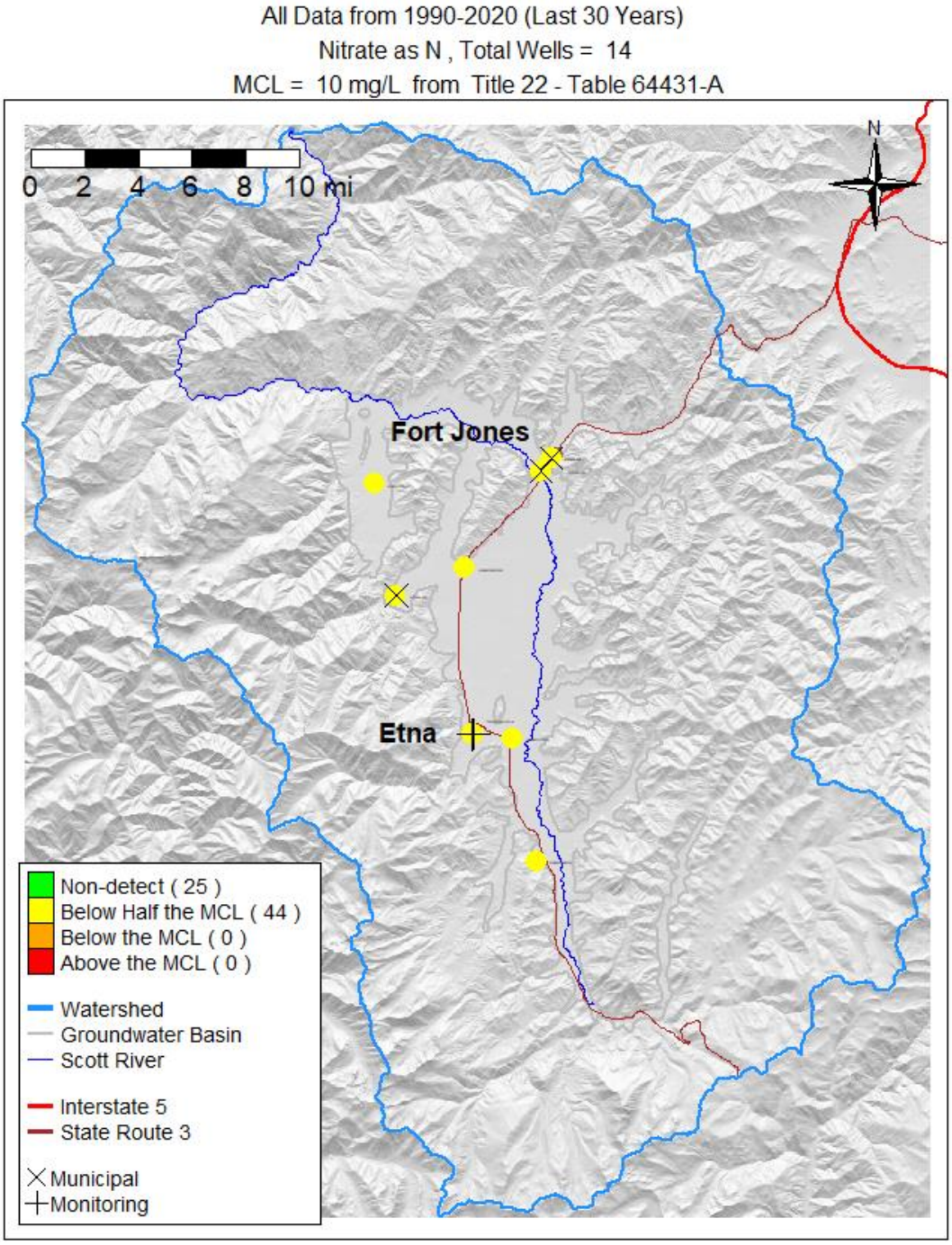

Figure 1: Well locations and detection magnitudes of nitrate data collected over the past 30 years in the Scott River Valley Groundwater Basin.

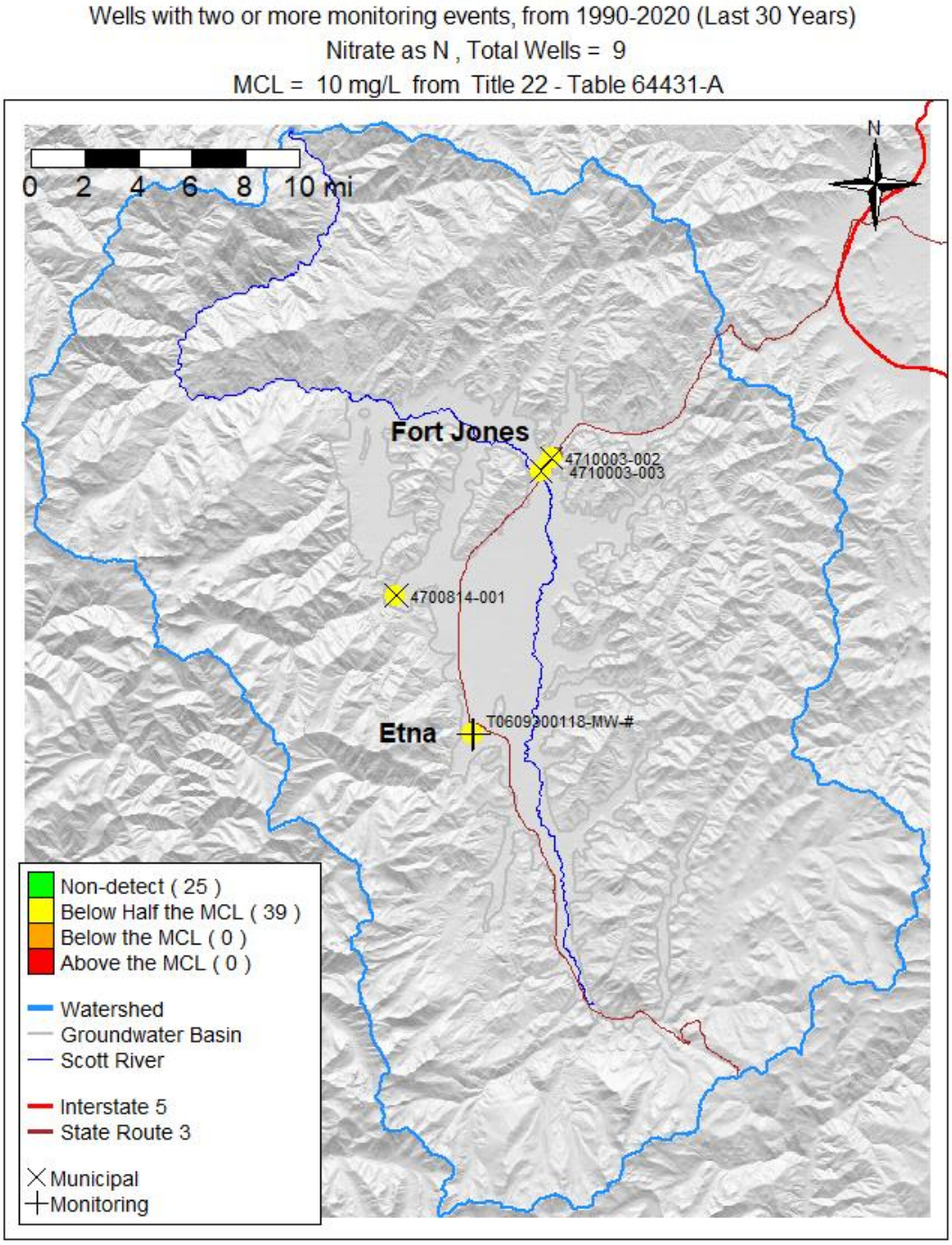

Figure 2: Well locations and detection magnitudes of nitrate data collected over the past 30 years in the Scott River Valley Groundwater Basin from wells with two or more monitoring events.

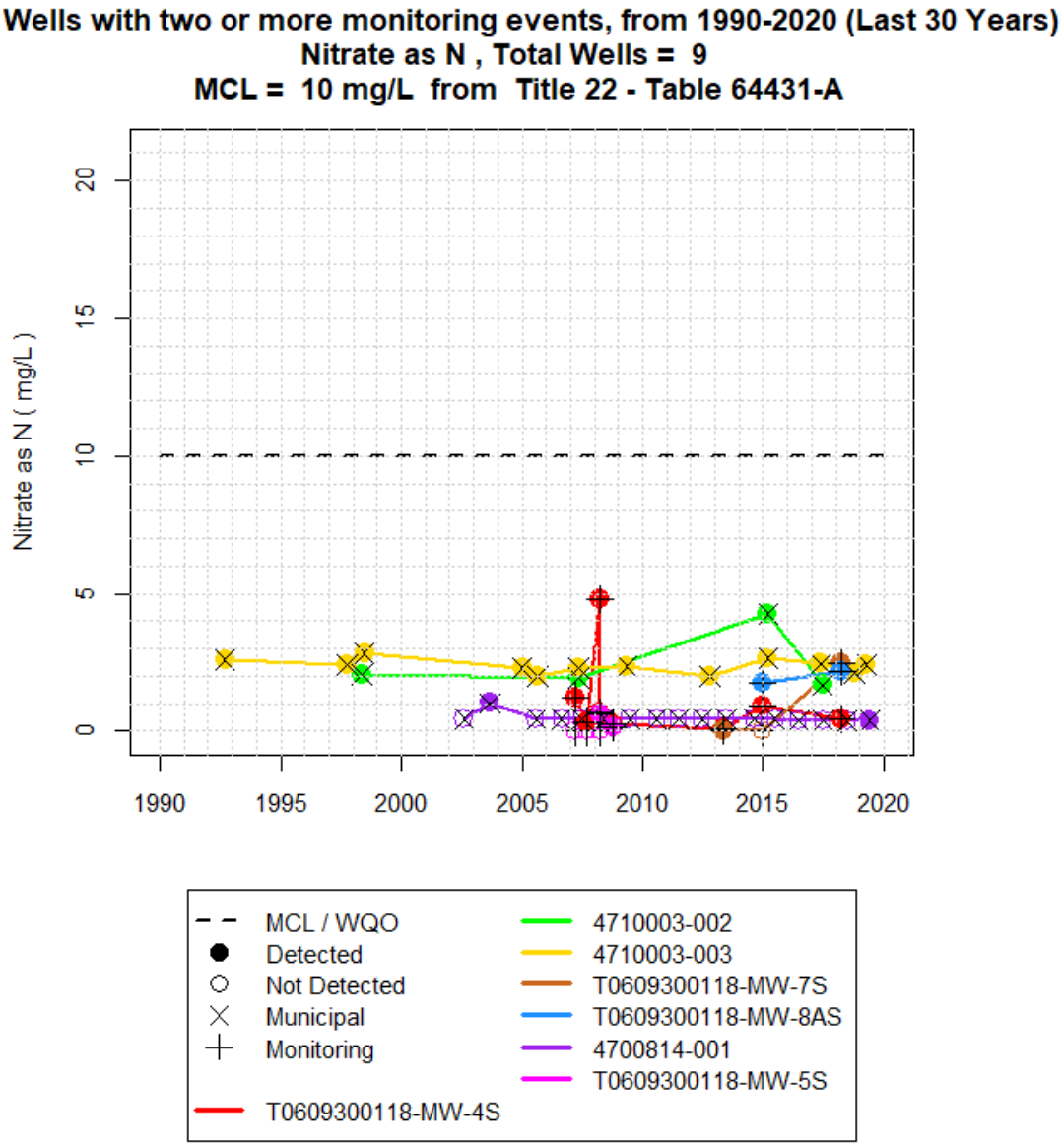

Figure 3: Timeseries plots of nitrate data collected over the past 30 years in the Scott River Valley Groundwater Basin from wells with two or more monitoring events

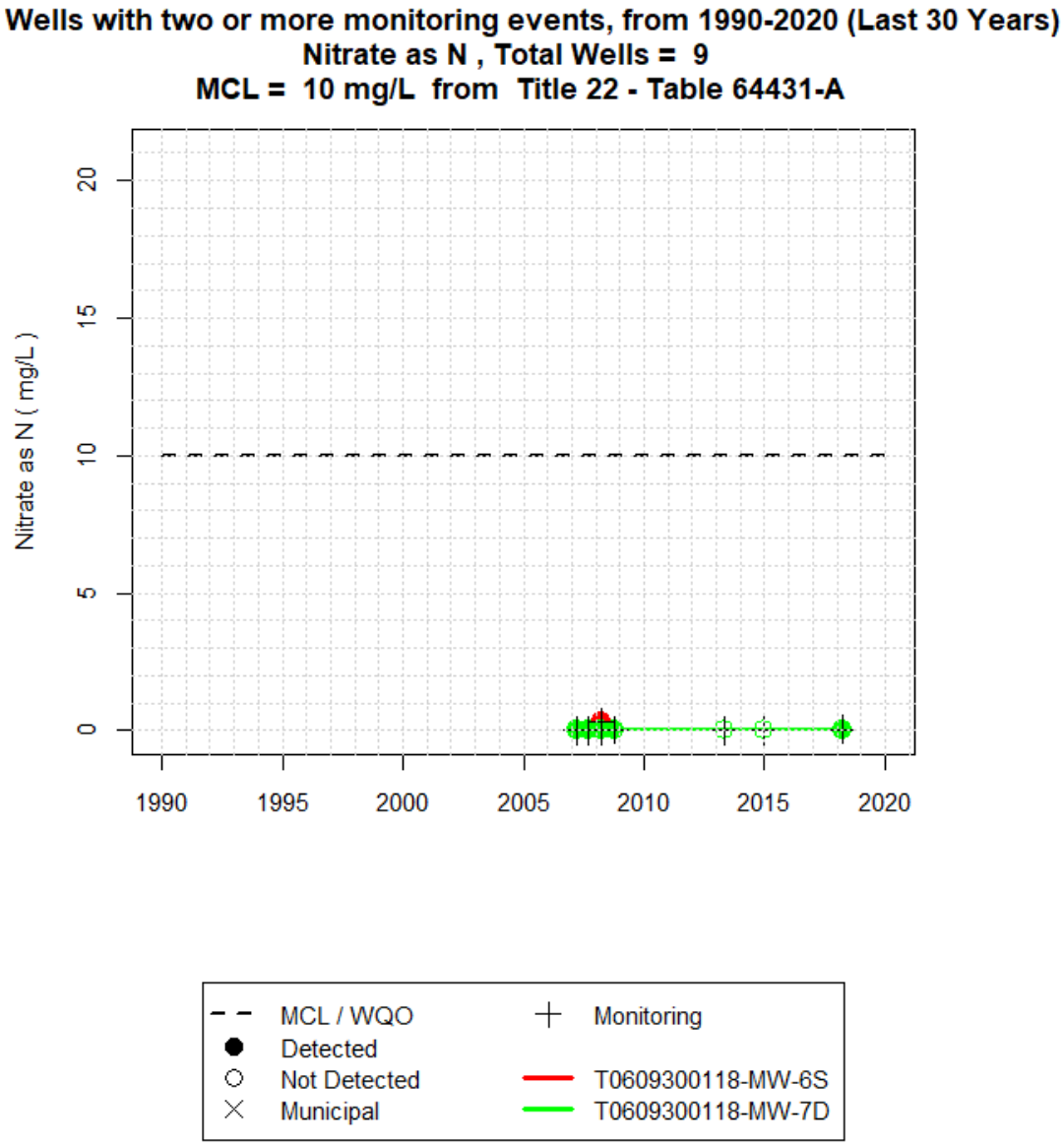

Figure 4: Timeseries plots of nitrate data collected over the past 30 years in the Scott River Valley Groundwater Basin from wells with two or more monitoring events

The maps and associated timeseries for specific conductivity data in the basin are shown below.

specific conductivity data are shown in Figure .

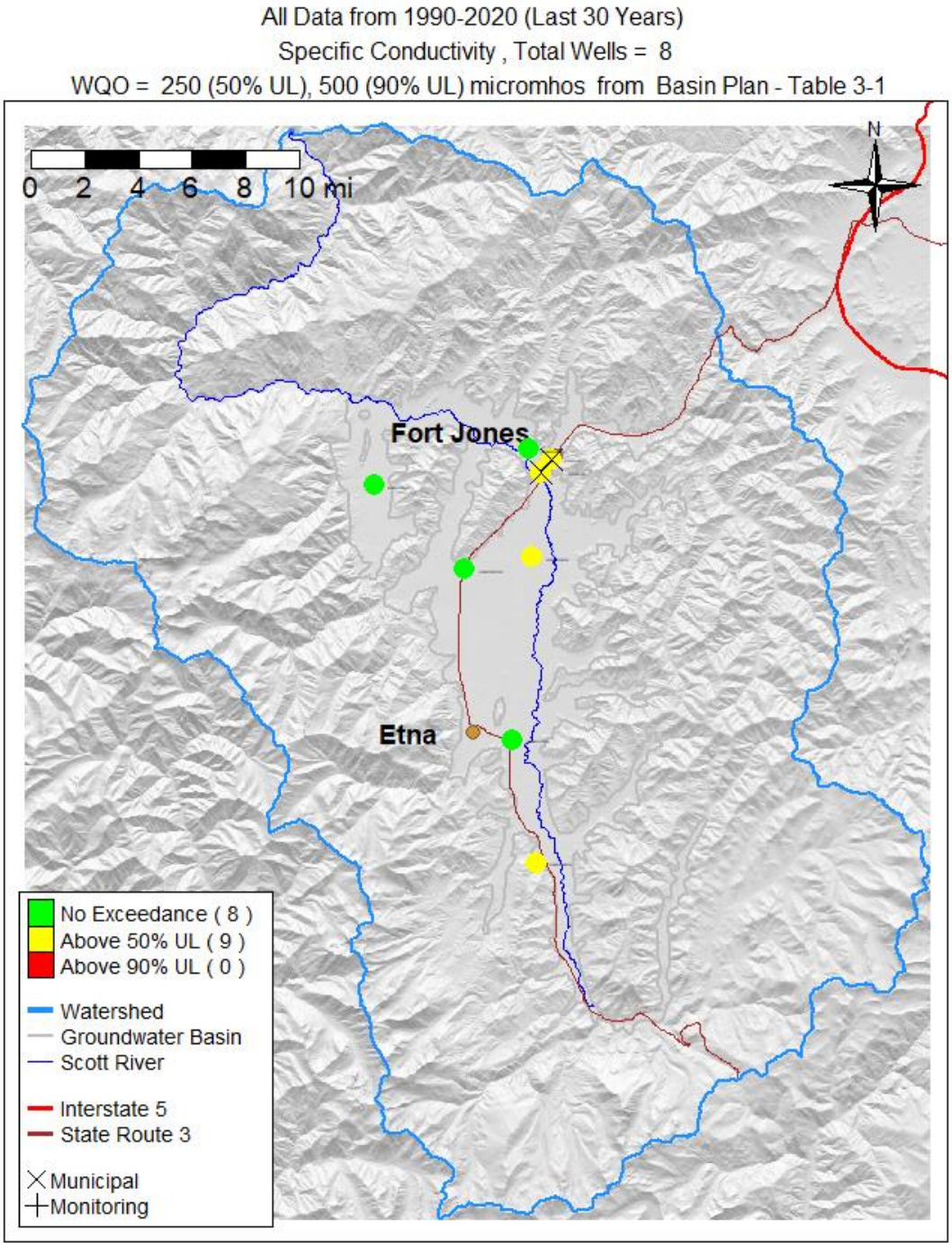

Figure 5: Well locations and detection magnitudes of specific conductivity data collected over the past 30 years in Scott River Valley Groundwater Basin.

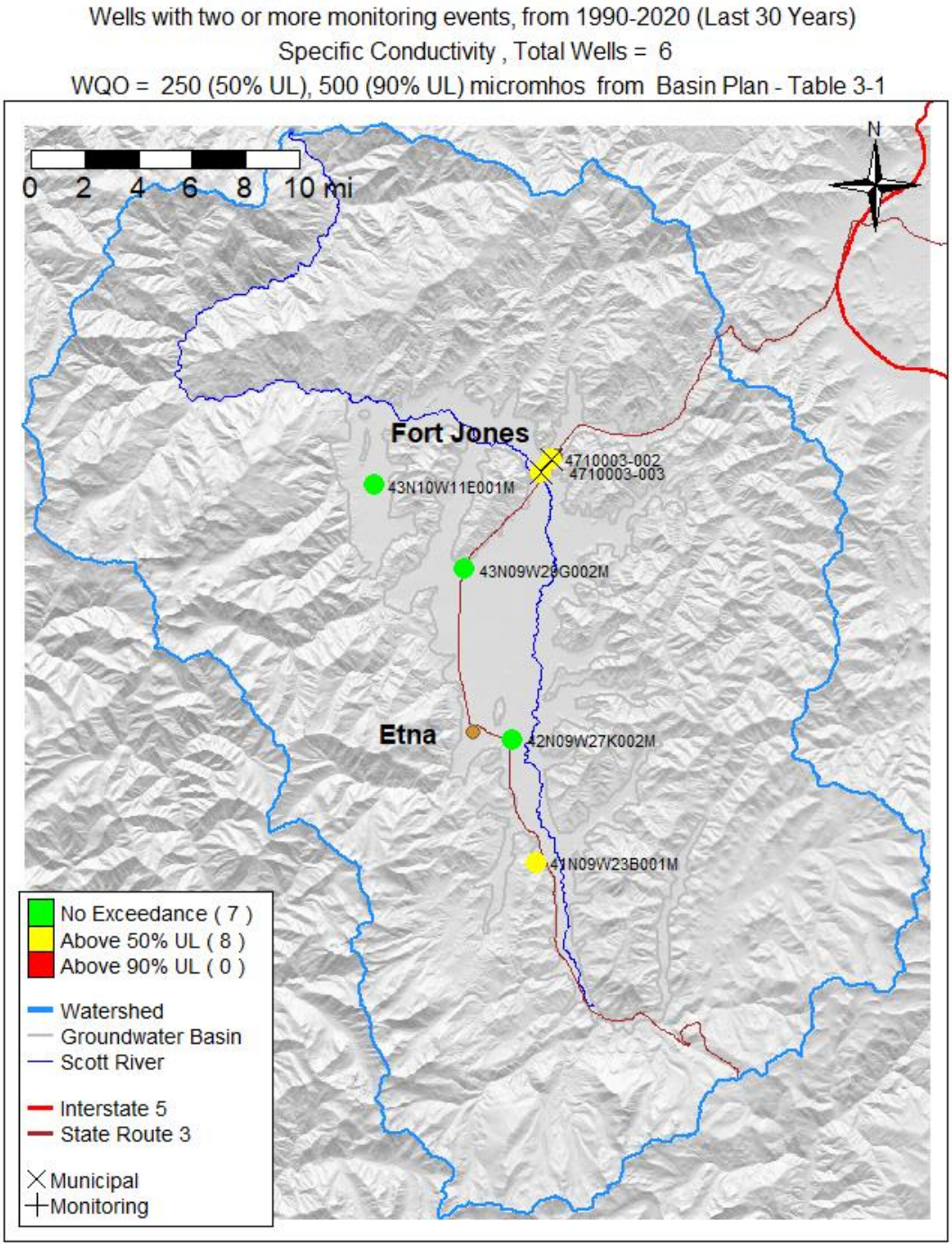

Figure 6: Well locations and detection magnitudes of specific conductivity data collected over the past 30 years in Scott River Valley Groundwater Basin from wells with two or more monitoring events.

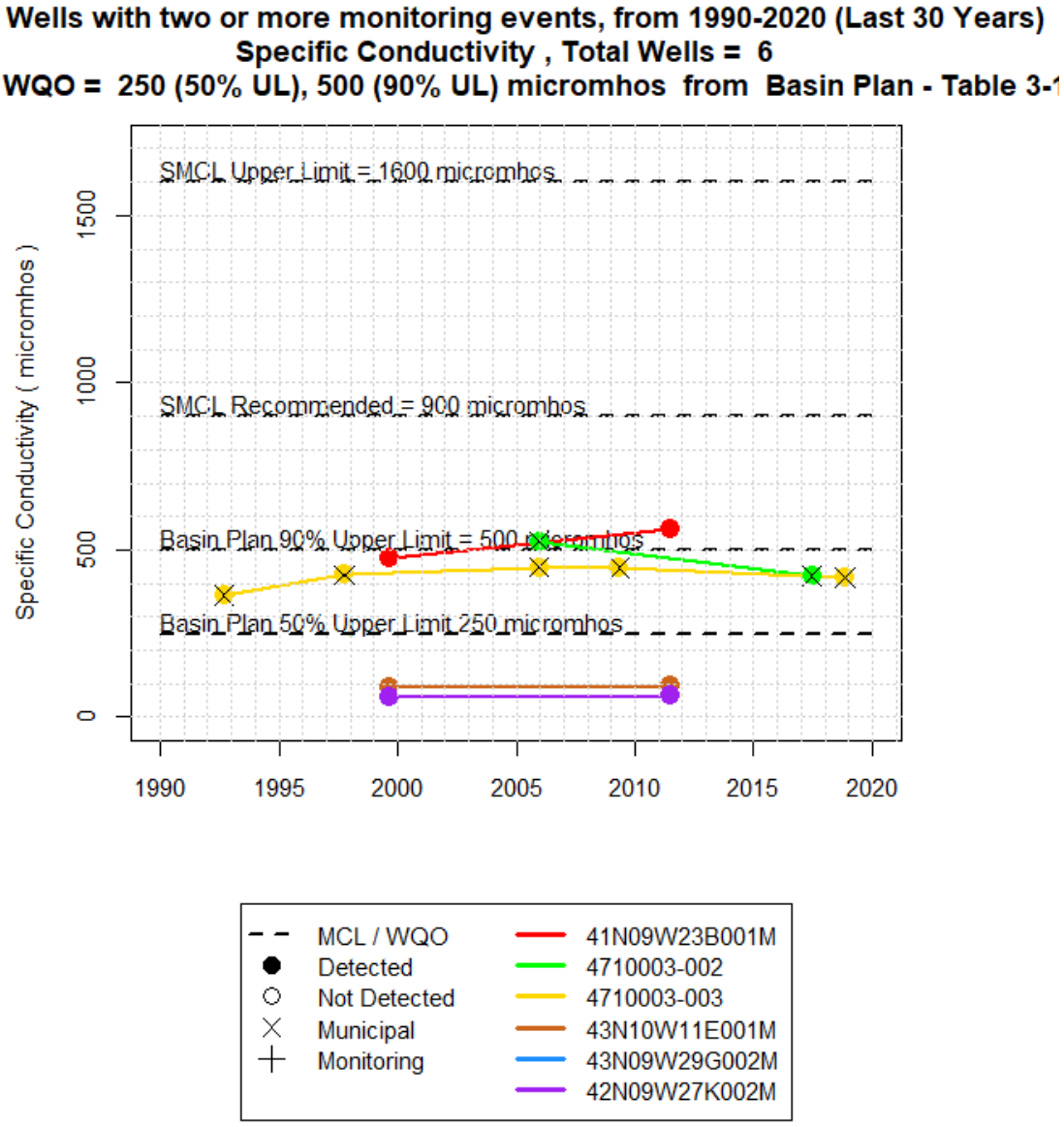

Figure 7: Timeseries plot of specific conductivity data collected over the past 30 years in Scott River Valley Groundwater Basin from wells with two or more monitoring events.

The maps and associated timeseries for benzene data in the Basin are shown below.

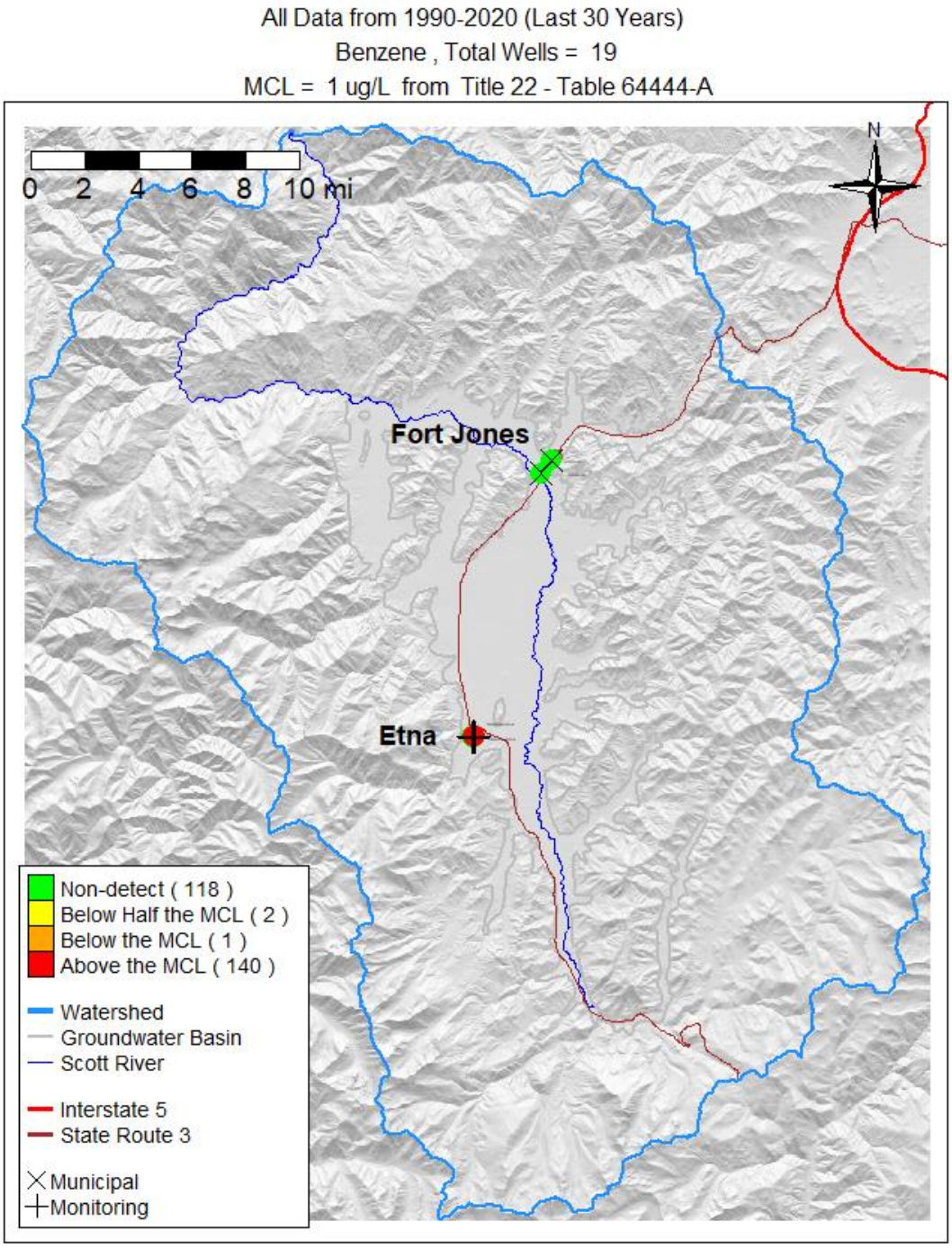

Figure 8: Well locations and detection magnitudes of benzene data collected over the past 30 years in the Scott River Valley Groundwater Basin.

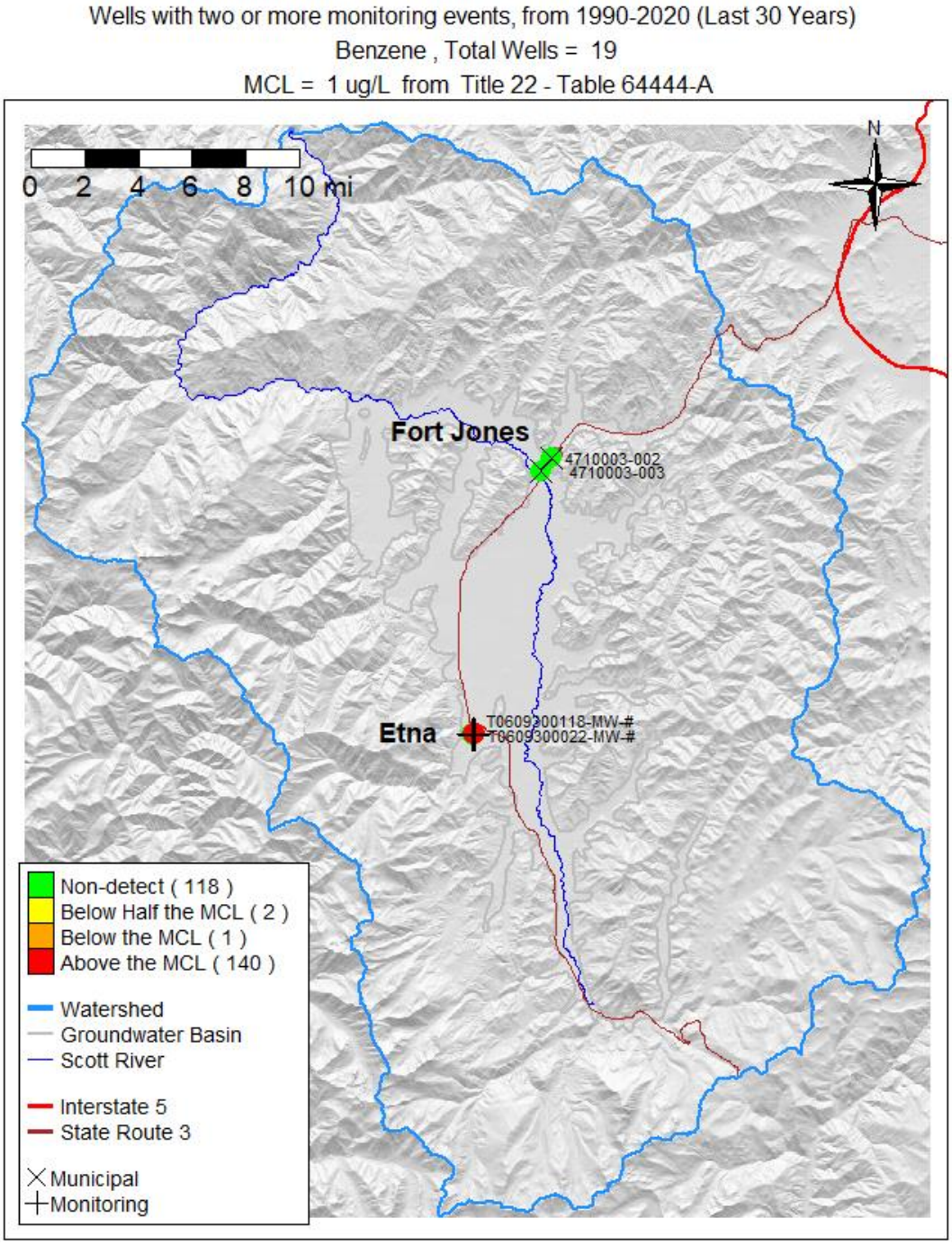

Figure 9: Well locations and detection magnitudes of benzene data collected over the past 30 years in the Scott River Valley Groundwater Basin for wells with two or more monitoring events.

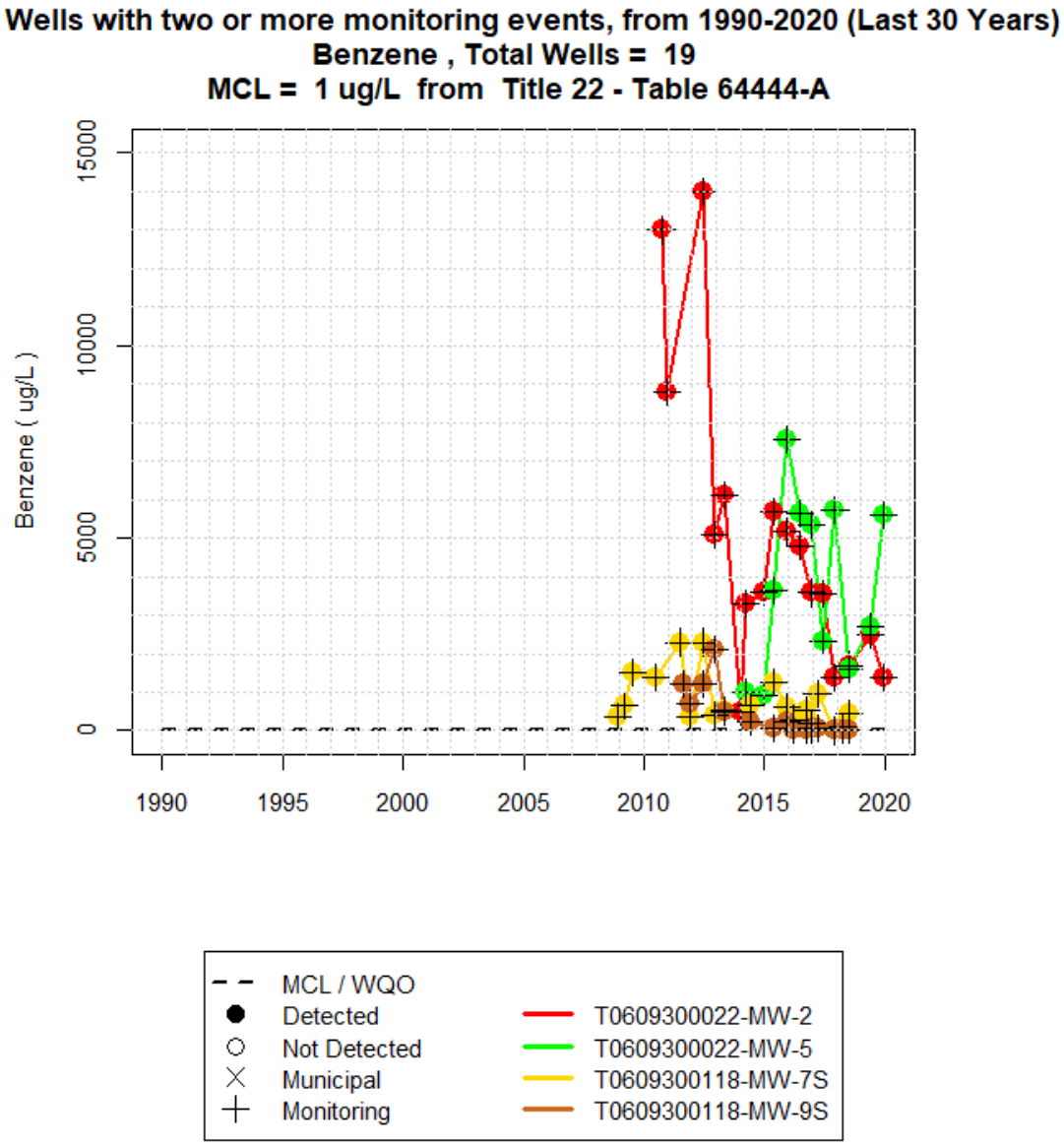

Figure 10: Timeseries plot of benzene data collected over the past 30 years in the Scott River Valley Groundwater Basin from wells with two or more monitoring events.

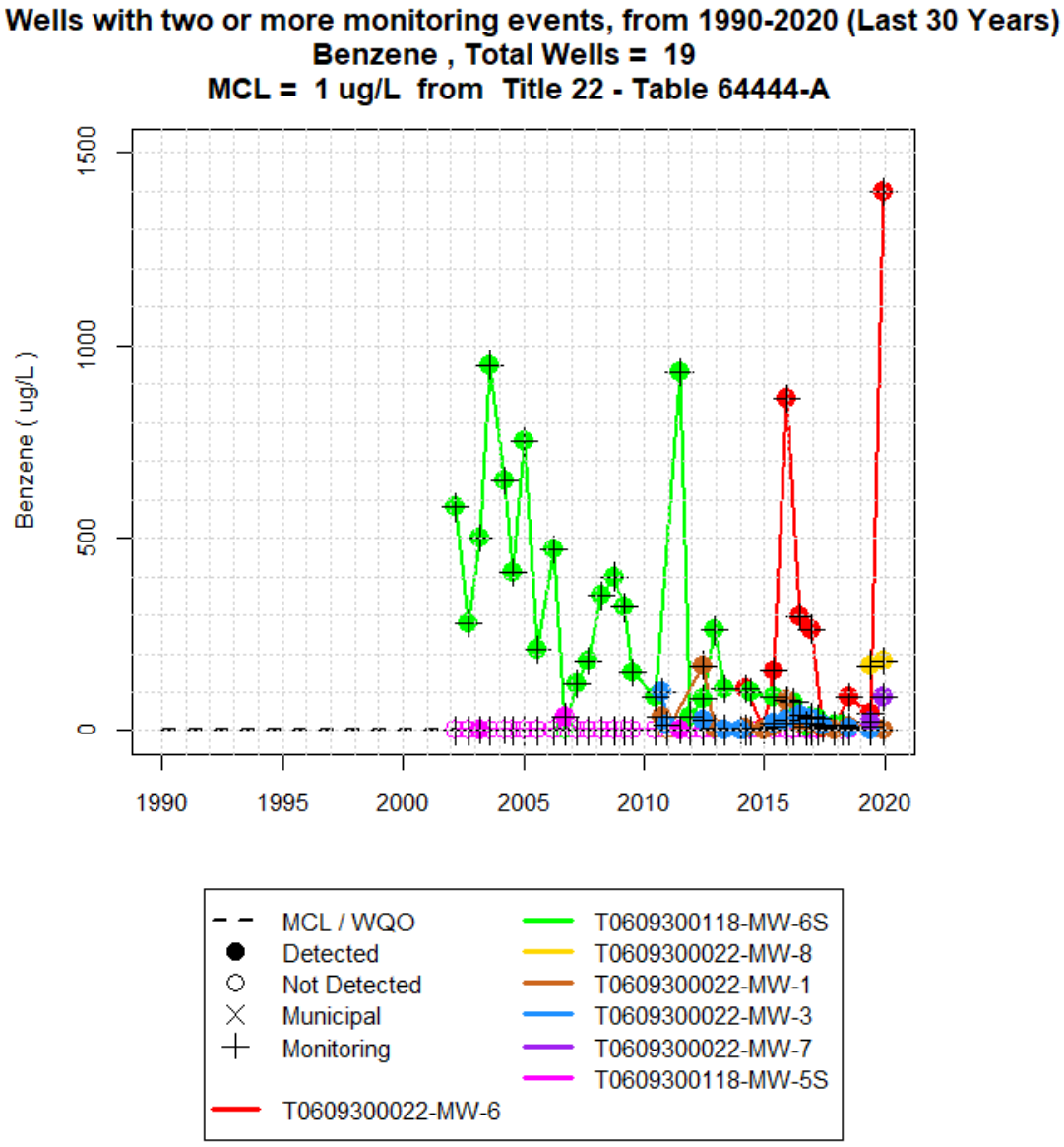

Figure 11: Timeseries plot of benzene data collected over the past 30 years in the Scott River Valley Groundwater Basin from wells with two or more monitoring events.

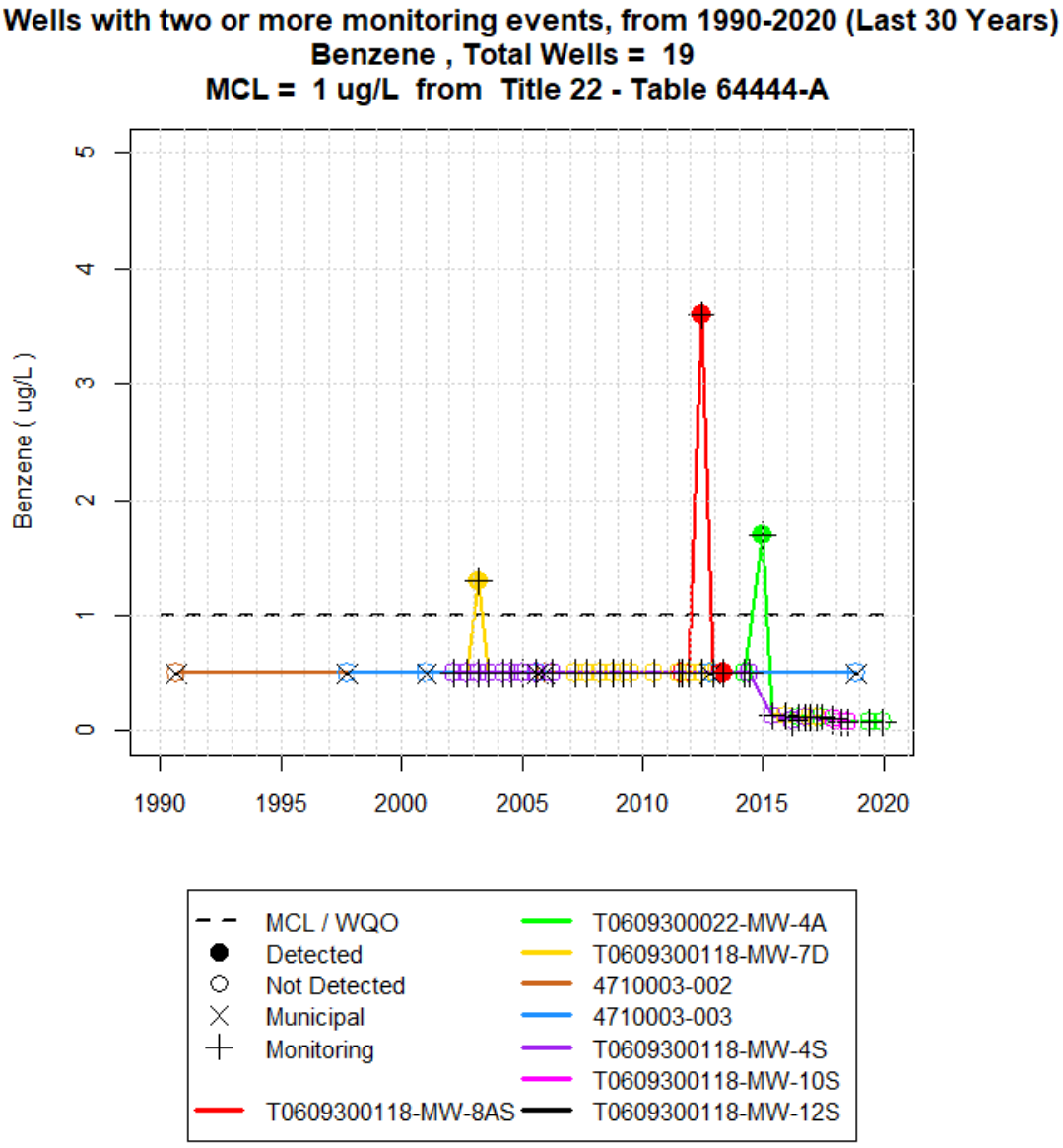

Figure 12: Timeseries plot of benzene data collected over the past 30 years in the Scott River Valley Groundwater Basin from wells with two or more monitoring events.

APPENDIX 2-E Scott Valley GSP Groundwater Model: Extension Documentation and Water Budget Tables

UC Davis Technical Team for The County of Siskiyou

9/10/2021

Contents

Introduction

This document is Appendix 2-D, supplemental to Chapter 2 of the Scott Valley Groundwater Sustainability Plan (GSP). The purpose of this appendix is to document the Scott Valley Integrated Hydrologic Model (SVIHM), which was used to estimate water budget components and predict potential future water use and hydrologic conditions, as required under the Sustainable Groundwater Management Act. Specifically, objectives of this appendix are to:

1. Summarize key numerical model specifications and direct readers to published studies in which the model structure is documented in more detail.
2. Document the time extension of the model inputs:
    - Original (documented) model period: Oct. 1, 1991 - Sept. 30, 2011 (Tolley, Foglia, and Harter 2019)
    - Updated model period for GSP: Oct. 1, 1991- Sept. 30, 2018
3. Document validation of model outputs for the extension period of water years 2012-2018.
4. Publish the full tables and figures of annual water budget values, a subset of which have been included in Chapter 2 of the GSP.

An earlier version of the SVIHM, which covers the model period of water years 1991-2011, is documented in the report by Foglia et al. (2013) and the study by Tolley, Foglia, and Harter (2019). Applications of the model are published in Foglia, McNally, and Harter (2013) and Foglia et al. (2018). It is currently available as a GitHub repository at the url `https://github.com/UCDavisHydro/SVIHM`. The extended version (covering 1991-2018) remains in development until official adoption of the GSP and will be publicly available after submittal of the GSP to DWR.

Model Structure and Validation

SVIHM Model Structure Summary

The integrated model consists of three cascading sub-models, utilizing 3 software platforms:

1. Streamflow regression model (a statistical model using the R programming language)
2. Soil water budget model, or SWBM (FORTRAN)
3. Groundwater-surface water flow model (MODFLOW)

The **streamflow regression model** is a statistical tool used to estimate surface flow into the SVIHM domain, and is described in futher detail in Section 5 in Foglia et al. (2013) and Section 3 of Tolley, Foglia, and Harter (2019). Surface water inflow (i.e., runoff from the upper watershed) is explicitly simulated at the SVIHM domain boundary on 12 major tributaries, and though some flow monitoring exists for these locations, the stream gauge records do not cover the entire model period and are largely incomplete. Statistical analysis showed that existing daily flow records for tributary streams are best estimated using linear regression of the normalized, log-transformed daily flow data at the tributary stream gauge against the normalized, log-transformed daily flow data at the USGS Gauge

11519500 (Fort Jones Gauge). The Fort Jones gauge represents stream outflow from the Scott Valley. Two separate linear regressions were performed - one for the period period prior to water year 1973, prior to the occurrence of frequent summer flows below 30 cfs, and one for records falling into the period October 1, 1973 to September 30, 2011. Normalization with respect to mean and standard deviation of log-transformed daily flow data was performed separately for the time series records at each gauging station. The streamflow regression model is used to estimate a continuous daily flow record for the model period at each of the 12 inflow points from the upper watershed (Foglia et al. 2013).

The **soil water budget model (SWBM)** is a FORTRAN-based calculator used to simulate water fluxes into and out of the soil zone, on a field-by-field basis, for 2,119 fields in the Scott Valley. It is described in more detail in Section 6 of Foglia et al. (2013) and Section 3 of Tolley, Foglia, and Harter (2019). In the SWBM, agricultural irrigation is calculated based on daily crop demand. Perfect farmer foresight of daily irrigation demand is assumed and the water volume is attributed to either diverted surface water (i.e., Surface Water Irrigation in Figure 4) or pumped groundwater (i.e., Groundwater Irrigation and Wells in Figure 4) depending on which source(s) is (are) available for each field. Irrigation technologies associated with each field (i.e., flood irrigation, wheel line or center pivot) are used to calculate irrigation efficiencies. Each field is treated as a “tipping bucket” object: at the end of each day, any water remaining in the soil zone beyond its field capacity is assumed to recharge to groundwater. A small number of fields in the so-called “discharge zone” between Greenview and Etna, east of Highway 3, are sub-irrigated; ET in these fields is assumed to come not only from soil water storage but also directly from shallow groundwater (rather than applied irrigation), where the latter is simulated by the groundwater model. Additionally, all precipitation falling on cultivated fields or native vegetation is assumed to infiltrate into the soil column (i.e., runoff is neglected).

The finite difference **groundwater-surface-water model** simulates spatial and temporal groundwater and surface water conditions in the valley within the alluvial basin (also referred to as the **MODFLOW model**). It is described in more detail in Section 3.4 of Tolley, Foglia, and Harter (2019).

Specifically, the MODFLOW model is built using MODFLOW-NWT (Niswonger, Panday, and Ibaraki 2005), a version of MODFLOW-2005 (Harbaugh 2005) that solves for unconfined flow using the Newton-Raphson solver. The packages used in the MODFLOW-NWT model include:

- SFR, streamflow routing package (Prudic, Konikow, and Banta 2004)
- WEL, well package (Harbaugh 2005)
- RCH, recharge package (Harbaugh et al. 2000; Harbaugh 2005)
- ETS, evapotranspiration segments package (Banta 2000)
- DRN, drain package (Harbaugh et al. 2000)

The integrated SVIHM is weakly coupled in that calculated fluxes are passed from the first two submodels to the MODFLOW model, but there are no direct feedbacks from the MODFLOW model to the streamflow regression model or the SWBM (Tolley, Foglia, and Harter 2019). The exception is direct uptake of evapotranspiration from groundwater in the “discharge zone”. An explicit iterative process between MODFLOW and SWBM ensures appropriate allocation of the ET demand to the unsaturated (soil) zone and to groundwater.

MODFLOW Numerical Model Construction Summary

A description of the structure of the MODFLOW groundwater-surface water model can be found in section 3.4 of Tolley, Foglia, and Harter (2019). Key model construction information is summarized below. The model domain (i.e. the extent of active cells) is outlined in Figure 1.

- 440 rows
- 210 columns
- 100-m (328 ft) gridcell lateral resolution
- cell depths of 0-61 m (0-200ft) thick
- 46,618 total acres within model domain (Figure 1)
  - 17,232 acres alfalfa
  - 16,362 acres pasture
  - 11,246 acres natural vegetation (ET, no irrigation)
  - 1,626 acres of pavement or cobbles (no ET, no irrigation)
  - 152 acres of water surface
- 164 irrigation wells and 55 monitoring wells
- Nine hydrogeologic zones and three surface water channel zones (see Figure 1 in Tolley, Foglia, and Harter (2019))

Summary of Model Calibration and Sensitivity Analysis

Explanation of terms

Model calibration is a process for estimating parameter values that are unavailable or difficult to measure, such as the hydraulic conductivity of a geologic formation. The goal of calibration is to select parameter values that minimize the error in the model output (e.g., minimizing the difference between simulated and observed values for surface flow rates and groundwater elevations). Typically, this involves building the model using initial “best-guess” values for the difficult-to-measure parameters, then running the model many times using different parameter values, and recording the output to evaluate which parameter set generates the minimum error. “Gradient-based” methods use the information from past runs to select the next set of parameters.

More generally, **sensitivity analysis** is used to calculate an overall index of how sensitive a desired model output (such as a flowrate in a single location, or the aggregate error in simulated groundwater elevation) is to a change in the value of a given parameter, such as the infiltration rate of a soil type. Sensitivity analyses can be “global” (covering the full range of possible values for all parameters) or “local” (starting with an initial parameter and deviating from it by set “perturbation” values).

In the calibration analysis, the end point of the analysis is typically determined by: 1) the convergence of the error function on an assumed irreducible value or 2) limitations imposed by computational resources. For a model like the SVIHM, which takes 4-5 hours to complete one simulation, global sensitivity analysis methods are commonly too expensive.

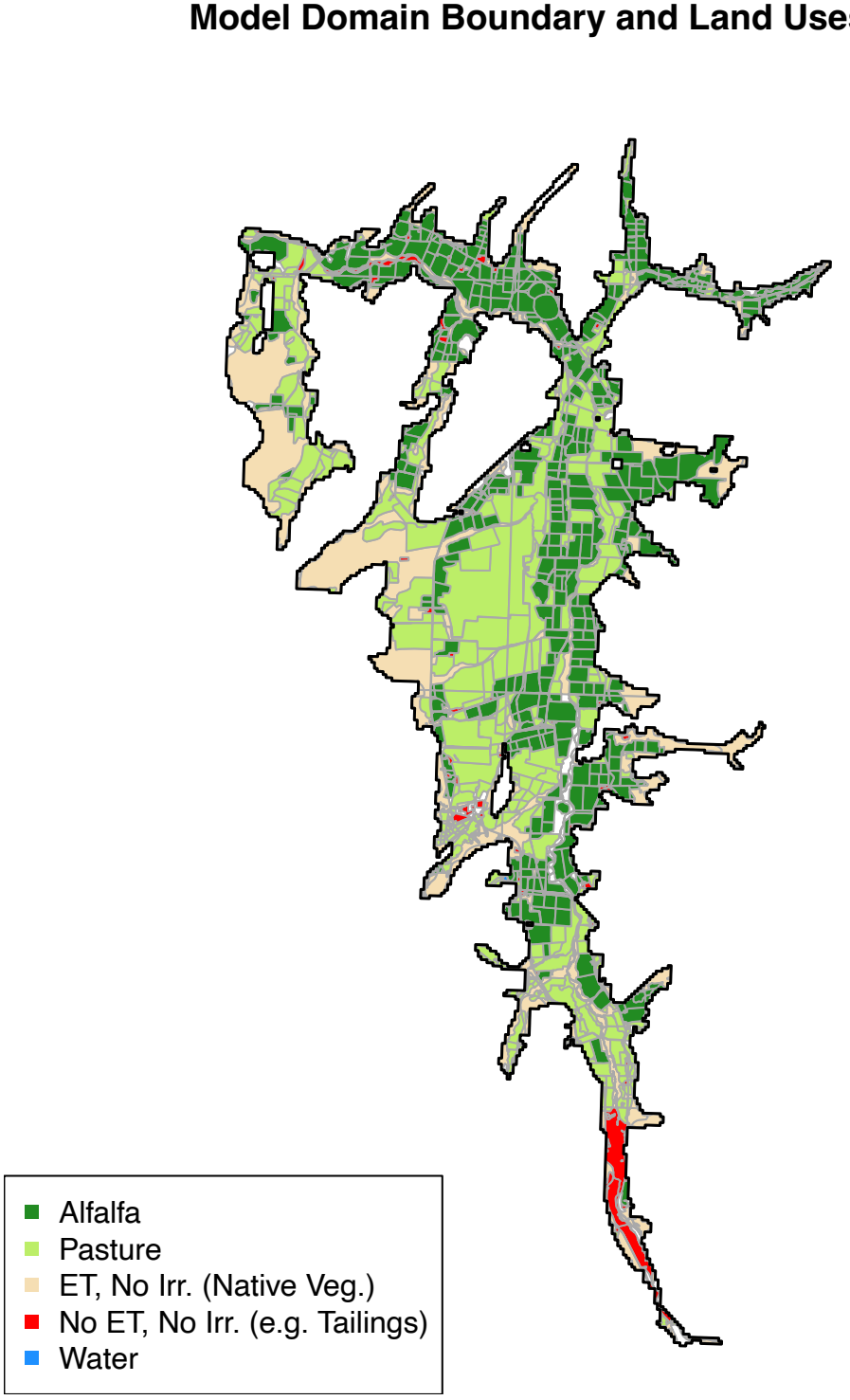

Figure 1: Land use categories used to represent irrigation behavior in the SVIHM.

SVIHM Calibration Results

Calibration and sensitivity analysis of the 1991-2011 version of SVIHM was performed using the inverse modeling software suite UCODE_2014 (Poeter and Hill 1998; Poeter et al. 2014) and is described in more detail Section 3.5 of Tolley, Foglia, and Harter (2019).

UCODE_2014 was used to automate the model calibration process, which included the following steps:

Sensitivity Analysis:

1. Select initial values for 61 parameters, including hydraulic properties of nine hydrogeologic zones, the amount of mountain front recharge, canal seepage, stream channel properties, and values in the SWBM related to deep soil moisture depletion, irrigation efficiency, and crop evapotranspiration.
2. Run the model forward to simulate groundwater heads and daily stream flowrates for the 1991-2011 model period.
3. Vary each of the 61 parameters by a small amount to determine sensitivity of simulated water levels and flow rates at monitored locations. Select the parameters for which model outcomes are significantly sensitive (14 parameters).

Calibration:

1. Run the model forward to simulate groundwater heads and daily stream flowrates for the 1991-2011 model period.
2. Compare the observed groundwater elevations and flowrates with corresponding simulated values. Record the difference; summarize the differences as the result of a weighted objective function. (Lower flow rates, for example, were weighted higher in the SVIHM calibration than higher flowrates to prioritize minimizing errors in low flows.)
3. Select a new set of 14 calibration parameters based on the results of past calibration runs and repeat steps 1-3 until parameters or the objective function no longer change significantly between calibration runs.

To account for the potential nonlinear effects of the initial parameter values, calibration of SVIHM was performed five times, using five sets of initial values for each of the 14 calibration variables (Table 2 in Tolley, Foglia, and Harter (2019)).

Sections 4 and 5 of Tolley, Foglia, and Harter (2019) describe the SVIHM calibration results in detail; key summary quotations are included below for convenience.

> The largest variations were observed in Kx1, Kx3, and Sy1, which ranged over an order of magnitude for hydraulic conductivity and varied up to 50% for specific yield. Parameters contained within SWBM showed similar variations across runs but with much less variability due to tighter imposed constraints. None of the parameters were calibrated to unreasonable values, with only a few limited by upper or lower calibration bounds.
>
> Values of DFBETAS and Cook's D (Figure 9) show that timing of the most influential observations occurs during or immediately following the lowest period of streamflow during the year.

The most sensitive parameters in SVIHM are crop coefficients for alfalfa and pasture, which control water demand (ET), and the SMDF for alfalfa/grain fields, which affects how much irrigation water is applied and therefore recharge rates for that land use type.

Model Extension and Validation

SVIHM development began nearly a decade ago in 2011, and the initial data summary and model input production was documented in Foglia et al. (2013). As a consequence, the version of SVIHM calibrated and documented in Tolley, Foglia, and Harter (2019) (or, the 2019 version) simulated conditions in the 21-year period between Oct. 1990 and Sept. 2011.

SGMA requires water budgets to include the 20 years prior to 2015, so an extension of SVIHM was necessary in order to use it for the Scott GSP. Work on this model extension began in 2019, so the extension period was 7 years, ending in Sept. 2018.

Model results for this extension period are an opportunity for a natural validation experiment, which analyzes how closely the parameter values, calibrated on observations in water years 1991-2011, can replicate observations from Oct. 2011 - Sept. 2018.

Methods for Extending Precipitation, Tributary Inflow, and ET

Extending the model period consists of extending key climate records that drive model behavior: valley floor precipitation, tributary inflow, and ET.

Precipitation

The precipitation record consists of a daily depth value, and is calculated as the average of the rainfall values for the Callahan and Fort Jones weather stations. On days with missing values in these two rain records, the value is calculated based on data at other stations. More details are included in Section 4 of Foglia et al. (2013) and below.

Though evidence exists of higher rainfall on the western side of the valley, the location of existing gauges did not allow estimation of a rainfall gradient at the time, so a single daily value was used. In a future version of the model, it may be possible to develop a spatially-explicit rainfall record that reflects this rainfall gradient, using the data from several new private rain gauges installed during monitoring efforts for the GSP in 2019-2021.

Based on methodology described in Foglia et al. (2013), the original rainfall record was generated in Excel. To extend the model, a researcher implemented the same methodology in R (R Core Team 2020), the statistical programming language. The steps in the method are:

1. Align all available precipitation data by date in one table. For this extension, the records used were from the following weather stations (with their NOAA identification code):
    - Callahan (USC00041316)
    - Fort Jones (USC00043182)
    - Etna (USC00042899)
    - Greenview (USC00043614)

- Yreka (USC00049866), long-term record
- Yreka (US1CASK0005), more recent record

The original precipitation record relied only on the first four stations in this list, but for this extension, it was necessary to add the two Yreka stations (which, notably, are outside the Scott River watershed) to fill in gaps with no records at the other stations in the 2012-2018 period.

2. Make a table of relevant values (slope and R^2) for the set of 0-intercept linear regressions in which the Callahan and Fort Jones stations' precipitation record is predicted using each other station's record, segregated by month. The total set of linear models calculated is [2 predicted values] * [6 predictors] * [12 months] - [24 combinations where x = y] = 120 total linear regressions.

3. For each missing value in the daily Callahan and Fort Jones records, estimate the precipitation on that day using the linear regression model for the relevant month with the highest R^2 value.

4. Once all gaps have been filled in this manner, average the values for each day for Callahan and Fort Jones.

Due possibly to corrections in the online databases from which records were obtained, this method was unable to exactly reproduce the original 1991-2011 precipitation record in the 2019 version of SVIHM. Therefore, the daily rainfall values produced using the R software were used only for water years 2012-2018 (and for five leap days, which were not included in the 2019 version).

Evapotranspiration

The evapotranspiration data that drives irrigation demand in SVIHM is denoted as ET_{ref}, or the ET measured over a reference short grass crop. Crop coefficients are used to convert this daily value into irrigation demand for different crops. The ET_{ref} model input for the 2019 version of SVIHM was calculated using the NWSETO program (Snyder, Orang, and Matyac 2002). Additional details are in Section 6 of Foglia et al. (2013). For this extension, two data sources were used. CIMIS Station 225 was installed in northeastern Scott Valley in 2015, and this ET_{ref} record is used for the days in which it is available (DWR 2021). The second source, used to bridge the gap between the end of the 2019 ET_{ref} record in Sept. 2011 and the start of the CIMIS Station 225 record in 2015, was interpolated Spatial CIMIS data products (DWR 2007). The location used to generate the Spatial CIMIS output was the location of the current CIMIS Station 225.

Tributary Inflow

The daily flow records for tributary inflow to the model domain were extended using the Fort Jones record, Oct. 2011 - Sept. 2018, and the existing Streamflow Regression Model script in R. Although at least one tributary flow gauge has recorded additional observations since 2011, the tributary flow records used to build regression models with the Fort Jones record were kept consistent between the 2019 SVIHM version and the extended version. In future work, expanding the tributary datasets may improve the Fort Jones Gauge-tributary flow predictions.

Flow Matching

Methods of validating the quality of flow-matching include:

- Visual comparison on time series plots (Figure 2, Panel A)
- Exceedance plots to compare overall abundance of high and low values (Figure2, Panel B)
- Calculations of flow-matching indices, such as the Nash-Sutcliffe Efficiency (NSE) (Nash and Sutcliffe 1970) and, to account for high variability in flow, a modified NSE (Tolley, Foglia, and Harter 2019) (Table 1)

These results indicate that SVIHM flow-matching performance in the 2012-2018 period is about the same, or slightly better, than in the 1991-2011 period (Table 1). This might simply be a consequence of the fact that SVIHM generally performs better at low flows, and that the 2012-2018 period (18.4 average annual inches of rainfall) was drier than 1991-2011 (21.8 inches).

A known limitation of the model is that it does not capture large storm flow peaks, because these happen in a matter of days, while the stress periods in SVIHM are monthly (Figure 2, Panel A). This is reflected in the seasonal difference in NSE values: SVIHM matches dry season flows better than wet season flows. The season in which flow-matching performance is highest is during the spring recession and early growing season. This probably reflects the fact that longer-term processes control streamflow during this time, such as snowmelt or the draining of the subsurface, rather than short-term storm events.

Due to the aforementioned limitation, SVIHM tends to underpredict flows >1,000 cfs (Figure 2, Panel B). Conversely, it tends to overpredict flows <10 cfs. This overprediction may be due to the high sensitivity of the low-flow hydrologic system to small deviations from simulated conditions or behaviors (e.g., irrigation behavior not captured by the logical statements in the SWBM). However, overpredictions during low-flow conditions tend to be small, on the order of 1-5 cfs. The middle area of discrepancy in the exceedance plots ranges from 10-70 cfs; SVIHM simulates fewer of these daily flowrates than are observed. This may reflect a lag in the fall, i.e., the model is slower to respond to fall rain events than the physical watershed (Figure 2).

Table 1: Nash-Sutcliffe Efficiencies (NSE) and modified NSE values for various time periods.

Time Period	NSE	MNSE
Water years 1991-2011	0.472	0.929
water years 2012-2018	0.529	0.935
All water years 1991-2018	0.485	0.931
Wet Season (Dec-Mar)	0.334	0.790
Spring Recession (Apr-Jul)	0.641	0.912
Dry Season (Aug-Nov)	0.449	0.840

Groundwater Head Matching

The model performance regarding groundwater head (elevation) matching can be evaluated using several methods or indices:

- Visual inspection of scatter plots

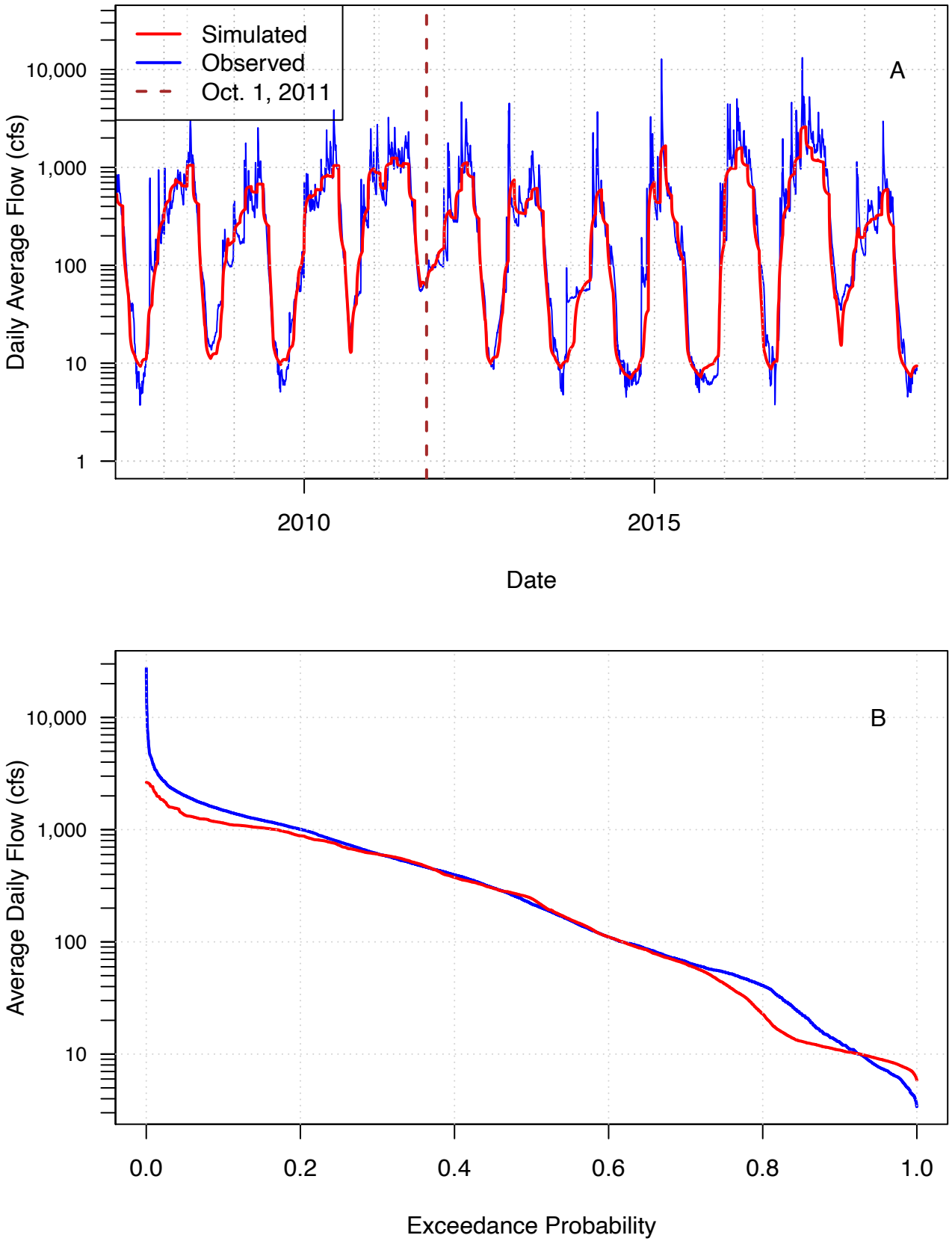

Figure 2: Daily flow at the Fort Jones Gauge, simulated vs. observed. Furthest extent of 2019 model version is indicated as a brown dashed line.

- The R^2 of the correlation between simulated and observed values
- The root mean squared error (RMSE) of simulated and observed values
- The percentage of groundwater elevation residuals less than a given number of feet or meters

Based on these results, the extended version of SVIHM performs about the same, and slightly worse, than the original 1991-2011 version at matching groundwater heads.

Observed and simulated groundwater head values show a strong correlation (Figure 3, Panel A; R^2 value of 0.98). The RMSE for the 1991-2018 period is 9.31 feet, compared with 7.48-9.12 feet in the 1991-2011 version (Tolley, Foglia, and Harter 2019).

Residuals range from -38 to 72 feet (Figure 3, Panel B). The proportion of residuals less than 3.3, 6.7, or 10 ft (1, 2, or 3 m) is 48%, 67%, and 78%, respectively, compared with 50%, 70%, and 80% in the 1991-2011 version.

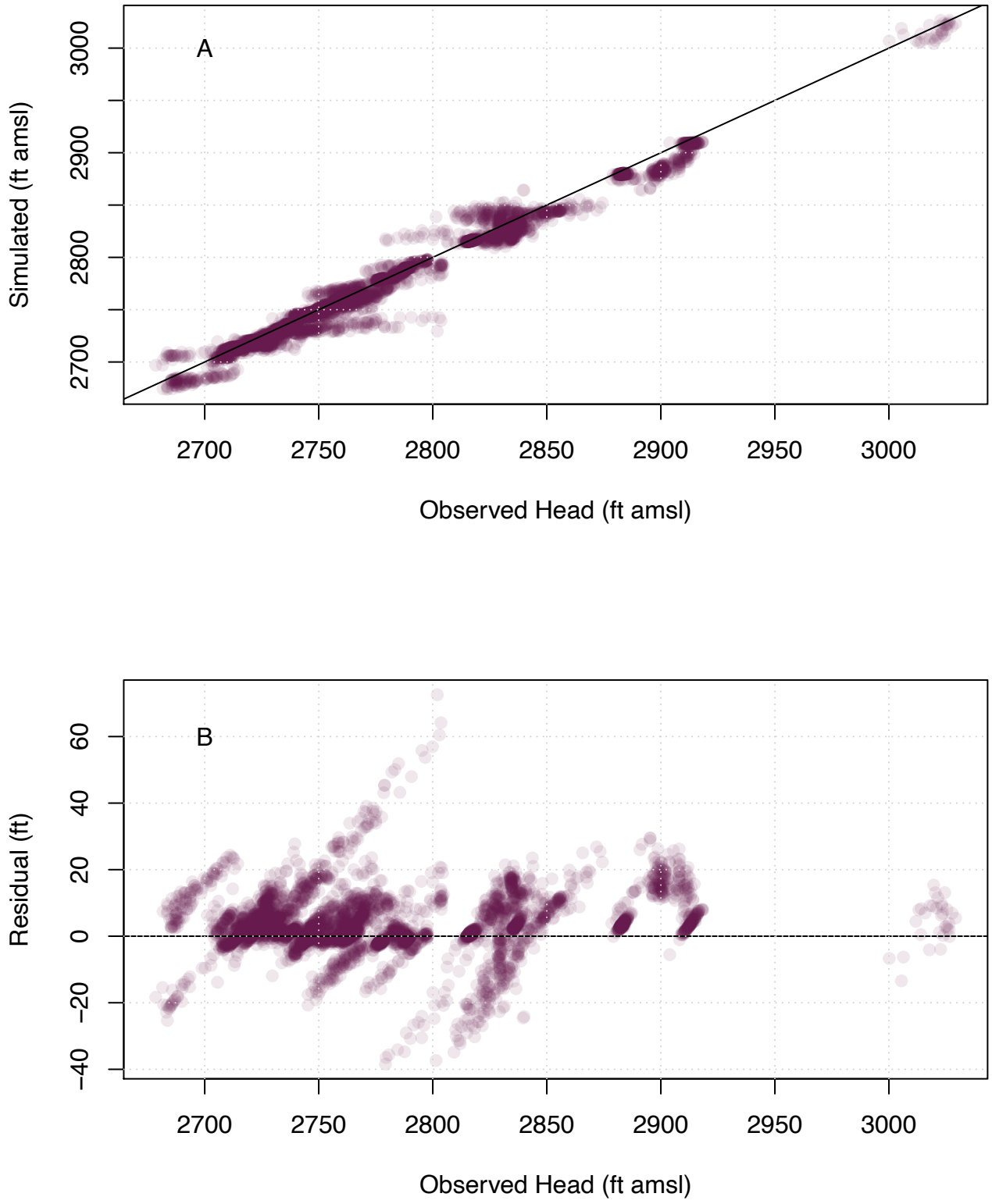

Figure 3: Groundwater elevations or heads, observed vs. simulated and observed vs. residuals (calculated as [simulated] - [observed]).

Water Budget

Water budget components are described in Chapter 2, Section 2.2.3, and in the reports referenced therein. For convenience they are listed below. Land cover used to calculate water useage in the SWBM is shown in Figure 1.

The water budget is visualized and tabulated for each of three subsystems: the Surface Water, the (Land/)Soil Zone, and the Aquifer subsystem. Thus, water budget components that flow from one subsystem to another appear in two tables or graph panels (i.e., Stream Leakage to groundwater is represented as negative in the Surface water and positive in the Aquifer subsystem). Tables shown here represent annual fluxes for each water year in the simulation period. Tables with monthly fluxes for each water budget component in each subsystem, for historic and future simulations, are available upon request.

1. Inflows
    - Precipitation
    - Surface inflow (tributaries)
    - Subsurface inflow (mountain front recharge or MFR)
2. Outflows
    - Surface water outflow
    - Subsurface water outflow (negligible)
    - Evapotranspiration
3. Flow between surface water and soil zone
    - Surface water irrigation
4. Flow between surface water and groundwater
    - Stream leakage
    - Drains/overland flow
    - Canal seepage from Farmes Ditch and SVID Ditch
5. Flow between soil zone and groundwater
    - Recharge to aquifer
    - Groundwater irrigation
6. Change in storage
    - Surface water storage
    - Soil zone storage
    - Aquifer storage

Historical Water Budget Figures and Tables

Historical Water Budget Barcharts

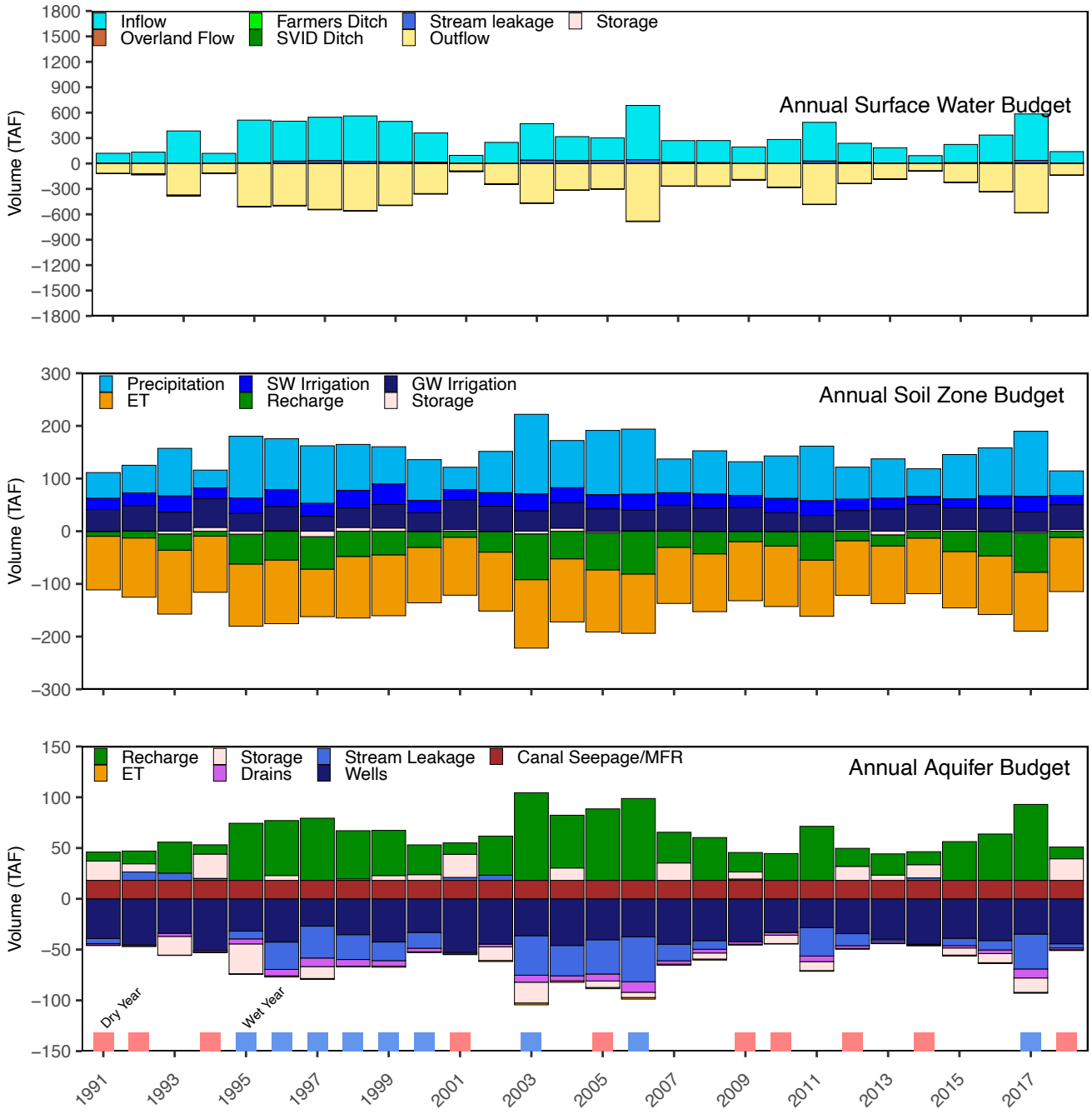

Figure 4: Annual water budgets for the three conceptual subsystems used to represent the hydrology of the Basin: the surface water system, the soil zone, and the aquifer.

Historical Water Budget - Annual and Summary Tables

Historical Water Budget - Streams Subsystem

Table 2: Annual and summarized annual values (TAF) for water budget components simulated in the Surface Water (SW) subsystem of the SVIHM. Positive values are water entering the stream network as inflows from tributary streams and overland flow entering streams; negative values are water leaving the stream network as diversions to the Farmers and SVID ditches and outflow from the valley through the Scott River. The net direction of stream leakage and the overall change in water stored in the stream system can be both negative and positive in different water years.

Water Year	Inflow	Overland	Farmers Div.	SVID Div.	Stream Leakage	Outflow	Storage
1991	115	0	-2	-4	5	-115	0
1992	133	0	-2	-4	-8	-120	1
1993	384	0	-2	-4	-7	-371	0
1994	118	0	-2	-4	-2	-111	1
1995	504	0	-2	-4	8	-506	0
1996	472	0	-2	-4	27	-494	0
1997	515	0	-2	-4	31	-541	0
1998	537	0	-2	-4	24	-555	0
1999	478	0	-2	-4	18	-491	0
2000	345	0	-2	-4	16	-355	0
2001	94	0	-2	-4	-3	-87	1
2002	249	0	-2	-4	-5	-238	0
2003	431	0	-2	-4	39	-464	0
2004	287	0	-2	-4	30	-311	0
2005	269	0	-2	-4	34	-297	0
2006	640	0	-2	-4	44	-679	0
2007	253	0	-2	-4	16	-264	1
2008	262	0	-2	-4	8	-265	0
2009	195	0	-2	-4	-1	-188	0
2010	283	0	-2	-4	0	-277	-0
2011	458	0	-2	-4	28	-480	-0
2012	227	0	-2	-4	12	-233	0
2013	183	0	-2	-4	2	-180	1
2014	91	0	-2	-4	-2	-84	2
2015	216	0	-2	-4	7	-219	1
2016	326	0	-2	-4	9	-330	0
2017	550	0	-2	-4	34	-579	0
2018	135	0	-2	-4	4	-134	1
Minimum	91	0	-2	-4	-8	-679	-0
25th %ile	192	0	-2	-4	-0	-483	0
Median	276	0	-2	-4	9	-287	0
Mean	312	0	-2	-4	13	-320	0
75th %ile	461	0	-2	-4	27	-186	1
Maximum	640	0	-2	-4	44	-84	2

Historical Water Budget - Soil Zone Subsystem

Table 3: Annual and summarized annual values (TAF) for water budget components simulated in the Surface Water (SW) subsystem of the SVIHM. Positive values are water entering the stream network as inflows from tributary streams and overland flow entering streams; negative values are water leaving the stream network as diversions to the Farmers and SVID ditches and outflow from the valley through the Scott River. The net direction of stream leakage and the overall change in water stored in the stream system can be both negative and positive in different water years.

Water Year	Precip	SW Irrig.	GW Irrig.	ET	Recharge	Storage
1991	49	21	41	-102	-9	-1
1992	53	24	48	-112	-13	0
1993	90	31	36	-121	-31	-5
1994	34	21	54	-107	-9	7
1995	117	29	34	-118	-57	-6
1996	97	32	45	-121	-55	1
1997	109	25	28	-90	-62	-10
1998	87	33	37	-117	-48	7
1999	71	39	45	-116	-45	6
2000	78	23	35	-105	-30	-1
2001	42	19	56	-110	-11	3
2002	78	26	47	-112	-39	-1
2003	151	32	38	-130	-87	-5
2004	90	28	49	-120	-52	5
2005	122	27	42	-118	-71	-2
2006	124	30	39	-113	-81	1
2007	64	24	47	-107	-31	2
2008	82	27	43	-110	-42	-0
2009	64	23	45	-112	-19	-0
2010	81	27	35	-115	-27	-1
2011	104	28	30	-107	-54	-1
2012	61	22	36	-104	-18	3
2013	74	21	42	-109	-21	-7
2014	53	15	48	-106	-13	3
2015	84	17	41	-107	-39	3
2016	91	24	43	-111	-46	-1
2017	124	30	36	-112	-75	-2
2018	47	18	47	-103	-12	3
Minimum	34	15	28	-130	-87	-10
25th %ile	63	21	36	-116	-54	-2
Median	81	25	42	-112	-39	-0
Mean	83	26	42	-111	-39	0
75th %ile	99	29	47	-107	-19	3
Maximum	151	39	56	-90	-9	7

Historical Water Budget - Aquifer Subsystem

Table 4: Annual and summarized annual values (TAF) for water budget components simulated in the Surface Water (SW) subsystem of the SVIHM. Positive values are water entering the stream network as inflows from tributary streams and overland flow entering streams; negative values are water leaving the stream network as diversions to the Farmers and SVID ditches and outflow from the valley through the Scott River. The net direction of stream leakage and the overall change in water stored in the stream system can be both negative and positive in different water years.

Water Year	Recharge	ET	STorage	Drains	Stream Leakge	Wells	Canals, MFR
1991	9	-1	19	-1	-5	-39	18
1992	13	-1	8	-1	8	-45	18
1993	31	-0	-18	-3	7	-34	18
1994	9	-1	24	-1	2	-51	18
1995	56	-1	-29	-5	-8	-32	18
1996	54	-1	5	-6	-27	-43	18
1997	61	-1	-12	-8	-31	-27	18
1998	48	-1	1	-7	-24	-35	18
1999	45	-1	5	-5	-18	-43	18
2000	29	-1	6	-4	-16	-33	18
2001	11	-1	23	-1	3	-53	18
2002	39	-1	-13	-3	5	-45	18
2003	86	-2	-20	-7	-39	-36	18
2004	52	-2	12	-5	-30	-46	18
2005	70	-1	-6	-7	-34	-40	18
2006	81	-2	-5	-10	-44	-37	18
2007	30	-1	17	-3	-16	-45	18
2008	42	-1	-6	-4	-8	-41	18
2009	19	-1	7	-2	1	-42	18
2010	27	-1	-8	-3	-0	-33	18
2011	53	-1	-9	-6	-28	-28	18
2012	18	-1	14	-3	-12	-34	18
2013	21	-1	5	-2	-2	-40	18
2014	13	-1	13	-1	2	-45	18
2015	38	-1	-7	-2	-7	-39	18
2016	46	-1	-9	-4	-9	-41	18
2017	75	-1	-14	-9	-34	-35	18
2018	12	-1	21	-2	-4	-44	18
Minimum	9	-2	-29	-10	-44	-53	18
25th %ile	19	-1	-9	-6	-27	-44	18
Median	38	-1	3	-3	-9	-40	18
Mean	39	-1	1	-4	-13	-40	18
75th %ile	54	-1	12	-2	0	-35	18
Maximum	86	-0	24	-1	8	-27	18

Future Water Budget Figures and Tables (Basecase and 4 Climate Change Scenarios)

To inform long-term hydrologic planning, the Future Projected Water Budget was developed using the following method:

1. Observed weather and streamflow parameters from water years 1991-2011 were used multiple times to make a 50-year "Basecase" climate record (see Table 5 for details). The Basecase projection represents a hypothetical future period in which climate conditions are the same as conditions from 1991-2011.
2. The climate-influenced variables Precipitation (as rain), Reference Evapotranspiration (ET_{ref}), and tributary stream inflow were altered to represent four climate change scenarios:
    - Near-future climate, representing conditions in the year 2030
    - Far-future climate, Central Tendency, representing the central tendency of projected conditions in the year 2070
    - Far-future climate, Wet with Moderate Warming (WMW), representing the wetter extreme of projected conditions in the year 2070
    - Far-future climate, Dry with Extreme Warming (DEW), representing the drier extreme of projected conditions in the year 2070

For convenience, these scenarios will be referred to as Near, Far, Wet, and Dry, respectively.

Future Water Budget Barcharts

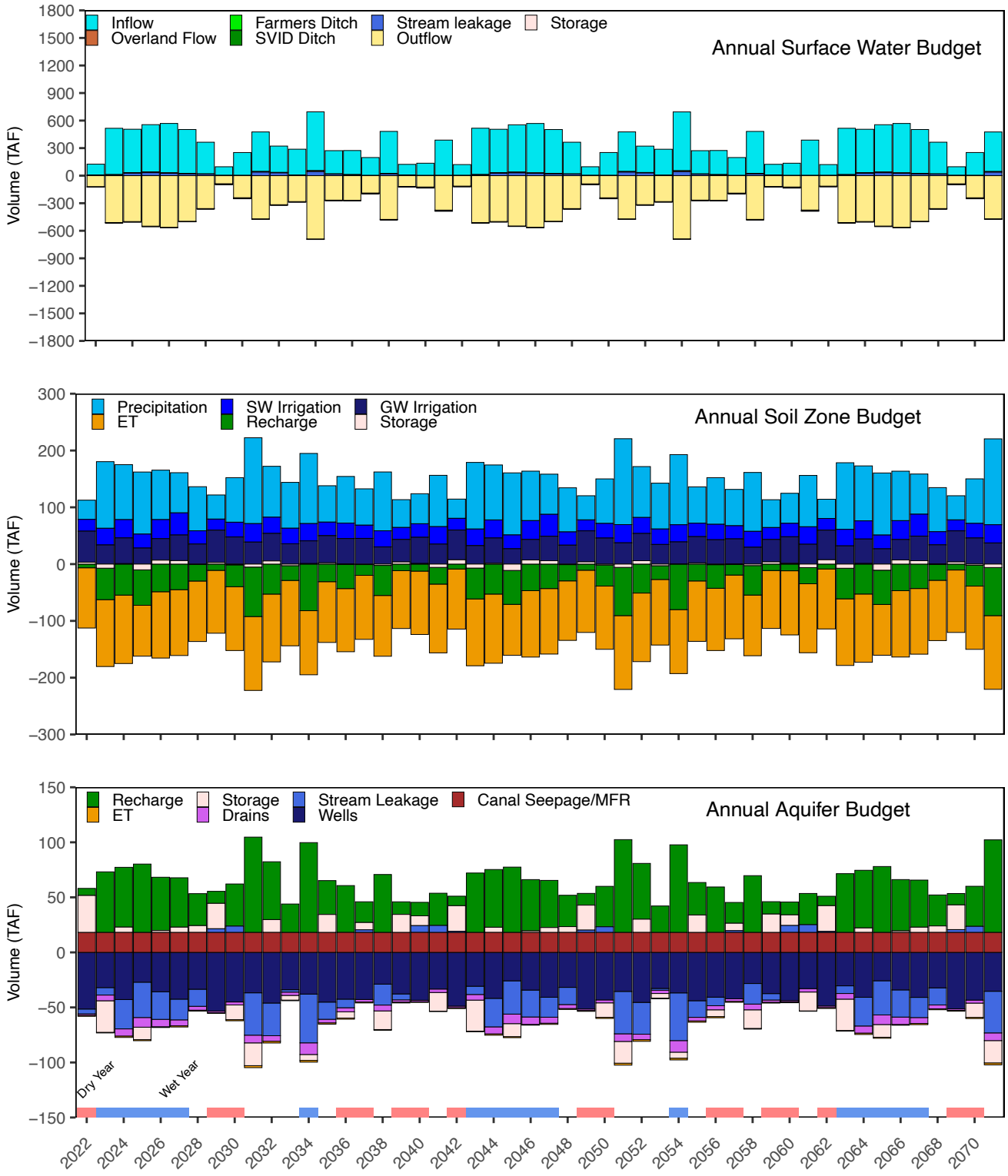

Figure 5: Scenario: Future Basecase. Annual water budgets for the three conceptual subsystems used to represent the hydrology of the Basin (the surface water system, the soil zone, and the aquifer) for 50 potential future years, with future climate data constructed from the past climate data of water years 1991-2011.

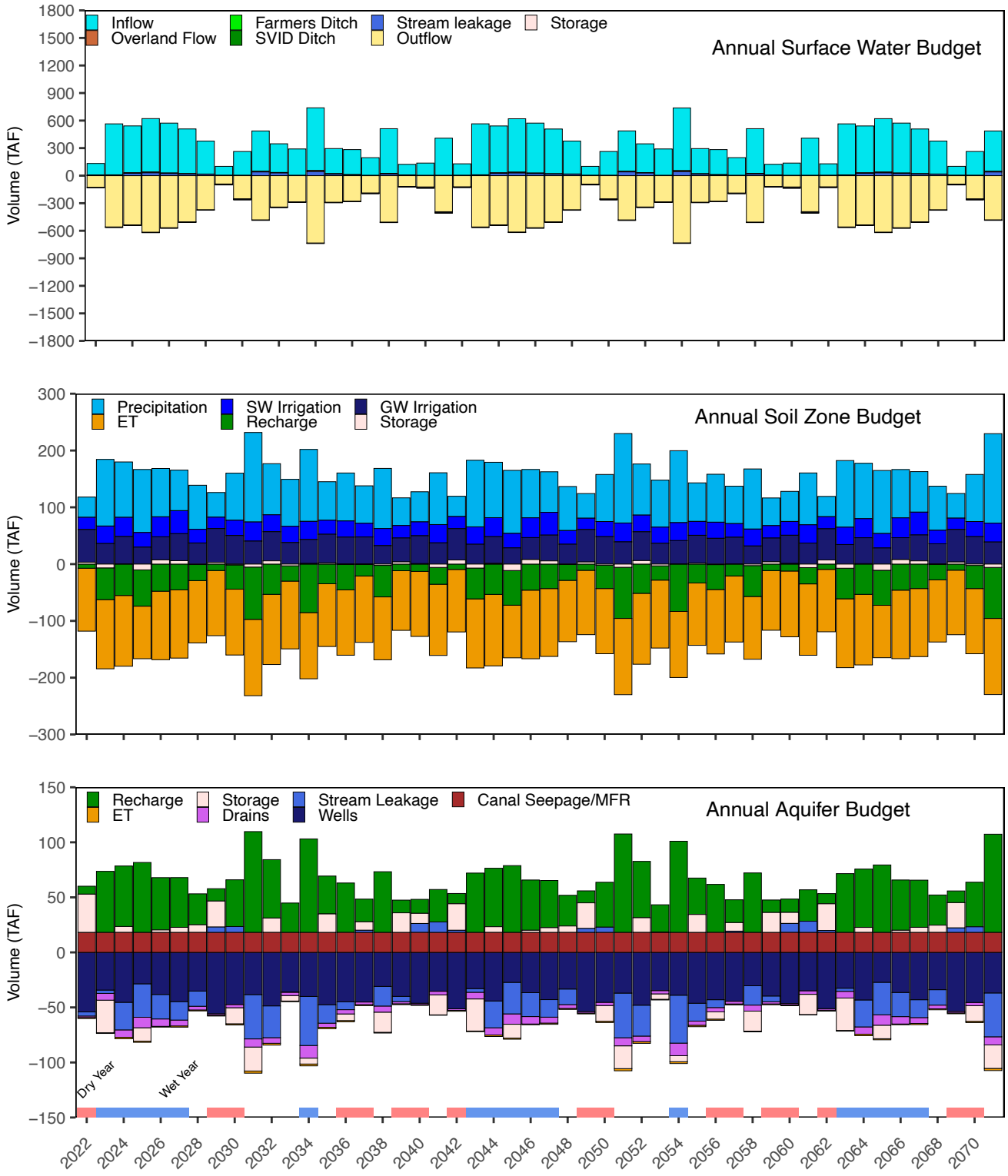

Figure 6: Scenario: Near Future (2030). Annual water budgets for the three conceptual subsystems used to represent the hydrology of the Basin (the surface water system, the soil zone, and the aquifer) for 50 potential future years, with basecsae future input data multiplied by change factors for the 2030 (Near) future climate scenario.

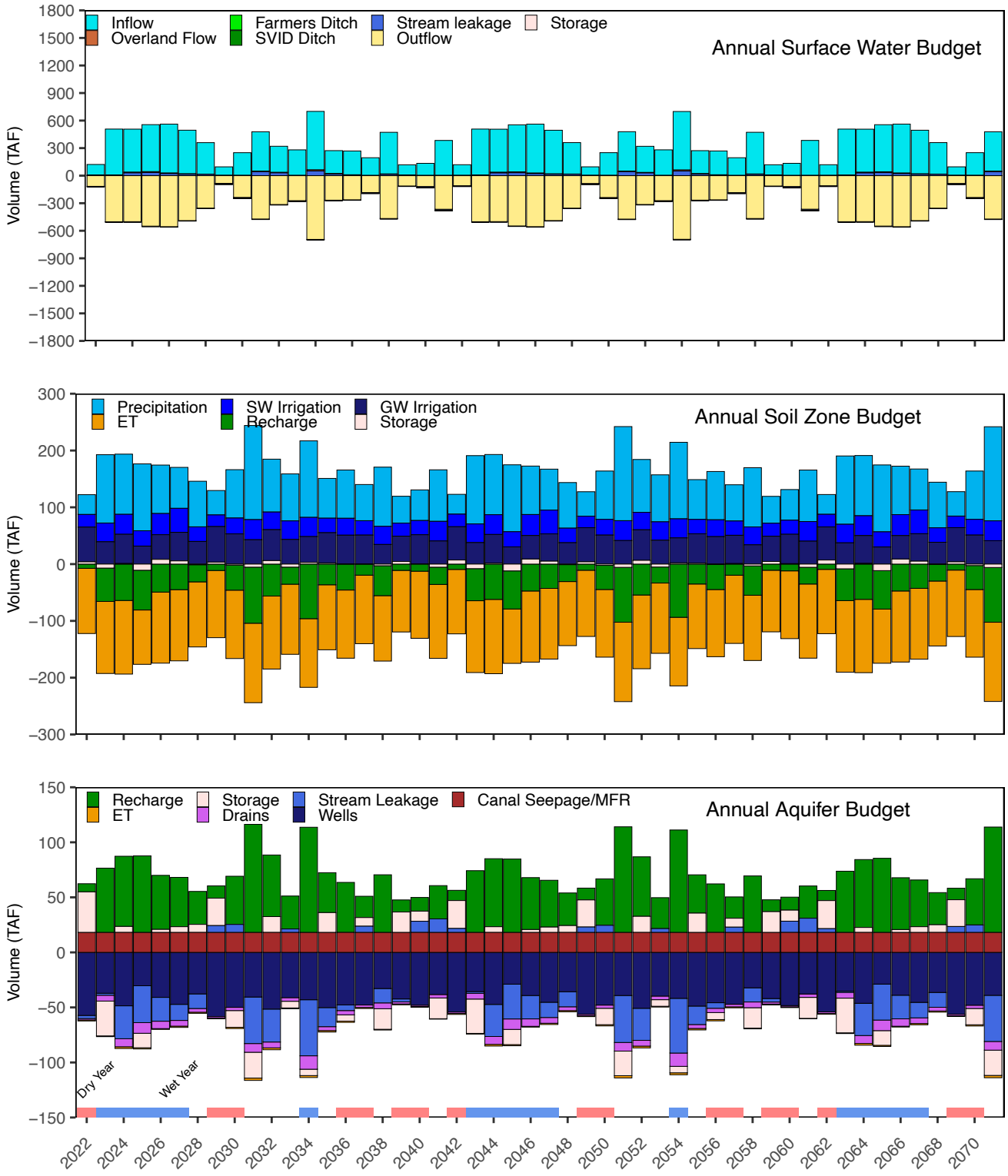

Figure 7: Scenario: Far Future (2070), Central Tendency.Annual water budgets for the three conceptual subsystems used to represent the hydrology of the Basin (the surface water system, the soil zone, and the aquifer) for 50 potential future years, with basecsae future input data multiplied by change factors for the 2070 Central Tendency (Far) future climate scenario.

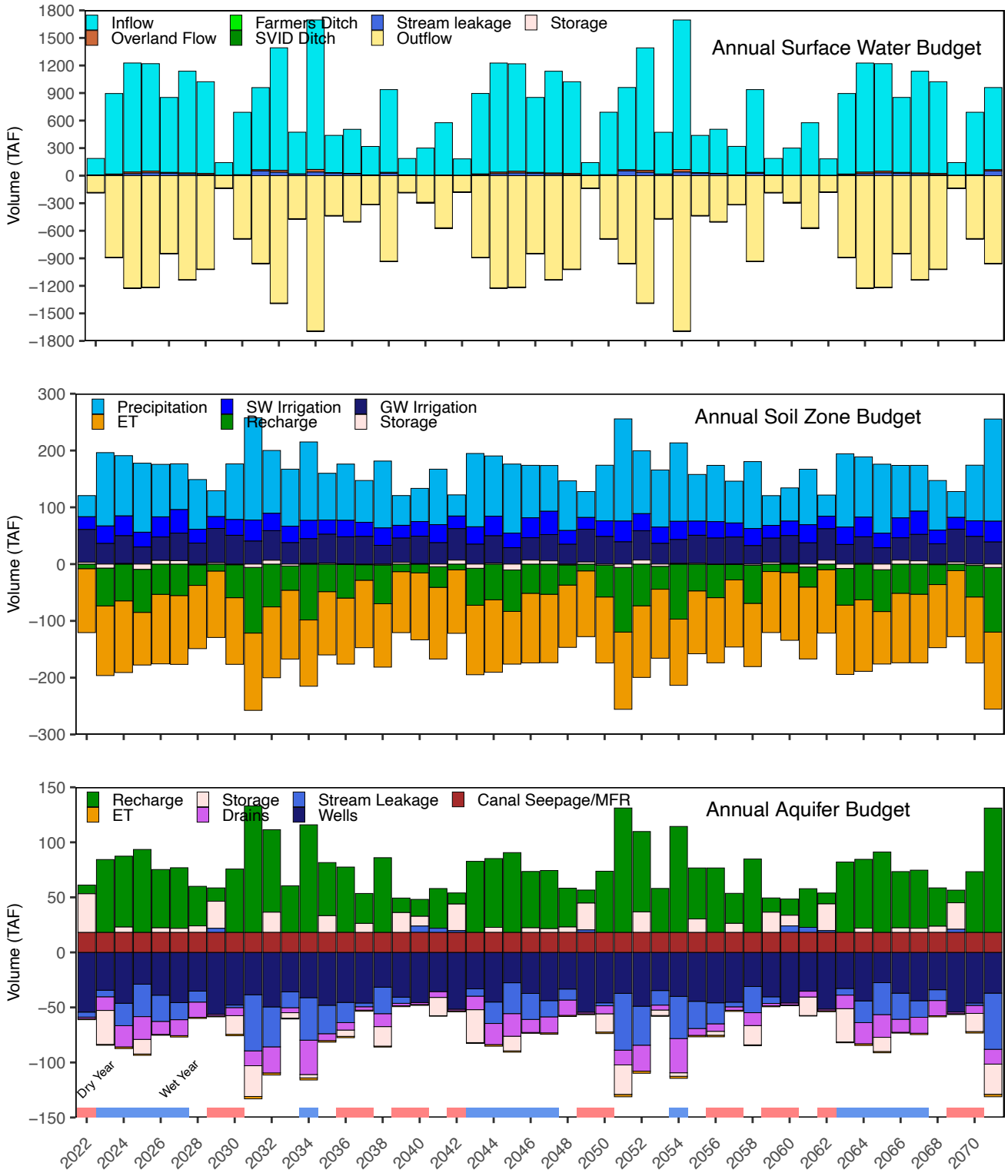

Figure 8: Scenario: Far Future (2070), Wet. Annual water budgets for the three conceptual subsystems used to represent the hydrology of the Basin (the surface water system, the soil zone, and the aquifer) for 50 potential future years, with basecsae future input data multiplied by change factors for the 2070 Wet with Moderate Warming (Wet) future climate scenario.

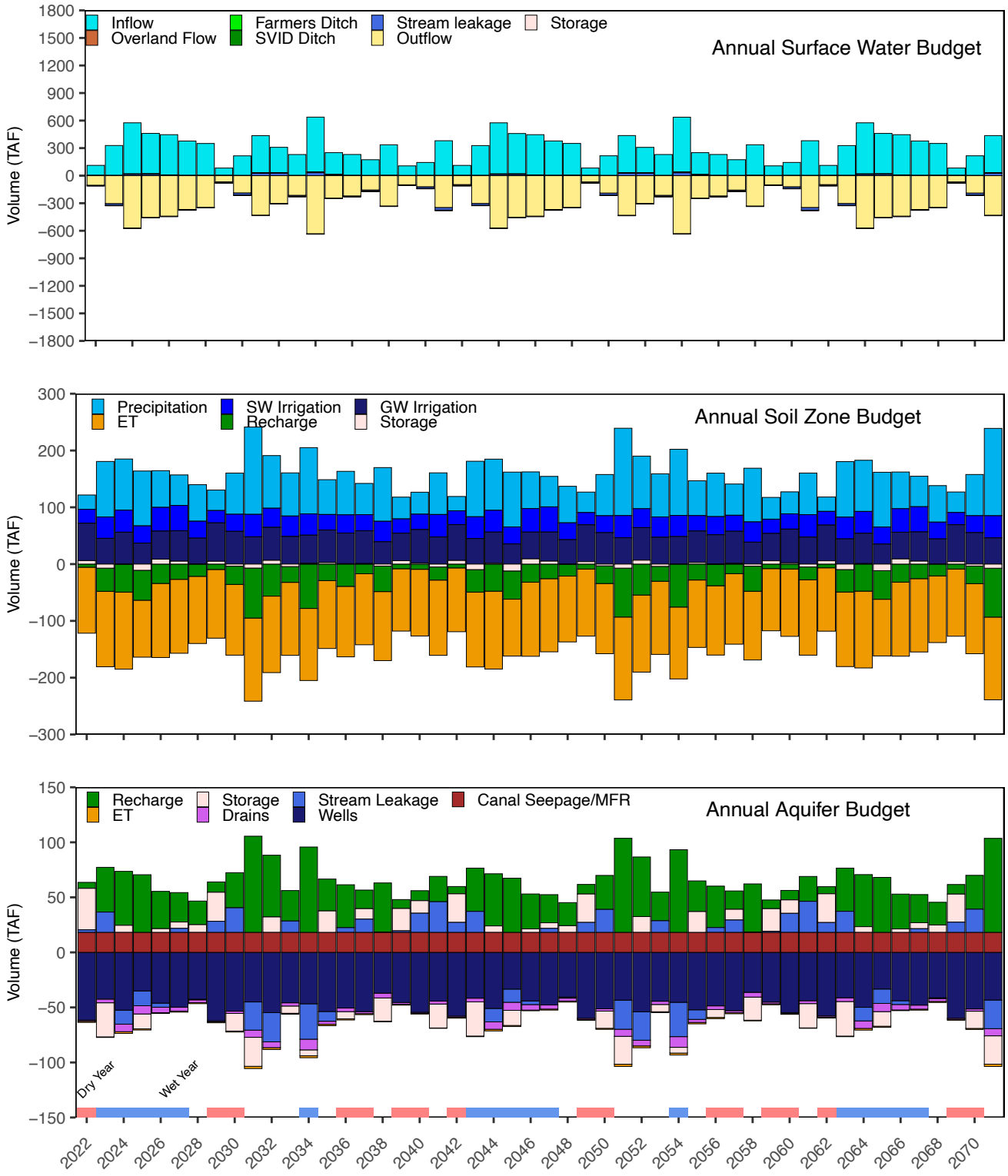

Figure 9: Scenario: Far Future (2070), Dry. Annual water budgets for the three conceptual subsystems used to represent the hydrology of the Basin (the surface water system, the soil zone, and the aquifer) for 50 potential future years, with basecsae future input data multiplied by change factors for the 2070 Dry with Extreme Warming (Dry) future climate scenario.

Table 5: The data used to build the 50-year future projected climate record is specified below, including the historical water year type. To account for leap days, some years were transposed.

Historical Year	Future Year	Water Year Type
1994	2022	Critical
1995	2023	Wet
1996	2024	Wet
1997	2025	Wet
1998	2026	Wet
1999	2027	Wet
2000	2028	Below Normal
2001	2029	Critical
2002	2030	Dry
2003	2031	Above Normal
2004	2032	Above Normal
2010	2033	Below Normal
2006	2034	Wet
2007	2035	Below Normal
2008	2036	Dry
2009	2037	Dry
2011	2038	Above Normal
1991	2039	Critical
1992	2040	Critical
1993	2041	Above Normal
1994	2042	Critical
1995	2043	Wet
1996	2044	Wet
1997	2045	Wet
1998	2046	Wet
1999	2047	Wet
2000	2048	Below Normal
2001	2049	Critical
2002	2050	Dry
2003	2051	Above Normal
2004	2052	Above Normal
2010	2053	Below Normal
2006	2054	Wet
2007	2055	Below Normal
2008	2056	Dry
2009	2057	Dry
2011	2058	Above Normal
1991	2059	Critical
1992	2060	Critical
1993	2061	Above Normal
1994	2062	Critical
1995	2063	Wet
1996	2064	Wet
1997	2065	Wet
1998	2066	Wet
1999	2067	Wet
2000	2068	Below Normal
2001	2069	Critical
2002	2070	Dry
2003	2071	Above Normal

Future Water Budget - Annual and Summary Tables

Future Basecase Stream Subsystem

Table 6: Annual flow volumes (TAF). Scenario: Future Basecase; Subsystem: Streams.

Water Year	Inflow	Overland	Farmers Div.	SVID Div.	Stream Leakage	Outflow	Storage
2022	118	2	-2	-4	4	-119	1
2023	504	5	-2	-4	7	-510	0
2024	472	6	-2	-4	27	-500	0
2025	515	9	-2	-4	32	-550	0
2026	537	7	-2	-4	25	-563	-0
2027	478	5	-2	-4	19	-497	0
2028	345	4	-2	-4	16	-358	0
2029	94	1	-2	-4	-3	-88	1
2030	249	3	-2	-4	-6	-240	0
2031	431	7	-2	-4	38	-470	-0
2032	287	5	-2	-4	30	-316	0
2033	283	3	-2	-4	2	-282	0
2034	640	10	-2	-4	44	-689	0
2035	253	3	-2	-4	16	-267	1
2036	262	4	-2	-4	8	-268	0
2037	195	2	-2	-4	-2	-189	0
2038	457	5	-2	-4	19	-476	-0
2039	115	2	-2	-4	5	-117	0
2040	133	1	-2	-4	-6	-123	1
2041	384	3	-2	-4	-6	-375	-0
2042	118	1	-2	-4	-1	-114	1
2043	504	5	-2	-4	8	-511	0
2044	472	6	-2	-4	26	-499	0
2045	515	8	-2	-4	30	-548	0
2046	537	7	-2	-4	24	-562	0
2047	479	5	-2	-4	18	-497	-0
2048	345	4	-2	-4	16	-358	0
2049	94	1	-2	-4	-2	-89	1
2050	249	3	-2	-4	-5	-241	0
2051	431	7	-2	-4	38	-471	-0
2052	287	5	-2	-4	29	-316	0
2053	283	3	-2	-4	2	-282	0
2054	640	10	-2	-4	43	-688	0
2055	253	3	-2	-4	15	-266	1
2056	262	4	-2	-4	8	-268	0
2057	195	2	-2	-4	-2	-190	0
2058	458	5	-2	-4	19	-476	0
2059	115	2	-2	-4	6	-118	0
2060	133	1	-2	-4	-6	-123	1
2061	384	3	-2	-4	-7	-374	0
2062	118	1	-2	-4	-1	-114	1
2063	504	5	-2	-4	7	-510	-0
2064	472	6	-2	-4	26	-499	0
2065	515	8	-2	-4	31	-549	0
2066	537	7	-2	-4	25	-563	-0
2067	479	5	-2	-4	18	-497	0
2068	345	4	-2	-4	16	-359	0
2069	94	1	-2	-4	-3	-89	1
2070	249	3	-2	-4	-6	-241	0
2071	431	7	-2	-4	38	-470	0
Minimum	94	1	-2	-4	-7	-689	-0
25th %ile	249	3	-2	-4	-1	-499	0
Median	345	4	-2	-4	15	-358	0
Mean	345	4	-2	-4	14	-358	0
75th %ile	479	6	-2	-4	26	-240	0
Maximum	640	10	-2	-4	44	-88	1

Future Basecase Soil Zone Subsystem

Table 7: Annual flow volumes (TAF). Scenario: Future Basecase; Subsystem: Soil Zone.

Water Year	Precip	SW Irrig.	GW Irrig.	ET	Recharge	Storage
2022	34	21	55	-106	-6	3
2023	117	29	34	-118	-55	-7
2024	97	32	45	-120	-55	1
2025	109	25	28	-90	-62	-10
2026	87	34	38	-117	-49	7
2027	71	39	45	-116	-45	6
2028	78	23	35	-106	-29	-1
2029	42	19	57	-111	-11	3
2030	78	26	48	-112	-38	-1
2031	151	32	39	-130	-87	-5
2032	90	28	49	-119	-53	6
2033	81	27	36	-115	-26	-3
2034	124	30	40	-113	-82	1
2035	64	24	48	-107	-31	2
2036	82	27	45	-111	-43	-0
2037	64	23	45	-113	-19	-1
2038	104	28	30	-107	-53	-2
2039	49	21	40	-102	-12	4
2040	53	24	46	-112	-12	1
2041	90	31	35	-121	-29	-6
2042	34	21	52	-106	-9	8
2043	117	29	33	-118	-54	-7
2044	97	32	44	-122	-53	2
2045	109	24	27	-90	-60	-11
2046	87	33	36	-117	-47	7
2047	71	39	43	-115	-43	6
2048	78	23	33	-105	-29	-1
2049	42	19	55	-110	-11	4
2050	78	26	46	-111	-37	-2
2051	151	32	37	-130	-85	-6
2052	90	28	48	-121	-51	6
2053	81	27	35	-115	-24	-3
2054	124	30	39	-113	-80	0
2055	64	24	46	-106	-30	2
2056	82	27	43	-110	-42	-1
2057	64	23	44	-112	-19	-0
2058	104	28	30	-107	-52	-3
2059	49	21	40	-102	-11	4
2060	53	24	47	-113	-12	1
2061	90	31	35	-121	-29	-6
2062	34	21	52	-106	-9	8
2063	117	29	32	-117	-54	-7
2064	97	32	43	-120	-53	1
2065	109	24	27	-89	-60	-11
2066	87	33	36	-117	-47	7
2067	71	39	43	-116	-43	6
2068	78	23	34	-106	-28	-0
2069	42	19	55	-110	-10	4
2070	78	26	46	-111	-37	-2
2071	151	32	37	-130	-85	-6
Minimum	34	19	27	-130	-87	-11
25th %ile	64	23	35	-117	-53	-3
Median	81	27	41	-113	-42	0
Mean	84	27	41	-112	-40	-0
75th %ile	102	31	46	-107	-25	4
Maximum	151	39	57	-89	-6	8

Future Basecase Aquifer Subsystem

Table 8: Annual flow volumes (TAF). Scenario: Future Basecase; Subsystem: Aquifer.

Water Year	Recharge	ET	STorage	Drains	Stream Leakge	Wells	Canals, MFR
2022	6	-1	34	-1	-4	-51	18
2023	55	-1	-29	-5	-7	-32	18
2024	54	-1	5	-6	-27	-43	18
2025	62	-1	-11	-9	-32	-27	18
2026	48	-1	2	-7	-25	-36	18
2027	45	-1	5	-5	-19	-42	18
2028	29	-1	6	-4	-16	-33	18
2029	11	-1	23	-1	3	-53	18
2030	38	-1	-13	-3	6	-45	18
2031	87	-2	-21	-7	-38	-37	18
2032	53	-2	12	-5	-30	-46	18
2033	26	-1	-4	-3	-2	-34	18
2034	82	-2	-5	-11	-44	-38	18
2035	31	-1	16	-3	-16	-45	18
2036	43	-1	-6	-4	-8	-42	18
2037	19	-1	7	-2	2	-43	18
2038	53	-1	-17	-5	-19	-29	18
2039	11	-1	16	-2	-5	-38	18
2040	12	-1	9	-1	6	-44	18
2041	29	-0	-17	-3	6	-33	18
2042	9	-1	23	-1	1	-49	18
2043	54	-1	-28	-5	-8	-31	18
2044	52	-1	5	-6	-26	-42	18
2045	59	-1	-12	-9	-30	-26	18
2046	47	-1	1	-7	-24	-34	18
2047	43	-1	4	-5	-18	-41	18
2048	28	-1	5	-4	-16	-32	18
2049	11	-1	23	-1	2	-51	18
2050	37	-1	-13	-3	5	-43	18
2051	84	-2	-20	-7	-38	-35	18
2052	51	-2	12	-5	-29	-45	18
2053	24	-1	-4	-3	-2	-33	18
2054	80	-2	-5	-11	-43	-37	18
2055	30	-1	16	-3	-15	-44	18
2056	41	-1	-6	-4	-8	-41	18
2057	19	-1	7	-2	2	-42	18
2058	52	-1	-17	-5	-19	-28	18
2059	11	-1	17	-2	-6	-37	18
2060	12	-1	10	-1	6	-44	18
2061	28	-0	-17	-3	7	-33	18
2062	9	-1	23	-1	1	-49	18
2063	53	-1	-28	-5	-7	-30	18
2064	52	-1	4	-6	-26	-41	18
2065	60	-1	-12	-9	-31	-26	18
2066	47	-1	1	-7	-25	-34	18
2067	43	-1	5	-5	-18	-41	18
2068	28	-1	6	-4	-16	-32	18
2069	10	-1	22	-1	3	-51	18
2070	36	-1	-13	-3	6	-43	18
2071	84	-2	-20	-7	-38	-35	18
Minimum	6	-2	-29	-11	-44	-53	18
25th %ile	25	-1	-13	-6	-26	-43	18
Median	42	-1	3	-4	-15	-39	18
Mean	40	-1	0	-4	-14	-39	18
75th %ile	53	-1	9	-3	1	-33	18
Maximum	87	-0	34	-1	7	-26	18

Near Future (2030) Stream Subsystem

Table 9: Annual flow volumes (TAF). Scenario: Near Future (2030); Subsystem: Streams.

Water Year	Inflow	Overland	Farmers Div.	SVID Div.	Stream Leakage	Outflow	Storage
2022	126	2	-2	-4	4	-127	1
2023	555	6	-2	-4	3	-558	0
2024	510	7	-2	-4	25	-536	0
2025	581	9	-2	-4	30	-615	0
2026	543	7	-2	-4	22	-566	0
2027	487	5	-2	-4	17	-503	0
2028	359	3	-2	-4	14	-371	0
2029	99	1	-2	-4	-5	-91	2
2030	260	3	-2	-4	-5	-252	0
2031	439	7	-2	-4	40	-481	-0
2032	313	5	-2	-4	29	-341	0
2033	288	3	-2	-4	0	-285	0
2034	683	11	-2	-4	45	-733	0
2035	274	4	-2	-4	17	-289	1
2036	272	4	-2	-4	7	-278	0
2037	193	2	-2	-4	-2	-188	0
2038	488	6	-2	-4	18	-505	-0
2039	116	2	-2	-4	5	-117	0
2040	135	1	-2	-4	-8	-123	1
2041	405	3	-2	-4	-10	-393	0
2042	126	1	-2	-4	-2	-121	1
2043	555	6	-2	-4	3	-559	-0
2044	510	6	-2	-4	24	-536	0
2045	581	9	-2	-4	29	-614	0
2046	544	7	-2	-4	22	-566	0
2047	487	5	-2	-4	16	-502	0
2048	359	3	-2	-4	14	-371	0
2049	99	1	-2	-4	-4	-92	1
2050	260	3	-2	-4	-5	-252	0
2051	440	7	-2	-4	41	-482	0
2052	313	5	-2	-4	28	-341	0
2053	288	3	-2	-4	-0	-285	-0
2054	683	11	-2	-4	44	-732	0
2055	274	4	-2	-4	16	-289	1
2056	272	4	-2	-4	7	-278	0
2057	193	2	-2	-4	-1	-189	0
2058	488	5	-2	-4	18	-505	-0
2059	116	2	-2	-4	5	-118	0
2060	135	1	-2	-4	-8	-123	1
2061	405	3	-2	-4	-10	-392	0
2062	126	1	-2	-4	-2	-121	1
2063	555	6	-2	-4	3	-558	-0
2064	510	7	-2	-4	24	-536	0
2065	582	9	-2	-4	30	-615	0
2066	544	7	-2	-4	22	-566	-0
2067	487	5	-2	-4	16	-503	0
2068	359	3	-2	-4	14	-371	0
2069	99	1	-2	-4	-4	-92	2
2070	260	3	-2	-4	-5	-252	0
2071	440	7	-2	-4	40	-481	0
Minimum	99	1	-2	-4	-10	-733	-0
25th %ile	260	3	-2	-4	-2	-536	0
Median	359	4	-2	-4	14	-371	0
Mean	364	5	-2	-4	12	-376	0
75th %ile	510	7	-2	-4	24	-252	0
Maximum	683	11	-2	-4	45	-91	2

Near Future (2030) Soil Zone Subsystem

Table 10: Annual flow volumes (TAF). Scenario: Near Future (2030); Subsystem: Soil Zone.

Water Year	Precip	SW Irrig.	GW Irrig.	ET	Recharge	Storage
2022	36	21	58	-111	-7	3
2023	117	31	36	-122	-56	-7
2024	98	34	48	-125	-55	0
2025	111	26	30	-93	-64	-10
2026	85	35	41	-121	-48	7
2027	71	41	48	-120	-45	6
2028	78	24	37	-110	-28	-1
2029	43	20	60	-115	-11	3
2030	83	27	50	-116	-43	-1
2031	158	34	40	-134	-92	-5
2032	90	30	51	-124	-53	6
2033	83	29	38	-119	-27	-3
2034	127	32	42	-117	-85	1
2035	68	25	50	-110	-35	2
2036	84	28	48	-115	-45	-0
2037	66	24	48	-117	-21	-0
2038	106	30	32	-111	-55	-2
2039	49	22	42	-105	-12	4
2040	53	24	49	-115	-13	1
2041	91	32	37	-125	-30	-6
2042	36	21	55	-110	-9	7
2043	117	31	35	-122	-54	-7
2044	98	33	47	-126	-53	1
2045	111	26	29	-93	-61	-11
2046	85	35	39	-121	-46	8
2047	71	40	45	-120	-43	6
2048	78	24	35	-108	-28	-1
2049	43	20	57	-113	-11	4
2050	83	27	48	-115	-41	-2
2051	158	33	39	-134	-90	-6
2052	90	29	51	-125	-51	6
2053	83	28	37	-120	-25	-3
2054	127	32	41	-116	-83	0
2055	68	24	49	-110	-33	2
2056	84	28	45	-113	-44	-1
2057	66	24	47	-116	-21	0
2058	106	30	32	-110	-54	-3
2059	49	22	42	-105	-11	4
2060	53	24	50	-116	-12	1
2061	91	32	37	-126	-29	-6
2062	36	21	55	-110	-9	7
2063	117	31	34	-121	-54	-7
2064	98	34	46	-124	-53	1
2065	111	25	28	-92	-62	-11
2066	85	35	39	-121	-46	8
2067	71	40	46	-120	-43	6
2068	78	24	36	-109	-28	-0
2069	43	20	57	-114	-11	4
2070	83	27	48	-115	-41	-2
2071	158	33	39	-134	-90	-6
Minimum	36	20	28	-134	-92	-11
25th %ile	68	24	37	-121	-54	-3
Median	84	28	44	-116	-43	0
Mean	85	28	43	-116	-41	-0
75th %ile	104	32	49	-111	-26	4
Maximum	158	41	60	-92	-7	8

Near Future (2030) Aquifer Subsystem

Table 11: Annual flow volumes (TAF). Scenario: Near Future (2030); Subsystem: Aquifer.

Water Year	Recharge	ET	STorage	Drains	Stream Leakge	Wells	Canals, MFR
2022	7	-1	35	-1	-4	-54	18
2023	56	-1	-30	-6	-3	-34	18
2024	55	-1	5	-7	-25	-45	18
2025	64	-1	-12	-10	-30	-29	18
2026	48	-1	2	-7	-22	-38	18
2027	45	-1	5	-5	-17	-45	18
2028	28	-1	7	-3	-14	-35	18
2029	11	-1	24	-1	5	-56	18
2030	42	-1	-15	-3	5	-47	18
2031	92	-2	-22	-7	-40	-38	18
2032	53	-2	13	-5	-29	-49	18
2033	27	-1	-5	-3	-0	-36	18
2034	85	-2	-5	-11	-45	-40	18
2035	34	-1	17	-4	-17	-48	18
2036	45	-1	-6	-4	-7	-45	18
2037	21	-1	8	-2	2	-45	18
2038	55	-1	-18	-6	-18	-31	18
2039	12	-1	18	-2	-5	-40	18
2040	13	-1	9	-1	8	-46	18
2041	29	-0	-18	-3	10	-35	18
2042	9	-1	24	-1	2	-51	18
2043	54	-1	-29	-6	-3	-33	18
2044	53	-1	5	-7	-24	-44	18
2045	61	-1	-13	-9	-29	-27	18
2046	46	-1	2	-7	-22	-37	18
2047	43	-1	4	-5	-16	-43	18
2048	28	-1	6	-3	-14	-33	18
2049	11	-1	23	-1	4	-54	18
2050	41	-1	-14	-3	5	-45	18
2051	89	-2	-21	-7	-41	-37	18
2052	51	-2	13	-5	-28	-48	18
2053	25	-1	-5	-3	0	-35	18
2054	83	-2	-5	-11	-44	-39	18
2055	33	-1	16	-4	-16	-46	18
2056	44	-1	-7	-4	-7	-43	18
2057	21	-1	8	-2	1	-44	18
2058	54	-1	-18	-5	-18	-30	18
2059	11	-1	18	-2	-5	-40	18
2060	12	-1	10	-1	8	-47	18
2061	29	-0	-18	-3	10	-35	18
2062	9	-1	24	-1	2	-51	18
2063	53	-1	-29	-6	-3	-33	18
2064	53	-1	5	-7	-24	-43	18
2065	61	-1	-12	-9	-30	-27	18
2066	46	-1	2	-7	-22	-36	18
2067	43	-1	5	-5	-16	-43	18
2068	27	-1	7	-3	-14	-34	18
2069	11	-1	23	-1	4	-54	18
2070	41	-1	-14	-3	5	-46	18
2071	89	-2	-21	-7	-40	-37	18
Minimum	7	-2	-30	-11	-45	-56	18
25th %ile	25	-1	-14	-7	-24	-46	18
Median	43	-1	3	-4	-14	-41	18
Mean	41	-1	-0	-5	-12	-41	18
75th %ile	54	-1	10	-3	2	-35	18
Maximum	92	-0	35	-1	10	-27	18

Far Future (2070), Central Tendency Stream Subsystem

Table 12: Annual flow volumes (TAF). Scenario: Far Future (2070), Central Tendency; Subsystem: Streams.

Water Year	Inflow	Overland	Farmers Div.	SVID Div.	Stream Leakage	Outflow	Storage
2022	116	1	-2	-4	3	-116	1
2023	500	5	-2	-4	2	-502	-0
2024	469	7	-2	-4	30	-501	0
2025	512	9	-2	-4	34	-550	0
2026	533	7	-2	-4	22	-555	0
2027	475	5	-2	-4	15	-489	0
2028	342	3	-2	-4	13	-354	0
2029	93	1	-2	-4	-6	-84	2
2030	247	3	-2	-4	-7	-237	0
2031	428	8	-2	-4	42	-472	-0
2032	284	5	-2	-4	30	-314	0
2033	278	3	-2	-4	-3	-272	0
2034	637	12	-2	-4	51	-694	0
2035	251	3	-2	-4	17	-267	1
2036	259	4	-2	-4	5	-263	0
2037	193	2	-2	-4	-6	-184	0
2038	454	5	-2	-4	13	-466	-0
2039	113	2	-2	-4	3	-112	0
2040	132	1	-2	-4	-10	-118	1
2041	380	3	-2	-4	-12	-366	0
2042	116	1	-2	-4	-4	-110	1
2043	501	5	-2	-4	2	-502	0
2044	470	7	-2	-4	29	-500	0
2045	512	9	-2	-4	32	-548	0
2046	533	7	-2	-4	21	-556	-0
2047	475	5	-2	-4	14	-489	0
2048	342	3	-2	-4	14	-354	0
2049	93	1	-2	-4	-5	-85	2
2050	247	3	-2	-4	-7	-238	0
2051	428	8	-2	-4	43	-473	-0
2052	285	5	-2	-4	29	-314	0
2053	278	3	-2	-4	-4	-272	0
2054	637	12	-2	-4	50	-693	0
2055	251	4	-2	-4	17	-267	1
2056	259	4	-2	-4	5	-263	0
2057	193	2	-2	-4	-5	-185	0
2058	454	5	-2	-4	13	-466	0
2059	113	2	-2	-4	3	-113	0
2060	132	1	-2	-4	-10	-118	1
2061	381	3	-2	-4	-13	-365	0
2062	116	1	-2	-4	-3	-110	1
2063	501	5	-2	-4	1	-501	0
2064	469	7	-2	-4	29	-500	0
2065	512	9	-2	-4	33	-549	0
2066	533	7	-2	-4	21	-556	0
2067	476	5	-2	-4	14	-489	0
2068	343	3	-2	-4	13	-354	0
2069	93	1	-2	-4	-5	-85	2
2070	247	3	-2	-4	-7	-238	0
2071	428	8	-2	-4	42	-472	-0
Minimum	93	1	-2	-4	-13	-694	-0
25th %ile	247	3	-2	-4	-4	-500	0
Median	342	4	-2	-4	13	-354	0
Mean	342	5	-2	-4	12	-354	0
75th %ile	475	7	-2	-4	27	-237	0
Maximum	637	12	-2	-4	51	-84	2

Far Future (2070), Central Tendency Soil Zone Subsystem

Table 13: Annual flow volumes (TAF). Scenario: Far Future (2070), Central Tendency; Subsystem: Soil Zone.

Water Year	Precip	SW Irrig.	GW Irrig.	ET	Recharge	Storage
2022	35	22	61	-115	-7	4
2023	120	33	39	-127	-59	-7
2024	106	35	51	-130	-64	1
2025	118	27	32	-96	-70	-11
2026	85	37	43	-125	-49	8
2027	72	42	50	-125	-45	6
2028	80	26	40	-115	-30	-1
2029	43	21	63	-118	-11	3
2030	85	28	53	-120	-44	-2
2031	166	35	43	-140	-99	-5
2032	93	31	54	-129	-56	6
2033	83	33	43	-123	-30	-5
2034	135	34	46	-121	-96	3
2035	70	26	53	-114	-36	2
2036	85	30	51	-120	-46	0
2037	64	25	51	-121	-19	0
2038	104	32	35	-115	-53	-3
2039	47	23	45	-108	-11	5
2040	54	25	51	-118	-12	1
2041	91	35	41	-130	-30	-5
2042	35	22	59	-113	-9	7
2043	120	33	38	-126	-57	-8
2044	106	35	50	-131	-62	2
2045	118	27	30	-96	-67	-12
2046	85	37	41	-125	-47	9
2047	72	42	48	-124	-43	5
2048	80	26	38	-113	-30	-1
2049	43	20	60	-117	-11	4
2050	85	28	51	-119	-42	-2
2051	166	35	41	-140	-97	-6
2052	93	31	54	-130	-54	7
2053	83	32	42	-124	-28	-5
2054	135	34	44	-121	-94	2
2055	70	25	52	-114	-35	2
2056	85	30	48	-118	-44	-0
2057	64	25	50	-120	-20	1
2058	104	31	34	-115	-52	-3
2059	47	23	44	-108	-11	5
2060	54	25	52	-119	-12	1
2061	91	34	40	-131	-29	-6
2062	35	22	58	-113	-9	7
2063	120	33	37	-126	-56	-8
2064	106	35	49	-129	-62	1
2065	118	27	30	-95	-68	-11
2066	85	37	41	-125	-47	9
2067	72	42	48	-125	-43	5
2068	80	25	38	-114	-29	-0
2069	43	20	60	-117	-11	4
2070	85	28	51	-119	-42	-3
2071	166	35	41	-140	-96	-6
Minimum	35	20	30	-140	-99	-12
25th %ile	70	25	41	-126	-56	-5
Median	85	30	47	-120	-43	1
Mean	88	30	46	-120	-44	-0
75th %ile	106	35	51	-115	-29	4
Maximum	166	42	63	-95	-7	9

Far Future (2070), Central Tendency Aquifer Subsystem

Table 14: Annual flow volumes (TAF). Scenario: Far Future (2070), Central Tendency; Subsystem: Aquifer.

Water Year	Recharge	ET	STorage	Drains	Stream Leakge	Wells	Canals, MFR
2022	7	-1	37	-1	-3	-57	18
2023	58	-1	-32	-5	-2	-37	18
2024	64	-2	5	-7	-30	-49	18
2025	70	-1	-13	-10	-34	-30	18
2026	49	-1	3	-7	-22	-41	18
2027	45	-1	5	-5	-15	-47	18
2028	30	-1	7	-3	-13	-38	18
2029	11	-1	25	-1	6	-58	18
2030	44	-1	-15	-3	7	-50	18
2031	98	-2	-23	-8	-42	-41	18
2032	56	-2	14	-5	-30	-52	18
2033	30	-1	-6	-3	3	-41	18
2034	96	-2	-6	-12	-51	-43	18
2035	36	-1	18	-4	-17	-50	18
2036	45	-1	-6	-4	-5	-48	18
2037	19	-1	8	-2	6	-48	18
2038	52	-1	-19	-5	-13	-33	18
2039	11	-1	19	-2	-3	-42	18
2040	12	-1	9	-1	10	-48	18
2041	30	-0	-19	-3	12	-38	18
2042	9	-1	25	-1	4	-54	18
2043	56	-1	-31	-5	-2	-36	18
2044	62	-2	5	-7	-29	-47	18
2045	67	-1	-14	-9	-32	-29	18
2046	47	-1	3	-7	-21	-39	18
2047	43	-1	5	-5	-14	-45	18
2048	30	-1	6	-3	-14	-36	18
2049	11	-1	25	-1	5	-56	18
2050	42	-1	-15	-3	7	-48	18
2051	96	-2	-22	-8	-43	-39	18
2052	54	-2	15	-5	-29	-51	18
2053	28	-1	-6	-3	4	-40	18
2054	93	-2	-6	-12	-50	-42	18
2055	35	-1	18	-4	-17	-49	18
2056	44	-1	-6	-4	-5	-46	18
2057	19	-1	8	-2	5	-47	18
2058	51	-1	-19	-5	-13	-32	18
2059	11	-1	19	-2	-3	-42	18
2060	12	-1	10	-1	10	-48	18
2061	29	-0	-19	-3	13	-38	18
2062	9	-1	25	-1	3	-54	18
2063	56	-1	-32	-5	-1	-35	18
2064	62	-2	5	-7	-29	-46	18
2065	67	-1	-13	-10	-33	-29	18
2066	47	-1	3	-7	-21	-39	18
2067	42	-1	5	-5	-14	-45	18
2068	29	-1	7	-3	-13	-36	18
2069	10	-1	24	-1	5	-56	18
2070	42	-1	-15	-3	7	-48	18
2071	96	-2	-23	-8	-42	-39	18
Minimum	7	-2	-32	-12	-51	-58	18
25th %ile	28	-1	-15	-7	-27	-48	18
Median	43	-1	4	-4	-13	-44	18
Mean	43	-1	-0	-5	-12	-44	18
75th %ile	56	-1	10	-3	4	-38	18
Maximum	98	-0	37	-1	13	-29	18

Far Future (2070), WMW Stream Subsystem

Table 15: Annual flow volumes (TAF). Scenario: Far Future (2070), Wet; Subsystem: Streams.

Water Year	Inflow	Overland	Farmers Div.	SVID Div.	Stream Leakage	Outflow	Storage
2022	180	2	-2	-4	5	-182	1
2023	877	12	-2	-4	6	-889	-0
2024	1188	18	-2	-4	20	-1221	0
2025	1171	19	-2	-4	29	-1214	0
2026	817	11	-2	-4	24	-846	-0
2027	1109	14	-2	-4	16	-1132	-0
2028	1000	13	-2	-4	10	-1017	0
2029	139	1	-2	-4	-4	-132	1
2030	681	7	-2	-4	2	-684	0
2031	895	13	-2	-4	51	-953	0
2032	1334	22	-2	-4	36	-1387	0
2033	455	5	-2	-4	14	-468	-0
2034	1628	29	-2	-4	39	-1690	0
2035	406	6	-2	-4	26	-433	1
2036	480	7	-2	-4	18	-499	0
2037	311	3	-2	-4	3	-312	0
2038	902	11	-2	-4	24	-931	0
2039	179	2	-2	-4	6	-181	0
2040	298	2	-2	-4	-6	-289	1
2041	571	5	-2	-4	-4	-567	0
2042	180	1	-2	-4	-2	-175	1
2043	877	12	-2	-4	7	-889	0
2044	1189	18	-2	-4	19	-1221	0
2045	1171	19	-2	-4	28	-1213	0
2046	817	11	-2	-4	24	-846	-0
2047	1109	14	-2	-4	15	-1132	0
2048	1000	13	-2	-4	10	-1017	0
2049	139	2	-2	-4	-2	-134	1
2050	681	7	-2	-4	3	-685	0
2051	896	13	-2	-4	52	-954	0
2052	1334	22	-2	-4	35	-1386	0
2053	455	4	-2	-4	13	-467	-0
2054	1628	29	-2	-4	38	-1690	0
2055	406	6	-2	-4	25	-433	1
2056	480	7	-2	-4	19	-499	-0
2057	311	3	-2	-4	4	-313	0
2058	902	11	-2	-4	24	-931	-0
2059	179	2	-2	-4	6	-182	0
2060	298	2	-2	-4	-6	-289	1
2061	571	5	-2	-4	-5	-566	0
2062	180	1	-2	-4	-2	-176	1
2063	877	12	-2	-4	6	-889	-0
2064	1189	18	-2	-4	20	-1221	0
2065	1171	19	-2	-4	29	-1214	0
2066	817	11	-2	-4	24	-846	0
2067	1109	14	-2	-4	15	-1132	-0
2068	1000	13	-2	-4	10	-1017	0
2069	139	1	-2	-4	-3	-133	1
2070	681	7	-2	-4	2	-685	0
2071	896	13	-2	-4	51	-954	-0
Minimum	139	1	-2	-4	-6	-1690	-0
25th %ile	406	4	-2	-4	4	-1103	0
Median	817	11	-2	-4	15	-846	0
Mean	746	10	-2	-4	15	-766	0
75th %ile	1082	13	-2	-4	24	-433	0
Maximum	1628	29	-2	-4	52	-132	1

Far Future (2070), WMW Soil Zone Subsystem

Table 16: Annual flow volumes (TAF). Scenario: Far Future (2070), Wet; Subsystem: Soil Zone.

Water Year	Precip	SW Irrig.	GW Irrig.	ET	Recharge	Storage
2022	37	22	58	-113	-8	3
2023	129	31	36	-123	-67	-7
2024	106	35	49	-126	-65	1
2025	122	26	30	-93	-76	-9
2026	92	35	41	-122	-53	6
2027	81	41	48	-121	-55	6
2028	87	24	37	-111	-36	-1
2029	46	21	60	-117	-12	2
2030	98	28	51	-117	-58	-1
2031	180	37	40	-136	-116	-6
2032	111	31	52	-125	-75	7
2033	101	29	38	-121	-43	-3
2034	138	32	43	-117	-98	1
2035	82	25	51	-111	-49	2
2036	99	29	48	-116	-60	-0
2037	74	25	49	-119	-27	-1
2038	118	31	33	-112	-68	-2
2039	52	23	43	-107	-13	3
2040	58	26	48	-118	-15	1
2041	98	32	38	-126	-36	-5
2042	37	22	55	-112	-10	7
2043	129	31	35	-122	-65	-7
2044	106	35	48	-128	-63	2
2045	122	26	29	-93	-73	-10
2046	92	35	39	-123	-51	7
2047	81	41	46	-121	-53	6
2048	87	24	35	-110	-35	-1
2049	46	21	58	-116	-12	4
2050	98	27	49	-116	-56	-2
2051	180	37	39	-136	-114	-6
2052	111	30	52	-126	-73	7
2053	101	29	36	-122	-40	-4
2054	138	32	42	-117	-97	1
2055	82	25	49	-111	-47	2
2056	99	29	46	-115	-58	-1
2057	74	25	48	-118	-27	-0
2058	118	30	32	-111	-67	-2
2059	52	22	43	-107	-13	3
2060	58	25	49	-119	-15	1
2061	98	32	37	-127	-35	-5
2062	37	22	55	-112	-10	7
2063	129	31	35	-122	-65	-8
2064	106	35	47	-126	-63	1
2065	122	26	29	-92	-74	-10
2066	92	35	39	-122	-51	7
2067	81	41	47	-121	-53	6
2068	87	24	36	-111	-35	-1
2069	46	21	58	-116	-12	4
2070	98	27	49	-116	-56	-2
2071	180	37	39	-136	-114	-6
Minimum	37	21	29	-136	-116	-10
25th %ile	81	25	37	-122	-66	-3
Median	98	29	45	-118	-53	0
Mean	96	29	44	-117	-51	-0
75th %ile	116	32	49	-112	-35	3
Maximum	180	41	60	-92	-8	7

Far Future (2070), WMW Aquifer Subsystem

Table 17: Annual flow volumes (TAF). Scenario: Far Future (2070), Wet; Subsystem: Aquifer.

Water Year	Recharge	ET	STorage	Drains	Stream Leakge	Wells	Canals, MFR
2022	8	-1	35	-1	-5	-54	18
2023	66	-1	-31	-12	-6	-34	18
2024	64	-2	5	-19	-20	-46	18
2025	75	-1	-13	-21	-29	-29	18
2026	53	-1	4	-12	-24	-39	18
2027	55	-1	4	-14	-16	-46	18
2028	36	-1	6	-14	-10	-35	18
2029	12	-1	25	-1	4	-56	18
2030	58	-1	-17	-7	-2	-48	18
2031	115	-2	-28	-13	-51	-38	18
2032	75	-2	18	-24	-36	-50	18
2033	42	-1	-5	-5	-14	-36	18
2034	98	-2	-3	-31	-39	-41	18
2035	48	-1	15	-6	-26	-48	18
2036	59	-1	-6	-7	-18	-45	18
2037	27	-1	8	-3	-3	-46	18
2038	68	-1	-18	-12	-24	-32	18
2039	13	-1	18	-2	-6	-41	18
2040	15	-1	9	-2	6	-46	18
2041	36	-0	-17	-5	4	-36	18
2042	10	-1	24	-1	2	-52	18
2043	65	-1	-30	-12	-7	-33	18
2044	63	-1	5	-19	-19	-45	18
2045	73	-1	-13	-21	-28	-28	18
2046	51	-1	4	-12	-24	-37	18
2047	53	-1	3	-15	-15	-44	18
2048	35	-1	5	-14	-10	-33	18
2049	12	-1	24	-2	2	-54	18
2050	56	-1	-17	-7	-3	-46	18
2051	113	-2	-27	-13	-52	-37	18
2052	73	-2	19	-24	-35	-49	18
2053	40	-1	-5	-4	-13	-35	18
2054	96	-2	-3	-31	-38	-40	18
2055	46	-1	12	-6	-25	-44	18
2056	59	-1	-4	-7	-19	-46	18
2057	27	-1	8	-3	-4	-45	18
2058	67	-1	-18	-12	-24	-31	18
2059	13	-1	18	-2	-6	-40	18
2060	15	-1	10	-2	6	-46	18
2061	35	-0	-17	-5	5	-35	18
2062	10	-1	24	-1	2	-52	18
2063	64	-1	-30	-12	-6	-33	18
2064	63	-2	4	-19	-20	-44	18
2065	73	-1	-13	-21	-29	-28	18
2066	51	-1	4	-12	-24	-37	18
2067	53	-1	4	-14	-15	-44	18
2068	35	-1	6	-14	-10	-34	18
2069	12	-1	24	-1	3	-54	18
2070	55	-1	-17	-7	-2	-46	18
2071	113	-2	-27	-13	-51	-37	18
Minimum	8	-2	-31	-31	-52	-56	18
25th %ile	35	-1	-16	-14	-24	-46	18
Median	53	-1	4	-12	-15	-42	18
Mean	51	-1	-0	-11	-15	-41	18
75th %ile	66	-1	9	-4	-4	-35	18
Maximum	115	-0	35	-1	6	-28	18

Far Future (2070), DEW Stream Subsystem

Table 18: Annual flow volumes (TAF). Scenario: Far Future (2070), Dry; Subsystem: Streams.

Water Year	Inflow	Overland	Farmers Div.	SVID Div.	Stream Leakage	Outflow	Storage
2022	109	1	-2	-4	-2	-104	2
2023	325	3	-2	-4	-19	-304	-0
2024	556	7	-2	-4	13	-570	0
2025	439	7	-2	-4	13	-455	1
2026	437	5	-2	-4	4	-440	0
2027	373	4	-2	-4	-4	-368	0
2028	347	3	-2	-4	1	-345	0
2029	80	1	-2	-4	-10	-67	2
2030	213	2	-2	-4	-22	-188	0
2031	403	6	-2	-4	26	-430	0
2032	276	5	-2	-4	27	-303	0
2033	227	3	-2	-4	-10	-214	-0
2034	596	9	-2	-4	32	-632	0
2035	238	3	-2	-4	9	-245	1
2036	227	3	-2	-4	-4	-220	0
2037	171	2	-2	-4	-12	-156	0
2038	332	4	-2	-4	-0	-330	0
2039	104	2	-2	-4	-2	-99	0
2040	142	1	-2	-4	-17	-120	1
2041	377	3	-2	-4	-28	-347	0
2042	109	1	-2	-4	-9	-97	2
2043	324	3	-2	-4	-19	-303	-0
2044	556	7	-2	-4	12	-569	0
2045	439	7	-2	-4	12	-453	1
2046	438	5	-2	-4	3	-440	0
2047	374	4	-2	-4	-4	-368	0
2048	347	3	-2	-4	1	-345	0
2049	80	1	-2	-4	-9	-68	2
2050	214	2	-2	-4	-21	-189	0
2051	404	6	-2	-4	26	-431	0
2052	277	5	-2	-4	26	-303	0
2053	227	3	-2	-4	-11	-214	-0
2054	596	9	-2	-4	31	-631	0
2055	238	3	-2	-4	9	-245	1
2056	227	3	-2	-4	-4	-220	0
2057	171	2	-2	-4	-11	-157	0
2058	332	4	-2	-4	-0	-330	-0
2059	105	2	-2	-4	-1	-100	0
2060	142	1	-2	-4	-17	-121	1
2061	378	3	-2	-4	-28	-346	0
2062	109	1	-2	-4	-9	-97	2
2063	324	3	-2	-4	-19	-303	-0
2064	556	7	-2	-4	12	-570	0
2065	439	7	-2	-4	13	-454	1
2066	438	5	-2	-4	3	-440	-0
2067	374	4	-2	-4	-3	-369	0
2068	347	3	-2	-4	1	-345	0
2069	80	1	-2	-4	-9	-68	2
2070	214	2	-2	-4	-21	-189	0
2071	404	6	-2	-4	26	-431	0
Minimum	80	1	-2	-4	-28	-632	-0
25th %ile	214	2	-2	-4	-11	-430	0
Median	325	3	-2	-4	-2	-303	0
Mean	305	4	-2	-4	-1	-303	1
75th %ile	404	5	-2	-4	11	-188	1
Maximum	596	9	-2	-4	32	-67	2

Far Future (2070), DEW Soil Zone Subsystem

Table 19: Annual flow volumes (TAF). Scenario: Far Future (2070), Dry; Subsystem: Soil Zone.

Water Year	Precip	SW Irrig.	GW Irrig.	ET	Recharge	Storage
2022	25	24	66	-116	-5	6
2023	98	38	45	-133	-41	-7
2024	90	39	56	-136	-49	0
2025	97	30	37	-100	-53	-11
2026	65	42	49	-130	-34	9
2027	54	45	54	-130	-27	5
2028	64	30	45	-118	-22	0
2029	36	22	68	-121	-9	5
2030	73	30	58	-125	-32	-4
2031	154	40	48	-146	-88	-7
2032	93	34	58	-135	-56	7
2033	76	36	49	-128	-28	-4
2034	117	37	50	-127	-78	1
2035	61	27	57	-119	-29	3
2036	77	32	54	-124	-39	1
2037	55	28	58	-125	-17	1
2038	95	36	39	-122	-45	-4
2039	38	25	48	-110	-8	6
2040	39	27	59	-117	-9	2
2041	73	40	48	-133	-23	-5
2042	25	24	63	-112	-7	6
2043	98	38	45	-132	-40	-10
2044	90	38	55	-137	-48	2
2045	97	30	35	-100	-50	-12
2046	65	41	47	-131	-32	9
2047	54	44	51	-129	-26	5
2048	64	30	43	-116	-21	0
2049	36	22	65	-118	-9	4
2050	73	30	55	-124	-31	-3
2051	154	39	46	-146	-86	-7
2052	93	33	57	-136	-54	7
2053	76	36	47	-129	-26	-4
2054	117	37	48	-127	-76	0
2055	61	27	55	-119	-28	3
2056	77	32	52	-122	-38	-0
2057	55	28	56	-124	-17	1
2058	95	36	39	-121	-44	-4
2059	38	25	48	-109	-8	6
2060	39	27	59	-118	-9	2
2061	73	39	48	-133	-23	-5
2062	25	24	63	-112	-7	6
2063	98	38	44	-131	-40	-10
2064	90	38	53	-135	-48	1
2065	97	30	35	-100	-50	-12
2066	65	41	47	-130	-32	9
2067	54	44	52	-129	-26	5
2068	64	30	44	-117	-21	0
2069	36	22	65	-118	-9	4
2070	73	30	55	-123	-31	-3
2071	154	39	46	-146	-86	-7
Minimum	25	22	35	-146	-88	-12
25th %ile	54	28	47	-131	-47	-4
Median	73	33	50	-124	-31	1
Mean	74	33	51	-124	-34	-0
75th %ile	94	38	57	-118	-21	5
Maximum	154	45	68	-100	-5	9

Far Future (2070), DEW Aquifer Subsystem

Table 20: Annual flow volumes (TAF). Scenario: Far Future (2070), Dry; Subsystem: Aquifer.

Water Year	Recharge	ET	STorage	Drains	Stream Leakge	Wells	Canals, MFR
2022	5	-1	38	-1	2	-62	18
2023	41	-1	-31	-3	19	-42	18
2024	49	-2	6	-7	-13	-53	18
2025	52	-1	-14	-7	-13	-35	18
2026	34	-1	3	-5	-4	-46	18
2027	27	-1	6	-4	4	-50	18
2028	21	-1	7	-3	-1	-43	18
2029	9	-1	26	-1	10	-62	18
2030	32	-1	-16	-2	22	-53	18
2031	87	-2	-26	-6	-26	-45	18
2032	56	-2	14	-5	-27	-55	18
2033	28	-1	-7	-3	10	-46	18
2034	78	-2	-5	-10	-32	-47	18
2035	29	-1	20	-3	-9	-54	18
2036	39	-1	-7	-3	4	-51	18
2037	17	-1	10	-2	12	-54	18
2038	45	-1	-21	-4	0	-37	18
2039	8	-1	20	-2	2	-46	18
2040	9	-1	11	-1	17	-54	18
2041	23	-0	-22	-3	28	-44	18
2042	7	-1	26	-1	9	-58	18
2043	39	-1	-31	-3	19	-42	18
2044	47	-2	6	-7	-12	-51	18
2045	49	-1	-14	-7	-12	-33	18
2046	32	-1	3	-5	-3	-44	18
2047	26	-1	5	-4	4	-48	18
2048	21	-1	6	-3	-1	-41	18
2049	9	-1	26	-1	9	-60	18
2050	31	-1	-16	-2	21	-51	18
2051	86	-2	-25	-6	-26	-43	18
2052	54	-2	14	-5	-26	-54	18
2053	26	-1	-7	-3	11	-44	18
2054	75	-2	-5	-10	-31	-45	18
2055	28	-1	19	-3	-9	-52	18
2056	38	-1	-7	-3	4	-49	18
2057	17	-1	10	-2	11	-53	18
2058	44	-1	-21	-4	0	-36	18
2059	8	-1	20	-2	1	-45	18
2060	9	-1	12	-1	17	-55	18
2061	23	-0	-22	-3	28	-44	18
2062	6	-1	26	-1	9	-58	18
2063	39	-1	-31	-3	19	-41	18
2064	47	-2	5	-7	-12	-50	18
2065	50	-1	-13	-7	-13	-33	18
2066	32	-1	3	-5	-3	-44	18
2067	26	-1	5	-4	3	-48	18
2068	21	-1	7	-3	-1	-41	18
2069	9	-1	26	-1	9	-60	18
2070	31	-1	-16	-2	21	-51	18
2071	86	-2	-26	-6	-26	-43	18
Minimum	5	-2	-31	-10	-32	-62	18
25th %ile	21	-1	-15	-5	-11	-53	18
Median	31	-1	4	-3	2	-47	18
Mean	34	-1	-0	-4	1	-48	18
75th %ile	47	-1	12	-2	11	-44	18
Maximum	87	-0	38	-1	28	-33	18

References

Banta, Edward R. 2000. “MODFLOW-2000, the U.S. Geological Survey Modular Ground-Water Model - Documentation of Package for Simulating Evapotranspiration with A Segmented Function (ETS1) and Drains with Return Flow (DRT1). Open-File Report 00–466.”

DWR. 2007. “Spatial CIMIS Dataset.” https://cimis.water.ca.gov/SpatialData.aspx.

———. 2021. “CIMIS Station Reports.” https://cimis.water.ca.gov/WSNReportCriteria.aspx.

Foglia, Laura, Alison McNally, Courtney Hall, Lauren Ledesma, Ryan Hines, and Thomas Harter. 2013. “Scott Valley Integrated Hydrologic Model : Data Collection , Analysis , and Water Budget.” April. University of California, Davis. http://groundwater.ucdavis.edu/files/165395.pdf.

Foglia, Laura, Alison McNally, and Thomas Harter. 2013. “Coupling a spatiotemporally distributed soil water budget with stream-depletion functions to inform stakeholder-driven management of groundwater-dependent ecosystems.” *Water Resources Research* 49: 7292–7310. https://doi.org/10.1002/wrcr.20555.

Foglia, Laura, Jakob Neumann, Douglas G. Tolley, Steve Orloff, Richard L. Snyder, and Thomas Harter. 2018. “Modeling guides groundwater management in a basin with river–aquifer interactions.” *California Agriculture* 72 (1): 84–95.

Harbaugh, Arlen W. 2005. “MODFLOW-2005 , The U .S. Geological Survey Modular Ground-Water Model — the Ground-Water Flow Process.”

Harbaugh, Arlen W., Edward R. Banta, Mary C. Hill, and Michael G. McDonald. 2000. “Modflow-2000 , the U.S. Geological Survey Modular Ground-Water Model User Guide To Modularization Concepts and the Ground-Water Flow Process, Tech. Rep. 00-92.” https://pubs.usgs.gov/of/2000/0092/report.pdf%0Ahttp://www.gama-geo.hu/kb/download/ofr00-92.pdf%0Ahttp://doi.wiley.com/10.1029/2006WR005839.

Nash, J. E., and J. V. Sutcliffe. 1970. “River flow forecasting through conceptual models part I - A discussion of principles.” *Journal of Hydrology* 10 (3): 282–90. https://doi.org/10.1016/0022-1694(70)90255-6.

Niswonger, Richard G., Sorab Panday, and Motomu Ibaraki. 2005. “MODFLOW-NWT , A Newton Formulation for MODFLOW-2005. USGS Techniques and Methods 6-A37.” In *Section a, Groundwater; Book 6, Modeling Techniques*, 1–44. U.S. Geological Servey Groundwater Resources Program. https://pubs.usgs.gov/tm/tm6a37/pdf/tm6a37.pdf.

Poeter, Eileen P., and Mary C. Hill. 1998. “Documentation of UCODE, a Computer Code for Universal Inverse Modeling. U.S. Geological Survey Water-Resources Investigations Report 98-4080.”

Poeter, Eileen P., Mary Hill, D. Lu, and C. R. Tiedeman. 2014. IGWMC: Colorado School of Mines.

Prudic, David E., Leonard F. Konikow, and Edward R. Banta. 2004. “A New Streamflow-Routing (SFR1) Package to Simulate Stream-Aquifer Interaction with MODFLOW-2000.”

R Core Team. 2020. “R: A Language and Environment for Statistical Computing.” Vienna, Austria: R Foundation for Statistical Computing. https://www.r-project.org/.

Snyder, R. L., M. Orang, and S. Matyac. 2002. “A long-term water use planning model for California.” *Acta Horticulturae* 584: 115–21. https://doi.org/10.17660/ActaHortic.2002.584.13.

Tolley, Douglas G., Laura Foglia, and Thomas Harter. 2019. “Sensitivity Analysis and Calibration of an Integrated Hydrologic Model in an Irrigated Agricultural Basin with a Groundwater-Dependent Ecosystem.” *Water Resources Research* 55 (8). https://doi.org/10.1029/2018WR024209.

Appendix 2-F Scott Valley Integrated Hydrologic Model (SVIHM) Documentation - Previous Reports

Technical Team Note for Appendix 2-F, July 20, 2021

Appendix 2-F includes one report and three papers published in academic journals which document the development of the Scott Valley Integrated Hydrologic Model (SVIHM) over several years. The citations for these papers are listed below.

Foglia, Laura, Alison McNally, Courtney Hall, Lauren Ledesma, Ryan Hines, and Thomas Harter. 2013. "Scott Valley Integrated Hydrologic Model: Data Collection, Analysis, and Water Budget." http://groundwater.ucdavis.edu/files/165395.pdf.

Foglia, Laura, Alison McNally, and Thomas Harter. 2013. "Coupling a Spatiotemporally Distributed Soil Water Budget with Stream-Depletion Functions to Inform Stakeholder-Driven Management of Groundwater-Dependent Ecosystems." *Water Resources Research* 49: 7292–7310. https://doi.org/10.1002/wrcr.20555.

Foglia, Laura, Jakob Neumann, Douglas G. Tolley, Steve B. Orloff, Richard L. Snyder, and Thomas Harter. 2018. "Modeling Guides Groundwater Management in a Basin with River–Aquifer Interactions." *California Agriculture* 72 (1): 84–95.

Tolley, Douglas G., Laura Foglia, and Thomas Harter. 2019. "Sensitivity Analysis and Calibration of an Integrated Hydrologic Model in an Irrigated Agricultural Basin with a Groundwater-Dependent Ecosystem." *Water Resources Research* 55 (8). https://doi.org/10.1029/2018WR024209.

UCDAVIS
UNIVERSITY OF CALIFORNIA

April 2013

North Coast Regional Water Board, SWRCB Contract 09-084-110 and 11-189-110.

Scott Valley Integrated Hydrologic Model: Data Collection, Analysis, and Water Budget

Final Report

Prepared by:

Laura Foglia, Alison McNally, Courtney Hall, Lauren Ledesma, Ryan Hines, and Thomas Harter

Department of Land, Air, and Water Resources

University of California, Davis

Prepared for:

North Coast Regional Water Board

With funding by:

North Coast Regional Water Board, Contract #09-084-110

State Water Resources Control Board, Contract #11-189-110

FINAL REPORT

Version

April 22, 2013

Suggested Citation:

Foglia, L., A. McNally, C. Hall, L. Ledesma, R. J. Hines, and T. Harter, 2013. Scott Valley Integrated Hydrologic Model: Data Collection, Analysis, and Water Budget, Final Report. University of California, Davis, http://groundwater.ucdavis.edu, April 2013. 101 p.

Corresponding author:

Thomas Harter, ThHarter@ucdavis.edu

Table of Contents

List of Figures

List of Tables

Executive Summary

The Scott Valley is an agricultural groundwater basin in Northern California, within the Scott River watershed and part of the much larger Klamath Basin watershed straddling the California-Oregon border. The Scott River provides important habitat for salmonid fish, including spawning and rearing habitat for coho and fall-run Chinook salmon and steelhead trout. Sufficient flows at adequately low temperatures during summer, for rearing, and fall, for spawning, are critical for healthy fish habitat in the mainstem and tributaries.

This report presents the data assembled and the methods used for data analysis and data modeling to prepare the Scott Valley Integrated Hydrologic Model Version 2, which is currently under development. The report includes precipitation data analysis, streamflow data analysis and modeling, geology and groundwater data review and analysis, evapotranspiration and soils data analysis, and preparation of relevant watershed, land use, topography, and irrigation data. The data collection and analysis efforts culminate in the development of a spatio-temporally distributed soil water budget model for the Scott Valley. The soil water budget model is used to determine spatially and temporally varying groundwater pumping rates, surface water diversion rates, and groundwater recharge across the groundwater basin. The spatial resolution of the soil water budget model is by individual fields (land use polygons). Temporal discretization is in daily time steps for the period from October 1, 1990 to September 30, 2011. This period includes several dry years, average years, and wet year periods. Methods and results of the soil water budget model are presented in this report. This report represents the next step toward a better understanding of the interactions between groundwater, surface water, landuse, and agricultural practices with a specific focus on the seasonal impacts of groundwater pumping on streamflow during critical low flow periods.

The work presented here relies on an extensive data collection facilitated by the voluntary and active collaboration of communities, landowners, the Scott River Watershed Council (SRWC), the Siskiyou Resource Conservation District (SRCD), and the Scott Valley Groundwater Advisory Committee (GWAC) which has been appointed by the Board of Supervisors in January 2011, meeting monthly since April 2011 and advising UC Davis on its data collection and modeling efforts.

In the data analysis and during the model development, numerous assumptions have been made as is common in building a conceptual and numerical integrated hydrologic model. Models cannot represent the complexity of the real system, but are an effort to capture salient hydrologic features with sufficient accuracy to develop modeling results that are useful for a better understanding of the watershed dynamics and water balance.

A key feature of the integrated hydrologic model includes that individual fields and other individual land use parcels are characterized by a set of properties (or attributes) that include:

- Land use: all land use has been simplified in that we divided the diversity of land use into four main categories: 1) Alfalfa/grain rotation, 2) Pasture, 3) land use with evapotranspiration but no irrigation (includes natural vegetation, natural high water meadow, misc. deciduous trees,

trees, riparian vegetation), and 4) land use with no evapotranspiration and no irrigation, but with potential recharge from precipitation via soil moisture storage (barren, commercial, dairy, extractive industry, municipal, industrial, paved, etc);

- Soil type: characterized by water holding capacity. For the Scott Valley, we are using a root-zone depth of 4 ft and also evaluate a hypothetical root-zone depth of 8 ft;
- Irrigation efficiency, which is usually determined by irrigation type. In the Scott Valley, flood, center pivot sprinkler, and wheel-line sprinkler irrigation are used almost exclusively; we also consider historic conversion of some fields from flood or sprinkler irrigation to center pivot irrigation, based on a review of 1990 - 2011 aerial photos;
- Water source: groundwater, surface water, subirrigated (shallow groundwater table), mixed groundwater-surface water, and non-irrigated (dry land farming).

Other key assumptions and simplifications include:

- the attributes of each polygon (landuse, irrigation type, irrigation source) do not change throughout the 21 year period except for conversion from sprinkler to center pivot on documented alfalfa/grain rotation fields;
- irrigated water is applied continuously and uniformly over the entire irrigation period, a simplification of the actual irrigation practice, where irrigation is applied during a number of specific irrigation events, the timing of which varies from field to field; also, the simulation does not account for irrigation non-uniformity within fields or between fields;
- applied irrigation amounts are computed based on crop evapotranspiration, which has been estimated from climate data; irrigation amounts are adjusted for precipitation, soil moisture availability, and account for commonly assumed irrigation efficiency of the irrigation system. This concept has been developed for the California Department of Water Resources (CDWR) Consumptive Use Program (Orang et al., 2008);
- reference ET, a key driver for simulating irrigation applications, is calculated from climate station data using the NWSETO program developed at UC Davis and is based on the Hargreaves and Samani (1982) equation;
- the start of the irrigation season is triggered by soil water depletion to 45% of soil water holding capacity (equivalent to a depletion factor of 0.55), recommended by FAO Publication 56, Table 22.
- direct uptake from shallow groundwater table is not accounted for in the soil water budget approach, but will be simulated in the integrated hydrologic model that is currently under development

The soil water budget approach presented here does not represent a complete water budget for either the surface watershed or the groundwater basin, since it does not include stream-groundwater interaction or evapotranspiration off shallow water-table from non-irrigated crops or natural landscapes. However, a streamflow regression analysis is performed to estimate all monthly tributary inflows into the Scott Valley based on incomplete sets of measured data. A complete surface watershed or groundwater basin budget requires an integrated groundwater-

surface water model which is now under development (Scott Valley Integrated Hydrologic Model Version 2, to be completed by early 2014).

Output from the soil water budget simulation includes daily land use polygon (field) specific soil water fluxes in water years 1991 through 2011. These are aggregated to provide monthly, yearly and long-term average rates by polygon, by land use, and by subwatershed. The report presents and discusses the following output results obtained from the soil water budget simulation:

- irrigation from surface water and groundwater sources;
- recharge;
- crop evapotranspiration under optimal irrigation (no shortage);
- actual evapotranspiration after accounting for limited available water in the root zone (limited surface water supplies, no irrigation);
- water uptake deficiency.

Results of the soil water budget model are typical of Northern California, given the land use, irrigation water source, irrigation type, and precipitation and given the limitations listed above to build the soil water budget model. For example, average monthly recharge and pumping rates indicate strong seasonal changes. Most pumping occurs during summer months and most recharge occurs in late winter and early spring. On pasture, significant recharge may also occur during the irrigation season due to widespread surface water flooding at rates that are significantly higher than crop water use (relatively lower irrigation efficiency). In August-September, streamflow available for flood irrigation decreases significantly leading to increased pumping on some pasture fields, typically at higher efficiency than with flood irrigation and, hence, less recharge. Recharge in alfalfa is highest in July and August, when all fields are fully irrigated. Fields in grains (12.5% of the alfalfa/grain cropping area) are fallow after their harvest in July without significant recharge or pumping in August and September. During the winter months, differences in the amount of recharge between the three land use categories reflect varying levels of soil moisture depletion and slight differences in average soil characteristics across each land use type, mainly hydraulic conductivity and water holding capacity.

Simulated irrigation amounts have been compared with field-estimated applied water values provided by alfalfa and pasture irrigators engaged in the Scott Valley Groundwater Advisory Committee (GWAC). We find that the water budget model significantly overestimates the amount of applied water compared with grower-reported rates and compared with recent field measured amounts. Hence, the current approach will need further development to reconcile the differences between the ET-based soil water budget model and field irrigation rate data. The largest discrepancy is found in the amount of irrigation applied to alfalfa, which the model overestimates by 25% or more given the reported values. Probable explanations for the discrepancy include uncertainty in the available evapotranspiration and reference evapotranspiration rates for alfalfa and the lack of accounting for irrigation non-uniformity. The latter may effectively lead to higher than assumed irrigation efficiency. New data are collected in an ongoing field campaign. These will be critical to update irrigation rates in future versions of the soil water budget model.

The current soil water budget model has two important characteristics that make it rather useful for understanding the hydrology of Scott Valley: 1) it has been developed to allow for rapid adjustment of inputs and/or model assumptions. Results can be refined in the future, and further sensitivity analysis and tests can be performed as new data become available; and 2) it is a tool that has been developed in close collaboration with local stakeholders, agency personnel, and scientists, which is critical for constructive discussion of different water management scenarios and to mitigate conflicts.

1 Acknowledgments

Many people have supported our efforts of collecting, analyzing, and interpreting data. We acknowledge the feedback, support, and reviews that we have received from the Scott Valley Groundwater Advisory Committee, the Siskiyou Resources Conservation District, the Scott River Watershed Council, the Natural Resources Conservation Service Yreka Office, the County of Siskiyou, Ric Costales with the County of Siskiyou, Steve Orloff with University of California Cooperative Extension, Bryan McFadin with the North Coast Regional Water Board, Deborah Hathaway with Papadopulos and Associates, and from Sari Sommarstrom at Sommarstrom & Associates. These collaborations were critical for developing a better understanding of agricultural practices in Scott Valley. Review comments were helpful in clarifying this report. We are also grateful to Prof. Samuel Sandoval Solis, University of California, Davis, for his collaboration on analyzing precipitation data and providing a new classification of the water year types.

Funding has been provided by the North Coast Regional Water Board, through Contract #09-084-110 and the State Water Resources Control Board, through Contract #11-189-110. The opinions and conclusions in this report are those of the authors and are not necessarily shared by the funding agency or any of the project partners, cooperators, or reviewers.

2 Introduction

The Scott Valley is an agricultural groundwater basin in Northern California, within the Scott River watershed and part of the much larger Klamath Basin watershed straddling the California-Oregon border. The Scott River provides important habitat for salmonid fish, including spawning and rearing habitat for coho (*Onchorhynchus kisutch*) and fall-run Chinook salmon (*Onchorhynchus tschawytscha*) and steelhead trout (*Onchorhynchus mykiss*). Sufficient flows at adequately low temperatures during summer, for rearing, and fall, for spawning, are critical for healthy fish habitat in the mainstem and tributaries.

During the dry summer, streamflow in the Scott River system is low and relies almost entirely on groundwater return flow (baseflow) from the alluvial aquifer system underlying Scott Valley. Summer streamflows in dry years have been markedly lower since the late 1970s, when compared to the 1940s to 1960s. Both Van Kirk and Naman (2008) and Drake et al. (2000) concluded that a statistically significant contribution of this downward trend is due to climate effects represented by reduced snowpack at lower elevations, while Van Kirk and Naman (2008), using statistical analysis, also asserted that groundwater pumping for irrigation and increased consumptive water use was a significant cause. A physically-based groundwater model was used by S.S. Papadopulos & Associates (2012) to estimate potential late summer/early fall stream depletion impacts associated with groundwater pumping for irrigation.

As a result of low streamflow, but also due to the lack of widespread riparian vegetation, temperatures in the Scott River may exceed critically high temperatures during the summer months (North Coast Regional Water Quality Control Board, Staff Report for the Action Plan for the Scott River Watershed Sediments and Temperature TMDLs, 2011).

A groundwater (GW) study plan was requested of Siskiyou County and its Scott Valley stakeholders, as set forth in the Action Plan for the Scott River Watershed Sediment and Temperature Total Maximum Daily Load (TMDL, adopted Dec. 2005 by the Regional Water Board [RWB]). The Action Plan sets forth the elements to be contained in the GW Study Plan; it also identifies the needs of the RWB for certain information to be developed from the groundwater studies proposed in the GW Study Plan. It has been agreed by Siskiyou County and Regional Water Board staff that better knowledge of the hydrology and alluvial aquifer is needed to develop a possible array of solutions to water issues and associated problems. Siskiyou County with its management jurisdiction over groundwater (the RWB has water quality jurisdiction over GW under the Porter-Cologne Act) is committed to taking a community-based approach to implementing the GW Study Plan. The Scott Valley Community Groundwater Study Plan was developed by the University of California at Davis (Harter and Hines, 2008) with the voluntary assistance of communities, landowners, the Scott River Watershed Council (SRWC), and the Siskiyou Resource Conservation District (SRCD). The GW Study Plan was adopted by the Siskiyou County Board of Supervisors in February 2008. The primary goal of the GW study plan is: *"To provide a scientific approach that can be used by Siskiyou County, the Scott Valley community, the State of California, and other interested parties to objectively assess the Scott Valley's groundwater resources and their effect on surface water resources."* (Harter and Hines, 2008).

Subsequently, the Board of Supervisors appointed the Scott Valley Groundwater Advisory Committee (GWAC) in January 2011, a group which has been meeting monthly since April 2011. This committee supersedes the role of the Watershed Council (SRWC) for representing the community on groundwater matters.

The GW Study Plan provides an overall course of action to achieve the following overall study objectives:

1. consider groundwater occurrence throughout Scott Valley,
2. evaluate effects of groundwater on health of riparian vegetation,
3. evaluate effects of water use on Scott River flows,
4. identify opportunities and potential solutions for increasing water storage and/or addressing Scott River temperature issues, and
5. develop a tool capable of investigating groundwater hypotheses, such as those developed by the Scott River Watershed Council.

The GW Study Plan was intended to be a living blueprint of the hydrologic, ecologic, water resource management, and agricultural management research needs and of the investigative approaches that can be taken to develop management practices that meet the mandate for protection of water, agricultural, and ecological resources in the Scott Valley. The GW Study Plan summarizes the current status of knowledge about the hydro-agro-eco-geography of the Scott Valley and outlines potential approaches to addressing critical current research needs. Individual future study projects and tasks are described and scheduled to efficiently and timely make best use of funds to collect the information and data needed.

The GW Study Plan identifies further comprehensive analysis of existing data and development of new integrated groundwater-surface water assessment tools as a critical need. These tools are needed to understand the groundwater hydrology of the Scott River system and its relationship to surface hydrology, especially in areas where groundwater could affect Scott River water temperatures, potential riparian vegetation, and habitat connectivity for anadromous fish. Without integrated, interdisciplinary knowledge of the groundwater hydrology of Scott Valley and its dynamic linkages with streamflow, solutions to specific issues outlined in the Scott River TMDL and Action Plan will not be possible. Baseline data are needed to determine the best approach in the design and implementation of water projects, water management alternatives, and strategies to protect anadromous fish while also providing for current users of water, including agricultural operations.

With the voluntary assistance of communities, landowners, the SRWC, the GWA, and the Siskiyou RCD, this report provides key elements proposed by the GW Study Plan as set forth in the Scott River TMDL Action Plan. This report provides a review of data collected since the publication of the GW Study Plan and the various analyses performed to prepare the Scott Valley Integrated Hydrologic Model. It includes precipitation data analysis, streamflow analysis and modeling, evapotranspiration data analysis and modeling, soils and groundwater data assembly and analysis,

landuse and topography data analysis, and development and analysis of a soil water budget model to estimate field-by-field daily pumping and groundwater recharge in the Scott Valley for Water Years 1991-2011. A separate report will be prepared on the integrated hydrologic modeling efforts with MODFLOW, once completed, by early 2014.

In this report we occasionally refer to Version 1 and Version 2 of the Scott Valley Integrated Hydrologic Model: Version 1 corresponds to the initial groundwater flow model developed with MODFLOW-2000 (Harbaugh et al., 2000) by a graduate student (Ryan Hines) and hand-calibrated against measured water level data. While unpublished, several presentations have been given on this tool at the community and agency level, which is the main reason for distinguishing the version currently in development from these earlier efforts. Version 2 is a revised integrated hydrologic model, also using MODFLOW-2000 and its Stream-Flow Routing Package, but with an improved water budget representation including a more detailed and realistic representation of irrigation practices and cropping patterns in the Scott Valley. For the development of Version 2, additional data collection and analysis was conducted to develop the new soil water budget model and to improve the conceptual basis of the integrated hydrologic model. This report combines relevant data first collected during the Version 1 development phase and all of the additional data and data analysis prepared for the Version 2 modeling effort in a single, comprehensive document.

The motivation for developing these integrated hydrologic modeling tools is based on acknowledging the importance of:

1. understanding how past and current pumping affects groundwater flows to the Scott River and how alternative future water management activities affect groundwater flow;
2. helping mediation of conflicts between:
    a. Landowners in Scott Valley, mostly farmers depending on agricultural pumping for crop production,
    b. Indian tribes downstream and commercial fisheries off-coast that depend on healthy fish populations,
    c. California Department of Fish and Wildlife, the U.S. Fish and Wildlife Service and the U.S. National Marine Fisheries Service responsible for the implementation of the state and federal Endangered Species Act (ESA; 16 U.S.C. 1531 et seq.)
    d. North Coast Regional Water Quality Control Board, State Water Resources Control Board, and U.S. Environmental Protection Agency responsible for the implementation of California's Porter-Cologne Water Quality Control Act and the Federal Clean Water Act.

A collaborative and open approach has been established involving many stakeholders, including local landowners, Valley residents, native tribes, and fisheries to develop acceptable concepts consistent with scientific as well as local knowledge of the system. Furthermore, there is a general need to improve communication between scientists, regulatory and planning agencies, environmental advocacy groups, and diverse local/regional stakeholder groups to develop sustainable water resources management. This study is designed as part of an effort to benefit

these diverse stakeholder groups and communities by fully integrating currently available data, modern scientific methods, local-regional education, and public outreach.

In the following chapters, an overview of the study area, a detailed description of the data collection effort and of the methods used for data analysis, a description of the concepts of the soil water budget model, and extensive results are presented. This information provides the foundation for the forthcoming integrated hydrologic model (Version 2) of the Scott Valley.

3 Study Area

3.1 Physical Setting

The Scott Valley is located in the Klamath Mountains of Northern California, approximately 30 miles south of the Oregon border in Siskiyou County. Scott Valley is approximately 25 miles long and 10 miles wide at the largest point, although much of Scott Valley is less than 3 miles wide. The Scott River flows through the eastern and northern part of the valley, from south to north and across its northern flank to exit the Valley at its northwest corner toward the Klamath River. Approximately 8,000 people live in Scott Valley and its two towns of Fort Jones and Etna. Land use and the local economy are dominated by agriculture, primarily beef cattle-raising and forage production (alfalfa and grain hay and pasture).

3.2 Geologic Setting

The geologic formations in the Scott Valley can be divided into two units, the surficial alluvial deposits, and the underlying bedrock that also comprises the upland areas surrounding the Valley. The consolidated bedrock history of the Scott Valley area consists of a complex process and accretion and metamorphosis of several Klamath terranes. The Scott Valley is a tectonic Quaternary basin situated within the Palezoic/Mesozoic Klamath Mountains Province. The terranes identified in the Scott Valley area contain similar rock type and all are of marine origin, with the exception of plutons and intrusions. The formation of the modern alluvial Scott Valley occurred in recent geologic time, approximately 2 million years ago (MYA), by Basin and Range extensional tectonics.

Consolidated bedrock terranes in the Scott Valley area are, from east to west, progressively younger, with older terranes situated structurally beneath younger deposits. The Trinity and Rail Creek terrane plagiogranites, located in the southeastern uplands of the Scott Valley area and forming a portion of the uplands drained by the East Fork of the Scott River, are the oldest tectonic rocks identified in North America and mark the oldest convergent (non-cratonic) margin identified in North America (Elder, personal communication, 2009). A succession of terranes were accreted or deposited on the area between 450 and 130 MYA and are, in succession: Yreka terrane, Central Metamorphic belt, Stuart Fork terrane, and Western Paleozoic and Triassic belt (Sawyers Bar, Western Hayfork, Rattlesnake terranes). Several intrusive events occurred over this time period as well, creating the mafic intrusive complex (MIC) rocks that intruded into the Trinity terrane and consist of pyroxenite and gabbro, and the intrusion of major Klamath plutons (Russian Peak) consisting of diorite to granodiorite in the period between 174 to 138 MYA (Elder, personal communication, 2009).

Structurally, the Scott Valley consolidated bedrock deposits range from pre-Silurian to Jurassic and possibly Early Cretaceous age, and consist of the following strata in order of upward succession: Abrams and Salmon schists, the Chanchelulla formation of Hinds, greenstones which correlate to either the Copley greenstone or the Applegate group, and ultrabasic and granitic intrusive rocks (Mack, 1958; State of California, State Water Resources Control Board, 1975).

Over time, the current Klamath Mountains underwent an uplifting sequence with the last major episode occurring 4 MYA, which accompanied a tilting of the Western Cascade ranges. Faulting and subsequent uplift of the Klamath Mountains caused the formation of a tectonic graben, of which Scott Valley is the western-most portion (Elder, personal communication, 2009). The current hydrographic position of the Scott Valley is controlled by activity that occurred along two of the principal faults forming the tectonic graben, the northern Greenhorn fault and the western Scott Valley fault. Indications are that the early course of the Scott River ran south-north and intersected the Klamath River at a point further to the east than currently, with the area comprising the current lower Scott River canyon belonging to a separate watershed. The activity along the Greenhorn and Scott Valley faults, however, caused a dip in the alluvial Scott Valley during the Quaternary period which resulted in the Scott River altering its course in the northern section of the alluvial valley and turning almost due west, capturing several tributaries as well. The activity along the Scott Valley fault also contributed to this stream capturing, and resulted in the realignment of several existing tributaries, which has left remnant alluvial fans which are now stranded (referred to as Pleistocene alluvium in Mack, 1958). The dip associated with activity along the Scott Valley fault has also resulted in a tilting of the bedrock across the valley floor from east to west, with a dip also in the northerly direction associated with the Greenhorn fault (Elder, personal communication, 2009).

The maximum exposed thickness of these remnant alluvial fan deposits is projected to be less than 50 feet. The deposits are poorly sorted and consist of sand and silty clay with well-rounded granodiorite, serpentine, chert, and quartzite boulders that average 1 foot in diameter. In the northern portion of the Scott Valley, the remnant alluvial fan deposits are found in isolated patches along the edges of the Oro Fino Creek Valley and Quartz Valley, and possibly near Etna Creek near the town of Etna. Those deposits along Quartz Valley and Etna Creek represent old alluvial fans formed by Shackleford and Etna Creeks. The alluvial fans consist of poorly sorted boulders of western-mountain origin set in a matrix of brown sandy clay to a depth of approximately 100 feet (Mack, 1958).

The remainder of the alluvium located in the Scott Valley is from a more recent time. It is composed of alluvial fan deposits, and stream-channel and floodplain deposits related to the present course of the Scott River and its tributaries. The recent alluvium ranges in thickness from 0 feet to possibly greater than 400 feet in the western portion of the Scott Valley, at its widest point. However, there is no evidence of alluvial material sufficiently coarse to support groundwater pumping below depths of 250 feet. The thickness of the alluvium decreases to both the north and the south. The alluvial deposits vary greatly in composition based on spatial distribution. Along the west side of the valley, from Etna northward to Quartz Valley, the principal streams have built large bouldery and cobbly alluvial fans which are generally most permeable in their mountainward reaches (fan apex). The channel deposits of these streams differ with regard to the percentage of granitic bouldery material which they contain, ranging from mainly finer clay and sand to larger gravel and granitic boulder debris. The composition of the alluvium deposited by the tributary streams to the Scott River differs widely. While most of the tributaries run dry during the early part of the summer, due to irrigation diversions and infiltration of streamflow into the coarse

gravel of the fanhead areas, other tributaries such as Crystal Creek maintain flow throughout the year owing to the relatively impervious nature of the underlying granitic rocks which prevent infiltration of streamflow to the groundwater aquifer (Mack, 1958).

At the downstream edge of the alluvial fans, the alluvium becomes progressively less coarse ranging to fine sand, silt, and clay. Groundwater well logs from these areas have shown that alluvium consists of lenses of water-bearing gravel confined between fairly impermeable beds of clay. The alluvium in this zone is much less permeable than the floodplain and stream channel deposits of the Scott River (Mack, 1958).

3.3 Data Availability and Assessment

Table 1 presents a summary of available data with information on data sources. In the following sections, data sources and methods of data analyses are described in more detail. Extensive analysis has been performed on all of these datasets to prepare input for the soil water budget model described in Sections 10 and 11, and for the Scott Valley Integrated Hydrologic Model Version 2 currently being developed. All data are archived either in Microsoft Excel spreadsheets or in an ESRI ArcGIS geospatial database using UTM 10 (NAD83) projection. The soil water budget model is written in FORTRAN code, which reads the necessary text files prepared using ArcGIS and Excel.

Table 1 Summary of available data

Data	Data source	Contact person or website	Notes
Climate Data			
• Average max daily temperature • Average min daily temperature • Max and min humidity • Wind speed • % cloud cover • Precipitation	National Climatic Data Center (NCDC)	http://www.ncdc.noaa.gov/oa/ncdc.html	These inputs are used in the NWSETO program to calculate the reference evapotranspiration (ET_0). Stations examined included Callahan (CAL), Fort Jones Ranger Station (FJN), and Greenview. However, the Greenview data was incomplete and was not used. For both CAL and FJN, data for precipitation, snow amounts (in water equivalents), and minimum and maximum temperatures was downloaded from the NCDC.
Streamflow Data			
Streamflow	USGS, DWR, SRCD	http://cdec.water.ca.gov/ SRCD data: see table 4	Gauging data available for: Scott River Ft. Jones (USGS 11519500), Shackleford Creek near Mugginsville (F25484); Mill Creek near Mugginsville (F25480); French Creek at Highway 3 near Callahan (F25650); Sugar Creek near Callahan (F25890); Scott River, East Fork, at Callahan (F26050); and Scott River, South Fork, near Callahan (F28100). Mofett Creek, Etna Creek, Patterson Creek, and Kidder Creek.
Data used to create the GIS layers			
Elevation data	Gesch, 2002, 2007 LiDAR data, 2010 (North Coast Regional Water Quality Control Board, NCRWQB)	http://ned.usgs.gov Watershed Sciences, Inc. , obtained from the NCRWQB	Used for the thalweg definition
Model extent	Mack Report	Mack, 1958	Modified for this project.
Land use, water source, irrigation methods	California Department of Water Resources, Division of Planning and Local Assistance (DPLA)	http://www.water.ca.gov/landwateruse/lusrvymain.cfm	Detailed inputs were provided by GWAC and have been used to update the DWR map.
Soil type, water holding capacity	Soil Survey Geographic (SSURGO) database	The Natural Resources Conservation Service (NRCS) National Geospatial Management Center. http://soildatamart.nrcs.usda.gov/	
Wells	California Department of Water Resources		Wells were geo-located using a multi-step procedure depending on the information contained within the well records obtained from DWR (see Section 8). Some well locations were visually verified in the field. No measurements were performed.
Scott Valley Tributaries	Mack report	Mack, 1958	

4 Precipitation

Precipitation in Scott Valley is dominated by storms approaching the Valley from the west and south. The Valley is therefore in the rain shadow of the mountain ranges surrounding it to the west and south. Precipitation stations in Scott Valley are sparse, mainly concentrated in the central and west part of the valley. Two stations have a nearly complete record of daily data since the 1940s. To determine the most representative precipitation time series for the soil water mass balance, several methods of precipitation estimation for the valley were evaluated.

4.1 Precipitation - CDEC Dataset, Monthly Values for Callahan and Ft. Jones Only

The California Data Exchange Center provides monthly precipitation records (accumulated precipitation in each month), in inches/month, for the Callahan (CAL) and Fort Jones (FJN) stations. Both sets of data were retrieved from the CDEC website on 6/28/2012 (http://cdec.water.ca.gov/). The National Weather Service operates the CAL station, the U.S. Forest Service is responsible for the FJN station. To obtain annual precipitation totals, monthly data were added for each site for each water year (WY). A water year, commonly used in hydrological statistics, begins on October 1 of the previous calendar year and ends on September 30 of the current calendar year.

Years 1981-1983 at the CAL station were recorded as "missing data", so these years were removed from the initial analysis. Both, monthly and annual total precipitation at the CAL and FJN stations for WY 1944-2011 show a relatively strong linear trend (Figure 1). The correlation coefficient (r^2) is 0.82 for the monthly data and 0.77 for the annual totals indicating moderate correlation between the upper and lower valley precipitation. This data set was originally employed to develop a representative monthly precipitation time series (uniform across the Scott Valley groundwater basin) as part of a Version 1 (a draft version) of the Scott Valley Integrated Hydrologic Model. The average (mean) of the two annual data values was used to estimate the Scott Valley rainfall per WY. The linear regression equation obtained from the monthly totals was used to fill in the years 1981-1983 at the CAL station (Figure 1). With the CAL data series filled in, the average annual precipitation at CAL and FJN is 21.3 in/yr for 1944-2011, and 21.4 in/yr for 1991-2011. For WYs 1991-2011 (21 years), the average annual precipitation is 21.2 in/yr at FJN and only slightly higher, 21.5 in/yr, at CAL.

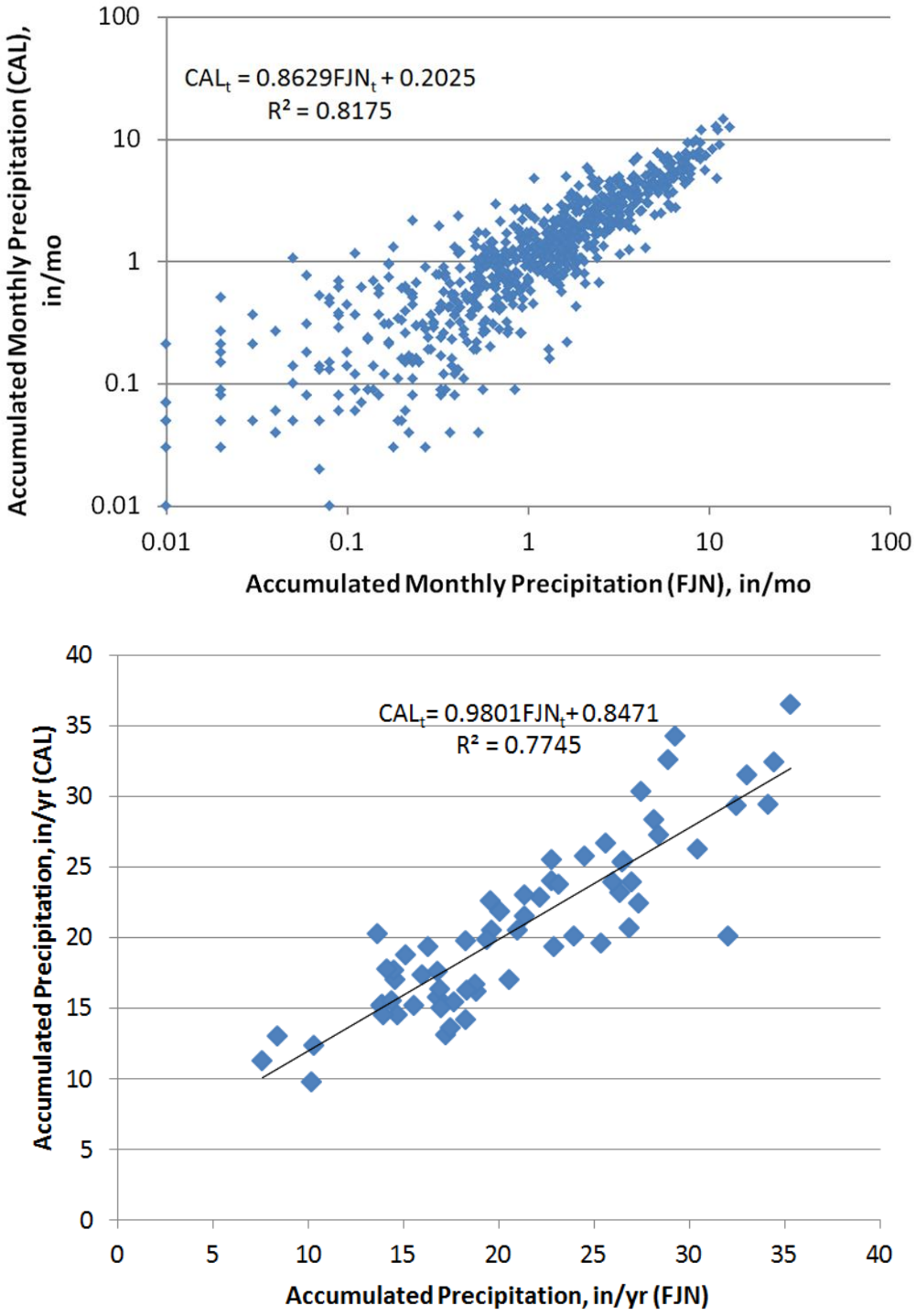

Figure 1. Linear regressions of the monthly (top) and annual (bottom) precipitation totals at Callahan (CAL) and Fort Jones (FJN) precipitation stations from 1944 to 2011, not including 1981-1983, for which CAL data are missing in the CDEC dataset. Note that the plot of the monthly precipitation data is on a log-log scale and does not show months in which either of the two stations recorded zero precipitation. The linear regression function is only shown for the annual precipitation data.

4.2 Precipitation - NOAA Dataset, Daily Values for Callahan and Ft. Jones Only

Daily precipitation data reported in units of tenth of millimeter [1/10 mm] was retrieved from the NOAA website (http://www.ncdc.noaa.gov/cdo-web/) for the Callahan and Fort Jones sites, GHCND:USC00041316 and GHCND:USC00043182, respectively, on June 29, 2012 (Figure 2). Ft. Jones station data begin in 1936, Callahan station data begin in 1943.

Summing daily precipitation data, not including missing days, for WYs 1944-2011, the average annual total precipitation is 17.8 in/yr for the Fort Jones station and 21.0 in/yr for the Callahan station. The average of monthly totals (unadjusted for missing values, occurring predominantly at the Fort Jones station), is 19.4 in/yr for WYs 1944-2011. Figure 3 shows the monthly distribution of the unadjusted monthly totals for the complete period of record. The average annual totals are significantly lower than those obtained from the CDEC monthly dataset (which are based on the same station values, but the CDEC data are aggregated differently). This is due to missing values being interpreted here as zero precipitation. This introduces a bias toward lower precipitation, which is addressed in two ways: by replacing missing values at one station with the values measured at the second station (this section), and by using statistical analysis (described in Section 4.4).

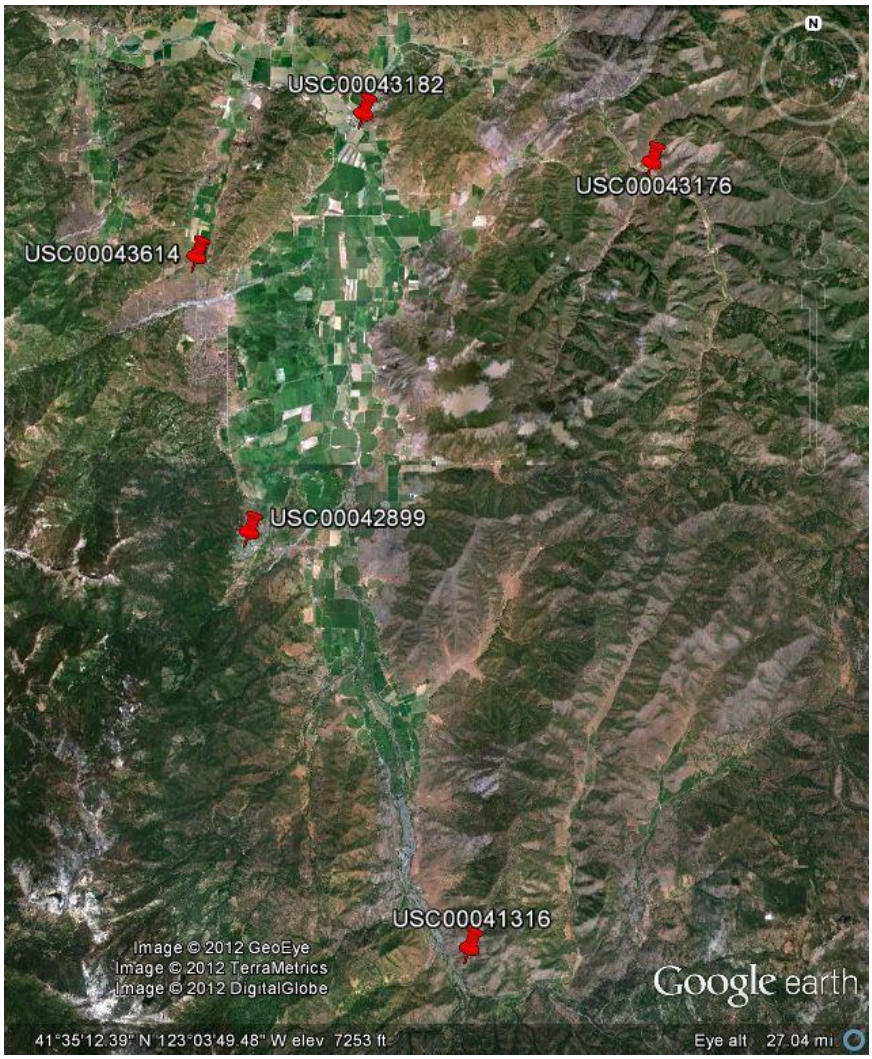

Figure 2. Precipitation gauges in Scott Valley with data available through NOAA. USC00043176 was not used, since it is outside of the Valley floor. USC00043182 corresponds to the CDEC "FJN" station and USC00041316 corresponds to the CDEC "CAL" station.

A plot of the precipitation time series at Fort Jones and Callahan shows that the sites follow similar precipitation patterns. Additionally, the peaks and troughs in the yearly precipitation are of similar magnitudes for the comparison time period, 1943-present.

The Wilcoxon rank-sum test was used to determine if the average precipitation (from the average of the precipitation at Callahan and Fort Jones) provided a good approximation for each site. Both time series compare to the average valley precipitation with 95% confidence, therefore the average valley precipitation can be considered a reliable model for the Scott Valley.

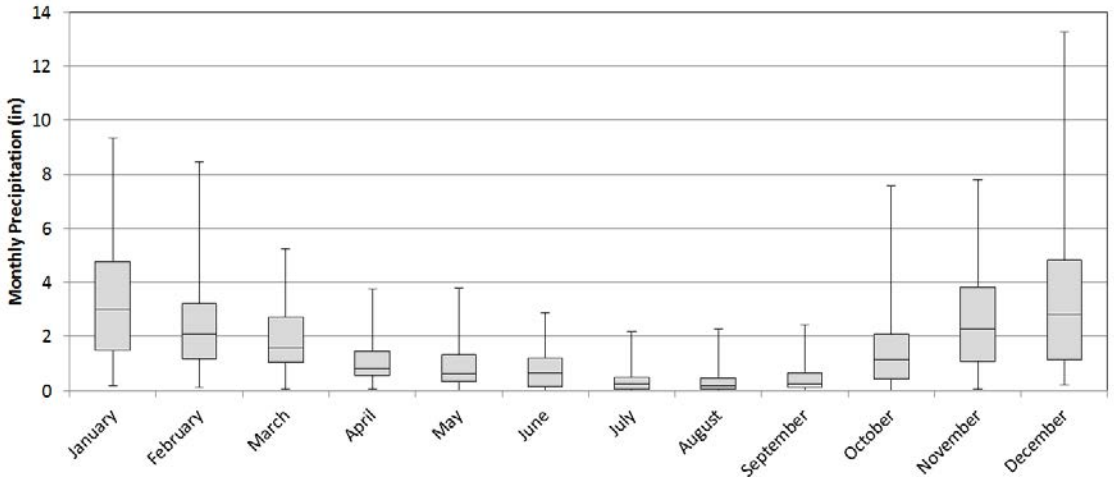

Figure 3. Minimum, 25% quartile, median, 75% quartile and maximum unadjusted monthly precipitation (average of Fort Jones and Callahan), 1944-2011. Missing daily data (mostly at the Fort Jones station) here counted as zero precipitation. See below for adjusted dataset results.

For purposes of classifying the water year type and for the soil water budget model presented below, missing data at one station (usually Ft. Jones) were replaced with measured data from the other station, rather than assuming zero precipitation on days with missing values and averaging the two stations' values. This procedure yielded a second, spatially uniform time-series of Scott Valley groundwater basin precipitation, with daily varying values for WY 1991-2011. This data series is in addition to the monthly average time series (Section 4.1). A more refined method for estimating missing data in this data series is described in Section 4.4.

Table 2 and Table 3 summarize the information collected from the NOAA internet site. Note that the elevation difference between the CAL and FJ stations is approximately 460 ft. Yearly total precipitation used in the soil water budget model is presented in Figure 4.

Table 2. Information about the two precipitation stations used: Fort Jones and Callahan (from NOAA, http://www.noaa.gov)

Fort Jones Ranger Station STN	**Callahan**
NOAA Station Id: CA043182	NOAA Station Id: CA041316
Latitude: 41°36'00N	Latitude: 41°18'40N
Longitude: 122°50'52W	Longitude: 122°48'16W
Elevation: 2725'	Elevation: 3185'

Table 3. Long-term historical averaged monthly precipitation and annual total for Fort Jones and Callahan in inches (from NOAA, http://www.noaa.gov). For this analysis, missing data at one station are replaced by the value measured at the other station prior to computing averages and totals.

Monthly Precipi-tation	Jan	Feb	Mar	Apr	May	Jun	Jul	Aug	Sep	Oct	Nov	Dec	Avg. Annu-al Total
Fort Jones	3.72	2.95	2.43	1.34	0.95	0.67	0.42	0.58	0.74	1.22	3.26	3.52	21.8
Callahan	3.72	2.94	2.44	1.34	1.15	0.82	0.46	0.35	0.64	1.39	2.95	3.1	21.3

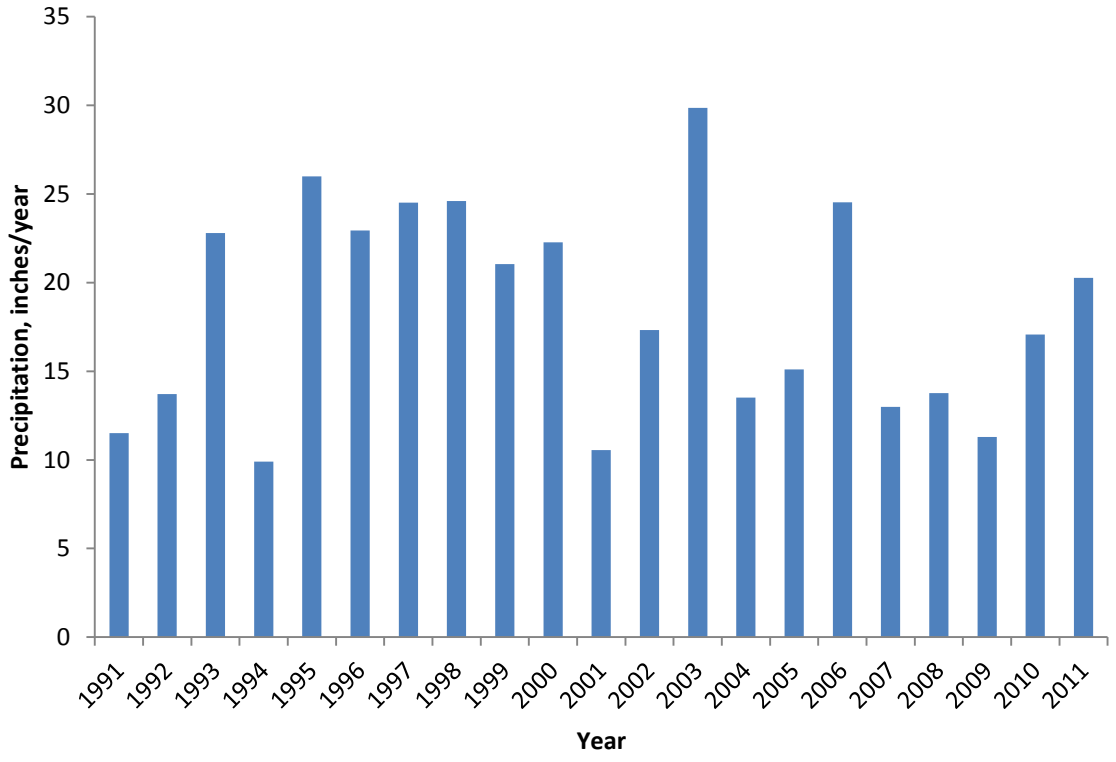

Figure 4. Precipitation in inches/year. One single value is used daily across the whole valley. For this analysis, missing data at one station are replaced by the value measured at the other station prior to computing averages and totals.

The adjusted precipitation data are used to recalculate year types. Our analysis principally relies on the analysis presented in Deas and Tanaka (2006). We updated their analysis to also include years 2005 through 2011. We recalculated the exceedance probability curve for the period 1936-2011, then used the percentile thresholds suggested in Table 4 (here: Figure 5) of Deas and Tanaka (2006), which identifies dry years, and then select these years in our 21 year modeling period, from 1990 - 2011. Results are presented in Figure 6.

Table 4. Expert Judgment Sample Classification System with Three and Four Year Types.

Year Type	October through March 31 Accumulated Precipitation (in)	Non-Exceedence Probability	Year Type	October through March 31 Accumulated Precipitation (in)	Non-Exceedence Probability
Dry	X < 10.2	X < 14%	Dry	X < 10.2	X < 14%
Normal	10.2 ≤ X < 21.7	14% ≤ X < 75%	Below Normal	10.2 ≤ X < 17.2	14% ≤ X < 50%
Wet	21.7 ≤ X	75% ≤ X	Above Normal	17.2 ≤ X < 21.7	50% ≤ X < 75%
			Wet	21.7 ≤ X	75% ≤ X

Figure 5. Expert judgment classification from Deas and Tanaka (2006), Table 4.

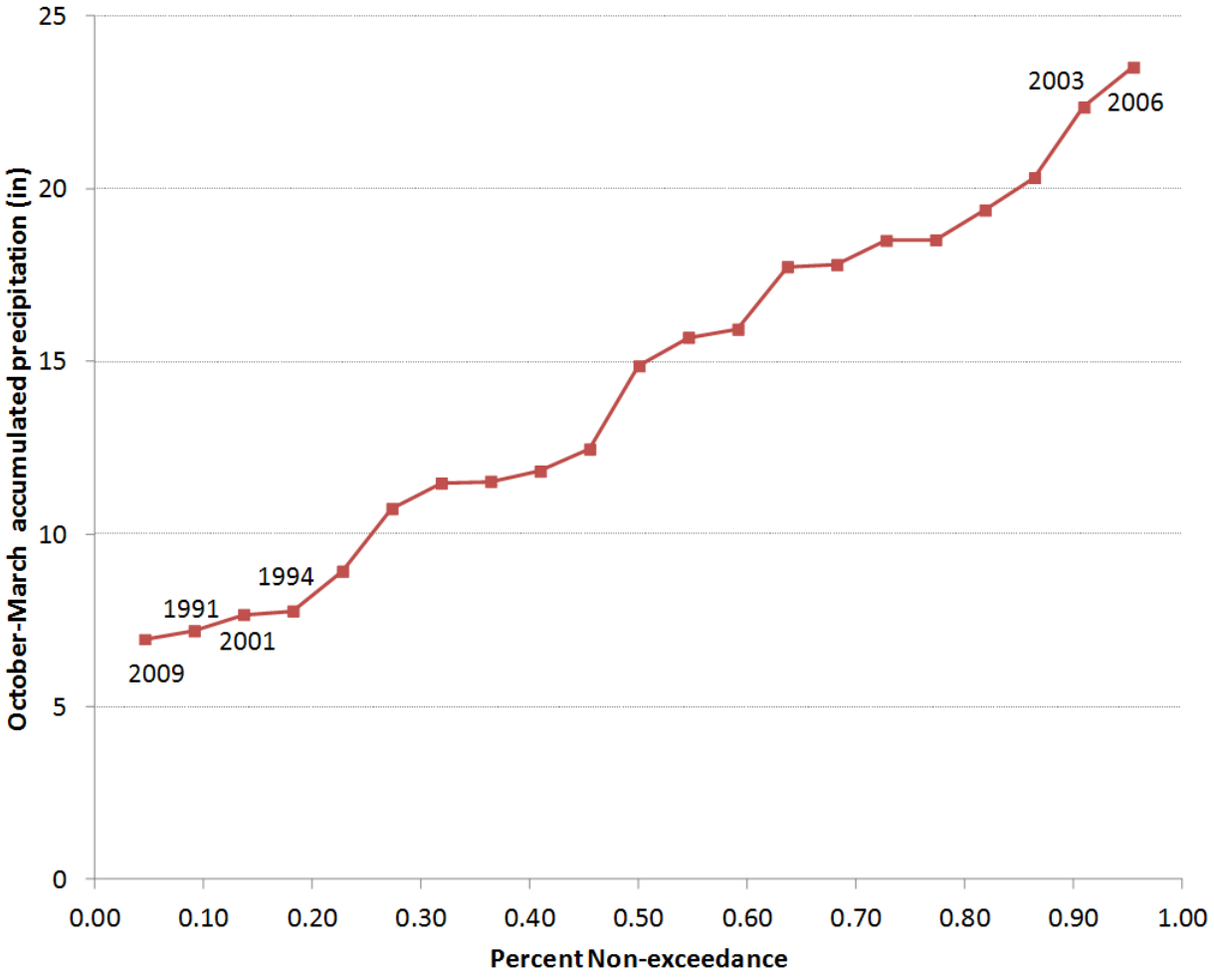

Figure 6. Analysis of precipitation to evaluate the year type.

Our results are in agreement with previous reports (Deas and Tanaka, 2005, 2006, 2009). The dry and below normal years identified in our study period are (listed in order from most dry to less dry): 2009, 1991, 2001, 1994, 1992, 2005, 2004, 2007, 2010, 2008, 2002, and 1993. The wettest years in the WY 1991 – 2011 period are 2006 and 2003. This order is slightly different from that

shown in Figure 4, since the year classification is based on October-March data and does not include precipitation in April through September.

4.3 Precipitation - Watershed Method, Annual Average Total Precipitation

California Rivers Assessment (CARA) is a computer-based data management system designed to provide access to information and tools with which to make sound decisions about the conservation and use of California's rivers (http://endeavor.des.ucdavis.edu/newcara/). For the Scott River Basin, CARA reports an average precipitation of 35.87 inches per year. The precipitation coverage is represented in a precipitation map showing lines of equal rainfall ("isohyets") based on long-term mean annual precipitation data compiled from maps and information sources at the USGS, the California Department of Water Resources, and the California Division of Mines. Source maps are based primarily on National Weather Service data for approximately 800 precipitation stations throughout California collected over a sixty-year period (1900-1960). The minimum mapping unit is 1000+ acres and the isohyet contour intervals are variable due to the degree of variation of annual precipitation with horizontal distance. The CARA database utilizes a weighted average to determine a single value of mean annual precipitation; the isohyet areas, after intersection, are multiplied by the average rainfall for each isohyet-derived polygon and divided by the total area of the CARA watershed[1].

The CARA Model suggests an average precipitation of 35.87 in/yr across the watershed, much higher than the 21.6 in/yr measured on the valley floor overlying the groundwater basin (see Section 4.2). The CARA watershed area of the Scott Valley includes the high precipitation and snowfall areas of the uplands and mountains. Spatial analysis of the CARA isohyet contour map against a satellite image of the Scott Valley (Figure 7) shows that the valley floor overlying the groundwater basin has average annual precipitation values of 18-22.5 inch isohyets. A spatial analysis of the contributing isohyet areas (Table 4) yields an estimated yearly precipitation of 20 in for the area overlying the Scott Valley groundwater basin comparable to the NOAA-derived estimation (Table 3).

[1] On 6/29/2012 the UC Davis Information Center for the Environment (ICE) was contacted to see how they created the CARA model. The response from ICE suggested that the model was outdated and use of PRISM (http://www.prism.oregonstate.edu/) or other more recent models would be more appropriate.

Table 4. Scott Valley precipitation, CARA model approach.

Average Precip per Isohyetal unit (in)	Area (acres)	Basin Relative Contribution	Valley Floor Relative Contribution
18	72130.97	0.14	0.56
22.5	57635.41	0.11	0.44
27.5	88116.19	0.17	N/A
35	127505.25	0.24	N/A
45	88614.9	0.17	N/A
55	55521.7	0.11	N/A
65	20445.65	0.04	N/A
75	10077.12	0.02	N/A
85	933.1	0.00	N/A
Average Precip (in/yr)=		35.87	20.00

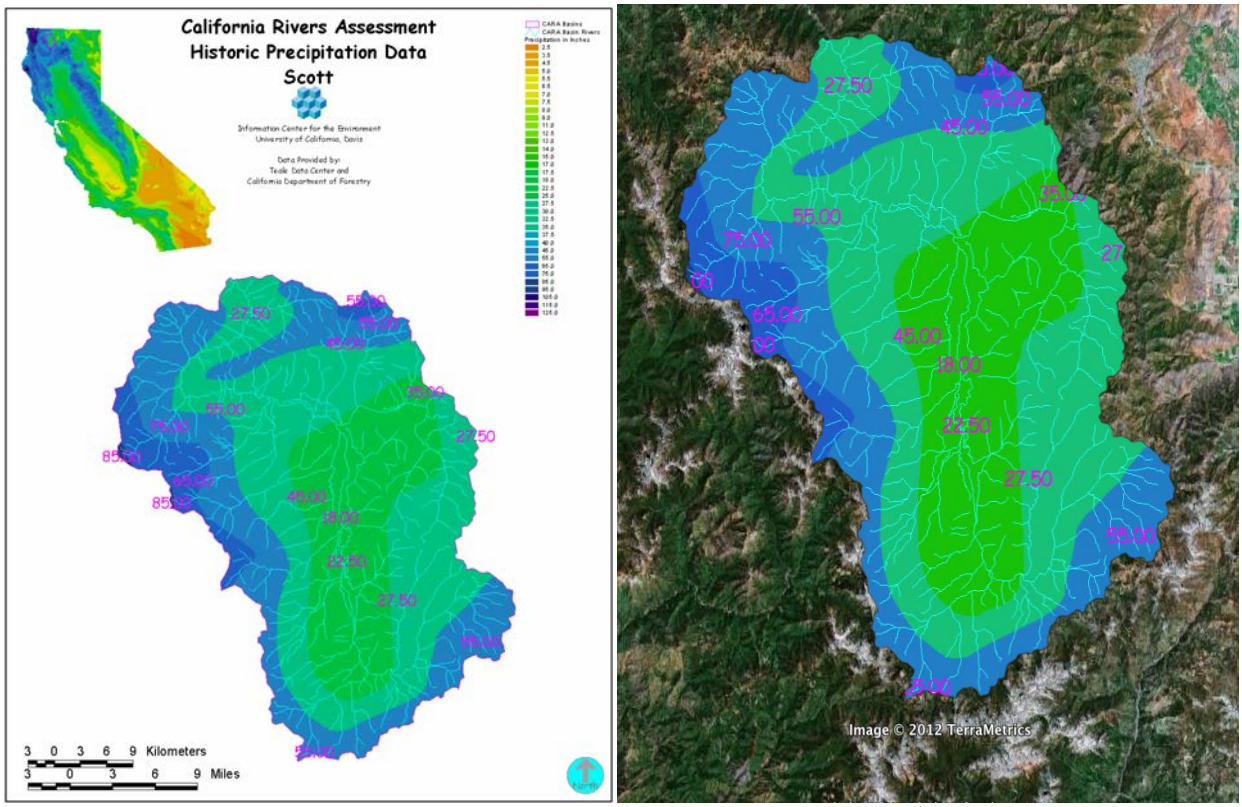

(A) (B)

Figure 7. CARA isohyet overlay for the Scott Valley (A) with aerial photo (B).

4.4 Considering Spatial Trends in the Precipitation Modeling Method

NOAA has precipitation stations not only at Fort Jones (station ID USC00043182) and Callahan (station ID USC00041316), but at two additional locations on the Scott Valley floor, at Greenview and at Etna (Figure 2). As mentioned above, the Fort Jones data series is the longest, beginning in 1936, while Callahan data are available from 1943 to present. Other stations have significantly shorter observation periods. The long historical datasets at Fort Jones and Callahan provide the most representative view of the highly variable precipitation record compared to other stations. But additional stations are valuable to determine possible spatial trends in precipitation patterns across Scott Valley. Furthermore, missing values at the Ft. Jones station (and the few missing values at the Callahan station are here replaced with statistically based estimates of the precipitation on missing data days to obtain a more accurate record of daily, monthly, and annual precipitation totals.

We use the NOAA precipitation data at all four Valley floor stations for further analysis and for developing regression equations. First, data were inspected visually and extreme outliers were removed. Then, with use of StatPlus®, the upper outlier boundary was calculated (Outlier≥Q3+1.5*IQR, where IQR is the inner quartile range). The subsequent data analysis was completed without those outling values.

The NOAA stations overlying the groundwater basin are located at Fort Jones, Callahan, Greenview, and Etna. The Fort Jones and Callahan stations are discussed in sections 2.1 and 2.2. The additional two stations are located in Etna and Greenview. Local residents report that precipitation is generally lower near the eastside of the valley floor than the westside of the valley floor. We used the additional precipitation records from Etna and Greenview to determine whether the climate station data available within the area overlying the Scott Valley groundwater basin are sufficient to verify such significant spatial trends..

Besides being of significantly less extent in time, the temporal resolution of the reported data differs across the precipitation stations: the Fort Jones and Callahan stations report precipitation values daily in 1/10th mm. The Greenview station reports precipitation values only as monthly totals in 1/10th mm. The Etna station reports precipitation values hourly in 1/100th in.

We applied a linear regression analysis to reconstruct complete precipitation records for the Etna and Greenview stations for 1943-2011, using StatPlus® software. The same regression procedure was used to also fill in the few missing values in the Fort Jones and those in the Callahan records during that time period. Separate regression equations were generated for each of twelve calendar months. For each month of the year, separate regressions were generated for each of the four stations against all other three station records (12 x 4 x [4-1] regression equations). At each of the four precipitation stations, the three regression equations were ranked separately for each of the twelve calendar months by their correlation coefficient. Missing daily precipitation data were then computed using the highest ranked station-to-station specific regression equation for

which data at any of the other three stations were available. For the Greenview station, regression equations were used to generate daily data from monthly total reported precipitation.

Daily data from October 1990 to September 2011 were compared for spatial precipitation trends across the Scott Valley groundwater basin. Over the 20 year study period, the average yearly precipitation, computed from the annual totals during 1990-2011 for Callahan, Fort Jones, and Greenview differed by less than 0.8 in (less than 4%), with values of 21.34, 22.05, and 21.27 inches respectively. At the Callahan station, 88% of the yearly precipitation occurs from October to April, while it is 90% at Fort Jones. Only about 2-inches of precipitation occur during the irrigation season, most of which would likely not reach the groundwater basin.

The Etna station recorded an average annual precipitation of 27.98 inches, approximately 30% higher than the other three stations. From Figure 7, we can see that the location of the Etna station places it on the edge of the model extent along the western mountains, not unlike the Greenview station.

To determine the quality of the estimated Greenview values, monthly precipitation from NOAA was compared with estimated monthly totals of daily data obtained from the regression analysis using a two sample homoscedastic t-test at alpha level 0.05. The test failed to reject the null hypothesis $H_0: \mu_1=\mu_2$ ($p=.05593$), so we can conclude that the regression precipitation values do not significantly differ from the NOAA values.

With all missing values at Greenview, Ft. Jones, and Callahan replaced by regression estimated values (but not considering the Etna data series), the average annual precipitation across all three stations, for WYs 1944-2011 is 21.3 in/yr, for WYs 1991-2011, it is 21.8 in/yr (Figure 11). In comparison, the average annual precipitation at Ft. Jones and Callahan only, with missing values replaced by estimated values, is 21.5 in/yr for WY 1944-2011 and 22.0 in/yr for WY 1991-2011, consistent with the average annual precipitation obtained from the CDEC dataset of monthly precipitation totals (see above). The precipitation data from the NOAA and CDEC online repositories are very similar, but not quite identical due to different handling of missing values in the aggregation of daily data to monthly data. They also differ in the time steps and measurement units of the reported values. But for practical purposes, these differences are negligible.

The precipitation measured at the Etna station often differs markedly from the values measured at the other stations, which prompted additional data analysis. In the 20 year period from October 1990 to September 2011, there are 167 days for which the difference between Etna and the average valley precipitation, computed from the Fort Jones, Callahan, and Greenview data, is greater than 0.5 inches. As shown in Figure 8A, Etna precipitation is frequently greater than the average valley precipitation. Figure 8B shows the same comparison but only for cases when Etna has precipitation exceeding 0.5 in. In some instances, Etna's precipitation is two orders of magnitude higher than the average valley precipitation. Of 167 days with differences exceeding 0.5 inches, only 40 days show Etna precipitation to be less than the average valley precipitation. Thirty-nine days return a difference between Etna and the average valley value that is larger than 1 inch. Of these, Etna has the lower precipitation on only 10 days. Notably, on each day where

Etna records a value that is more than 0.5 inches lower than the average, the Etna recording is 0 inches. It is therefore unclear, whether there are operating or local positioning biases to the Etna data series.

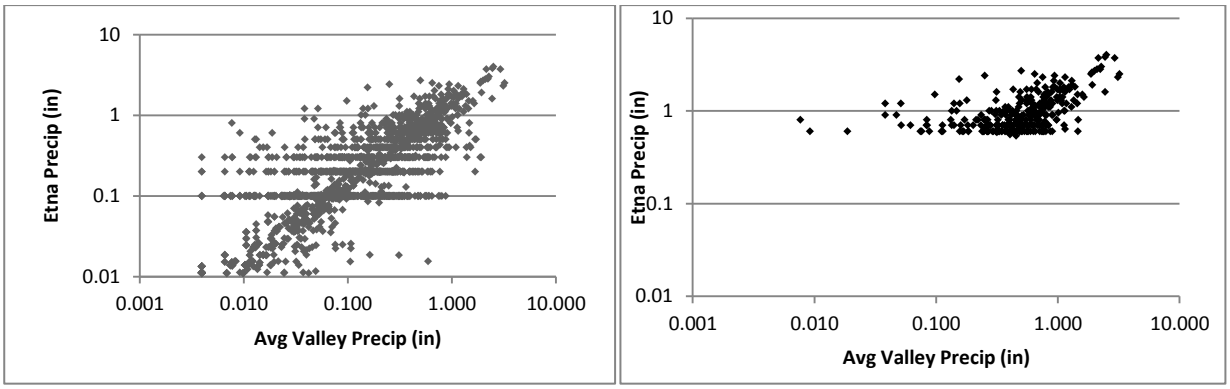

(A) (B)

Figure 8. Etna precipitation compared to average Scott Valley precipitation. A: all Etna precipitation; B: only Etna precipitation exceeding 0.5 in.

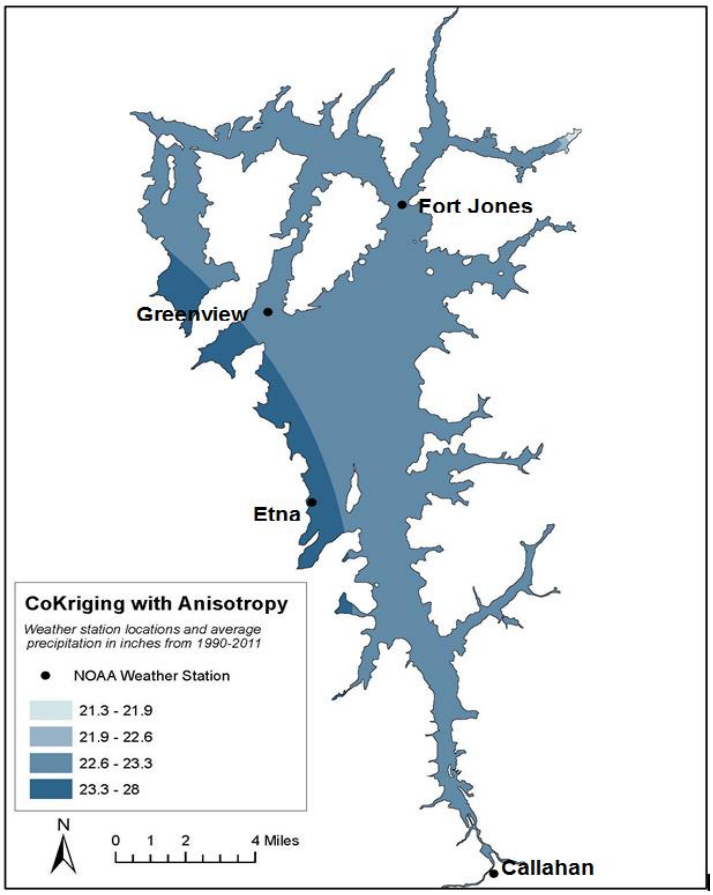

Figure 9. Valley floor precipitation cokriging interpolation with anisotropy.

Average annual total precipitation measured at Etna, Greenview, Fort Jones, and Callahan were interpolated (using ArcGIS®) and mapped across the groundwater basin (Figure 9). We used cokriging with large NNW-SSE anisotropy to map spatially variable precipitation across the valley. The anisotropy reflects the hypothesized strong precipitation gradient across the West-East extent of the valley. However, even if the Etna precipitation were considered relatively accurate, the high precipitation at the western-most margin of the Scott Valley groundwater basin only affects a relatively small area of the basin and would exclude the Greenview area. The Greenview station, also on the westside of the Valley, agrees well with those at Callahan and Fort Jones.

While of nearly identical yearly averages, daily values at Greenview, Callahan, and Fort Jones exhibit significant variance among each other, as would be expected across the significant extent of the groundwater basin (25 miles long and up to 10 miles wide at its widest point). But given that the integrated hydrologic model for which this data series is developed operates effectively at monthly stress periods, a spatially averaged daily precipitation value, obtained from the relatively complete Callahan and Fort Jones stations, is considered adequately representative of precipitation dynamics across the Scott Valley groundwater basin.

In conclusion, using the four available precipitation stations, it was not possible to either support or disprove the observation of a strong west-east gradient in precipitation totals reported by local residents. Additional stations on the eastern margin of the Valley and on the Valley's southwest side would be needed to support these qualitative observations. Furthermore, the number and location of the precipitation stations for which data were available, and the temporal extent of the data currently do not justify a spatially distributed precipitation map for the groundwater basin. Future precipitation gauges would be needed to enhance our understanding of orographic precipitation mechanisms in the valley, which may lead to alternative rainfall estimates. Until such additional data are available, daily precipitation across the entire Scott Valley groundwater basin is assumed to be uniform, represented by the arithmetic average of the measured daily Fort Jones and Callahan or at Fort Jones, Callahan, and Greenview, with missing data replaced by the regression estimated data. This time series, developed from daily data, was used for the streamflow regression analysis described in the next section.

The choice of uniform precipitation does not preclude future alternative approaches in the integrated hydrologic modeling effort. Spatially variable precipitation, if additional data become available, could be accommodated by the water budget model described in this report and hence become part of a groundwater-surface water model.

5 Streamflow

The Scott Valley groundwater basin and its overlying streams are fed by runoff from the surrounding mountains. Tributaries to the Scott River, including the two forks of the Scott River itself, emanate from the mountains carrying significant runoff.

Understanding groundwater-surface water interactions in the Scott Valley requires some knowledge of the streamflow amounts that enter the valley floor overlying the groundwater basin. In this section, we describe and investigate available data. We also construct time series of streamflow in all major tributaries of the Scott River and for the South Fork and East Fork of the Scott River, which join at the upper end of the Scott Valley floor. The main purpose for developing these time series is to provide an approximation of surface flows into the Scott Valley as part of the Scott Valley Integrated Hydrologic Model.

The eight tributaries of interest here are Sugar, French, Etna, Patterson, Kidder, Mill (a tributary to Shackleford Creek), Shackleford, and Moffett Creeks. There are other tributaries to the Scott River, but their flows tend to be ephemeral, relatively smaller, and their exact magnitude is not as critical to understanding groundwater-surface water interactions in Scott Valley. In an integrated hydrologic model, these may be represented as a diffuse source of recharge along the mountain front around Scott Valley. The Scott River itself is gauged near Callahan at both the East and South Forks (upstream of the confluence). An additional long-standing gauge ("Ft. Jones") is located downstream of Scott Valley, west of Fort Jones on the Scott River.

Location of the flow gauges has been provided by SRCD and is shown in Figure 10. The gauges at Sugar Creek, Moffet Creek, and Kidder Creek are located above irrigation diversions and do not reflect tributary inflows to the Scott River. Gauges at French Creek, South Fork, and East Fork are located at the margin, but within the Scott Valley.

Most of the tributaries have very limited records of streamflow gauging, while the Ft. Jones gauge has a complete record for the past seventy years (Figure 11). To develop an appropriate groundwater-surface water model for the Scott Valley groundwater basin, it is therefore necessary to also develop a model of the main stem and tributary streamflows, at the upgradient boundary of the Scott Valley floor, for those time periods for which no streamflow data are available.

Here, we chose to determine missing tributary and main stem streamflow data at the upstream margins of the groundwater basin through statistical regression analysis. A number of independent predictor variables are considered for the regression analysis: streamflow of the Scott River at the downstream Fort Jones gauging station, streamflow at the East Fork and South Fork gauging stations in Callahan, streamflows on the tributaries when measured (Table 5), precipitation data, temperature data, and snowpack data. The program R® was used to create linear regression models with accompanying diagnostic plots (see Appendix A).

5.1 Snow Water Content for Regression Modeling

Snow water content stations are located throughout the Scott Valley. The measurements considered here are those taken in the month of April. The stations at Box Camp (BXC) and Marble Valley (MBV) were not used since the snowmelt from these stations enters the Scott River downstream (north) of the Scott Valley. For the model, the yearly average of the measured snow water content at Middle Boulder 1 (MBL), Etna Mountain (ETN), Dynamite Meadow (DYM), Swampy John (SWJ), and Log Lake (LOG) were used to aggregate across intra-watershed variabilities and to obtain a representative dataset of the snow water content for the regression analysis.

An additional snowmelt-related variable investigated here is the number of days in a given calendar year (not water year), on which the temperature at Callahan exceeded 21°C. At this temperature the entire watershed is under snowmelt conditions.

5.2 Precipitation for Regression Modeling

Daily mean precipitation computed from measured data at the Fort Jones, Greenview, and Callahan stations for 1943 – 2011 (see Section 4.4) were used to compute the following additional independent variables in the regression:

“MoPrecip”: sum of the average daily precipitation during the current month t

“PrevMoPrecip”: sum of the average daily precipitation during the prior month, t -1

“WYPrecip2Date”: sum of the average daily precipitation between the beginning of the current water year (starting on October 1) and the beginning of the current month, t

“WYPrecip”: sum of the average daily precipitation for the entire water year, of which the current month, t, is part (a model with “perfect foresight” because it includes information that represents events in the future relative to the date of the estimated streamflow).

5.3 Flow Gauges

Daily mean discharge has been recorded at Scott River near Fort Jones CA (USGS 11519500) since October 1, 1941 (Figure 11). This data is available at http://waterdata.usgs.gov/nwis, with average daily values reported in cubic feet per second (cfs). For the regression, daily data were converted to units of acre-feet per day (1.9835 AF/day equals 1 cfs). This dataset is the most robust of all the streamflows in the Scott Valley. The published record has no missing daily flows. On some days, data are estimated by the USGS, and then approved for publication. Because of the abundant data available, the Scott River near Fort Jones flow was a major component of the regression model. Table 5 lists the dates of available tributary streamflow data used for the regression analysis, including the east and south fork of the main stem Scott River.

Tributary flow was downloaded from the Water Data Library (http://www.water.ca.gov/waterdatalibrary/). The following list includes the code for each tributary: Shackleford Creek near Mugginsville (F25484); Mill Creek near Mugginsville (F25480);

French Creek at Highway 3 near Callahan (F25650); Sugar Creek near Callahan (F25890); Scott River, East Fork, at Callahan (F26050); and Scott River, South Fork, near Callahan (F28100). Dates for which data are available are listed in Table 5. Data are provided as average daily flows (cfs) and were converted to units of (AF/day).

Daily data were used for the regression analysis. Complete sets of daily data with measured values, when available, and with regression estimated values otherwise, were aggregated to monthly totals (AF/mo) for each individual month in the time series.

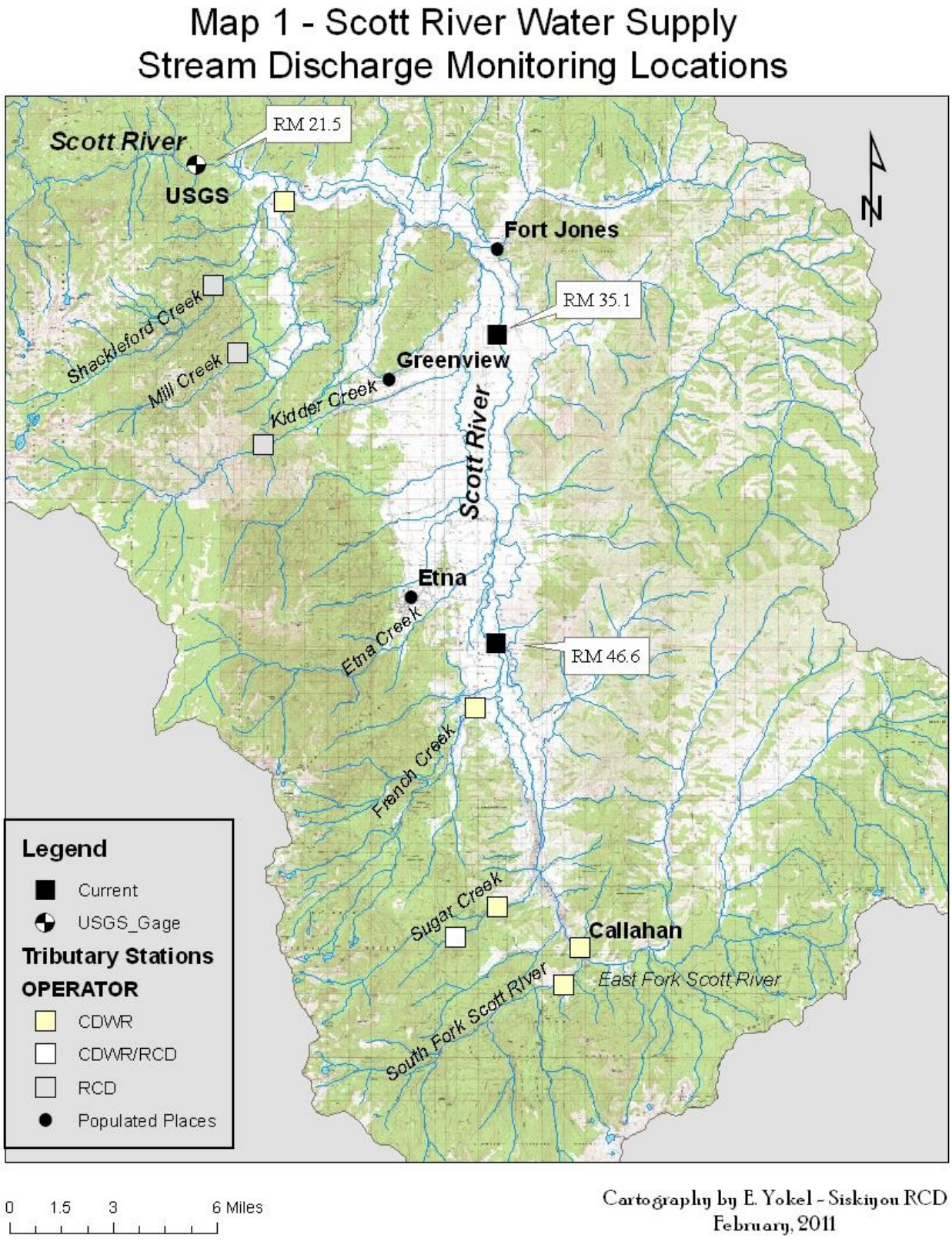

Figure 10. Streamflow measurements in Scott Valley (E. Yokel, Siskiyou RCD, 2011).

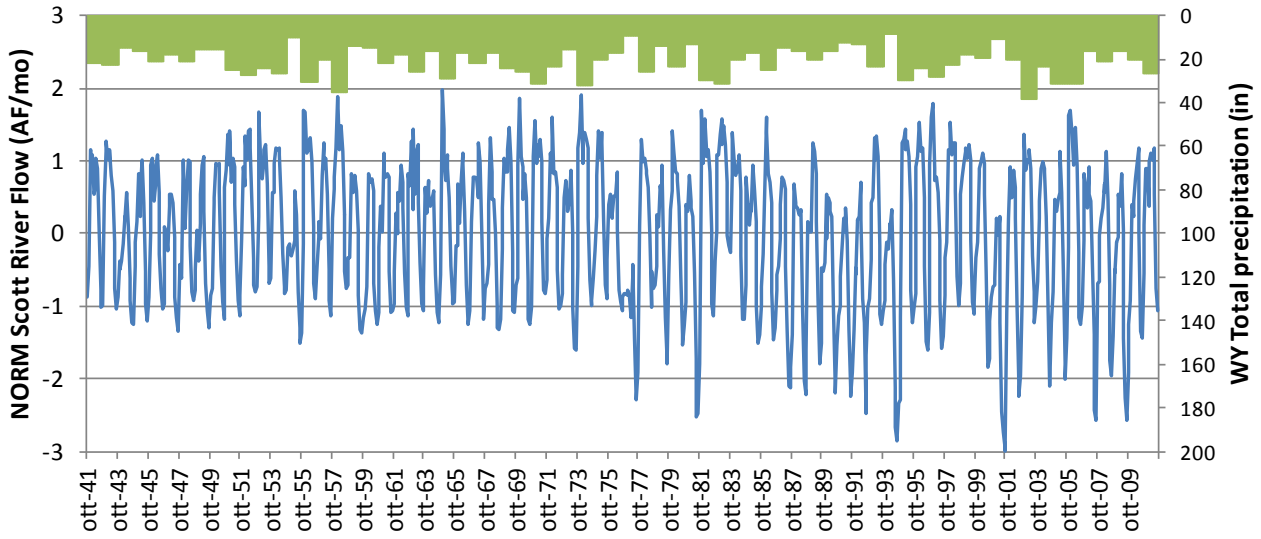

Figure 11. Log-transformed, normalized monthly average Scott River streamflow at Fort Jones, October 1941 through September 2011, computed from reported daily discharge (blue line). Water year total precipitation(green hanging bars) are computed as the average of measured and estimated daily precipitation data at the Fort Jones, Callahan, and Greenview stations (Section 4.4).

Missing data from the CDEC database are noted with a quality code of 160 or 255. Code 160 indicates that the flow was higher than the gage capacity, a situation for which it is difficult to estimate an exact value. Similarly, the tributaries that are measured manually are measured only under wadeable, non-flooding, conditions. Because many of the high value flows are missing from the raw data, the regression models have difficulty replicating the peak flows. However, the goal of the model is to understand the late summer/fall flows, which may affect fish, particularly juvenile coho and fall-run Chinook salmon. Inaccurate prediction of high flow events is not significantly affecting our analysis of late summer low flows. High flood flow may impact late summer low flows indirectly – if at all - through groundwater recharge. Recharge from flood events is difficult to predict, even if high flood flows were known precisely. While it is important for the model to represent the streamflows accurately each month, more focus was therefore placed on the accuracy of low flow events.

Table 5. Dates of available tributary streamflow data used for the regression analysis, including the east and south fork of the main stem Scott River.

	Pre-WY1972 Data Range	Post-WY1972 Data Range
Kidder	4/72-9/72	10/02-9/11
Mill	-	12/04-9/05
Shackleford	10/56-9/60	10/04-9/11
Sugar	9/57-9/60, 5/72-9/72	10/09-9/11
Moffett	10/58-9/67, 4/72-9/72	-
East Fork	10/59-9/72	10/72-9/74, 7/02-9/11
South Fork	10/58-9/60, 4/72-9/72	7/02-9/11
French	-	10/04-9/11
Etna	4/72-9/72	-
Patterson	4/72-9/72	-

The degree to which unmeasured and poorly (under)predicted high flows may affect groundwater recharge will need to be determined through sensitivity analysis with the integrated hydrologic model.

5.4 Statistical Analysis: Streamflow Regression Methods

Monthly averages of reported daily streamflow data for the Scott River gauge at Fort Jones and at the two gauges in Callahan are log-normally distributed. For the regression analysis, all existing monthly average streamflow data, $x_{i,t}$, at gauging station *i* and month (time) *t* were therefore log-transformed and normalized to obtain a normally distributed data series of monthly flows, Norm($x_{i,t}$), for each gauging station *i*:

$$Norm(x_{i,t}) = \frac{\log(x_{i,t}) - \mathrm{M}[\log(\boldsymbol{x}_i)]}{\mathrm{STD}[\log(\boldsymbol{x}_i)]}$$

where M is the arithmetic mean (of the log-transformed data series xi) and STD is the standard deviation.

Four transformed data series computed from known data sets were alternately used as independent variables to build regression models of normalized log-transformed tributary flows using linear regression:

- "Norm(Scott)": Norm(Scott River Flow at Fort Jones)
- "ProductWeightedNorm(Scott)": $\sqrt[3]{\mathrm{Norm(Scott\ River\ Flow\ at\ Fort\ Jones)} \times \mathrm{WYPrecip} \times \mathrm{AvgSnowWC}}$
- "RatioWeightedNorm(Scott)": $\frac{\mathrm{Norm(Scott\ River\ Flow\ at\ Fort\ Jones)}}{\sqrt{\mathrm{Total\ WYPrecipt} \times \mathrm{AvgSnowWC}}}$
- "SumWeightedNorm(Scott)": [Norm(Scott River Flow at Fort Jones) + WYPrecip + WYPrecip2Date + MoPrecip + PrevMoPrecip + AvgSnowWC]

The following dependent variable time series were separately used against each of the above four independent variables to build a number of regression models for comparison:

- "Norm(*Streamname*)": each individual normalized tributary flow gauge time series, all times
- "Norm(EastTribs)": the combined record of all normalized tributary flow time series of tributaries along the east side of Scott Valley, all times
- "Norm(WestTribs)": the combined record of all normalized tributary flow time series of tributaries along the west side of Scott Valley, all times
- "Norm(Tribs)": the combined record of all normalized tributary flow time series, all times

To investigate seasonal biases in the regression models, the combined dataset of all normalized, log-transformed tributary data, "CombinedTribs", was dissected into

- "Norm(Tribs-Season)": season-of-the-year data (4 datasets) and

- "Norm(Tribs-Month)": month-of-the-year data (12 datasets)

These 4 and 12 datasets were used to compute separate regressions for each season (fall: Oct-Nov, winter: Dec-Feb, spring: Mar-Jun, summer: Jul-Sep) and separate regressions for each calendar month (Oct through Sep), respectively.

Over the period of record, the normalized flow data for the Scott River show a significant shift that occurs sometime during the long drought-free period between the 1955 drought and the 1977 drought. Beginning with the 1977 drought, summer month low flows (but not winter month high flows) are significantly lower than in the 1955 drought and earlier. We therefore created another set of regressions using a split "Norm(Tribs)" dataset:

- Norm(Tribs)-Pre-WY1972, which includes WY 1943 to WY 1972, and
- Norm(Tribs)-Post-WY1972, which includes WY 1973 to WY 2011 data.

Note that in the above lists, "tributary flow" and "tribs" include the South and East Fork of the Scott River. For all of the above regressions, subsets of each log-transformed, normalized data series were used for the time period of interest. However, across all analyses, the normalization of each stream gauge's dataset by its mean and standard deviation remains the same and is always based on the total period of record for each stream gauge. In other words, we did not renormalize the individual data series from original data for the particular time series used in the analysis, neither for the independent nor for the dependent data series.

Additional regressions were implemented using the number of days in the calendar year to date at which the temperature exceeded 21°C. This temperature was selected by computing the temperature difference between Fort Jones and the highest point in the watershed, using the dry adiabatic lapse rate (DALR). At 21°C, all of the surrounding snow-capped mountains have temperatures above freezing, and they are contributing flow to the tributaries.

Goodness of fit was determined in a number of ways. First, the diagnostic plots from R were visually examined. "Residuals vs Fitted" shows residual values as a function of the fitted value. If the assumption of linear dependency between dependent and independent variable is justified, these bounce randomly around the 0 line. If the results in the plot are closer together on one part of the x-axis (e.g., the left side) than on the other part of the axis (where they would be more spread apart or fanned out), then this would indicate a violation of the homogeneity assumption that the residuals are independent of the magnitude of the predicted value. The "Q-Q plot" should show linearity if the data are normally distributed. "Residuals vs. Leverage" should show no pattern. "Scale-Location" plots should also show no patterns and issues of heteroscedasticity would be noticeable through fan-like patterns in the plots.

5.5 Streamflow Regression: Results and Discussion

The regression slopes of the normalized tributary flows against the Scott River flows are all less than 1 with a positive regression intersect (Table 6). This indicates that the geometric mean flows of the tributaries have a tendency to occur when the Scott River below Ft. Jones is at less than

geometric mean flow; and the low flow on the tributaries tend to be less extreme than on the Scott River, or the high flows are not as extreme as on the Scott River, or both (relative to the standard deviation). The only exception is Moffett Creek, which has regression slope slightly larger than 1 with a slightly negative regression intersect.

The behavior observed on most tributaries is even more exaggerated when the normalized data are separated into a pre-WY1972 and post-WY1972 series: prior to (and including) WY 1972, tributary geometric mean flow occurs at approximately the Scott River geometric mean flow, with the slope being slightly larger than 1 (high flows and/or low flows on the tributaries tend to be slightly stronger than on the Scott River). After WY1972, tributary geometric mean flows occur when the Scott River is at less than geometric mean flow and the extreme events (highs or lows or both) are less exaggerated on the tributaries than on the main stem of the Scott River below Ft. Jones: the log-transformed flows on the tributaries vary only at 84% of the relative variation on the main stem below Scott Valley. Separating the time-series into two series, however, yields an only slightly better correlation coefficient, r^2.

Fitting each tributary separately against the Scott River data, or fitting the combined west side tributaries separately from the combined east side tributary data also does not produce a much higher correlation coefficients (Table 6). It therefore appears that a single regression for the combined dataset of normalized, log-transformed tributary flows is adequate and also takes advantage of the information that may be collected on some tributaries but not at others, given that tributary flows are highly correlated among each other.

When weighting the regressions by additional information, two models emerge with correlation coefficients similar to (and not much higher than) the unweighted regressions: the product-weighted regression and the sum-weighted regression. The ratio-weighted regression, on the other hand, performed very poorly.

The product-weighted regression provides large weights when high flow events coincide with wet years and large snow pack, and low weights when low flow events coincide with dry years and small snow packs. The product-weighted regression implies that tributary flows are relatively smaller (compared to Scott River flows) in dry years with low snow pack than in average or wet years or in years with higher snowpacks.

The sum-weighted regression provides the best correlation coefficient, if only slightly better than the unweighted correlations. The sum-weighted correlation assigns additional weights to several precipitation and snow-pack related data. But that does not significantly improve the predictive capability, if the Scott River dataset alone was used.

In the Q-Q plot, most models showed some tailing off the line y=cx for low x values. Also, some trends appear in residuals. For many regressions against Norm(Scott) and SumWeightedNorm(Scott), the correlation coefficient, r^2, is larger than 80% (Table 6) indicating an overall strong, but not perfect, goodness of fit. R-squared can give an approximate indication of how well the estimated data fit the measured data overall, but it is important not to base all

judgment on this value alone. Some models had r^2 larger than 70%, yet failed to model the high and low streamflow values well.

A visual comparison of the plotted estimated and actual values was made (see Appendix A). This method of determining goodness of fit was the best way to see how well the regression modeled the flow, especially the important summer/early fall flow.

Mill, Etna, and Patterson were difficult to analyze since these tributaries were only gauged for one year. With so few points to compare, it is difficult to tell which regression provides the best fit. To be conservative, the regression that shows the best for the other tributaries should also be used for these three flows.

Table 6. Key regression slopes, intersects, and regression coefficients. Availability of data from individual streams is listed in Appendix (also see Table 5).

Dependent Variable	Independent Variable	Regression Slope [-]	Regression Intersect [-]	r^2 [%]
Norm(Tribs)	Norm(Scott)	0.903	0.122	81.2
Norm(Tribs)-Pre-WY1972	Norm(Scott)	1.053	-0.000405	84.7
Norm(Tribs)-Post-WY1972	Norm(Scott)	0.840	0.218	82.4
Norm(WestTribs)	Norm(Scott)	0.881	0.205	81.4
Norm(EastTribs)	Norm(Scott)	0.964	0.00975	83.7
Norm(Kidder)	Norm(Scott)	0.804	0.129	76.7
Norm(Shackleford)	Norm(Scott)	0.952	0.243	89.9
Norm(Sugar)	Norm(Scott)	0.979	0.0406	83.0
Norm(Moffett)	Norm(Scott)	1.044	-0.0567	78.0
Norm(EastFork)	Norm(Scott)	0.941	0.0364	87.4
Norm(SouthFork)	Norm(Scott)	0.900	0.317	82.1
Norm(French)	Norm(Scott)	0.879	0.350	82.2
Norm(Tribs-Summer)	Norm(Scott)	0.758	-0.123	50.1
Norm(Tribs)	RatioWeighted-Norm(Scott)	18.66	0.14	37.0
Norm(Tribs)	ProductWeighted-Norm(Scott)	0.1118	0.006066	76.3
Norm(Tribs)	SumWeighted-Norm(Scott)	0.930	0.370	82.3
Norm(Tribs)	SumWeighted-Norm(Scott) – Pre-WY1972	1.111	0.240	85.6
Norm(Tribs)	SumWeighted-Norm(Scott) – Post-WY1972	0.876	0.682	83.7

For the best fit, we were particularly interested in matching flows during the low flow season, if not perfectly, then at least such that flows are over-predicted in some years and under-predicted in other years. Ideally, the regression would have zero bias, where bias is here defined as

$$\text{Bias} = \text{Norm(Trib)}_{\text{actual}} - \text{Norm(Trib)}_{\text{predicted}}$$

Bias was calculated separately for each calendar month and each tributary for the time period of record, using two example regressions. Data are not available in all months to compute bias (Table 7 - Table 10).

Comparing prediction results between various regression methods, qualitative differences in the overall pattern of fit are small compared to the large annual variations in streamflow. Weaknesses in one prediction are repeated, at slightly better or worse levels, in other predictions.

A large number of negative bias occurs during the summer months at the East Fork, in particular. Visual inspection of predicted vs. measured time series indicates that predicted values for the earlier time period at the East Fork seemed to have a particularly significant bias, not being able to predict the low flows in most summer months. While the East Fork has significant bias, especially for September's low flows, no adjustments were made to correct this bias or any other stream's bias. Not enough month-specific data are available to correct for potential bias.

For the pre- and post-1972 regressions (Norm(Tribs)Pre-WY1972, Norm(Tribs)Post-WY1972), streams had at most 13 datapoints, and commonly much less (Table 7-Table 10).

From the many individual regressions, we found that those regressions that included all tributaries in the equation provided a better fit overall than the regressions for individual tributaries, or the regressions for individual months or individual seasons.

The regressions of normalized tributary streamflows vs. RatioWeightedNorm(Scott) provided the relatively poorest fit ($r^2 < 0.4$), although some summer flows are better predicted than by other models. A much better correlation was obtained when computing a regression of tributary flows vs. ProductWeightedNorm(Scott) (r^2 =76.3%). Commonly, this regression, however, tends to significantly underestimate peak flows and overestimate low flows.

In summary, of the many regression models developed, two regression models stood out as having a significant better fit, particularly in the critical low-flow season: Norm(Tribs) vs Norm(Scott) and Norm(Tribs) vs SumWeightedNorm(Scott).

The best fit was obtained by the split time period regressions, Norm(Tribs)Pre-WY1972 and Norm(Tribs)Post-WY1972 vs. SumWeightedNorm(Scott), particularly in the critical summer months. Splitting the regression gave slightly better results (r^2 values of 84.7% and 82.4%) than the fully combined regression Norm(Tribs) vs. SumWeightedNorm(Scott) (r^2=81.2%). The split regression model would also provide the best possible fit for the flows at Mill, Etna, and Patterson given the lack of raw streamflow data for these tributaries. The regression is considered particularly good, given the large variability in flow volume and geographical range within the valley. The split Norm(Tribs)Post-WY1972 vs. SumWeightedNorm(Scott) and the split Norm(Tribs)Post-WY1972 vs. Norm(Scott) will be the best candidates for use in the groundwater-surface water model.

Table 7. Regression bias for Norm(Tribs)- Pre-WY1972 vs. SumWeightedNorm(Scott). White areas indicate that data are available to compute a bias for those months.

	Kidder Avg / #Datum	Mill Avg / #Datum	Shackleford Avg / #Datum	Sugar Avg / #Datum	Moffett Avg / #Datum	East Fork Avg / #Datum	South Fork Avg / #Datum	French Avg / #Datum	Etna Avg / #Datum	Patterson Avg / #Datum
January										
February			-0.28 / 4	-0.13 / 3		-0.16 / 13	-0.13 / 2			
March			-0.17 / 4	-0.14 / 3						
April				-0.17 / 3						
May					-0.45 / 10					
June					-0.65 / 10					
July				-0.13 / 4	-0.11 / 10					
August				-0.46 / 4		-0.15 / 13				
September				-0.26 / 5		-0.42 / 13				
October						-0.24 / 13				
November					-0.24 / 9					
December										

Indicates one or fewer years of data, so no average bias calculated
Indicates bias was > -0.1

Table 8. Regression bias for Norm(Tribs)- Post-WY1972 vs. SumWeightedNorm(Scott). White areas indicate that data are available to compute a bias for those months.

	Kidder Avg / #Datum	Mill Avg / #Datum	Shackleford Avg / #Datum	Sugar Avg / #Datum	Moffett Avg / #Datum	East Fork Avg / #Datum	South Fork Avg / #Datum	French Avg / #Datum	Etna Avg / #Datum	Patterson Avg / #Datum
January						-0.34 / 6	-0.12 / 5			
February	-0.11 / 6			-0.29 / 2						
March	-0.27 / 8									
April										
May										
June										
July										
August			-0.15 / 7			-0.23 / 10		-0.28 / 7		
September			-0.40 / 7	-0.19 / 2		-0.50 / 10		-0.16 / 7		
October	-0.58 / 8		-0.68 / 5			-0.13 / 8				
November										
December						-0.32 / 5	-0.12 / 4			

Indicates one or fewer years of data, so no average bias calculated
Indicates bias was > -0.1

Table 9. Regression bias for Norm(Tribs)- Pre-WY1972 vs. Norm(Scott). White areas indicate that data are available to compute a bias for those months.

	Kidder Avg / #Datum	Mill Avg / #Datum	Shackleford Avg / #Datum	Sugar Avg / #Datum	Moffett Avg / #Datum	East Fork Avg / #Datum	South Fork Avg / #Datum	French Avg / #Datum	Etna Avg / #Datum	Patterson Avg / #Datum
January			-0.14 / 4			-0.11 / 13				
February			-0.38 / 4	-0.26 / 3		-0.15 / 13	-0.19 / 2			
March			-0.20 / 4	-0.18 / 3						
April				-0.15 / 3						
May					-0.40 / 10					
June					-0.62 / 10					
July				-0.15 / 4	-0.12 / 10					
August				-0.50 / 4	-0.13 / 10	-0.24 / 13				
September				-0.30 / 5		-0.53 / 13				
October						-0.18 / 13				
November					-0.22 / 9					
December										

Indicates one or fewer years of data, so no average bias calculated
Indicates bias was > -0.1

Table 10. Regression bias for Norm(Tribs)- Post-WY1972 vs. Norm(Scott). White areas indicate that data are available to compute a bias for those months.

	Kidder Avg / #Datum	Mill Avg / #Datum	Shackleford Avg / #Datum	Sugar Avg / #Datum	Moffett Avg / #Datum	East Fork Avg / #Datum	South Fork Avg / #Datum	French Avg / #Datum	Etna Avg / #Datum	Patterson Avg / #Datum
January						-0.30 / 6				
February	-0.15 / 6			-0.27 / 2		-0.16 / 4				
March	-0.30 / 8									
April										
May										
June										
July										
August			-0.19 / 7			-0.23 / 10		-0.33 / 7		
September			-0.46 / 7	-0.27 / 2		-0.52 / 10	-0.16 / 8	-0.23 / 7		
October	-0.53 / 8		-0.60 / 5			-0.22 / 8				
November										
December						-0.26 / 5				

Indicates one or fewer years of data, so no average bias calculated

Indicates bias was > -0.1

6 Evapotranspiration and Crop Coefficients

Evapotranspiration was calculated using a program designed at UC Davis, the NWSETO program (Snyder, 2002). The NWSETO program is used to calculate reference evapotranspiration (ET_0) for short grass. The atmospheric inputs for this program include, for each month, average maximum daily temperature, average minimum temperature, maximum and minimum humidity, wind speed, and percent cloud cover. The NWSETO program provides two alternative reference ET_0 values based on either the Penman-Monteith (1965) or based on the Hargreaves and Samani equations (1982). The calculated ET_0 obtained from the climate records and NWSETO were compared and evaluated on the basis of observed values available for Scott Valley as discussed below, prior to using it within the water budget model. The two sets of data were generally in agreement. For this study, the ET_0 values calculated by NWSETO using the Hargreaves and Samani equation have been used.

Crop coefficients (k_c) and ET_0 are used to estimate specific crop evapotranspiration rates. The k_c is a dimensionless number (usually between 0.1 and 1.2) that is multiplied by the ET_0 value to obtain an estimate of the actual crop ET (ET). The estimate of actual crop ET is primarily designed to help an irrigation manager schedule irrigation frequency and amount, but is here used to estimate actual crop ET for simulating a daily soil water budget. Crop coefficients vary by crop, stage of growth of the crop, and by some cultural practices. Coefficients for annual crops vary widely throughout the season, with a small coefficient in the early stages of the crop (when the crop is just a seedling or, in the case of alfalfa, has been recently cut) to a large coefficient when the crop is at full cover (the soil completely shaded).

Crop coefficients have been assigned as follows:

- alfalfa: $k_c = 0.95$ (Steve Orloff and Blaine Hanson, University of California, personal communication) from February 15 to November 15, and $k_c=0$ for the remainder of the winter months. In alfalfa, a constant k_c value is used for two reasons: first, the growing period of alfalfa broadly coincides with that of the reference crop; secondly, alfalfa cuttings do not occur at the same time across the entire study area. A time-varying k_c value that reflects individual cutting events on individual fields would require knowledge (or simulation) of individual field cutting events over the period of interest. That level of detail in the spatio-temporal variability of field-by-field water budgets was deemed not critical for the current modeling effort. Also, using a slightly different growing period, such as March 1st- October 31st would not significantly change the final ET value because the ET in February and March is almost negligible. Simulations yield a 1990-2011 average annual ET in alfalfa of 1,200 mm (39.4 inches), very close to the field values measured by Blaine Hanson (Hanson et al., 2011a);
- grain (wheat, barley, oats and triticale): we use a daily varying k_c according to UCCE Leaflet 21427. Leaflet 21427 lists crop coefficients for two crops similar to the “grain” category here: summer barley in Northern California Mountain Valleys and small winter grain in the Sacramento Valley. The following is a combination of “barley” for “Mountain Valleys”

(planting date: 4/30, harvest date: 8/31) with the “small grain” for “Sacramento Valley” (planting date: 12/16, harvest date: 8/04) supported by the recommendation provided by Steve Orloff and general information provided by the GWAC:

  - planting date A: March 15, k_c=0
  - early season date B: April 20, k_c=0.27
  - mid season start date C: May 15, k_c=1.15
  - mid season end date D (after 70% of the 127 day period or 90 days): June 15, k_c=1.15
  - harvest date E, July 20, k_c=0

  The daily k_c values vary linearly between the above dates and values.

- pasture: k_c = 0.9 as suggested by the UCCE Leaflet 21427 for grazed pasture statewide, and confirmed by Steve Orloff. To account for winter frost, we set k_c=0.9 from February 15 to November 15, but zero over the winter (same as for alfalfa).
- natural vegetation: k_c = 0.6

7 Soils

The Soil Survey Geographic (SSURGO) Database, maintained by the Natural Resources Conservation Service (NRCS), was used to obtain spatial and tabular soils data for our project area. This database contains soil attributes, which describe variables such as texture, particle size or water holding capacity. We used information from this database to evaluate water holding capacity (WHC) for each of the land use polygons delineated by the California Department of Water Resources (DWR). The recommendation by UC Cooperative Extension personnel was to use a root-zone depth of 4 ft (122 cm) to compute WHC. Available information in the SSURGO database was WHC to 100 cm and to 150 cm. To simulate WHC at the recommended depth of 4 ft (122 cm), we mapped WHC for both 100 cm and 150 cm in each soil map unit, then obtained the WHC used for the soil water budget simulation using an area-weighted average of all intersecting soil type polygons and their WHCs at 100 cm and at 150 cm within each DWR land use polygon (Figure 12). For modeling purposes, the same root zone depth was assumed for all crops. In practice, grain and alfalfa are do not have the same rooting depth; however, a sensitivity analysis of the root zone depth, presented later in the report, shows that doubling the root zone depth does not significantly affect results. Selecting a uniform root zone depth for both crops in the soil water budget model is therefore a reasonable assumption.

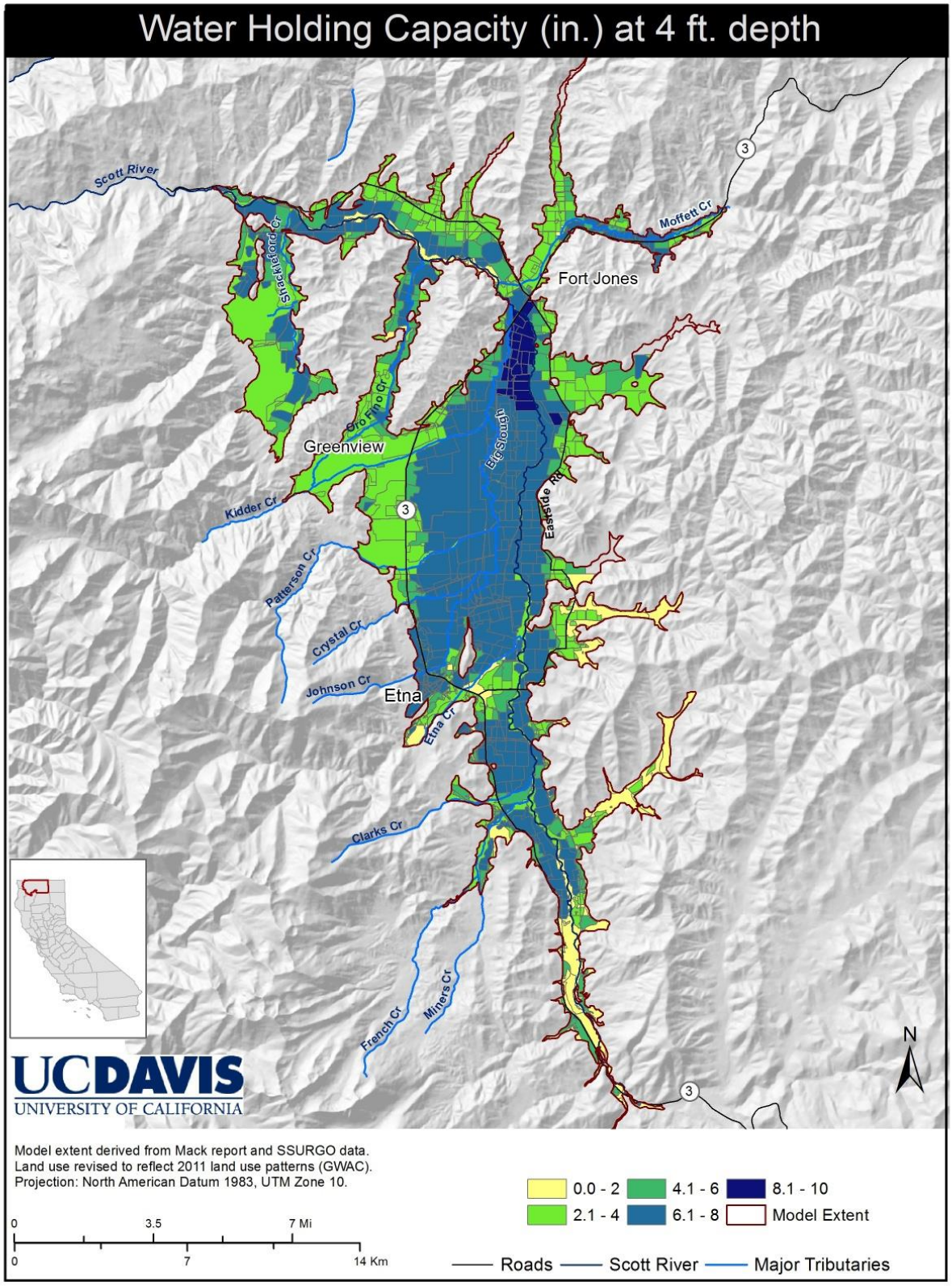

Figure 12. Map of water holding capacity in the top 4 ft (122 cm), in [inches of water].

8 Groundwater

8.1 DWR Well Log Review

The main focus of our well log analysis was on identifying geologic structure within the Scott Valley alluvium and on identifying the location of irrigation (agricultural) wells, regardless of whether these were active or inactive. Well locations are used in the water budget model to represent groundwater pumping required to meet agricultural water demands in wells nearest to each field, when not met by surface water supplies.

A scanned copy of all well logs available for the Scott Valley and immediately surrounding areas was obtained from the California Department of Water Resources (CDWR). An extensive review of these 1,701 well logs was conducted in order to gain a better understanding of the hydrogeology of the valley. Well logs typically provided information on the well's location, on geologic facies encountered during drilling, albeit at varying degrees of description detail and accuracy, and for some wells the logs provided information on the hydrologic characteristics of the well, including specific capacity or pumping data. Well logs also indicated the major use of the well. Our review included the following:

- Domestic Wells: 1,302
- Irrigation Wells: 240
- Industrial Wells: 3
- Public/Municipal Wells: 4
- Other (Monitoring, Test, etc.): 152

The number of wells identified to be in or near the Scott Valley was 598 wells. The number of wells located within the Version 2 model boundaries and included in our GIS database is 406 wells:

- Domestic Wells: 192
- Irrigation Wells: 182
- Other: 32

Well logs were first geo-located throughout the integrated hydrologic modeling area (see below) using a variety of information. The primary information used was the parcel number of the property where the well was situated. This information was typically provided on the well log itself. Parcel numbers and associated locations for the Scott Valley area were obtained from the Siskiyou County Assessor's Office files. The second datum used for geo-locating a well was the well owner and address listed on the well log. If neither of these two methods obtained a location match, the well logs were categorized by their township/range/section information, which was obtained by reviewing the well location sketch provided by the driller, and from a review of aerial photography to identify the parcels where the wells are situated. Additionally, a field survey was conducted throughout the valley to verify well locations where accessible or viewable from public access places.

In some instances, wells were only placed within the centroid of the property polygon based on a computerized geographic information system (GIS) geo-location process used to match well owners and parcel numbers with their location. In many instances, these locations were improved by canvassing the valley and through the reviews of aerial photographs as discussed above. Despite these extensive efforts and the multitude of approaches, the location of wells related to some well drilling logs could only be approximated in a very rough manner. A lack of confidence identifier was included in the GIS layer of the well location to convey the approximate nature of the geo-location. Ultimately, 598 wells were identified to be within the Scott Valley. Of these, 54 wells could not to be matched to a particular property. The remaining 544 wells were used to characterize the geologic deposits and heterogeneous character of the alluvial deposits comprising the Scott Valley aquifer (Section 8.2).

In the well database updated for Version 2 of the integrated hydrologic model, we consider a total of 406 wells located within the revised integrated hydrologic model domain (Figure 13). Out of these, 182 are irrigation wells and will be used in the model. Pumping for each field is assigned in the new conceptual model to the nearest well. This implies that each field has exactly one associated well, while one well can serve multiple fields.

After discussion with the GWAC, there was also the suggestion to try a simpler approach that equally distributes the amount of pumped water among all the wells within a subwatershed. A third option is to associate a “virtual” well with each field. These alternatives maybe considered as part of a sensitivity analysis on pumping representation in version 2 of the Scott Valley Integrated Hydrologic Model.

The model likely over-represents the actual number of active irrigation wells, as the well locations identified in Figure 13 were not adjusted for wells that are no longer in service. However, groundwater pumping values are obtained from the new soil water budget model explained in detail in chapter 10. They are not related to the number of wells. For modeling purposes, spreading groundwater pumping to more wells than are actually active does not cause significant error, because new wells are typically drilled nearby wells to be deactivated. The integrated hydrologic model lumps groundwater pumping within any 50 m (165 ft) model grid cell. The overall extraction of groundwater is unaffected by the number of wells. Instead, groundwater pumping is driven by the actual monthly irrigation demand.

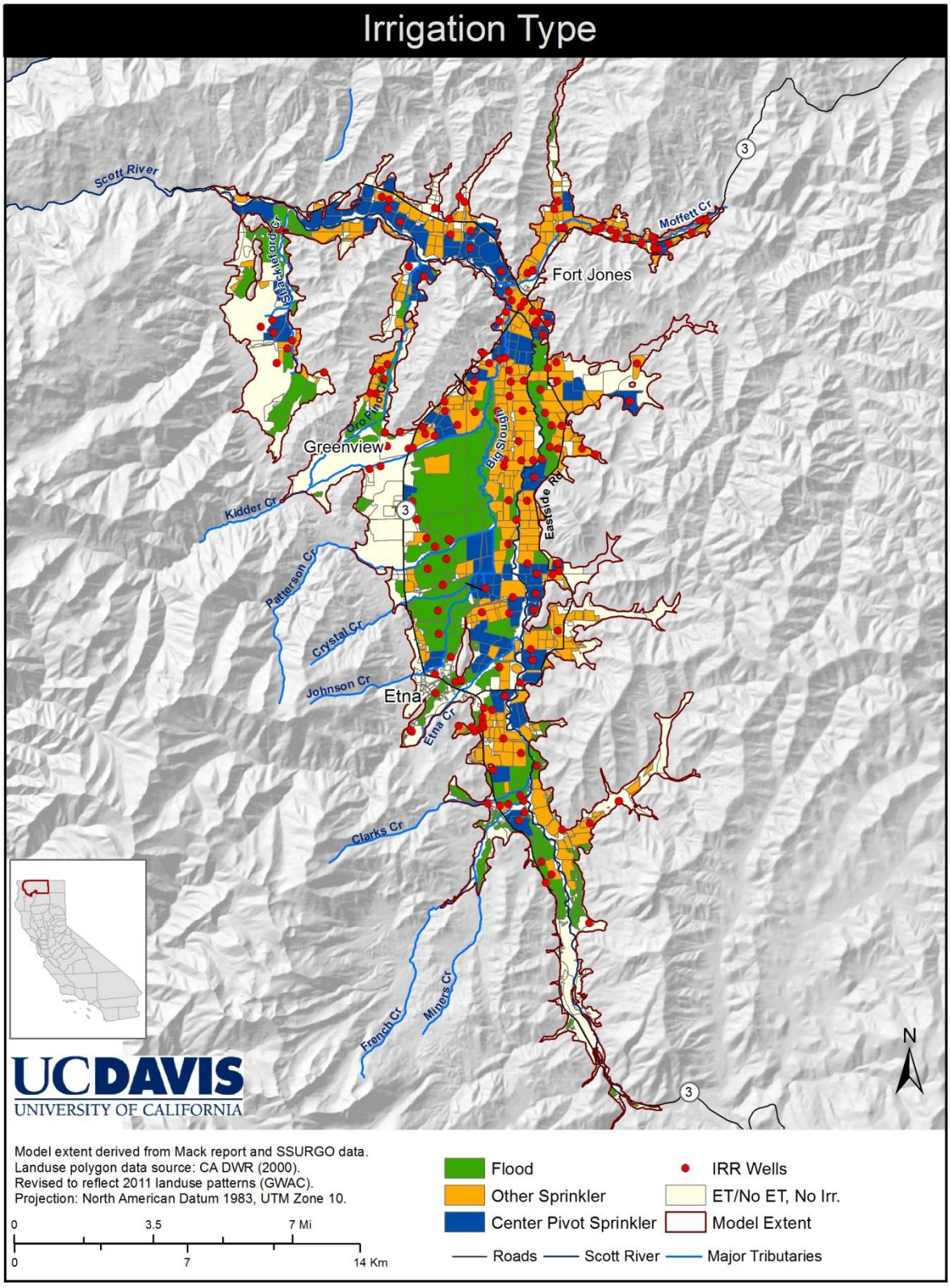

Figure 13. Map of the irrigation type and of the available irrigation wells for Version 2 of the integrated hydrologic model. Locations have been refined by inspection (see text) and may not coincide with those reported by the California Department of Water Resources. The irrigation type reflects recent (2011) conditions. The year of conversion from "Other Sprinkler" (typically wheelline) to "Center Pivot" is an attribute of the "Center Pivot Sprinkler" polygons, if the conversion occurred after 1990, and is taken into account in the soil water budget model.

8.2 Geologic Heterogeneity

The well logs obtained from DWR revealed a tremendous amount of heterogeneity within the alluvial deposits of the Scott Valley. A preliminary geostatistical analysis of the geologic heterogeneity was performed using the so-called transition probability approach (Carle and Fogg, 1996). The transition probability approach is a modified indicator variogram analysis that describes the joint probability distribution of a discrete set of hydrogeologic or geologic facies groups throughout the aquifer system. The transition probability is defined by:

a) a finite number of facies, typically the three to five most common facies observed in a set of geologic records (well logs), e.g., coarse-grained stream deposits, coarse-to-fine grained overbank deposits, and fine-grained flood-plain deposits. One of these facies (usually the facies with the largest volumetric proportion) is designated as "background facies".

b) The volumetric percentage of each facies within the aquifer system of interest.

c) The mean lengths (average straight-distance extent) of all but the background facies in the dip, strike, and vertical direction.

d) The juxtapositional preference among the facies sequence, in other words, the likelihood that one particular facies is located adjacent to another particular facies with a probability that is significantly higher or lower than that obtained if the facies are randomly assembled.

Within the context of groundwater modeling, the transition probability analysis provides a quantitative analysis of the geologic heterogeneity encountered in a groundwater basin. It also provides the simulation framework for generating equally-probable, random realizations of the highly heterogeneous aquifer architecture, conditioned to the specific well logs at the locations where these are available. These random realizations can also be conditioned to surficial geologic information available in soils maps (Weissman, 1999). The more concrete information available, the more specific the random realizations of the aquifer architecture (less variability between individual realizations).

To illustrate the geologic heterogeneity of the Scott Valley, a single realization of the Scott Valley aquifer was generated with the geostatistics software T-PROGS. T-PROGS utilizes the transition probability method, a modified form of indicator kriging, through calculation of transition probability measurements, modeling spatial variability with Markov Chain models, and conditional simulation of the well log information. In this context, the term "indicator" is used to denote categorical classification of aquifer sediments (e.g., coarse, intermediate, fine), as opposed to continuum values (numeric values, for example, hydraulic conductivity varying log-normally with a mean of 20 feet per day and a standard deviation of 10 feet per day).

The T-PROGS geostatistical analysis was based on the information obtained from the 544 wells that were geo-located in the valley. Following a review of these well log records, it was determined that three geologic facies would be modeled: clay or fine-grained sediments, sand, and gravel. As such, in one-foot vertical increments, the data from the well logs was interpreted

as one of the three listed facies, and transition probability statistics were calculated including mean length, proportion, and transition probabilities. Within the combined digitized well logs, a total of 3,982 geologic facies transitions were recorded in the vertical direction (z-direction).

In order to complete the analysis, a review of the SSURGO soil mapping of the 'C Horizon' soil (approximately 0.1 to 0.15m below ground surface) was undertaken to provide information on the nature of the lateral variability observed in geologic deposits. Each deposit identified by the SSURGO mapping (in the subreport entitled Wind Erosion Prediction System Related Attributes) was interpreted as one of the three facies chosen for analysis using at least one of the following indicators: percentage of silt/clay versus sand, and grain size analysis provided to determine between sand and gravel. If the percentage of silt and clay was greater than 50%, the texture was considered to be clay. This particular limit was chosen as it fit the qualitative description of deposits described as loam, clayey-loam, or clay. If the percentage of sand was greater than 50%, the texture was considered to be either sand or gravel with the fragment descriptor being the parameter deciding between the two. If the fragment percentage was greater than 40, the gravel indicator was selected. Also, in a few instances the description was "stratified sandy loam and clay loam". In these cases, sandy loam was chosen as the key layer depending on overall percentages. This seemed to match descriptions of gravel material versus sandy loam. If sandy loam was the description of the material, it was generally labeled as belonging to the sand fraction.

For the geostatistical analysis of the soils information, the deepest soil horizon profile was used. For example, most of the soils were given a description to a depth of approximately 150 cm (5 ft), split between at least two soil horizons: the upper soil horizon less than 50 cm (1.7 ft), and at least one deeper horizon which was typically close to 100 cm (3 ft) in depth. Often, the data for this deeper soil horizon were incomplete and only included the percentage of clay. In these cases, the information provided was often descriptive but sufficient to make a determination of the category to which the soil belonged (clay/sand/gravel).

To complete the analysis, the soil maps had to be discretized so that mean lengths, proportions, and transitions could be calculated. In previous applications, cross-sections of arbitrary discretization were used to accomplish the analysis. For this study, a 50 m by 50 m grid was used to discretize the soil map (not including the tailings area in the southern Scott Valley). In GIS, the grid was overlain on the soil map, and a Spatial Join operation was completed so that each model grid node was provided with a single soil type. This Spatial Join was completed based on the soil type with the highest percentage of area within the grid cell (as calculated by the GIS function). Essentially, the process allowed for 621 horizontal (rows) and 420 vertical (columns) cross-sections to be evaluated as input data. Once discretized, the transition probability data was calculated, including mean length, proportion, and transition for each of three facies.

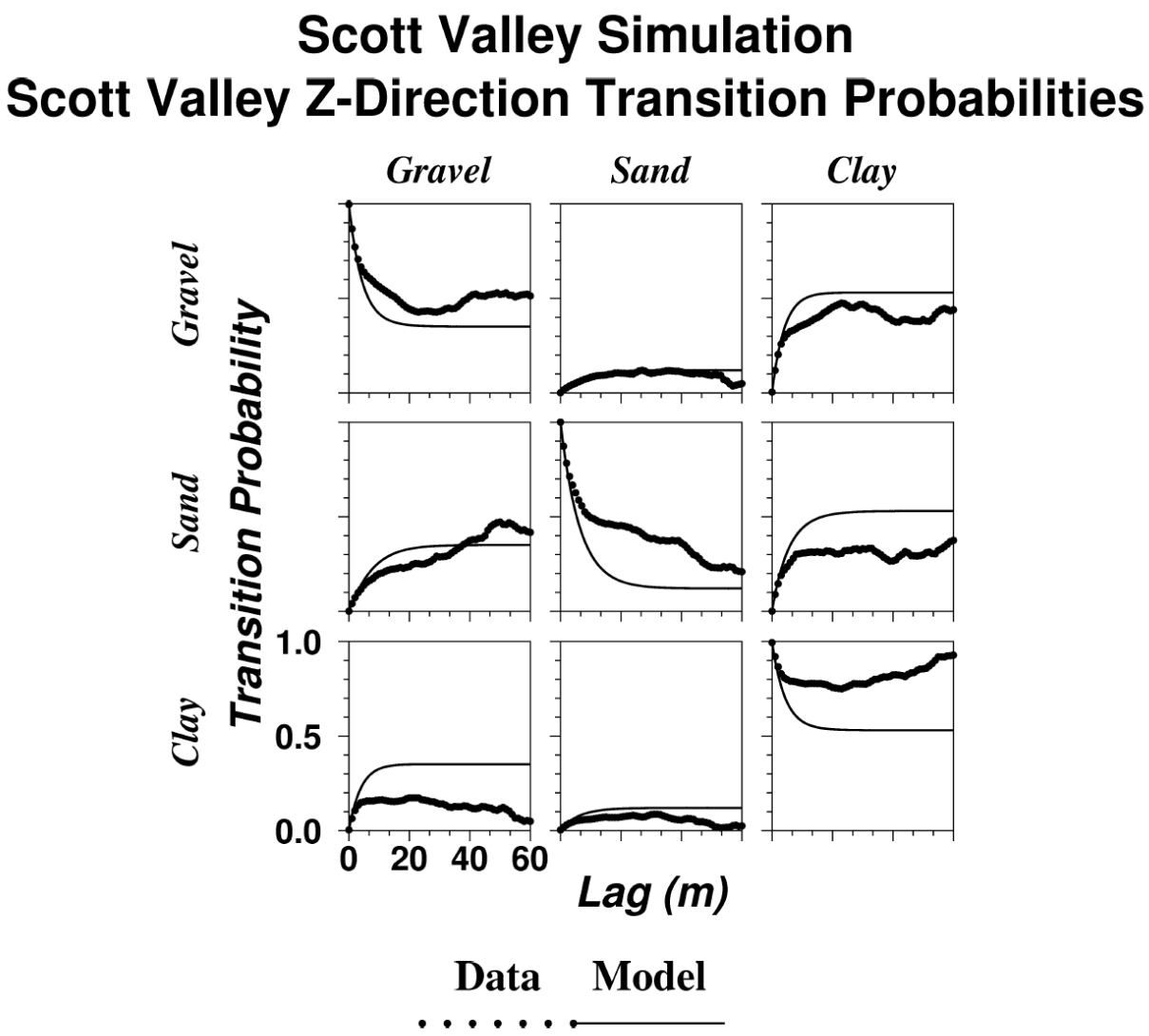

Figure 14. Vertical transition probability curves obtained from an analysis of 544 wellbore logs located within the study area in Scott Valley.

The results of the data analysis show the relative proportions of deposits and display the differing mean lengths of deposits in each of the ordinal directions. The above transition probability curves represent important aspects of the geologic facies deposits (Figure 14). The curves for each type asymptotically approach the value that represents the proportion of each facies deposit. From the z-direction analysis, the proportions of each facies obtained are 51% for clay, 37% for gravel, and 12% for sand. Similar proportions arose from the analysis of the soils map in the XY lateral plane, with proportions of 61% for clay, 28% for gravel, and 11% for sand. Furthermore, in the above transition probability diagram, one can draw a tangent along each auto-transition curve and extend the tangent to the x-axis. The value at which the tangent intersects the x-axis represents the mean length of the particular facies. The mean lengths of each deposit in the z-direction obtained from this analysis were 15.0 m (49 ft) for clay, 12.7 m (42 ft) for gravel, and 10.1 m (33 ft) for sand. The mean lengths of each deposit in the X direction (east-west cardinal directions) were 1,379 m (4,524 ft) for clay, 755 m (2,477 ft) for gravel, and 640 m (2,099 ft) for sand.

The results of the transition probability analysis above were used as input for a Markov-chain random field generator (included in the TPROGs software package) to generate random, equi-probable aquifer structure conditioned on the geologic facies information available for Scott Valley, obtained from the well logs (representative of the vertical dimension) and the soils maps available for Siskiyou County (representative of the lateral dimensions). Figure 15 represents one such realization created with the T-PROGs software with a discretization of 10 ft vertically, 500 ft in the x (W->E) direction and 1,000 ft in the y (S->N) direction. It should be noted that any number of realizations can be created, and although each one will be different, they all will have similar "patterns" with all realizations having the same overall proportion of each geologic facies, determined from the z-direction analysis, and the same mean lengths and juxtapositional preference in each of the three directions. At the surface and along well locations, each realization will preserve the actually known data.

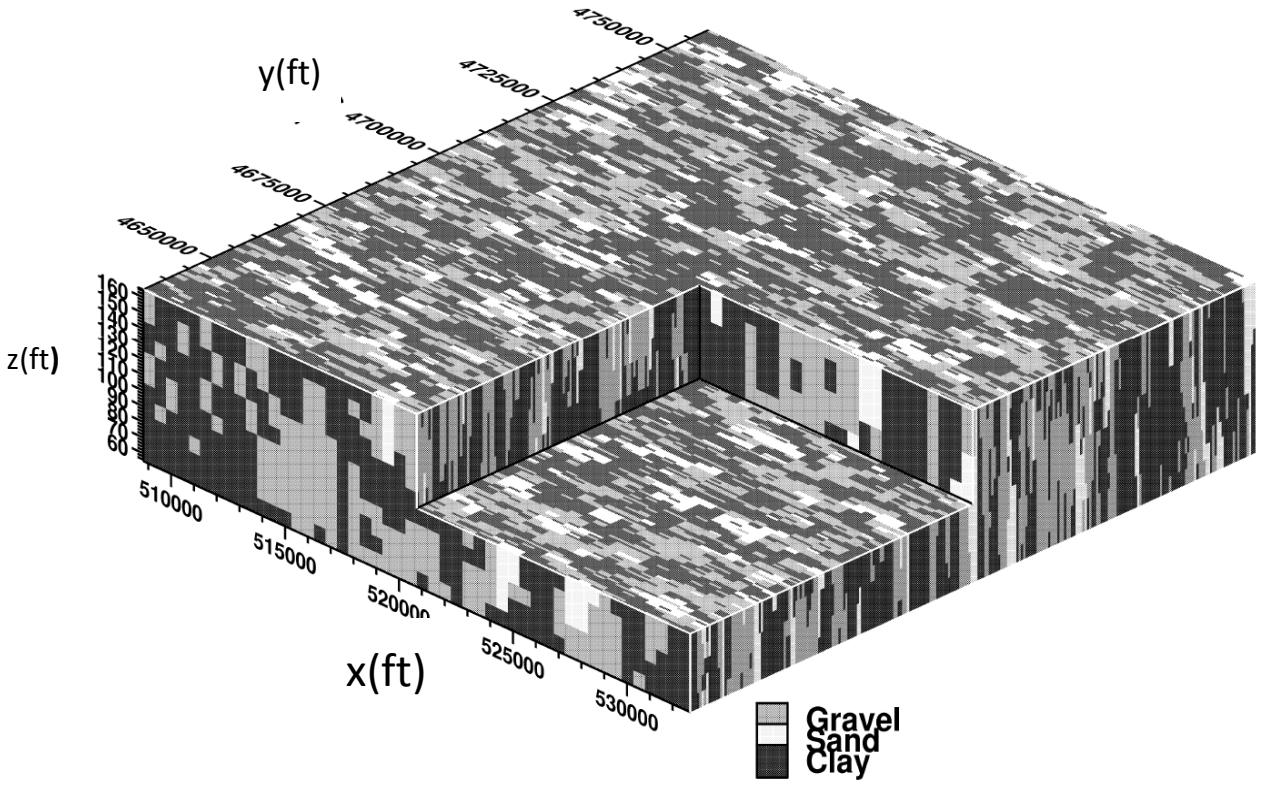

Figure 15. TPROGS Realization of the Scott Valley geologic deposits. Length units are in feet. The image shows a hypothetical aquifer volume that is approximately 100 ft thick, 6 miles in the x direction and 25 miles in the y direction. Note that this image is stretched in the X-direction relative to the y-direction and it does not consider the actual boundaries of the Scott Valley aquifer. It is shown only to conceptually illustrate the heterogeneity encountered in the alluvial deposits of Scott Valley.

While the realization shown in Figure 15 is random, it has important features to note that are shared by all realizations and that are indicative of the overall patterns in the Scott Valley aquifer architecture: the facies exhibit somewhat preferential, elongated connectivity in the y (north-south), but less connectivity in the x direction (east-west), a pattern that represents observations

in the well logs and in the soil map. It is also obvious from the above illustration that the gravel deposits, which are the hydraulically most conductive facies within the aquifer, are highly connected throughout the aquifer system and not isolated from one-another by clay-layers or clay walls. In particular considering that gravel and sand make up approximately half of the aquifer sediments, the connectivity of these coarser-grained sediments is very high and it appears unlikely that significant proportions of sand and gravel would be completely isolated from the regional aquifer system (i.e., encased and surrounded completely by clay). They are likely well-connected to the main-stem of the Scott River.

On the other hand, a review of the boring logs in certain areas shows that a clay layer exists over portions of the valley. This realization as well as hand-drawn cross-sections of the valley created from boring logs, show that these clay layers or lenses may not be broad enough to act as a true confining features. As such, portions of the aquifer may be semi-confined, where they are located below a local clay layer or a clay lens that is relatively broad in extent. However, a spatially extensive confined aquifer does not appear to be present in the Scott Valley. We also note that no sand and gravel has been recorded below about 76 m (250 ft) depth in the few existing logs that exceed such depth.

The geostatistical realization of the Scott Valley aquifer indicates that the Scott River, which intersects with the surficial layer of this aquifer model, is alternately passing along finer and coarse-grained sediments. It is important to keep in mind, however, that this model was created with a lateral resolution of 150 m (500 ft) and also largely depends on the resolution and surveying detail of soil mapping units, which is typically on the order of several hundred meters. The above illustration therefore ignores variability that inevitably occurs at scales smaller than about 150 m – 300 m (500 ft – 1,000 ft).

The analysis here provides an initial survey of spatial variability in the Scott Valley groundwater system. Spatial variability, such as that shown in Figure 15 may be incorporated into future groundwater models, after further analysis of well logs, additional review of streambed sediment studies not reviewed here, and perhaps an improved geostatistical assessment of facies variability in the alluvial system. However, Version 2 of the Integrated Hydrologic Model will not yet include such detailed hydrogeologic facies representation.

9 Watersheds, Land Use, Irrigation, and Land Elevation

A variety of data were used to create input for the model. The model extent was determined based on the extent of groundwater storage units outlined by Seymour Mack in 1958 (Mack, 1958), while the land use data were derived from the California Department of Water Resources (DWR) Land Use survey data. The most recent land use data for Siskiyou County available from the DWR is from the 2000 DWR land use survey. Although a more recent land use survey has been completed by CDWR in 2010, the processed data were not available for use in our project. Since the modeling period is 1990 -2011, the 2000 land use survey was used as the basis upon which we developed the spatial component of our model.

9.1 Model Boundaries and Subwatersheds

Our study area boundaries were selected to represent the Scott Valley area containing surficial alluvial deposits. To delineate these areas in a digital map, a spatial analysis was performed and we assumed that the extent of the alluvium was defined largely by the absence of steep topographic gradients (more than 3%). A digital elevation model (DEM), derived from National Elevation Data (NED), was created and topographic gradients (slope) were computed. The DEM with slopes was then draped over 2005 National Agriculture Imagery Program (NAIP) color aerial imagery, and used as a visual guide to manually digitize the contiguous areas of the Scott Valley that have a three percent slope or less.

The Scott Valley model area covers approximately 50,000 acres. It is subdivided into nine subwatersheds for purposes of modeling surface water supplies and the distribution of these supplies within subwatersheds (Table 11, Figure 16). The subwatersheds are Scott, French, Etna, Patterson, Kidder, Moffet, Mill, Shackleford, and the Scott River Tailings. These subwatersheds were created partly based on the water storage units delineated by Seymour Mack in his 1958 report. Crystal and Patterson Creek are combined into a single subwatershed. Similarly, Johnson and Etna Creek are combined into a single subwatershed. Other smaller subwatersheds are included with larger ones (Figure 16).

Mack (1958) and our Scott Valley model Version 1 data work did not include the Scott River Tailings subwatershed located in the upstream part of the valley. For Version 2 of the Scott Valley Integrated Hydrologic Model, the southern tailings area of the Scott Valley is included in the analysis and in the groundwater flow domain. From visual field inspection, it appears that the tailings aquifer consist primarily of large boulders, with very high hydraulic conductivity and rapid connectivity to the stream. During the late summer and fall low flow season, the Scott River, at the surface, is often disconnected across this highly permeable subwatershed.

Table 11: Total areas of subwatersheds (Figure 16), total area for various irrigation types (Figure 13), total area for various irrigation water sources (Figure 19), and total area of land use (Figure 18), in acres. All values represent 2011 conditions. Note that not all acreage in the alfalfa/grain and pasture category is irrigated.

Subwatershed Name	Area (acres)	Irrigation Type	Area (acres)	Water Source	Area (acres)	Land Use	Area (acres)
Etna Creek	4,223	Non-irrigated	18,549	DRY	3,356	Water	166
French Creek	501	Flood	10,864	GW	16,526	Alfalfa/Grain	17,421
Kidder Creek	9,298	Sprinkler	12,564	MIX	3,949	Pasture	16,578
Mill Creek	2,237	Center Pivot	6,928	SUB	2,106	ET/No Irrig.	14,151
Moffett Creek	2,437	Unknown	1,107	SW	7,596	No ET	1,695
Patterson Creek	4,032			None/unknown	16,478		
Scott River	20, 736						
Scott River tailings	3,562						
Shackleford Creek	2,984						
Study Area Total	**50,011**	**Total**	**50,011**	**Total**	**50,011**	**Total**	**50,011**

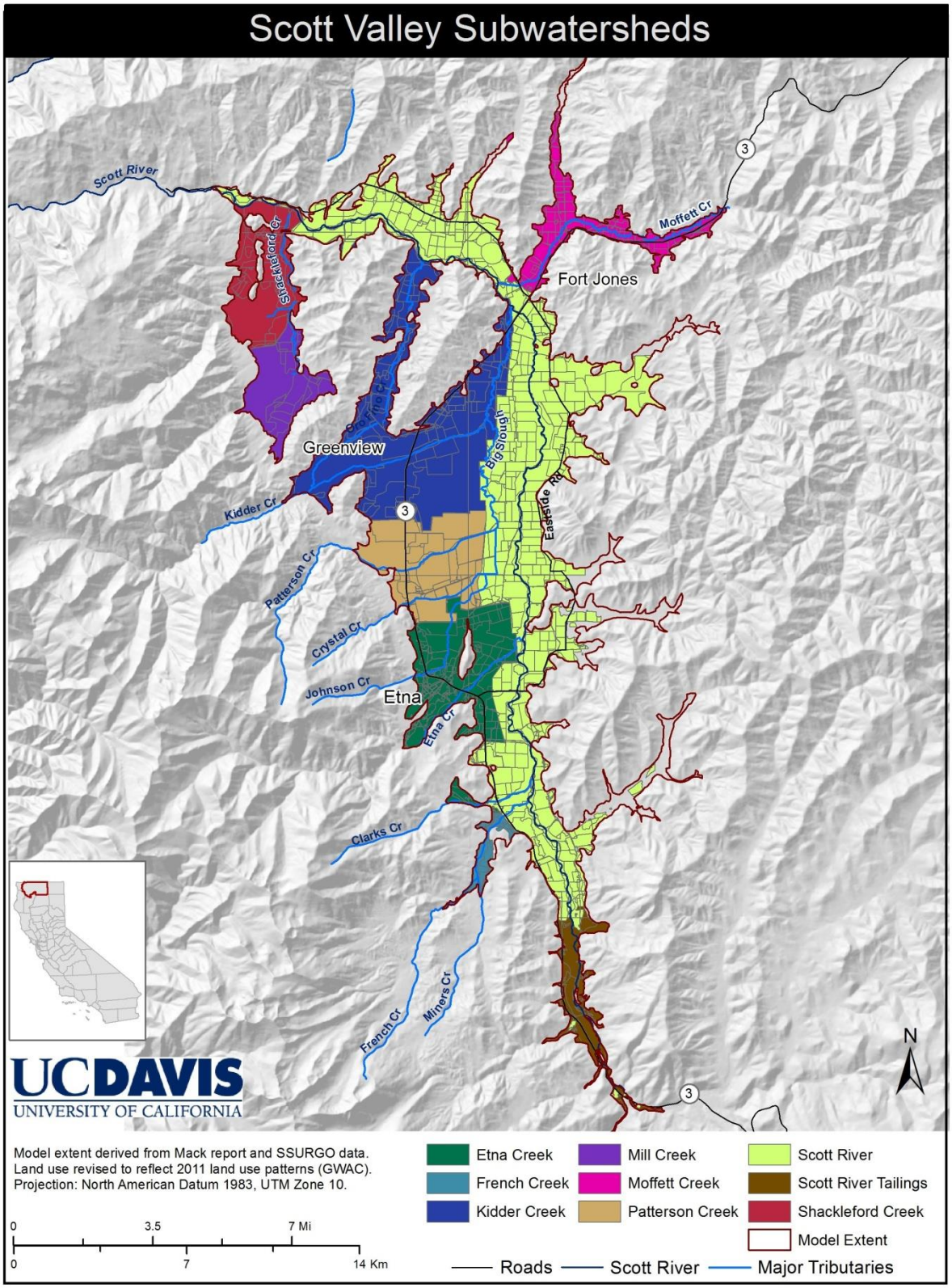

Figure 16. Map of the Scott Valley with the boundaries of the integrated hydrologic model study and the nine subwatersheds.

9.2 Land Use Categories

The CDWR land use surveys delineate polygon shapes identifying areas with various types of land use (i.e. residential, commercial, agriculture). We used the existing year 2000 land use database, which also includes attributes such as irrigation type, water source, and expanded the database to include values that describe water holding capacity, and soil hydraulic conductivity for each land use polygon. Using extensive feedback from the Scott Valley Groundwater Advisory Committee (GWAC), we confirmed or updated the water source, irrigation type and land use associated with each polygon. Feedback was provided by the GWAC and local landowners through marked up large maps that reflect the knowledge of local landowners about dominant 2000 – 2011 conditions and changes in irrigation type, water source, and land use that have occurred since the DWR survey in 2000. It is assumed that the feedback effectively reflects conditions in 2011 and the years immediately preceding 2011.

It is important to note that some of the feedback provided on land use, water source, and irrigation type reflects an outright correction of the CDWR 2000 landuse map (i.e., reflects year 2000 conditions as well as year 2011 conditions), some reflects land use changes since the year 2000 survey. For modeling purposes, we did not make a distinction between these two types of suggestions. However, the most important irrigation type change is that from sprinkler irrigation to center pivot irrigation due to the efficiency increase. That specific change was explicitly tracked in the land use database by adding a conversion date to those polygons that are in center pivots in 2011. The dynamics of that change are reflected in the soil water budget model (see below). With these dynamics simulated explicitly, and with the overall feedback from the GWAC and local landowners, the resulting landuse, irrigation type, and water source map is considered more representative of 1991 – 2011 conditions than the CDWR 2000 map. No changes were made to the shape of individual land use polygons defined in the CDWR 2000 survey.

We aggregated the land use polygons into four main categories each of which reflects a common water demand:

1. new “alfalfa/grain rotation” land use category: all land use parcels in this category are assumed to be on an alfalfa-grain rotation. Since we do not have exact data on the rotation, we simulate the rotation by creating an eight-year cycle. Each field in this category is randomly assigned one of the eight years in the cycle during which it goes into “grain” rotation. All other years, a field is assumed to be in “alfalfa” land use. Each year, one out of eight fields is in “grain” and the rest are “alfalfa”. The same eight-year rotation is followed throughout the simulation period (1990-2011). This new land use category includes the following CDWR land use classes:
    a. grain (wheat, barley, oat, triticale)
    b. corn
    c. alfalfa, mixed alfalfa/orchardgrass
    d. rice
    e. sudan
    f. miscellaneous truck crops

2. new “pasture” land use category. This includes the following CDWR land use classes:
    a. pasture
    b. highwater pasture
    c. improved pasture
    d. mixed pasture
    e. grass
    f. cemeteries
    g. lawns
    h. institutions
    i. schools
    j. residential
    k. recreation
    l. nursery
3. new land use category “ET without irrigation” representing pasture-like ET (crop coefficient, $k_c = 0.6$) but without irrigation. This includes:
    a. natural vegetation
    b. natural highwater meadow
    c. misc. deciduous trees
    d. trees
4. new land use category “no ET and no irrigation” for all land uses without ET ($k_c = 0$) and without irrigation (but with recharge from precipitation via soil moisture storage). This includes:
    a. barren
    b. commercial
    c. dairy
    d. extractive industry
    e. farmsteads
    f. industrial
    g. livestock feedlots
    h. municipal
    i. paved
    j. storage
    k. trailers
    l. unpaved
    m. vacant

Figure 17 presents the updated land use map using a lumped land use categorization scheme based on the definition of land use categories also used in the CDWR 2000 map. Figure 18 shows the same land use map after re-categorization into the newly assigned four land use categories as listed above. Both maps reflect the changes suggested by the GWAC. The new land use categories of Figure 18 are used in the water budget model development. A separate, fifth landuse category

is comprised of 166 acres of open water areas (streams, lakes, wetlands) within the study area (Table 11).

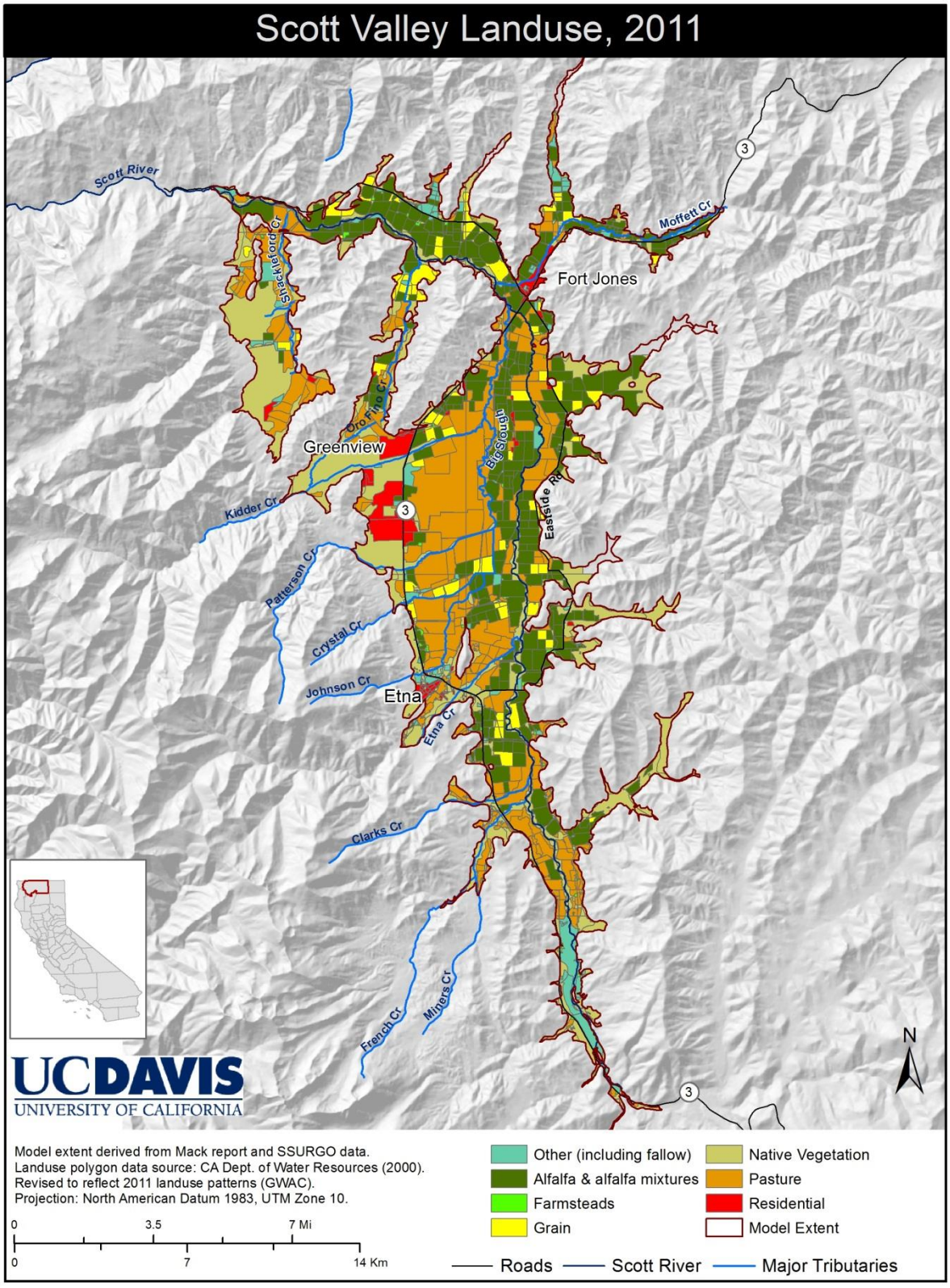

Figure 17. Land use categories based on DWR 2000 map and updated for 2011 using suggestions from GWAC and local landowners.

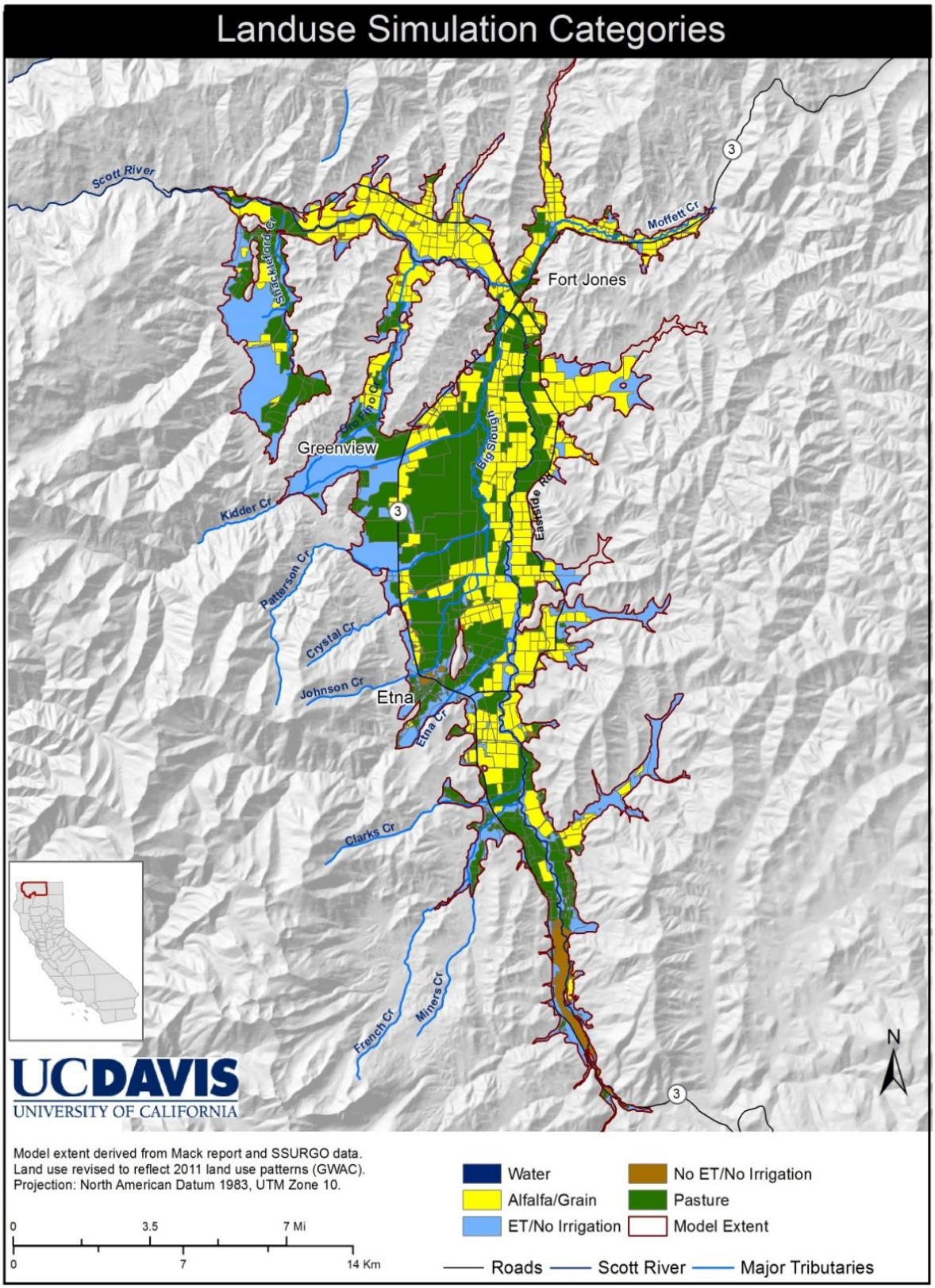

Figure 18. Aggregated five land use categories developed for the new conceptual soil water budget model from the landuse map shown in Figure 17.

9.3 Irrigation Type and Irrigation Water Source

Irrigation types were derived based on the DWR categories and summarized in three groups for modeling purposes as follows:

- "surface flood irrigation" consists of the following CDWR categories:
    - iB - border flood irrigation: the correspondent water source is surface water, mix or sub-irrigation (per June 2011 GWAC meeting, this is the same as wild flooding)
    - iF - furrow irrigation: it applies only to a few small fields, often now in center pivots with groundwater as water source for irrigation
    - iW - wild flooding: the correspondent water source for irrigation is surface water or sub-irrigation
- "center pivot sprinkler irrigation" consists of the following CDWR categories:
    - iC - center pivot: typically with groundwater as water source for irrigation
    - others that were converted to center pivot sometime in the last 20 years, with dates and prior crop specified in the new land use polygon table
- "other sprinkler irrigation" consists of the following CDWR categories:
    - iH - handmoved sprinkler irrigated
    - iR - wheel-line sprinkler irrigated

Unknown irrigation type affects 1107 acres (Table 11), of which 27 acres are classified as pasture and the remainder (1080 acres) as alfalfa/grain. In addition, 700 acres of alfalfa/grain and 1,861 acres of the pasture category, mostly residential land use in the original DWR classification (e.g., in the Ft. Jones and Etna area) are classified as non-irrigated in the year 2000 CDWR land use survey. In total, 18,549 acres are not irrigated within the study area, with or without ET.

The irrigation efficiency values used in the water budget model have been fixed based on suggestions from Steve Orloff and the GWAC. As a future modeling task, we will use irrigation efficiency as a calibration tool to check against the irrigation scheduling suggested by the GWAC. The values used in the model are:

- surface flood irrigation: 0.70 (Steve Orloff, 2011, oral communication)
- center pivot sprinkler: 0.9 (Steve Orloff, 2011, oral communication)
- other sprinkler irrigation: 0.75 (Steve Orloff, 2011, oral communication)

Irrigation water sources are represented in Figure 19 and are summarized in Table 11 as:

- Groundwater (GW)
- Surface water (SW)
- Subirrigation (SUB)
- Mixed surface water-groundwater (MIX)
- Dry (DRY)
- None/unknown/other

There are no known water sources on 177 acres of alfalfa/grain and on 475 acres of pasture, and on practically all open water and other unirrigated land uses (with or without ET).

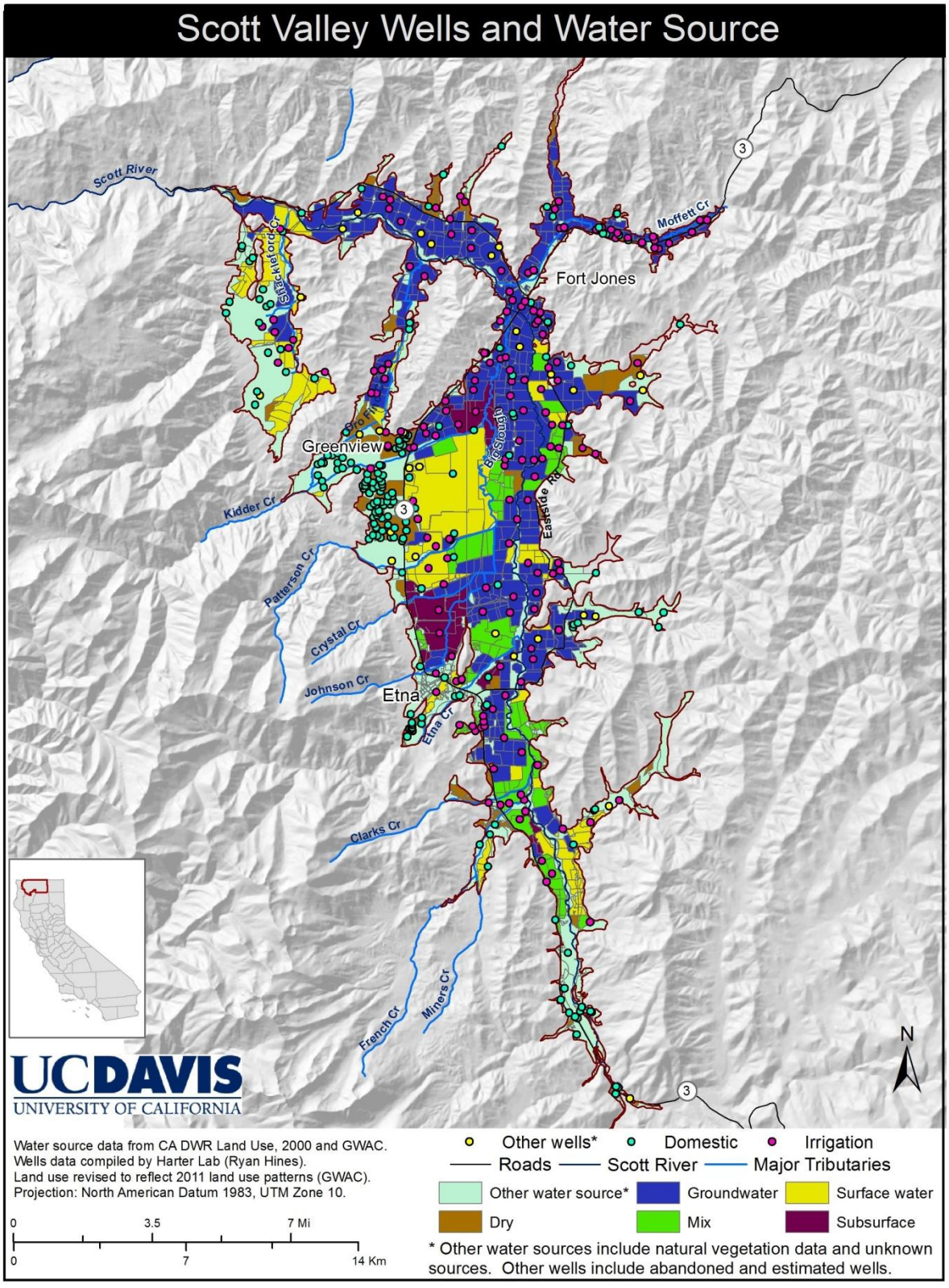

Figure 19. Water source assigned to each polygon, based on data from the CDWR Land Use, 2000, and based on revisions suggested by the Scott Valley GWAC (2011).

9.4 LiDAR Land Surface Elevation Data Analysis

LiDAR data, published by Watershed Sciences, Inc. (2010) and obtained from the NCRWQB in 2012, were used to create a bare earth digital elevation model of the Scott River area.

Because Light Detection and Ranging (LiDAR) data are typically of higher resolution than National Elevation Data (LiDAR is sub-meter accuracy while NED is available in three to 30 meter resolution), they provide a more accurate digital elevation model.

This high resolution bare earth DEM was then used to create a digitized model of the Scott River thalweg. Draped over the 2005 NAIP color aerial imagery, the bare earth DEM was categorized into 10 centimeter classifications, which showed the river channel morphology in great detail. Using the aerial imagery as a guide, the Scott River thalweg was digitized in ArcGIS, with a vertex placed every 1/3 of a meter. Elevation values from the bare earth DEM were then assigned to each of these vertices in ArcGIS. Average slope between vertices were also calculated in ArcGIS.

10 Soil Water Budget Model - Methods

10.1 Introduction and Overview

We have developed a soil water budget model that serves to define the spatio-temporal distribution of groundwater pumping, surface water diversions, groundwater recharge, and evapotranspiration throughout the Scott Valley. The soil water budget model computes spatially and temporally varying water fluxes across the approximately 50,000 acre study area. The spatial resolution is variable and equal to the individual fields and land use units (polygons) identified by the 2000 CDWR land use map, which has been updated (Figure 17), and converted into five major land use categories (Figure 18). In time, the model operates on daily information values, primarily driven by available climate and streamflow data resolution and the need to properly represent soil water storage dynamics. For surface water accounting purposes, the model domain is subdivided into nine major subwatersheds (Figure 16).

The field soil water budget method is a simple root zone bucket model at each land use polygon as described below. This model, however, does not represent a complete surface water budget of the Scott Valley, since it does not account for river-groundwater interaction or evapotranspiration off shallow water-table from non-irrigated crops or natural landscapes, or from open water surfaces (the latter being the "Water" land use category in Figure 18). The complete surface water budget will be considered when this model is coupled to the MODFLOW groundwater-surface water model which is under development.

The output from the soil water budget model is a 21 year time-series (1990-2011) of daily surface water diversions, pumping, irrigation, evapotranspiration, and recharge values at each land use polygon except those designated as "Water". The model also computes the theoretical irrigation deficiency, defined as the difference between optimal crop evapotranspiration and actual evapotranspiration. Using a daily time-step for the soil water budget model allows us to account for the often rapid dynamics in soil moisture and for carry-over storage of soil moisture for later plant evapotranspiration.

In contrast, the integrated hydrologic model will be driven by monthly stress periods, which means that pumping and recharge are constant within a month. For the integrated hydrologic model, daily water fluxes from the soil water budget model will be aggregated for each month to provide monthly, land use polygon specific recharge, pumping, evapotranspiration, and surface water delivery values. The monthly stress periods in the integrated hydrologic model reflect the generally slower dynamics of groundwater flow. However, if warranted, the budget model described here can also be applied to an integrated hydrologic modeling scenario with weekly or bi-weekly varying stress periods or to stress periods of varying period length.

The conceptual approach is largely derived from the approach taken for Version 1, but has been revised in close collaboration with UC Cooperative Extension personnel, the Scott Valley GWAC, and technical experts familiar with the Scott Valley. Some of the key differences between the

revised Version 2 soil water budget model and the earlier (unpublished) Version 1 soil water budget model include:

- daily rather than monthly time-step
- soil moisture storage changes in the soil root zone are tracked
- the southern part of Scott Valley with the tailings is included in the model domain
- revised and updated land use map and land use categories are used
- irrigation schedules and irrigation demands have been revised

Whereas the previous soil water budget model (Scott Valley Integrated Hydrologic Model Version 1) was compiled in a spreadsheet, the new soil water budget model has been developed and compiled as a Fortran program, which allows for more efficient control on various conceptual model scenarios and inclusion of soil water budget model variables in model sensitivity and calibration procedures. The development of this code and its linkage to a GIS database provides us with the capability to include detailed spatial information, readily adjust for newly available information from local parties, and provides flexibility to generate a multitude of future simulation scenarios.

10.2 Description of the Soil Water Budget Model

10.2.1 Model Input Preparation

The following data have been compiled in the previous sections to provide input for the soil water budget model:

- climate (digital climate station records)
  - precipitation
  - potential evapotranspiration
- streamflow
  - daily streamflow data on all tributaries including main stem forks
  - subwatershed delineation
- land use:
  - crops with crop coefficient
  - irrigation method
  - irrigation water sources
- soil properties (digital USDA soil maps with properties)
  - water holding capacity
- hydrogeology
  - location of pumping wells

Each land use polygon in the Scott Valley is characterized by a set of properties (or attributes) mainly derived from the GIS analysis:

- Land use, divided into the five main categories as described above (Figure 18): 1) alfalfa/grain rotation with seven years of alfalfa followed by one year of grain, 2) pasture

(including some urban landscapes, see above), 3) evapotranspiration without irrigation (includes natural vegetation, natural highwater meadow, misc. deciduous trees, trees), and 4) no evapotranspiration and no irrigation with recharge from precipitation via soil moisture storage (barren, commercial, dairy, extractive industry, municipal, industrial, paved, etc); 5) water surfaces (mostly streams), which are not included in the soil water budget model, but will be part of the integrated hydrologic model.

- Soil type derived water holding capacity (Figure 12). The model is assuming a root-zone depth of 4 ft (8 ft in the sensitivity analysis described below).
- Irrigation type (Figure 13): flood, center pivot, or sprinkler; some fields switch from flood or sprinkler to center pivot at some field-specific date between 1991 and 2011, based on review of historic aerial photos.
- Water source (Figure 19): groundwater “GW”, surface water “SW", subirrigated “SUB”, mixed groundwater-surface water “MIX”, and farming without irrigation “DRY”.

However, the alfalfa/grain land use and the pasture land use include areas for which either the irrigation type is not known or the water source is not known or both (Table 11). For the soil water budget model, the following assumptions are made to account for all potential combinations of land use, irrigation type, and water source:

If the land use is either alfalfa/grain or pasture, and:

a) water source is GW, MIX, or SW, but the irrigation type is unknown (480, 2, and 335 acres, respectively): assume that the irrigation type is “other sprinkler irrigation”;
b) water source “DRY” or “SUB”, but the irrigation type is unknown (200 and 34 acres, respectively): treat the land use as “ET without irrigation”;
c) irrigation type is unknown and the water source is unknown (56 acres): assume that the irrigation type is “other sprinkler irrigation” and the water source is GW;
d) irrigation type is “center pivot” or “other sprinkler” or “flood”, but the water source is unknown (177 acres of alfalfa/grain and 475 acres of pasture): assume that the water source is GW;
e) irrigation type is “non-irrigated”, regardless of water source (700 acres of alfalfa, 1861 acres of pasture land use, mostly in residential areas): treat the land use as “ET without irrigation”. This includes 484 acres of alfalfa/grain and 1275 acres of pasture classified as having a “DRY” water source; and 10 acres of pasture classified as having a “SUB” water source. No or unknown water source is specified for 120 acres of non-irrigated alfalfa/grain and for 469 acres of pasture land use.

These assumptions may not accurately reflect the irrigation type or water source in all cases, but due to the relatively minor acreage of these special cases, the above simulation process is a representative simplification that does not significantly affect the outcome of the soil water budget model.

10.2.2 Tipping Bucket Approach for Soil Water Budget Modeling

The soil water budget calculations are performed using a tipping bucket approach. The main concepts associated with the tipping bucket approach here are the following:

- The simulation starts with the beginning of water year 1991, on October 1, 1990 and is performed daily.
- We assume that the initial soil water content on October 1, 1990 is zero, since the starting point is after the completion of the irrigation season (the soil water profile fills during the first winter months).
- We assume that adjusted daily precipitation (Padj) is the portion of daily precipitation (P) that infiltrates into the soil and is available for daily evapotranspiration (ET) or recharge:
    - if $P > 0.2*ET_0$, Padj(*i*) = P
    - if $P <= 0.2*ET_0$, Padj(*i*) = 0 (FAO Bulletin 56)
    - ET_0 is the daily reference evapotranspiration (FAO Bulletin 56)

  This effectively assumes that precipitation events of less than 20% ET_0 on any given day will sit on leaves or bare ground and evaporate before the end of the day, without affecting soil water storage, plant evapotranspiration, etc. For all soil water budget computations, we use adjusted precipitation and not precipitation. Adjusted precipitation is the same across the valley, since we only use one ET_0 value.

With daily time-steps, the tipping bucket approach used to calculate daily soil moisture storage changes and deep percolation in each polygon can be expressed as follows:

Theta (i) = max(0, theta(i-1) + Padj(i) + Irrig(i) –actualET(i) –Recharge(i)) Eq. 1

Recharge (i) = max(0, theta(i-1) + Padj(i) + Irrig(i) –actualET(i) – WC4(i)) Eq. 2

Where:

- Theta(i) = water content at the end of day i
- Padj(i) = precipitation on day i
- Irrig(i) = irrigation on day i
- ET(i) = evapotranspiration on day i= ET_0*crop_coefficient
- Recharge (i) = deep percolation to groundwater
- Actual ET(i) = min (ET(i), theta(i-1) + Padj(i) + Irrig(i)) Eq. 3

Groundwater recharge is defined here as the amount of soil water that cannot be held against gravity, i.e., the amount of soil water that is above the water holding capacity, WC4, of the root zone in the land use polygon at the end of each day. The model does not account for the time delay between water leaving the root zone and water reaching the water table at the top of the groundwater system. Given that water table depth is generally less than 20 ft and that recharge values are aggregated monthly for the integrated hydrologic model, the assumption of

"instantaneous recharge" is justified, but can be evaluated as part of a sensitivity analysis with the integrated hydrologic model.

The above algorithm intrinsically exerts complete mass balance control on each land use polygon:
Padj(i) + Irrig(i) – actualET(i) – Recharge(i) = theta(i)-theta(i-1) Eq. 4

Furthermore, we can compute deficit irrigation for each polygon as follows:

Deficiency(i)= ET(i) – actualET(i) Eq. 5

10.2.3 Irrigation Water Source Simulation

Where does the irrigation water, Irrig(i), come from? The source of the irrigation water depends on the water source and land use specified for an individual land use polygon.

- For pasture, irrigation water typically is supplied by surface water. Groundwater pumping in pasture occurs only for polygons where the GIS land use coverage indicates that irrigation water is being sourced fully or partially from groundwater ("GW" or "MIXED", see below).
- Alfalfa/grain land use polygons can be irrigated with surface water, groundwater, or a mix of surface water/groundwater. Based on information from the GWAC, the distinction between "SURFACE WATER" and "MIXED" water source was ignored, and all alfalfa/grain fields with "SURFACE WATER" source were treated as if equipped for a "MIXED" source: in either case, alfalfa/grain is always fully irrigated. First with surface water and when surface water allocations dry up, groundwater is used for irrigation.

The simulated decision process that leads to a land use polygon switching from surface water irrigation to groundwater irrigation can be summarized as follows:

- Total monthly discharge rates in the Scott River and in its tributaries at the entry into the Scott Valley are obtained for each of the nine subwatersheds as calculated by the regression analysis (chapter 5).
- Within each subwatershed and for each month, the surface water used for irrigation by each polygon is subtracted from the total monthly discharge of the respective subwatershed stream in a given month.
- Once the total irrigation demand within a subwatershed, in a given month, exceeds (estimated) stream discharge, and if the field is alfalfa/grain, then groundwater is used to make up the difference between surface water available and the irrigation demand. The available amount of surface water is distributed to all polygons designated for use of surface water at equal water depth (water volume proportional to polygon size). For each polygon, the difference between surface water supply and irrigation demand for a given month with surface water shortage is obtained by groundwater pumping.

- Canal losses to groundwater are currently not considered separately. Effectively, these are included in the irrigation efficiency concept and therefore contribute to diffuse landscape recharge.

The surface water delivery and groundwater pumping rates are driven by irrigation schedules and by precipitation and evapotranspiration. Urban and domestic pumping for irrigation of lawns, golf courses, cemeteries, etc. is included in the soil water budget model, but allocated to nearby agricultural wells. Domestic and urban water use other than for domestic/urban/residential irrigation is currently neglected in the soil water budget model, but can be accounted for in the MODFLOW groundwater-surface water model. Domestic/urban water use other than that used for lawn/garden irrigation in Scott Valley is only a very small fraction of total water use in the Scott Valley.

In the current water budget calculations, we apply an irrigation management scheme in which irrigation is driven by crop ET and available precipitation (see below for details).

Recharge occurs across the entire integrated hydrologic modeling domain, either from irrigation and rainfall, or from rainfall only (non-irrigated land uses).

10.2.4 Irrigation Management and Scheduling Simulation

The irrigation simulation is based on irrigation efficiency and evapotranspiration as the drivers for computing applied water demand. It is based on the concepts developed for the CDWR Consumptive Use Program (Orang et al., 2008). Irrigation amount is calculated using the same approach for alfalfa, grain, and pasture, but the irrigation scheduling and irrigation demands differ depending on three variables: crop type, irrigation type, and water source. Details of the irrigation management model are described here. Note that land use designated as "Water" is not associated with recharge, irrigation, evaporation, groundwater pumping, or surface water deliveries.

1) Alfalfa/grain and pasture

Following the literature (FAO publication 56) for alfalfa, irrigation in each polygon *k* starts on the first day *i* on or after March 25th when the soil water content has dried to less than 45% of field capacity:

$$\text{Theta}(i) < (1-0.55)*\text{WC4}(k) \qquad \text{Eq. 6}$$

The depletion factor 0.55 is from FAO Publication 56, Table 22.

The last alfalfa irrigation application occurs on September 5th (typically it ends prior to the 3rd cutting which is anytime between the last week of August and the 3rd week of September. According to GWAC, few fields are irrigated after Labor Day). It is important to note that these "irrigations" are not simulated as individual events but are spread evenly across the irrigation season, i.e., the irrigation demand is computed daily based on the crop water demand (see below).

For grain, the first irrigation on a field *k* is determined exactly as for alfalfa but the earliest potential starting date is March 15th. However, the last day of continuous irrigation on grain is simulated to be much earlier than in alfalfa, on July 10th, after which the grain is harvested.

For pasture, the irrigation season is always from April 15th through October 15th (184 days). However, on pasture that is surface water irrigated (which represents most pasture), no irrigation occurs once surface water supplies become unavailable (the explanation of when surface water is considered unavailable is presented above). When applied, irrigation is applied continuously based on daily ET demand (again, we do not distinguish individual irrigation events).

The approach chosen here for simulating irrigation assumes that fields are all irrigated with the same, irrigation type-specific irrigation efficiency. This represents a simplification of reality, where some fields are relatively over-irrigated (mainly pasture fields) and others are relatively under-irrigated. However, the irrigation efficiencies are chosen to represent average irrigation management practices, given the irrigation type. The approach here also neglects irrigation non-uniformity within individual fields. Large non-uniformity with significant under-irrigation in some parts of the field may effectively increase field-scale irrigation efficiency.

For each polygon j and for each day i, the daily irrigation amount is calculated as shown in eq. 7 based on the evapotranspiration of the crop, adjusted for precipitation and considering the irrigation efficiency of the crop:

Irrig_j(i)=(1/irrigation_efficiency_j)*(Max(0, (ET_j(i)-Padj(i)) Eq. 7

Where:

- ET_j(i) = Kc_j* ET_0(i) where K_c is the crop coefficient,different for each crop
- Padj(i) is the adjusted precipitation on day i (Eq. 4)

For the soil water budget model, we assume that there is no contribution to evapotranspiration from groundwater. Groundwater contribution will be thoroughly evaluated once the integrated hydrologic model is developed, calibrated and coupled to the soil water budget model. This may require an iterative coupling process between the integrated hydrologic model development and the soil water budget model development.

2) ET/no irrigation category

The main assumption in this land use category is that, at all times:

Irrig(*i*) = 0

ET in this land use category is computed separately by two models: the soil water budget model and the groundwater flow model (MODFLOW).

In the first step, we use the soil water budget model to compute daily ET (on day *i*):

ET(*i*) = k_c* ET_0(*i*) = 0.6 * ET_0(*i*)

With the additional constraint that ET(*i*) <= Theta(*i*-1) + Padj(*i*)

This latter constraint is the key difference to an irrigated crop: here, ET is constrained to the naturally available water.

In a second step, ET that is due to direct uptake from the water table will be computed with the groundwater flow model (MODFLOW with the evapotranspiration, ET, package). The MODFLOW ET package uses root zone depth and maximum possible crop ET as input parameters.

The recharge is computed as indicated in the soil water budget model (Eq. 2, section 5.1). Note that recharge is computed without consideration of ET directly from the water table. This means that recharge may occur even if the water table is in the root zone. This conceptual dilemma results from the fact that:

- recharge computation is done *prior* to MODFLOW and is an input to MODFLOW
- direct ET from the water table is computed *as part* of the MODFLOW simulation

Effectively, the explicit coupling of these two components will not have much influence on the result, as water mass is still conserved by not allowing the sum of the two ET values (soil water budget model and MODFLOW) to be larger than the optimal ET from this land use category (0.6 * ET_0). Note that this simulation process only applies to non-irrigated ET land uses.

3) No ET / no irrigation category

Land use categories of this type have neither irrigation nor evaporation, or evapotranspiration from plants:

Irrig(*i*) = 0 at all times

ET(*i*) = 0 at all times

In the polygons within this category, we assume that runoff is negligible and that therefore recharge is equal to the adjusted precipitation:

Recharge (*i*) = Padj(*i*)

10.3 Calibration of Reference Evapotranspiration (ET_0)

Due to the sparse amount of observed data, calibration of the soil water budget model alone (i.e., not yet coupled to the groundwater MODFLOW model) is very difficult. Some values of reference ET and ET were provided by Hanson et al. (2011a) and have been used for a hand-calibration of the ET component used in the model.

Reference ET (ET_0) for the soil water budget model has been calculated with the NWSETO program developed at UC Davis, which is based on the Hargreaves and Samani (1982) equation. The

reference ET values are summarized in Table 12 for the years 2007-2010 and are compared against reference ET values calculated with the Hargreaves equation (Hargreaves et al., 1985).

Table 12 Reference ET (Seasonal Reference ET) calculated with the Hargreaves equation (Hargreaves et al., 1985) (modified from Hanson et al., 2011a) and obtained with the NWSETO program used here (Hargreaves and Samani, 1982).

	ET_0 (March 15-October 1)	
Year	NWSETO calculated values (in)	ET_0 values (March 15-October 1) with Hargreaves eq. (in)
2007	40.12	44
2008	39.48	42.6
2009	40.4	40.4
2010	38.12	37.4

The reference ET(ET_0) values calculated with the NWSETO program overall were in agreement with the reference ET values based on the Hargreaves equation (Table 12).

With the above reference ET values, crop evapotranspiration (which we call ET, as mentioned above) is calculated as:

$ET=k_c*ET_0$

where ET_0 is the reference ET described above and k_c is the crop coefficient.

Observed values of alfalfa ET in Scott Valley were also available (Hanson et al., 2011a) and have been compared with the calculated values.

As shown in Table 13 , observed and calculated alfalfa ET values for the period March 15-October 1 are in agreement for three of the years considered: 2007, 2009 and 2010. The values for 2008 are in disagreement because of a significant number of smoke days that occurred in June-July 2008 and are not accounted for in the NWSETO-based ET estimate.

Table 13 Measured and calculated ET values for alfalfa using a crop coefficient k_c =0.95 . Measured values were obtained from Hanson et al., 2011a, Table 2).

Crop coefficient for Alfalfa= 0.95	ET (March 15-October 1)	
Year	Calculated values with k_c=0.95	Measured values (March 15-October 1)
2007	38.11	38.3
2008	37.34	29.4
2009	38.48	38.8
2010	36.13	36.03

* values for 2008 are expected to be lower than other years because of the numerous smoke days

11 Soil Water Budget Model: Results

This section presents the results of the soil water budget analysis. Results are compared against irrigation, evapotranspiration and recharge data available from relevant literature and against data provided by the local GWAC.

The water budget simulation provides daily, field-by-field land use polygon specific outputs for all of the following variables, which are aggregated to provide yearly and long-term average rates by polygon, by land use, and by subwatershed:

1. Pumping: each polygon is assigned to the nearest well in the irrigation well database. If there are multiple wells in one polygon, the total pumping need is evenly split between the wells, while the pumping rate in a well that is serving multiple polygons is the sum of all daily water needs in the associated fields;
2. Recharge, deep percolation, as calculated with Eq. 2;
3. Crop Evapotranspiration (ET) under optimal irrigation (=crop coefficient multiplied by ET_0);
4. Actual ET- the ET actually occurring, limited by the available water in the root zone including the amount of irrigation and precipitation on a given day *i* (Eq. 3);
5. Deficiency - the difference between optimal crop ET and actual ET, which may be limited by the amount of water available (e.g., where surface water is the only source of irrigation water or where no irrigation water is supplied) (Eq. 5).

Daily pumping and recharge rates are aggregated to monthly totals for the MODFLOW groundwater-surface water simulation.

As part of the extensive GIS analysis described above, the watershed has been subdivided into a total of 2,119 polygons, 710 of which are alfalfa/grain (with an 8 year rotation, i.e., 1 year grain followed by 7 years alfalfa), 541 are pasture, 451 polygons are in the category with evapotranspiration but no irrigation, 417 do not have evapotranspiration nor irrigation (Figure 18). Each polygon is also associated with a subwatershed, an irrigation type, and a water source. Table 14 presents a summary of polygon area, and the fraction of the area irrigated by different water sources used in the soil water budget model.

Table 14. Summary of number of polygons, area, and % of the area irrigated with each of the water sources used in the soil water budget model. The area of alfalfa/grain changes slightly every year because of the rotation, but the overall ratio is of alfalfa area to grain area is 7:1. 177 acre (1%) of alfalfa/grain and 475 acres (3%) of pasture have no or unknown water sources.

	Total /Irrigated Area (ac)	*% area with SW irrigation*	*% area with GW irrigation*	*% area with mixed (GW/SW) irrigation*	*% area dry*	*% area subirrigated*
Alfalfa	15,200 / 13,900	7	77	7	6	1
Grain	2,200 / 2,000	7	77	7	6	1
Pasture	16,600 / 11,900	39	18	16	13	11

Results are presented for the entire 21 year period starting on October 1, 1990. As noted earlier, results reported here are based on the precipitation time series described in section 4.2 and based on a complete, mostly synthetic streamflow dataset obtained by regression as presented in Chapter 5.

11.1 Water Budget Analysis

Average annual values totaled over the project area are computed for irrigation, crop evapotransporation (ET), actual evapotranspiration, deficiency, recharge, and pumping. These are values estimated using the daily values calculated in the soil water budget model (Table 15). Simulation results must not be confused with measured values and they have not been calibrated against field data. For recharge and pumping, no field records exist. Irrigation and evapotranspiration totals are compared against reported field data later in this section.

Maps showing the polygon specific yearly average values over the 21 year period in inches/year for irrigation, recharge, pumping, recharge minus pumping and deficiency are also presented to provide information on the spatial distribution of the results (Figure 20 to Figure 25).

Table 15. Average simulated annual water budget terms averaged over the 21 year period. The numbers represent rates in inches/year for each land use (top) and in acre-feet/year over the entire study area (bottom). Note that these are soil water budget model simulation results and do not reflect actually measured values. Irrigation includes irrigation with surface water and irrigation with groundwater. Recharge also includes all landuse polygons irrespective of whether irrigation water is from surface water or from groundwater. All calculations assume that the water table is below the root zone.

Inches/Year	Crop ET[1]	Actual ET[2]	Irrigation	SW Irrigation	GW Pumping	Recharge	Deficiency	Area
Alfalfa	42.0	40.1	33.1	4.1	29.0	14.6	1.9	13,893 ac
Grain	16.2	16.1	14.1	2.1	11.9	18.4	0.1	1,985 ac
Pasture	40.0	33.9	29.7	20.8	9.0	17.2	6.1	11,909 ac
ET noIRR	11.2	10.8	0.0	0.0	0.0	10.8	0.4	20,363 ac
noET noIRR	0.0	0.0	0.0	0.0	0.0	21.5	0.0	1,695 ac

Acre-Feet/ Year	Crop ET[1]	Actual ET[2]	Irrigation	SW Irrigation	GW Pumping	Recharge	Deficiency	Area
Alfalfa	48,700	46,400	38,300	4,730	33,600	16,900	2,230	13,893 ac
Grain	2,670	2,660	2,330	355	1,970	3,040	11	1,985 ac
Pasture	39,700	33,700	29,500	20,600	8,890	17,100	6,060	11,909 ac
ET noIRR	18,900	18,300	-	-	-	18,300	636	20,363 ac
noET noIRR	-	-	-	-	-	3,040	-	1,695 ac

[1] Crop ET = ET_0 * crop_coefficient

[2] Actual ET = estimated actual ET occurring, limited by available water in the root zone (with or without irrigation)

A total of 15,900 acres of the “alfalfa/grain” category, which includes miscellaneous crops, is irrigated. Total crop ET from alfalfa is nearly 49,000 acre-feet per year (af/y) and 2,700 af/y from grains. Crop ET is met by precipitation, soil moisture, and an estimated 38,000 af/y of irrigation onto alfalfa and 2,300 af/y of irrigation onto grains. Total pumping for those two crops is estimated to be about 35,600 af/y, while only about 5,000 af/y of irrigation water are estimated to be from surface water.

Irrigated “pasture” including some residential/urban lawn areas covers 12,000 acres with an estimated total crop ET of nearly 40,000 af/y. Two-thirds of the nearly 30,000 af/y of irrigation water is from surface water (20,600 af/y) with the remainder from groundwater (8,900 af/y).

Total surface water deliveries to irrigated areas are estimated to be about 26,000 af/y, groundwater pumping is estimated to be on the order of 44,500 af/y not including groundwater uptake in about 2,100 acres of subirrigated areas.

An additional 19,000 af/y of consumptive use occurs on lands in the “ET - no Irrigation” land use areas (including dry farmed or sub-irrigated crops). This estimated ET is supplied by precipitation and soil moisture storage and does not account for any groundwater uptake.

Analysis of the spatial and temporal distribution of irrigation and recharge fluxes suggests the following main findings:

- Highest irrigation and pumping rates occur in polygons with pasture as land use and groundwater as water source (Figure 20 and Figure 23): this can be explained by the fact that pasture has the longest irrigation season. In polygons with groundwater as water source, irrigation rate and pumping rate are the same.
- Highest recharge rates (Figure 21) occur in polygons with pasture as land use and with groundwater as water source, in vacant land use polygons located in the tailings subwatershed, and in polygons with very small water holding capacity. Recharge is expected to be higher where there is higher irrigation or less plant transpiration;
- The lowest recharge rates (almost zero recharge) occur, for example, in some polygons south of Greenview around Highway 3: as shown in Figure 19, they correspond to dryland. They rely on precipitation as water source for plants, which efficiently scour available moisture and therefore show little natural recharge, typical of a semi-arid climate;
- Low recharge rates (between 4 and 8 in/year) occur in some fields north of Etna: these have pasture as land use, but they are subirrigated (high water table);
- Deficiency (Figure 25) occurs in the months immediately following the end of the irrigation season (September, October, November).

A year-specific analysis of the water budget for the 21 year period has also been performed (Figure 26 to Figure 28).This analysis allows us to highlight differences in the water budget between dry and wet years (highlighted with red and blue arrows, respectively). Dry and wet year classification is identical to that shown in Figure 6.

As expected, dry years are marked by smaller amounts of recharge to groundwater and a smaller amount of applied surface water. Lower surface water use reflects the modeled constraints in irrigation of pasture, which is limited by the estimated or measured (when available) monthly flow in the stream associated with the subwatersheds to which a field belongs.

Typical characteristics contrasting alfalfa/grain soil water budgets with pasture water budget dynamics include:

1) Alfalfa/grain land use (Figure 27) is higher in actual evapotranspiration, higher in applied groundwater and has an overall low fraction of applied surface water. This is expected considering that alfalfa/grain is mostly groundwater irrigated (Table 14);
2) Pasture land use has higher applied surface water and almost no applied groundwater. The amount of applied groundwater does not change dramatically from year to year because there are no large differences in the length of the pasture irrigation season between different years. Large differences occur in the use of surface water between wet and dry years. Where the water source is groundwater, year-to-year differences in groundwater use are small and due to annual differences in the irrigation start date, but then irrigation continues for the entire season each year, regardless of year type (wet, normal, dry);
3) Recharge in alfalfa/grain is similar to pasture. A few pastures have high recharge rates due to being irrigated with groundwater at high irrigation rates (low irrigation efficiency assigned by the model).

Effects of dry and wet years on the amount of applied surface water and applied groundwater are shown in more detail for alfalfa and for pasture (Figure 29). In dry years, the amount of applied surface water generally decreases while the amount of groundwater use increases.

The results of the soil water budget model are generally in agreement with what would be expected considering the background information on land use, irrigation water source, irrigation type, and precipitation.

The soil water budget model can be adjusted to accommodate changes in inputs and/or operational assumptions. Further sensitivity analysis and tests can be performed to evaluate assumptions.

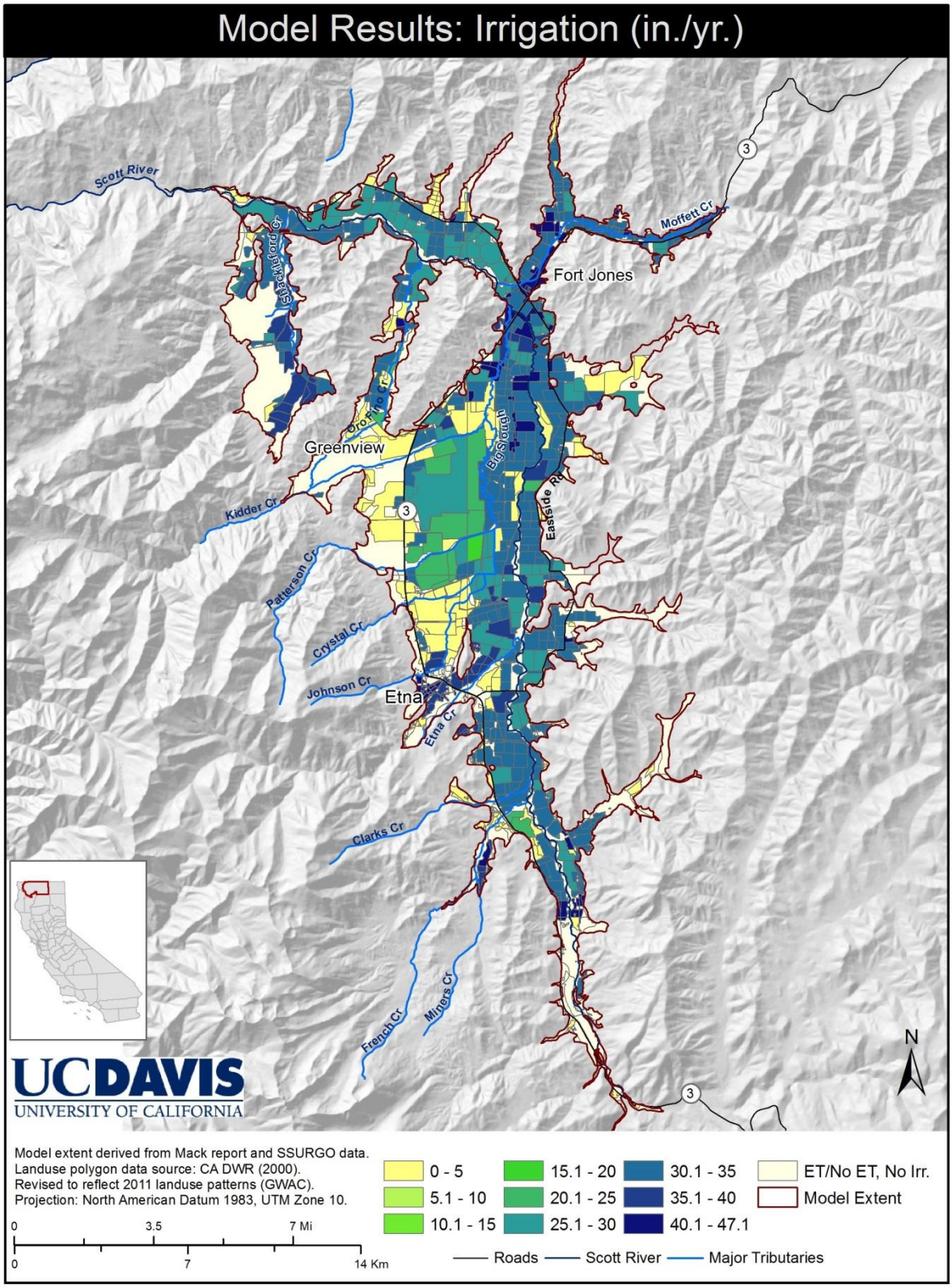

Figure 20. Map of land use polygon specific average annual irrigation rates (inches/year) between October 1990 and September 2011.

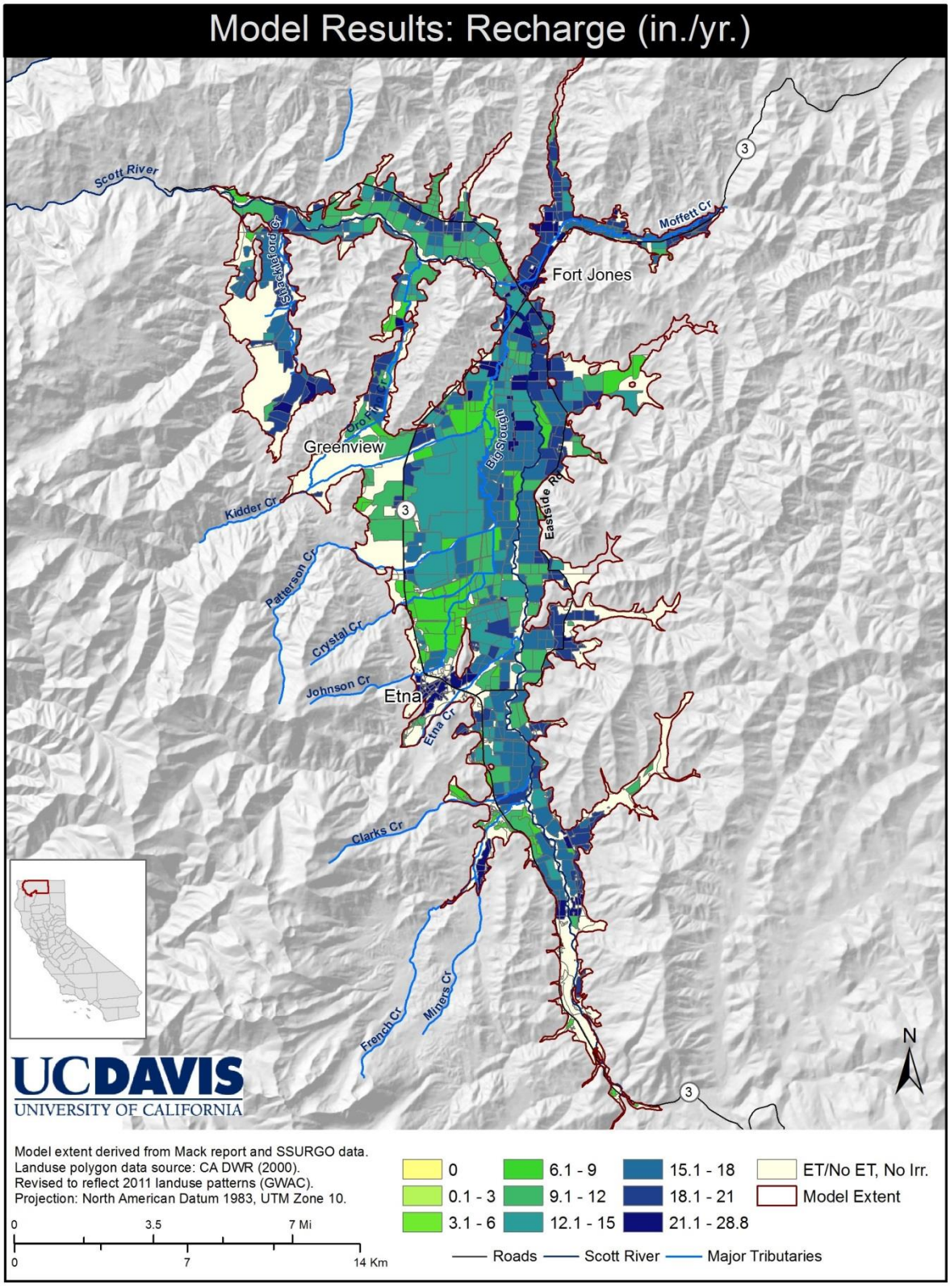

Figure 21. Map of land use polygon specific average annual recharge rates (inches/year) between October 1990 and September 2011.

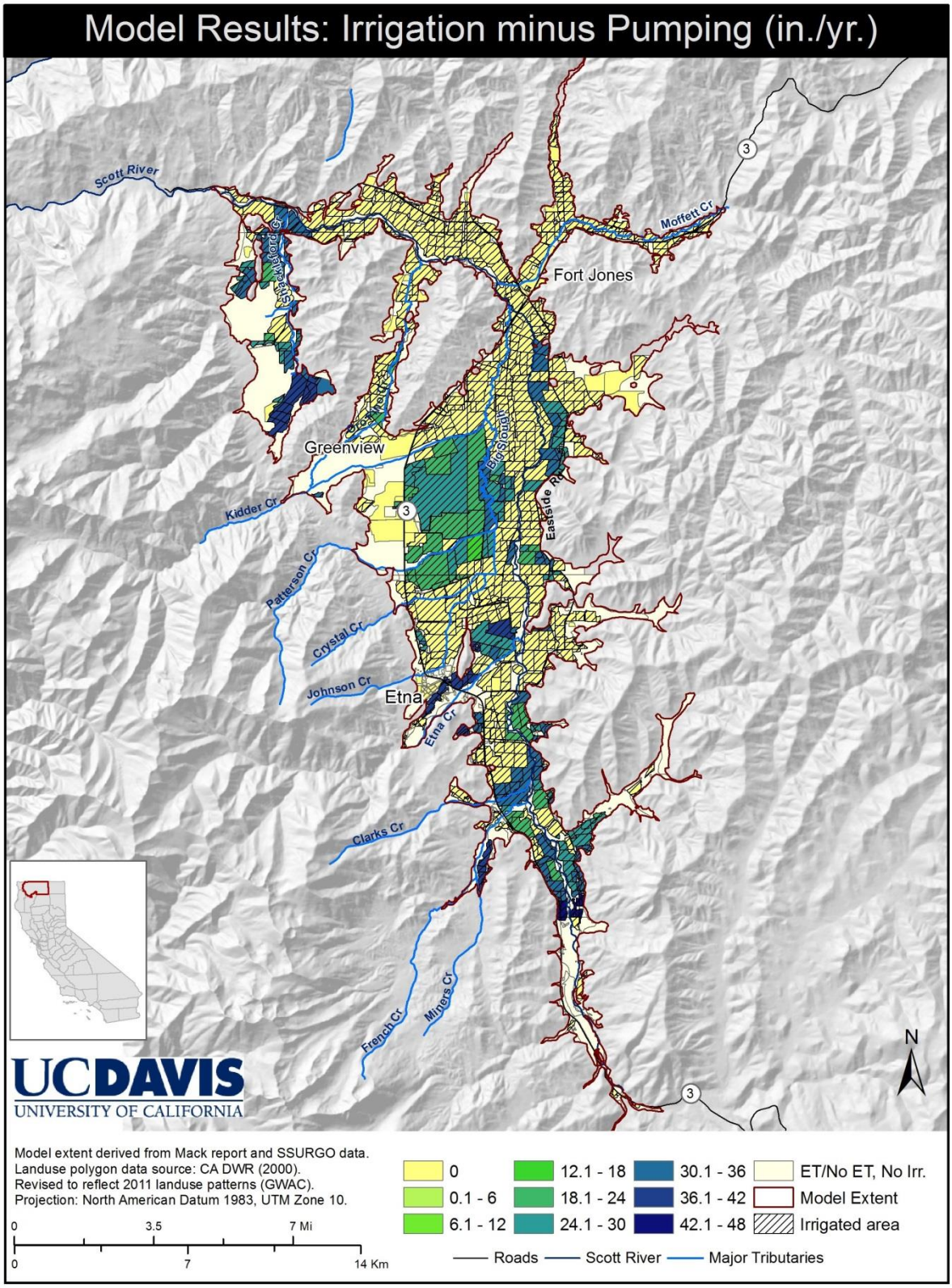

Figure 22. Map of land use polygon specific average annual applied surface water rates (inches/year) between October 1990 and September 2011. The amount of applied surface water is calculated as the difference between the total irrigation and the pumping.

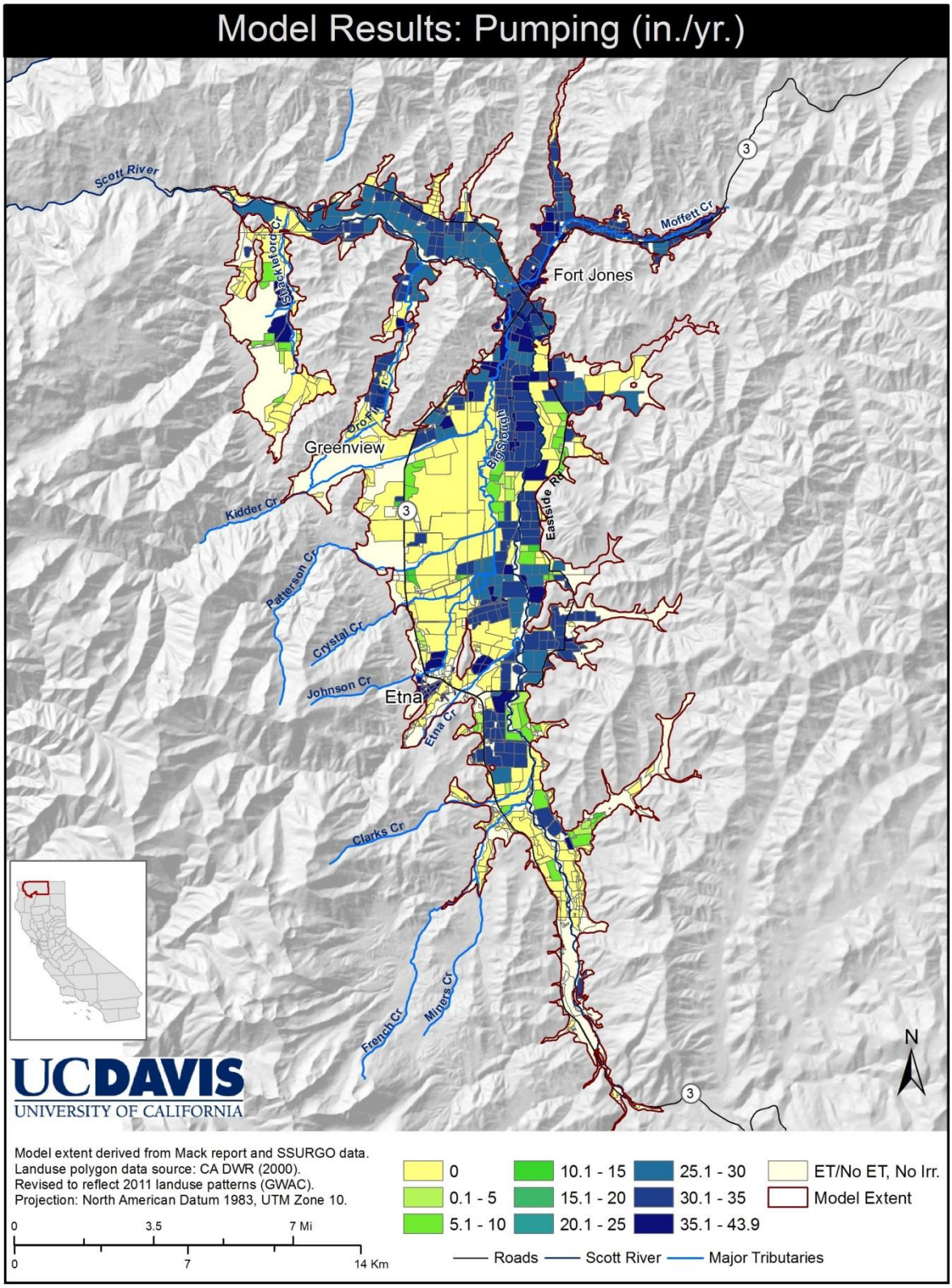

Figure 23. Map of land use polygon specific average annual pumping rates (inches/year) between October 1990 and September 2011.

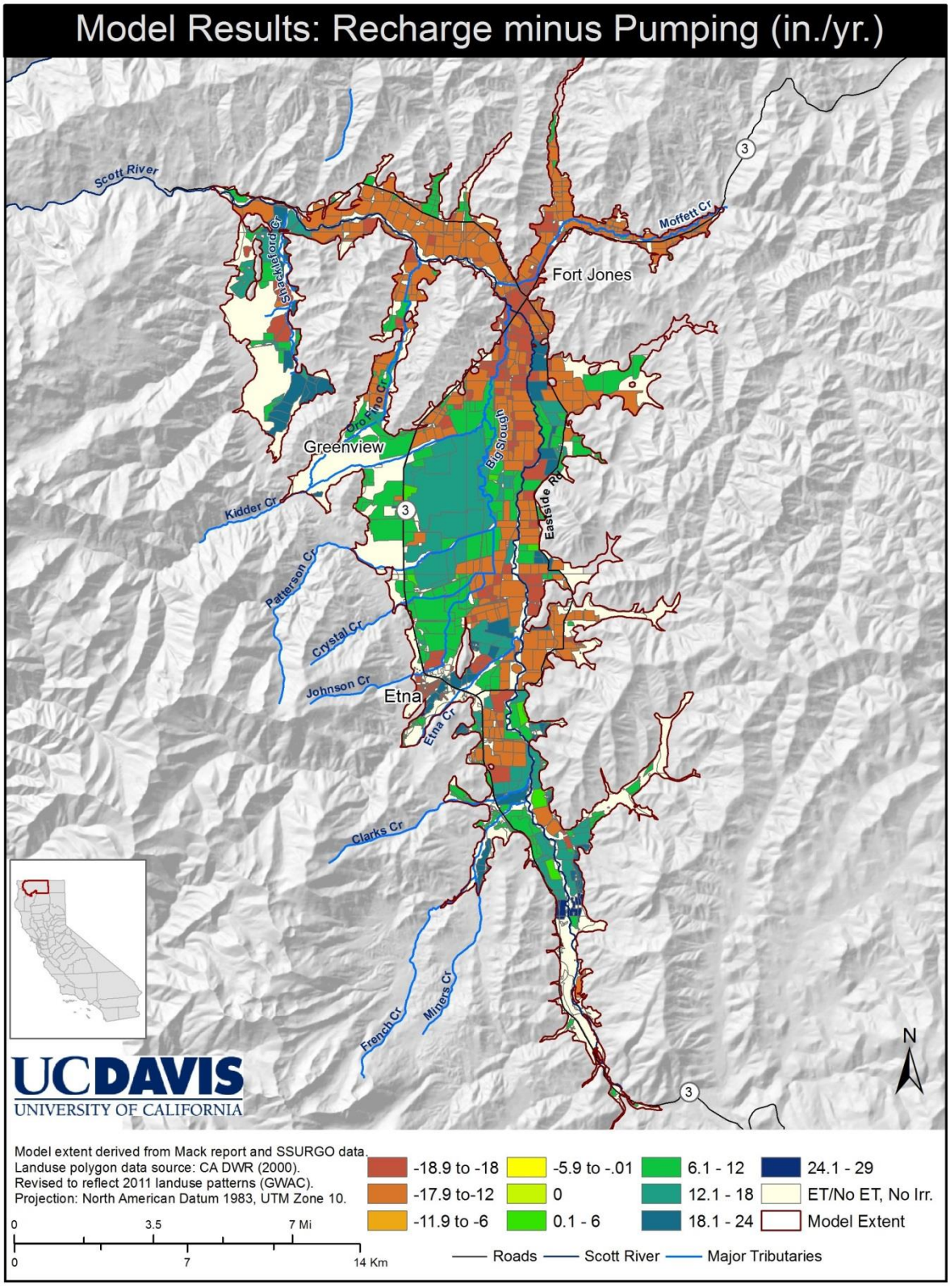

Figure 24. Map of land use polygon specific average annual recharge minus pumping rates (inches/year) between October 1990 and September 2011.

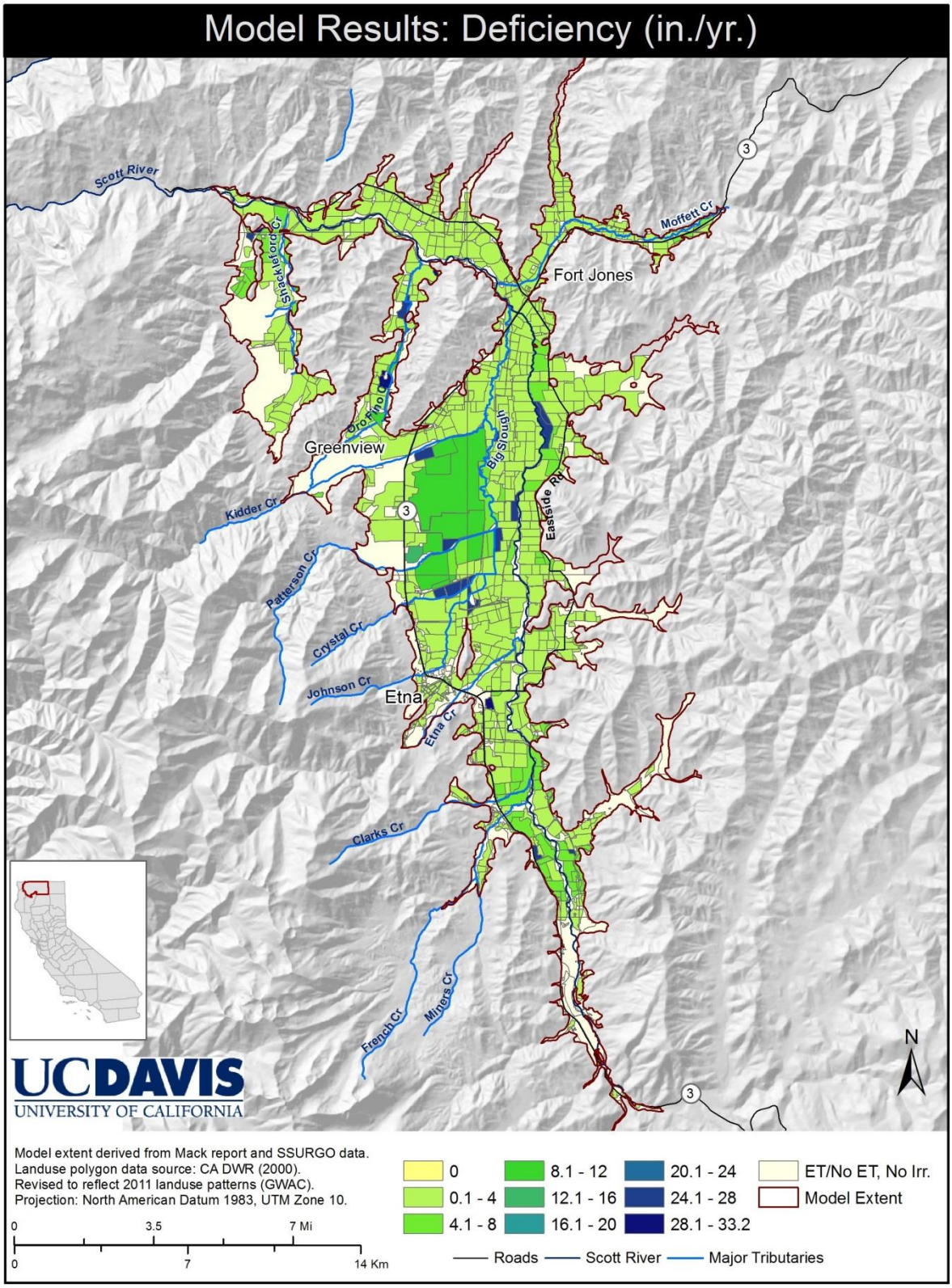

Figure 25. Map of land use polygon specific average annual deficiency rates (inches/year) between October 1990 and September 2011. Deficiency is defined as the difference between actualET and ET under optimal water supply conditions. Deficiency occurs in pasture or after the irrigation season ends in alfalfa

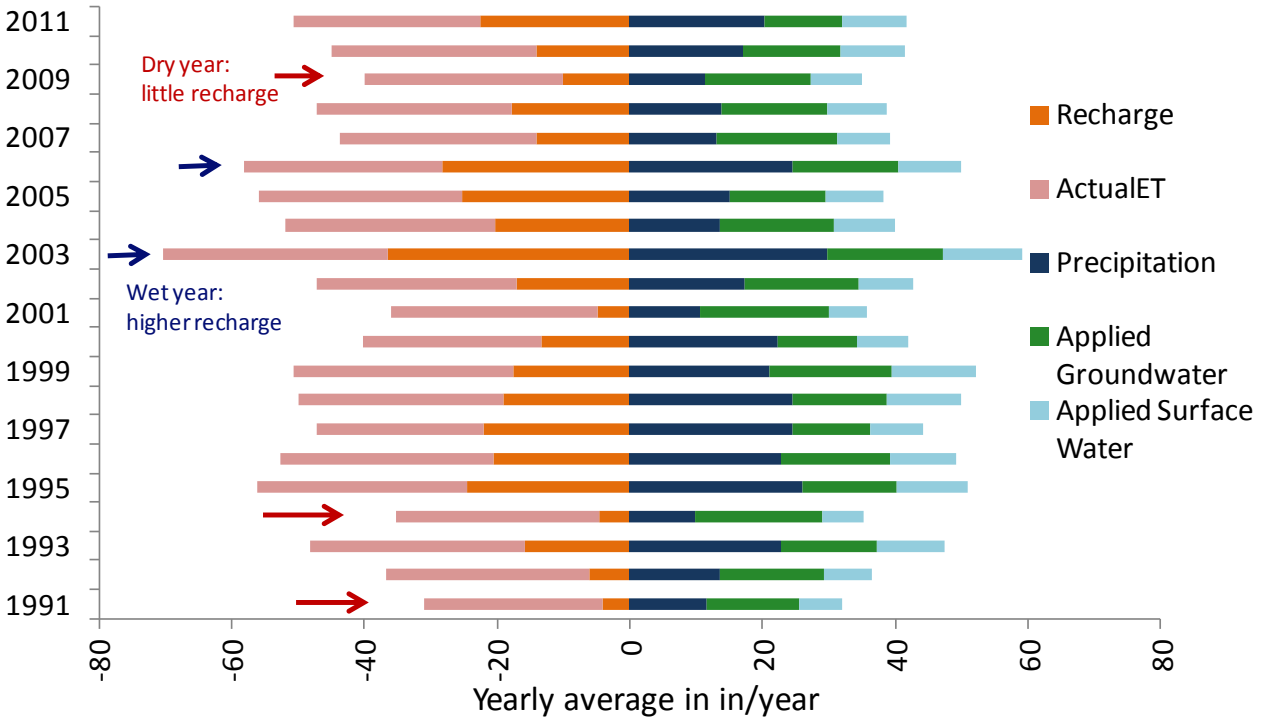

Figure 26. Yearly soil root zone water budget in in/year, area-weighted average for the entire Scott Valley project area. Input to the root zone shown as positive values (precipitation, applied groundwater and surface water). Output from the root zone shown as negative values (actual ET and recharge).

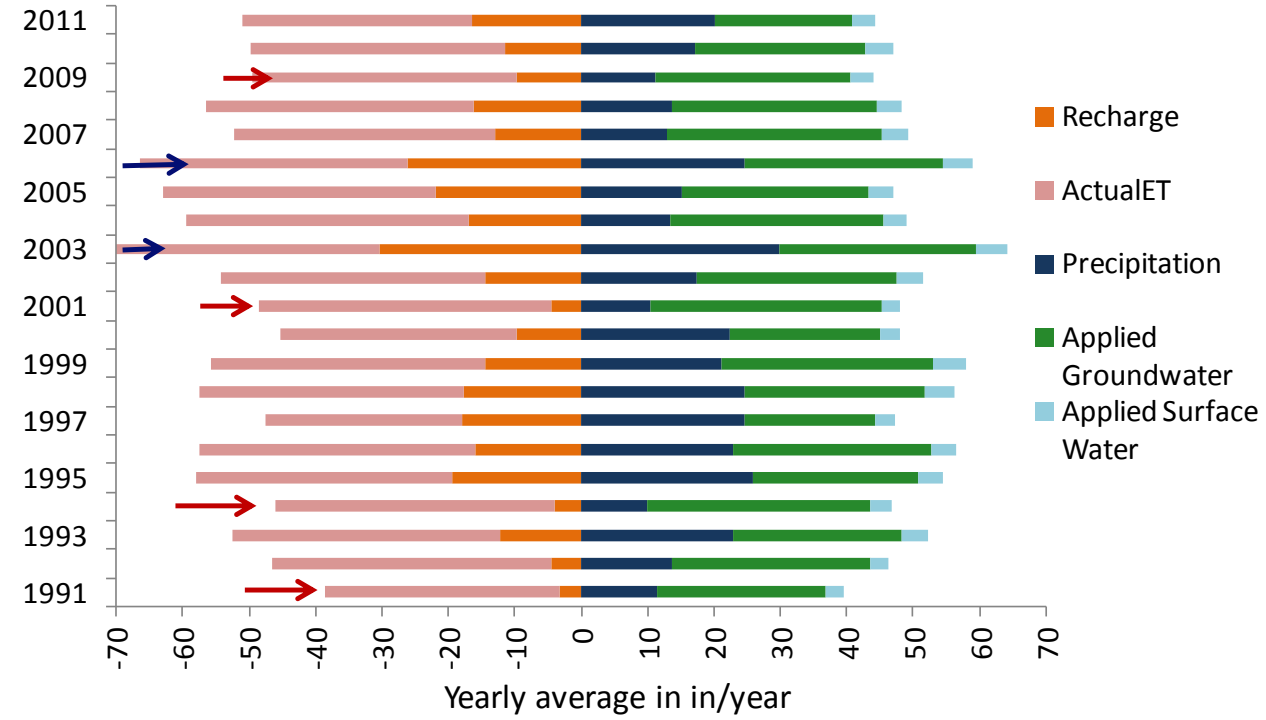

Figure 27. Yearly soil root zone water budget in in/year, area-weighted average for the alfalfa polygons over the entire Scott Valley project area. Input to the root zone shown as positive values (precipitation, applied groundwater and surface water). Output from the root zone shown as negative values (actual ET and recharge).

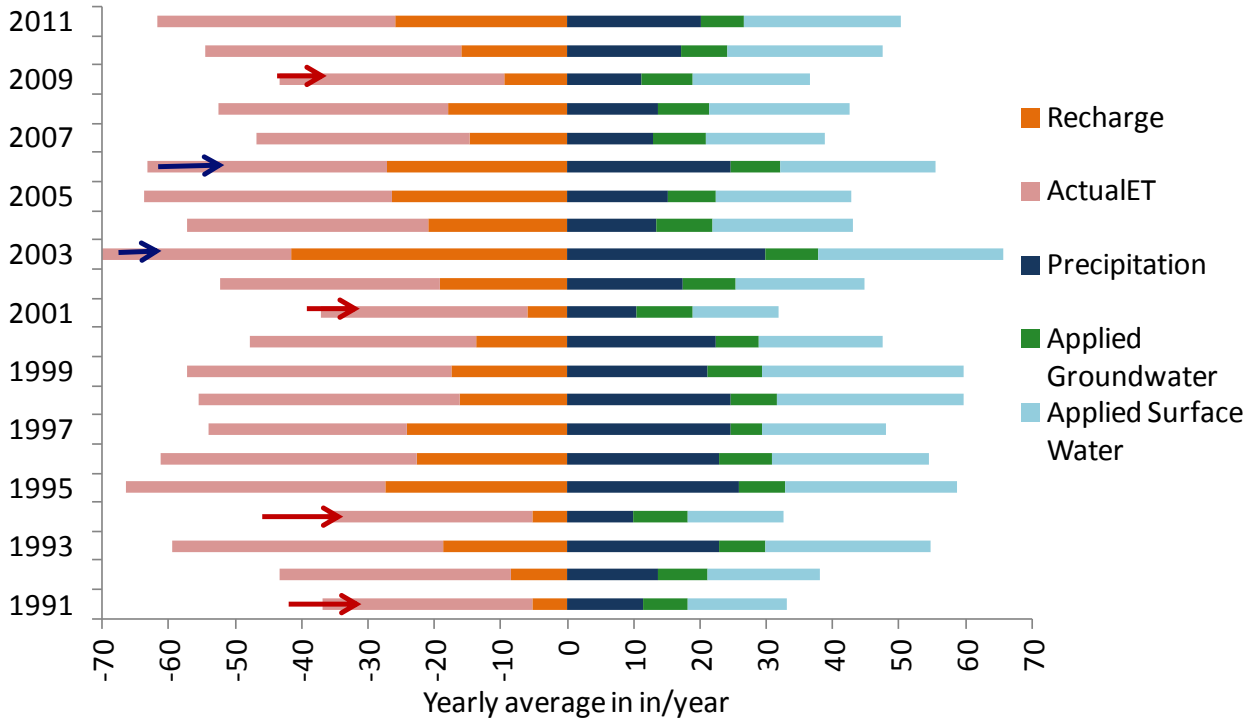

Figure 28 Yearly soil root zone water budget in in/year, area-weighted average for the pasture polygons over the entire Scott Valley project area. Input to the root zone shown as positive values (precipitation, applied groundwater and surface water). Output from the root zone shown as negative values (actual ET and recharge).

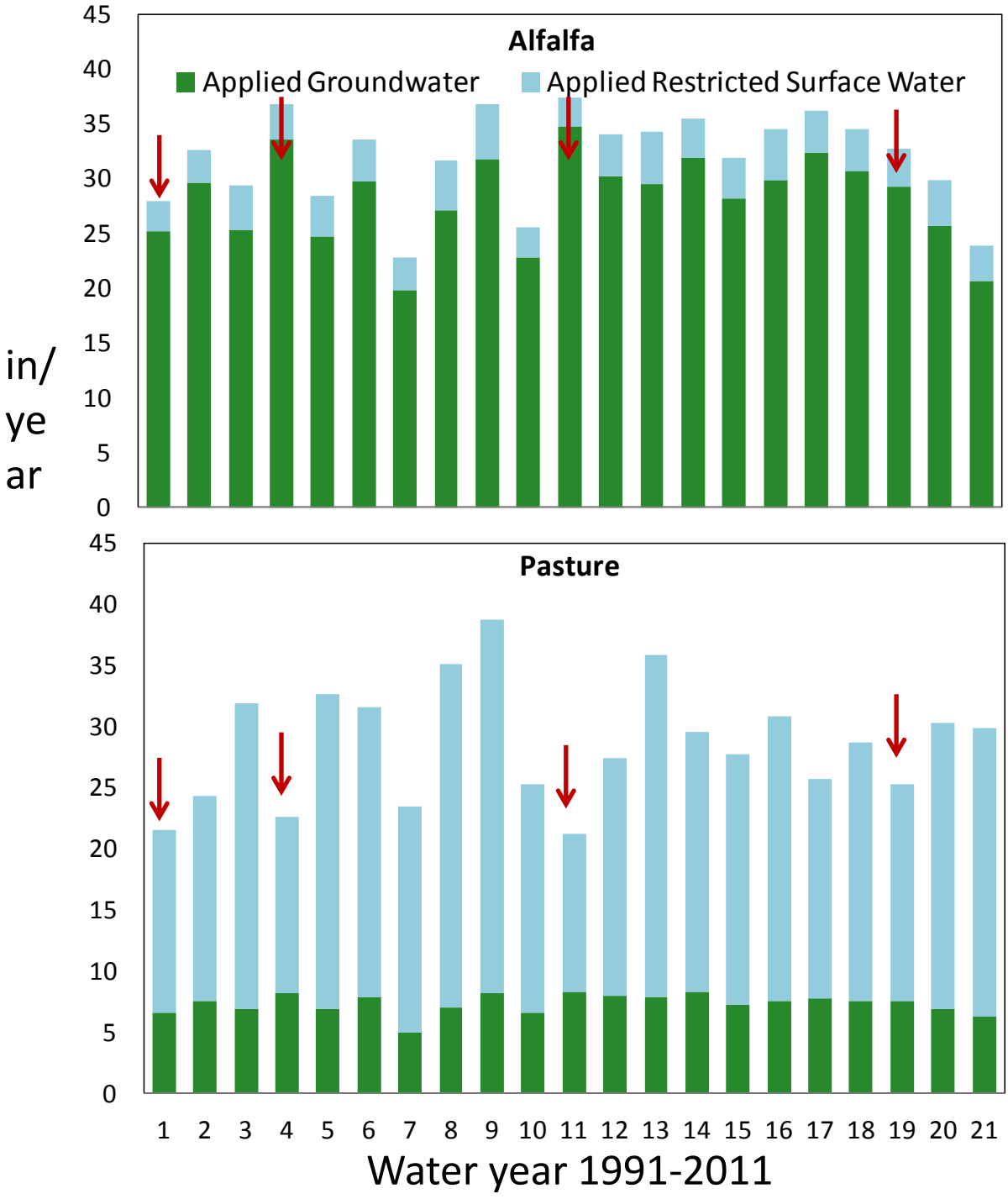

Figure 29. Yearly values of applied surface water and applied groundwater in in/year for alfalfa/grain (above) and pasture (below), area-weighted average over all alfalfa/grain land use polygons in the project area. Dry years are highlighted.

11.2 Sensitivity Analysis: Water Holding Capacity

Water holding capacity is a critical parameter in the soil water budget model. But the actual value of the parameter is quite variable and locally uncertain. Based on expert suggestions, to compute the above results we used a water holding capacity that corresponds to a rooting depth of 4 feet. Roots may eventually grow deeper than 4 feet and access deeper water if shallow moisture is depleted.

To test the sensitivity of the soil water budget simulation results to the value chosen for water holding capacity, a simple sensitivity test was implemented. A second simulation was run assuming that root zone depth is 8 ft depth with a water holding capacity that is exactly twice as large as that at 4 ft depth.

The results provided by the soil water budget model with the alternative water holding capacity are summarized and compared to the original values in Table 16. At double the water holding capacity, the irrigation amount for alfalfa decreases by about 1 in and, as expected, the only noticeable change is a substantial decrease in groundwater recharge. Because of the significant effect on recharge, additional sensitivity analyses should be carried out once the soil water budget model is coupled to the integrated hydrologic model.

Table 16. Sensitivity of average fluxes due to doubling of the soil water holding capacity. Changes (in percent) are relative to the original results (Table 15). Positive values indicate a relative increase compared to original results.

	CropET	Actual ET	Irrigation	SW irrigation	GW irrigation	Recharge
Alfalfa	0	3.7	-3.3	-4.6	-3.1	-24
Grain	0	1.2	-1.2	-1.0	-1.3	-13
Pasture	0	11.3	0.0	0.0	0.0	-23

11.3 Comparison with Available Data

The GWAC provided us with grower information on the amount of irrigation that is typically applied to different crops as a function of the irrigation type used (Table 17). The information was developed from the GWAC's knowledge of typical Scott Valley irrigation schedules, sprinkler spacing, sprinkler nozzle sizes, and sprinkler flow rates.

The irrigation rates computed from the information provided by the GWAC (Table 17) are significantly lower than the irrigation rates estimated from the soil water budget model. In the soil water budget model, the simulated irrigation rate is primarily driven by the assumption that evapotranspiration demands not met by precipitation and soil moisture are fully met by irrigation (Table 15). The largest discrepancy between reported data and simulated data is for the amount of irrigation applied to alfalfa (reported: 19.5-22 inches, simulated: 33 inches). Several factors may contribute to this difference:

- Reported irrigation rates underestimate actual irrigation rates used by growers;
- Reference evapotranspiration computed by the NWSETO method from Scott Valley and nearby climate data overestimates actual reference evapotranspiration;
- Irrigation practices result in deficit irrigation of alfalfa, which means that the crop coefficient for alfalfa used here assuming optimal irrigation is too large, and the field scale irrigation efficiency chosen is too low;
- The soil moisture profile remains relatively dry during the irrigation season. This would mean that irrigation efficiencies are higher than assumed during the irrigation season;

- The root zone depth is much larger than 4 feet and roots may possibly tap into the water table;
- A combination of the above.

To address this discrepancy, field experiments were developed in spring of 2012 to collect more information on alfalfa evapotranspiration, reference evapotranspiration, irrigation rates, soil moisture dynamics, groundwater levels, and forage yield. Eight alfalfa fields (four center pivot irrigated and four wheel-line sprinkler irrigated fields) were selected for monitoring over the 2012-2013 production season. Data collected include:

1. Three surface renewal system installed in three alfalfa fields (all of the irrigated with center pivots that have permanently installed flow meters) to calculate alfalfa ET.
2. A CIMIS type weather station installed in one irrigated pasture field to estimate ETo in order to determine the appropriate alfalfa crop coefficient.
3. Soil samples collected to 8 ft. depth in April, August, and early October to determine gravimetric soil moisture content.
4. Watermark soil moisture sensors installed at 1 ft. increments to 8 ft. depth at two locations in all fields to determine soil moisture tension and wetting and drying patterns over the season.
5. A tipping rain gauge installed in each field to monitor irrigation application rate and in-season rainfall.
6. Portable Ultrasonic Doppler flow meter used to determine flow rate in center pivot fields.
7. Nozzle discharge rate monitored in wheel-line fields.
8. Alfalfa yield determined in all eight fields by hand cutting a representative area and comparing with grower yield values.

The project is intended to be continued for at least one, possibly two years, depending on interannual variability in the dataset. The dataset will be critical to help refine the soil water budget model to minimize the difference between simulated and measured irrigation rates.

Table 17. Total seasonal irrigation amount computed from information on typical irrigation frequency, nozzle sizes, nozzle spacing, and nozzle flow rates, provided by the GWAC for each crop and each irrigation type.

Alfalfa		**Grain**		**Pasture**	
Irrigation Type	*Irrigation in inches*	*Irrigation Type*	*Irrigation in inches*	*Irrigation Type*	*Irrigation in inches*
Sprinkler	22”	Sprinkler	8.25”	Sprinkler	n/a
Center Pivot	19.5”	Center Pivot	6”	Center Pivot	n/a

12 Future Work

Work that is currently planned or ongoing will concentrate on four main tasks: 1) evaluation of the field experiments to determine alfalfa irrigation and evapotranspiration rates, 2) refinement of the soil water budget model, 3) development of Version 2 of the Scott Valley Integrated Hydrologic Model, and 4) initiation of scenario alternatives to simulate future streamflow and groundwater conditions under various management/project options.

The dataset produced with the effort presented in this report is used to build Version 2 of the Scott Valley Integrated Hydrologic Model. The model is implemented using MODFLOW-2000 and it will be coupled to the soil water budget model and streamflow data presented here. The soil water budget model provides groundwater pumping, surface water diversion, and groundwater recharge rates that are also used as inputs in the groundwater flow model. It also provides the evapotranspiration data for the water budget.

In summary, Version 2 of the Scott Valley Integrated Hydrologic Model will perform the following refinements that are improvements over the (draft) Version 1 of the model:

1. Extended modeling area to include the dredge-tailing area in the southern Scott Valley and make some minor adjustments to the edge of the modeling area, based primarily on land surface topography data.
2. Refined land surface elevation representation, especially of stream channels, using neìwly available LIDAR data obtained from the U.S. Forest Service.
3. Updated groundwater pumping, surface water diversion, and groundwater recharge using the values calculated with the new soil water budget model.
4. Revised regression model of streamflow data based on the evaluation of additional data that have become available since 2008.
5. Extension of the time period simulated by the integrated hydrologic model to include 2009, 2010, and most of 2011 (through September 30, 2011).
6. Extensive sensitivity analysis, calibration and uncertainty analysis.

Regarding this last task, parameters from both models (the soil water budget model and the MODFLOW integrated hydrologic model) will be included simultaneously in the sensitivity analysis allowing us to evaluate the sensitivity of model results to parameters and observations. The integrated hydrologic model will be calibrated and validated using measured groundwater level data available for the Scott Valley and using measured streamflow data downstream of Scott Valley.

The information that we obtain with this type of analysis will quantify and illustrate the sensitivity of model results to parameters and algorithm choice. It will also describe the relationship between different types of data and the processes represented. Furthermore, our approach will allow the evaluation of uncertainty in the model output for 1991-2011 and for any of the scenario analyses. The sensitivity analysis will be used to identify the most critical information needed to reduce model prediction uncertainty. The evaluation of data needs will include a determination of optimal

areas or locations at which to collect data and whether there are seasonal preferences to collecting certain data. All these tasks will be performed using an automatic inversion code such as UCODE_2005 (Poeter et al., 2005) or PEST (Doherty, 2010) which allow the coupling of the two models and the automatic calibration of parameters involved in all the processes.

The approach described in this report and the integrated hydrologic model currently under development provide a framework to efficiently and effectively develop and evaluate future data collection campaigns and alternative water management scenarios. In the soil water budget model much of the information related to a field is parameterized with parameters available from geospatial databases. Future water management scenarios can be efficiently coded into the soil water budget model and the integrated hydrologic model as needed to simulate future conditions.

13 Conclusions

Precipitation and streamflow data have been analyzed, a revised streamflow regression model to generated synthetic data for stations that have only a very limited period of record has been prepared specifically for use with the integrated hydrologic model, and a new conceptual model for the simulation of the soil water budget has been developed and used to estimate streamflow diversions, groundwater pumping, groundwater recharge, and crop evapotranspiration. The model is based on a spatially distributed soil water dynamics approach and puts together a wide array of information in a tractable, physically and hydrologically rigorous approach.

Comprehensive datasets were compiled, and we worked closely with local stakeholders and committees to refine these dataset as well as the conceptual framework used to represent various landuses, especially agricultural landuses, and irrigation management practices. The contributions of various stakeholders have been essential to update our GIS database and soil water budget model with the most complete, accurate reflection of land use and agricultural practices in Scott Valley.

The study shows that precipitation across the valley floor, while variable during any given rainfall event, is overall of similar magnitude between Callahan, Fort Jones, and Greenview. Significantly higher precipitation may occur at the far western margin of the valley (Etna), but available data do not allow for sufficient quantification of such effects. Precipitation patterns define streamflow. Years with low precipitation result in the lowest summer flows on the Scott River and its tributaries. We are able to estimate tributary flows with a newly developed statistical model that takes advantage of the long time series at the Ft. Jones streamflow gauging station immediately downstream from Scott Valley. The statistical model also shows that snow pack and precipitation data further aid in tributary streamflow estimation, even if only slightly. Also, developing separate regression models for the time period before fall of 1972 and the period since then, further improves statistical estimates of tributary streamflow into the Scott Valley. However, the data series for the tributaries are extremely limited. The synthetic dataset generated will be sufficient for purposes of the integrated hydrologic model. It will be important to continue streamflow monitoring on all tributaries.

Landuse in the Scott Valley, for hydrologic purposes, can be divided into four categories: irrigated fields in alfalfa-grain rotation (nearly 16,000 acres), irrigated fields with pasture (12,000 acres), non-irrigated parcels with natural or other vegetation that consumes water through evapotranspiration, and land parcels that are effectively barren of vegetation or open water bodies (no irrigation and no evapotranspiration).

Soil water budget simulations show that significant amount of groundwater recharge occurs across the Scott Valley from both precipitation and irrigation. We estimate that the average annual recharge is 15 inches in alfalfa, and about 17-18 inches in grain and pasture. Irrigation on alfalfa is highest (33 inches), followed by pasture (30 inches) and grain (14 inches), which has a relatively short growing season. Based on soil water budget simulations, groundwater pumping is estimated to be highest in alfalfa fields, averaging 29 inches per year, supplying most of the

irrigation water there. It is much lower in grain fields (less than 12 inches per year), and lowest in pasture (averaging 9 inches per year), since most pasture is irrigated with surface water. Rainfall also provides a significant amount of crop water supplies via soil moisture storage.

Large field-to-field and year-to-year variations occur both with groundwater pumping and recharge. The variability shown in this report is due to varying irrigation practices within the same crop type, varying water sources, and due to inter-annual climate variations. Variability within fields or between individual growers is not simulated, but further adds to actual variability in groundwater use and recharge.

The alfalfa irrigation results obtained with the simulation model are much higher than recently measured and grower-reported irrigation rates, thus clearly identifying the need for further research work to clarify actual irrigation practices and to measure evapotranspiration occurring in alfalfa fields. Work is needed to test to what degree the discrepancy between measured and simulated irrigation rates is due to soil moisture storage currently not accounted for, potential water table encroachment and root water uptake directly from groundwater, variability in actual irrigation rates, or possibly misleading ET rates published by the California Department of Water Resources and available in the scientific literature. It will be important to thoroughly validate and possibly improve the soil water budget model against new field data as part of performing water management scenario simulations and prior to making policy decisions.

Finally, we recognize that a tool such as the one presented here is critical for discussion of alternative water management scenarios with the Groundwater Advisory Committee and other stakeholders as an effective mechanism to mitigate conflicts.

14 References

Allen, R.G., Pereira, L.S., Raes, D., and Smith, M., 1998, Crop evapotranspiration-Guidelines for computing water requirements-FAO Irrigation and drainage paper 56. Food and Agriculture Organization of the United Nations, Rome, Italy: FAO.

California Department of Water Resources. 1963, Land and Water Use in Shasta-Scott Valleys Hydrographic Unit. Volume I: Text, Bulletin No. 94-5, pp. 232.

California Department of Water Resources, 2000, Land Use Survey, Siskiyou County. Available online at http://www.water.ca.gov/landwateruse/lusrvymain.cfm. Accessed May 14, 2009.

Carle, S., and Fogg, G., 1996, Modeling Spatial Variability with One and Multidimensional Continuous-Lag Markov Chains Mathematical Geology Volume 29, Number 7, 891-918, DOI: 10.1023/A:1022303706942.

Deas, M.L., and S.K. Tanaka, 2003, Scott River Water Balance Study: Data Analysis and Model Review. Prepared for the Scott River Watershed Council.

Deas, M.L., and S.K. Tanaka, 2004, Scott River Water Balance Study: Data Analysis and Model Review, Watercourse Engineering, June 2004.

Deas, M.L., and S.K. Tanaka, 2005, Scott River Runoff Forecast Model: Investigation of Potential Formulation, Watercourse Engineering, December 2005.

Deas, M.L., and S.K. Tanaka, 2006, Scott River Water Supply Indices: Year Types for the Scott River Basin, prepared for the Siskiyou RCD.

Deas, M.L., and S.K. Tanaka, 2008, Scott River Water Balance-Streamflow and Precipitation Gauging, prepared for the Siskiyou RCD.

Doherty, J., 2010, Methodologies and Software for PEST-Based Model Predictive Uncertainty Analysis, Watermark Numerical Computing, Australia.

Drake, D., Tate, K., and Carlson, H., 2000, Analysis shows climate-caused decreases in Scott River Fall Flows, California Agriculture, Vol. 54 n. 6, pp. 46-49.

Foglia, L., A. McNally, L. Ledesma, R. Hines, and T. Harter, 2012, Scott Valley Integrated Hydrologic Model: Background and Water Budget (Draft Report). Prepared for the North Coast RWQCB.

Gesch, D.B., 2007, The National Elevation Dataset, in Maune, D., ed., Digital Elevation Model Technologies and Applications: The DEM Users Manual, 2nd Edition: Bethesda, Maryland, American Society for Photogrammetry and Remote Sensing, p. 99-118.

Gesch, D., et al., 2002, The National Elevation Dataset: Photogrammetric Engineering and Remote Sensing, v. 68, no. 1, p. 5-11.

Hanson, B., Orloff, S., Bali, K., Sanden, B., Putnam, D., 2011a, Evapotranspiration of Fully-Irrigated Alfalfa in Commercial Fields, 2011 Conference Proceedings, Agricultural Certification Programs-Opportunities and Challenges.

Hanson, B., Orloff, S., Bali, K., Sanden, B., Putnam, D., 2011b, Mid-summer Deficit Irrigation of Alfalfa in Commercial Fields, 2011 Conference Proceedings, Agricultural Certification Programs-Opportunities and Challenges.

Harbaugh, A.W., Banta, E.R., Hill, M.C. and McDonald, M.G., 2000, MODFLOW-2000, The U.S. Geological Survey modular ground-water model – users guide to modularization concepts and the ground-water flow process: U.S. Geological Survey Open-File Report 00-92, 121 p.

Hargreaves, G. H., and Z. A. Samani, 1982, Estimating potential evapotranspiration, J. Irrig. Drain. Eng., 108(3), 225-230.

Hargreaves, G.H., and J.P. Riley, 1985, Irrigation water requirements for the Senegal river basin. Journal of Irrigation and Drainage Engineering 111(3): 265-275.

Harter, T., and R. Hines, 2008, Scott Valley Community Groundwater Study Plan. Groundwater Cooperative Extension Program, University of California, Davis.

Hines, Ryan. "MS Thesis Draft." October 2010.

Mack, S., 1958, Geology and Ground-Water Features of Scott Valley Siskiyou County, California: U.S. Geological Survey Water-Supply Paper 1462. Washington D.C.

Monteith, J.L. , 1965, Evaporation and environment. Symp. Soc. Exp. Biol. 19, 205-224.

North Coast Regional Water Quality Control Board, 2006, Action Plan for the Scott River Sediment and Temperature Total Maximum Daily Loads, September 2006.

North Coast Regional Water Quality Control Board, Staff report for the action plan for the Scott River Watershed Sediments and Temperature TMDLs, 2011, http://www.swrcb.ca.gov/northcoast/water_issues/programs/tmdls/scott_river/staff_report.shtml.

Orang, M.N., Snyder, R.L., Matyac, J.S., 2008, Consumptive Use Program +, California Department of Water Resources, http://www.water.ca.gov/landwateruse/models.cfm.

Poeter, E.P., Hill, M.C., Banta, E.R., Mehl, S.W., and Christensen, S., 2005, UCODE-2005 and six other computer codes for universal sensitivity analysis, inverse modeling, and uncertainty evaluation, U.S. Geological Survey Techniques and Methods, 6-A11.

Quigley, D., S. Farber, K. Conner, J. Power, and L. Bundy, 2001, Water Temperatures in the Scott River Watershed in Northern California." Prepared for U.S. Fish and Wildlife Service.

Snyder, R.L., M. Orang and S. Matyac, 2002, A long-term water use planning model for California. Proceedings of the Sixth International Symposium on Computer Modelling in Fruit Research and Orchard Management. Acta Hort., 584: 115-121.

Soil Survey Staff, Natural Resources Conservation Service, United States Department of Agriculture, 1975, Soil Survey Geographic (SSURGO) Database for [Survey Area, State]. Available online athttp://soildatamart.nrcs.usda.gov . State of California, State Water Resources Control Board, 1975.

S.S. Papadopulos & Associates, 2012, Groundwater conditions in Scott Valley, Report prepared for the Karuk Tribe, March 2012.

Swenson, M. 1947. Report on Scott River Watershed Basic Data Pertinent to Development of a Watershed Management Plan for the Klamath National Forest. Region 5. U.S. Forest Service.

Tanaka, S.K., and M.L. Deas, 2008, Scott River Water Balance: Streamflow and Precipitation Gauging." Watercourse Engineering, May 2008.

UCCE Leaflet 21427, Using Reference Evapotranspiration (ET0) and Crop Coefficients to estimate Crop Evapotranspiration (Etc) for agronomic crops, grasses, and vegetable crops, http://lawr.ucdavis.edu/irrigation/irrigation_leaflets/L21427.html

Van Kirk, R. W. and S. W. Naman, 2008, Relative Effects of Climate and Water Use on Base-Flow Trends in the Lower Klamath Basin. Journal of the American Water Resources Association (JAWRA) 44(4):1035-1052. DOI: 10.1111/j.1752-1688.2008.00212.x

Watershed Sciences, 2010, LiDAR Remote Sensing Data Collection: Scott Valley California. November 11, 2010. Watershed Sciences, 529 SW 3rd Avenue, Suite 300, Portland, OR 97204. 24 pages. Accessed through the California State Water Resources Control Board.

Streamflow - Data Sources

California Rivers Assessment (CARA). "Historic Precipitation for Scott Basin." Information Center for the Environment, University of California, Davis. January 1998. http://www.ice.ucdavis.edu/newcara/basin.asp?cara_id=15 (retrieved on 28 June 2012)

California Data Exchange Center (CDEC). "Historical Data for Scott River Basin." California Department of Water Resources. 2010. http://cdec.water.ca.gov/ (retrieved on 28 June 2012).

National Oceanic and Atmospheric Administration (NOAA). "Climate Data Online Data Search: Scott Valley." http://www.ncdc.noaa.gov/cdo-web/ (retrieved on 29 June 2012).

USGS Water Data for the Nation. "USGS Surface-Water Daily Data for the Nation." http://waterdata.usgs.gov/ (retrieved on 23 August 2012).

California Department of Water Resources. "Water Data Library." http://www.water.ca.gov/waterdatalibrary/ (retrieved on 23 July 2012)

Streamflow - Statistical Analysis Software

AnalystSoft Inc. StatPlus®: mac LE. 2011. http://www.analystsoft.com/en/products/statplusmacle/

R Core Team. R: A language and environment for statistical computing. R Foundation for Statistical Computing. Vienna, 2012. http://www.R-project.org

15 Appendix A

The appendix illustrates detailed results of the streamflow regression analysis (Section 5). Due to its size, this appendix is provided as a separate PDF file.

WATER RESOURCES RESEARCH, VOL. 49, 7292–7310, doi:10.1002/wrcr.20555, 2013

Coupling a spatiotemporally distributed soil water budget with stream-depletion functions to inform stakeholder-driven management of groundwater-dependent ecosystems

Laura Foglia,[1,2] Alison McNally,[1] and Thomas Harter[1]

Received 12 November 2012; revised 20 September 2013; accepted 23 September 2013; published 12 November 2013.

[1] Groundwater pumping, even if only seasonal, may significantly impact groundwater-dependent ecosystems through increased streamflow depletion, particularly in semiarid and arid regions. The effects are exacerbated, under some conditions, by climate change. In social sciences, the management of groundwater-dependent ecosystems is generally considered a "wicked" problem due to the complexity of affected stakeholder groups, disconnected legal frameworks, and a divergence of policies and science at the cross road between groundwater and surface water, and between ecosystems and water quality. A range of often simplified scientific tools plays an important role in addressing such problems. Here we develop a spatiotemporally distributed soil water budget model that we couple with an analytical model for stream depletion from groundwater pumping to rapidly assess seasonal impacts of groundwater pumping on streamflow during critical low flow periods. We demonstrate the applicability of the tool for the Scott Valley in Northern California, where protected salmon depend on summer streamflow fed by cool groundwater. In this example, simulations suggest that increased recharge in the period immediately preceding the critical low streamflow season, and transfer of groundwater pumping away from the stream are potentially promising tools to address ecosystem concerns, albeit raising difficult infrastructure and water trading issues. In contrast, additional winter recharge at the expense of later spring recharge, whether intentional or driven by climate may reduce summer streamflows. Comparison to existing detailed numerical groundwater model results suggests that the coupled soil water mass balance—stream depletion function approach provides a viable tool for scenario development among stakeholders, to constructively inform the search for potential solutions, and to direct more detailed, complex site-specific feasibility studies. The tool also identifies important field monitoring efforts needed to improve the understanding and quantification of site-specific groundwater-stream interactions.

Citation: Foglia, L., A. McNally, and T. Harter (2013), Coupling a spatiotemporally distributed soil water budget with stream-depletion functions to inform stakeholder-driven management of groundwater-dependent ecosystems, *Water Resour. Res.*, *49*, 7292–7310, doi:10.1002/wrcr.20555.

1. Introduction

[2] Groundwater-dependent ecosystems (GDEs) located within streams are among several types of GDEs including peats, terrestrial systems, and springs [*Howard and Merrifield*, 2010; *Bertrand et al.*, 2012]. Significant groundwater development can lead to reduction in base flow of nearby rivers and streams. Particularly in Mediterranean and similar semiarid climates, dry, warm periods coincide with the crop growing season supported by irrigation, often with groundwater. Regions in the Western and Central U.S., Mexico, Argentina, North Africa, the Middle East, Southern Europe, Northern India, China, and Southeast Asia are widely affected by use of groundwater with major impacts

Additional supporting information may be found in the online version of this article.

[1]Department of Land, Air, and Water Resource, University of California Davis, Davis, California, USA.
[2]Institute for Applied Geosciences, Technical University Darmstadt, Darmstadt, Germany.

Corresponding author: T. Harter, Department of Land, Air, and Water Resource, University of California Davis, Davis, CA 95616, USA. (thharter@ucdavis.edu)

0043-1397/13/10.1002/wrcr.20555

to surface water flows [*Wada et al*., 2010, 2012; *Gleeson et al*., 2010]. Irrigated agricultural systems provide 40% of the world's crop production [*United Nations World Water Development Report*, 2009] with over 100 million ha of land equipped for irrigation with groundwater and an estimated 545 km^3 of extracted water [*Siebert et al*., 2010].

[3] Groundwater management may follow a "safe yield" approach that balances long-term, annual water extraction with groundwater recharge, yet pumping induced decrease of dry season base flow may negatively impact ecosystems [*Sophocleous*, 2000, *Jolly et al*., 2010]. Statistical analyses of long-term precipitation, pumping, and streamflow records, e.g., in the High Plains aquifer system, have been used to show significant linkages between pumping and streamflow depletion [*Burt et al*., 2002; *Wen and Chen*, 2006; *Kustu et al*., 2010]. *Zume and Tarhule* [2008] used a fully three-dimensional groundwater-surface water model to investigate the effects of basin-wide pumping reductions on streamflow depletion in Oklahoma. A similar tool was used, at a much smaller scale, to analyze the hydroecology of mountain meadows fed by groundwater [*Loheide and Gorelick*, 2007]. Significant work has been conducted on optimizing conjunctive use of groundwater and surface water [*Singh*, 2012]. But economic analysis of groundwater-surface water systems does typically not account for hydrologic regimes important to ecosystem services.

[4] Improved implementation of conjunctive use schemes of surface water and groundwater resources are an important step toward improving conditions in GDEs with opportunities for improving the economy of these systems while significantly increasing the resilience to droughts [*Lefkoff and Gorelick*, 1990; *Schoups et al*., 2006; *Bredehoeft*, 2011]. But dynamics at the interface between groundwater and streams and the combined impacts of groundwater abstraction and climate change on streamflow depletion and GDEs are legally unrecognized [*Thompson et al*., 2006] and often ignored by water managers [*Kollet et al*., 2002; *Döll et al*., 2012]. In the United States, where groundwater management is delegated to individual states, water laws largely lack a comprehensive framework for the management of GDEs and even ignore the physical connection of surface water and groundwater [*Harter and Rollins*, 2008; *Nelson*, 2012]. Human modifications of water flows at local, regional, and continental scales interject multiple conflicting objectives into water management including food production and ecosystem services [*Maxwell et al*., 2007]. Climate change promises to incur further shifts with impacts rippling throughout the water network, in unanticipated ways [*Allen et al*., 2004; *Scibek and Allen*, 2006; *Maxwell and Kollet* 2008].

[5] Such "wicked" problems are characterized by a high level of complexity, uncertainty, and conflict [*Von Korff et al*., 2012; *Ker Rault and Jeffrey*, 2008; *Kreuter et al*., 2004; *Freeman*, 2000]. Addressing wicked problems requires new participatory approaches to the decision-making process and an active role of physical/hydrologic sciences in addressing such problems. Scientific understanding of hydrologic systems is advancing rapidly, but developing tools that communicate fundamental scientific understanding to decisions makers and citizens remain a challenge at all scales (global, regional, and local) [*Reid et al*., 2010; *UNESCO*, 2010].

[6] Efforts to address wicked water problems have been or are under development in different regions of the world and at different scales [*Ostrom et al*., 1999; *Sophocleous*, 2002; *Hare et al*., 2003; *Moellenkamp et al*., 2010; *Von Korff*, 2012]. Many include an effort to integrate scientists, decision makers (at the local and regional scale), and regulators within the workflow [*Sophocleous*, 2012]. Often, collaborative solutions to such wicked problems require conceptual representations of the water management system(s) at various levels of complexity.

[7] Simple conceptual models convey fundamental insights into the dynamics of hydrologic systems to non-technical stakeholders. Such models are also useful to develop worst-case/best-case scenarios given the conceptual simplification and data limitation underlying the model. Models representing additional complexity may then be used to further constrain insights into the hydrologic system and predictions of its future state. This process enables a better understanding of water resources and leads to a more informed approach toward developing strategies and scenarios for better water resources management.

[8] In this work, we couple two low order (conceptually and geometrically simple, mass balance based) hydrologic modeling tools to investigate aquifer-stream interactions. Simplified aquifer-stream interaction models to reduce computational costs have been applied in hydro-economic modeling efforts [e.g., *Pulido-Velazquez et al*., 2008], showing that a coupled water budget-stream depletion function analysis may be useful for optimizing groundwater management under ecosystem services constraints. Here we expand the approach to investigate spatiotemporally distributed groundwater management alternatives that may improve GDE conditions in basins with significant but unmeasured groundwater extractions and recharge.

[9] The tool is applied to the Scott Valley groundwater basin, California, to (1) evaluate and demonstrate the fundamental dynamics between landuse, groundwater use, and seasonally low streamflow that is affecting stream temperature [*Caissie*, 2006] and salmonid stream habitat [*Milner et al*., 2012]; (2) evaluate the role of data in understanding the key drivers of potential stream base flow depletion during the dry season in a semiarid, irrigated agricultural region with Mediterranean climate; (3) utilize the tool to cast an overall framework for developing potential groundwater management options and for defining project-specific feasibility work; and (4) employ the tool for education and outreach to diverse stakeholders seeking common, creative solutions. Stakeholders in the Scott Valley include local landowners (farms) and groundwater pumpers, native American tribes dependent on downstream salmon fisheries, environmental groups, as well as local, state, and federal agencies representing often conflicting interests in water rights regulation, water quality control, endangered species protection, and agricultural resources management—thus representing all the ingredients to a "wicked" water management problem.

[10] In the following, we provide further details on the study area and describe the spatiotemporally distributed

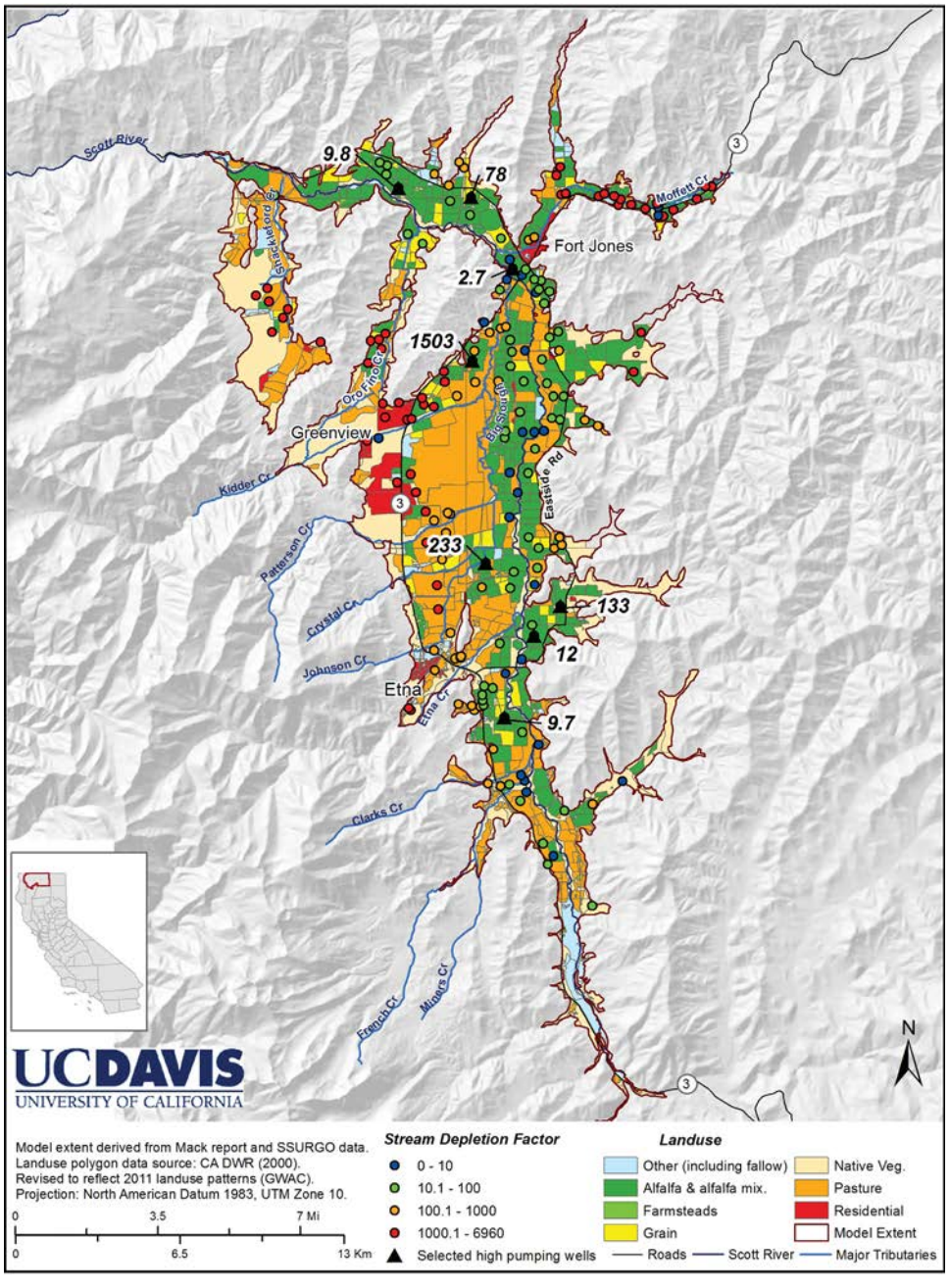

Figure 1. Map of the Scott Valley with the boundaries of the groundwater model study, landuse, and irrigation wells with their stream depletion factor (SDF in days) relative to the main-stem Scott River, calculated as described below. Highlighted are the SDF values of some wells used below for a detailed analysis (also see Table 4).

soil water budget approach and the theory of stream depletion analysis. We use the coupled water budget and stream depletion analysis to explore the role of groundwater pumping in the Scott River Valley with respect to late summer base flow in the Scott River. We then identify broad options for potential alternative water management scenarios to improve summer streamflow as a basis for discussion with stakeholders and for directing the selection and assessment of specific projects including necessary field work and higher level, more complex hydrological modeling efforts.

2. Methods

2.1. Study Basin

[11] The coupled water budget and stream depletion analysis is applied to the 202 km^2 Scott River Valley, Siskiyou County, Northern California. The major landuse is pasture, alfalfa hay, and grain farming (approximately 140 km^2) supported by summer irrigation with stream water and with groundwater. The valley is part of the Klamath Basin watershed straddling the California-Oregon border (Figure 1). The Scott River is one of four undammed

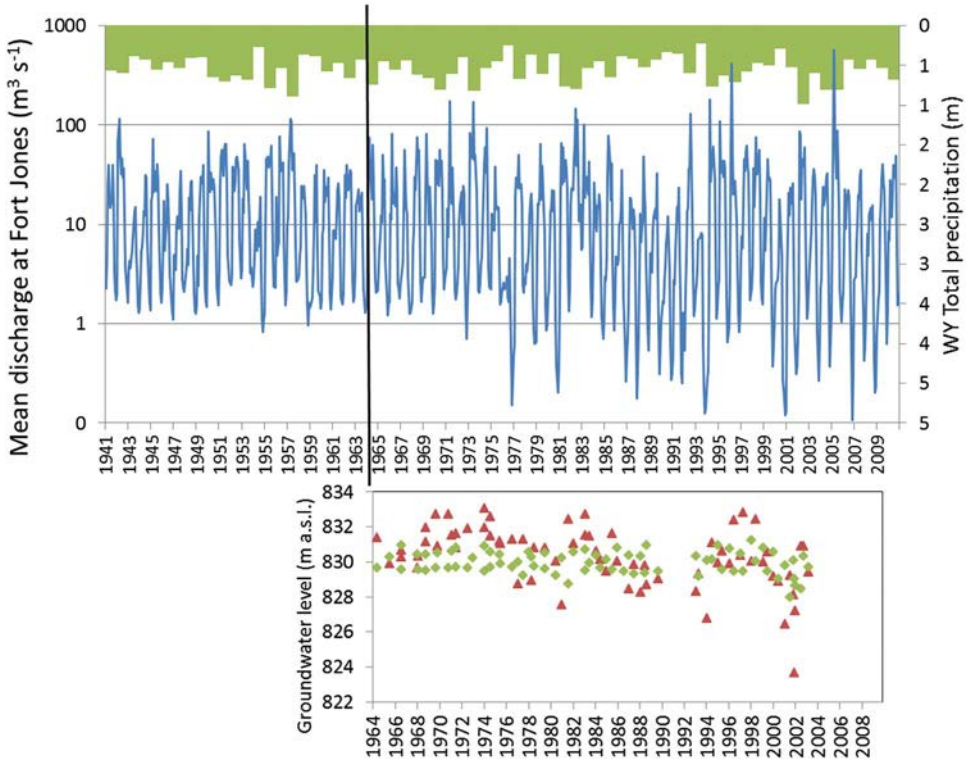

Figure 2. (a) Daily mean discharge ($m^3\ d^{-1}$) of the Scott River recorded at the USGS gauge near Fort Jones. Since the mid-1970s, dry year low flows (1977, early 1990s, 2001, 2007–2008) have been about half an order of magnitude lower than during the 1941–1976 measurement period (1945, 1955). (b) Scott River Valley well levels and precipitation, 1965–2012 [*California Department of Water Resources* (*CDWR*), 2012]. Beginning with the drought-year 1977, summer water levels in some dry years were lower than during the 1964–1976 period.

tributaries to the Klamath River. It provides key spawning habitat for salmonid fish in the Klamath Basin, including *Oncorhynchus tschawytscha* (Chinook salmon) and federally protected threatened *Oncorhynchus kisutch* (Coho salmon). The Scott River has been mapped as medium to high ranking for the presence of base flow-dependent ecosystems [*Howard and Merrifield*, 2010].

[12] Scott Valley overlies an intermontane alluvial basin within the Klamath Mountains Province, created by faulting along its northwestern outlet, and subsequent alluvial deposition during the late Tertiary and Quaternary. The alluvial fill, consisting of gravel, sands, and also silts and clays, may exceed 100 m thickness at the center of the basin and decreases in thickness to the valley margins [*Mack*, 1958]. Groundwater pumping is limited to the upper 60 m of the alluvial fill. Spring groundwater levels, while slightly variable from year to year, have not experienced a long-term decline that would indicate systemic overdraft [*Harter and Hines*, 2008; *S.S. Papadopoulos & Associates (SSPA)*, 2012].

[13] The climate is Mediterranean. Precipitation predominantly occurs during winter and early spring months but is negligible between June and September. Average July temperature is 21°C and average January temperature is 0°C. Total annual rainfall on the valley floor is 500 mm. Mountain ranges surrounding Scott Valley reach elevations of 2500 m with much higher precipitation rates than the valley. Annual runoff from the 1700 km^2 watershed is 560 Mm^3 [*U.S. Geological Survey* (*USGS*), 2012]. Winter flows in the main stem of the Scott River, immediately downstream of the groundwater basin, may exceed 1,000,000 $m^3\ d^{-1}$ (400 cfs) during winter months, but are as low as 25,000–125,000 $m^3\ d^{-1}$ (10–50 cfs) during the later summer months (July–September) (Figure 2a).

[14] During the dry summer, streamflow in the Scott River system significantly relies on groundwater return flow (base flow) from the alluvial aquifer system underlying Scott Valley. Historic records show that summer base flows in dry years prior to 1977 (1945, 1955) have been higher than during later dry years (1977, early 1990s, 2001, 2009) (Figure 2a). The decrease is generally attributed to climate change [*Drake et al*., 2000], but also to increased groundwater pumping for irrigation [*Van Kirk and Naman*, 2008]. As a result of lower summer/fall base flow, but also due to the lack of widespread riparian vegetation, temperatures in the Scott River may exceed critically high levels during the summer months [*NCRWB*, 2011]. Yet, ecologically necessary minimum flow requirements remain uncertain.

[15] Under regulatory efforts driven by federal *Clean Water Act* [1972] provisions (33 U.S.C. §1251 et seq., 1972, and 40 C.F.R. 130.2), stakeholders have agreed that better knowledge of the hydrology and the alluvial aquifer system is needed to develop a possible array of solutions to water issues and associated problems [*Harter and Hines*, 2008]. Siskiyou County has management jurisdiction over

groundwater and is taking a community-based approach to implementing groundwater management.

[16] Water and groundwater management is also affected by recent enforcement actions under the California Endangered Species Act (CESA; California Fish and Game Code, Sections 2050 et seq.), which allows the State of California to curtail diversions of irrigation water if instream flows are considered critically low with respect to threatened or endangered salmon species in the river system (California Fish and Game Code, Section 5937). Finally, a lawsuit has been brought against the County (as the groundwater management agency) and the State (as the licensor of water rights) to protect groundwater-dependent ecosystems under the so-called Public Trust doctrine [*Hart*, 1996]. If successful, this may give the State an unprecedented legal tool to enforce limits on current groundwater pumping not already controlled under existing adjudications. An existing groundwater adjudication in the Scott Valley, dating to the 1970s, prescribes the amount of groundwater that is reasonably required to irrigate within a groundwater—surface water "interconnected zone" (California Water Code 2500.2) extending approximately 500–1000 m from the main-stem Scott River [*California State Water Resources Control Board* (*CSWRCB*), 1980]. Elsewhere in Scott Valley, as is customary in California, groundwater pumping for overlying uses does not require state permitting [*California Department of Water Resources* (*CDWR*), 2003].

2.2. Soil Water Budget Model

[17] Land use specific water budgets have been used to allow for a better understanding of landuse linkages to groundwater and provide the basis for distributed groundwater-stream models [e.g., *Ruud et al*., 2004; *Faunt*, 2009; *Chung et al*., 2010]. In the study area, measurement data on groundwater extraction and recharge do not exist. Hence, a soil water budget model is used to estimate spatially and temporally varying recharge and pumping across the groundwater basin.

[18] The spatial resolution for the analysis is determined by the size of individual fields and other landuse parcels defined in a recent landuse survey [*CDWR*, 2000] that was further refined using aerial photo analysis and on-the-ground verification. A total of 2119 landuse parcels overly the Scott Valley groundwater basin (Figure 1). Of those, 710 parcels (70 km^2) are alfalfa/grain, typically on an 8 year rotation with 1 year of grain crops followed by 7 years of alfalfa, 541 parcels (67 km^2) are pasture, 451 parcels (58 km^2) belong to landuse categories with significant evapotranspiration but no irrigation (e.g., cemeteries, lawns, natural vegetation), and 417 parcels (6.8 km^2) represent landuses with no evapotranspiration or irrigation (e.g., residential, parking lots, roads, and—most significantly—historic mine tailings). For each landuse parcel, the soil water budget is computed with daily time steps [e.g., *Gassman et al*., 2007] for the period from 1 October 1990 to 30 September 2011, a period that includes several dry years as well as average year and wet year periods.

[19] The soil water budget approach includes the managed components of the surface water system (diversions) and of the groundwater system (extraction), as well as groundwater recharge from managed and unmanaged landuses. The budget does not account for stream recharge or for groundwater discharge downstream resulting from stream recharge upstream. It also does not account for evapotranspiration due to root water uptake from the water table by nonirrigated crops or in natural landscapes with shallow water table. A complete surface watershed or groundwater basin budget requires a more complex, integrated groundwater-surface model.

[20] To compute the soil water budget, each landuse polygon is characterized by a set of properties (attributes) assembled from existing databases, through field work, survey, and by applying spatial analysis within a geographic information system (GIS). The concepts applied represent some simplification over detailed root zone water models, but are commensurate given available data and the overall framework of the approach:

[21] 1. Daily precipitation for 1990–2011 is obtained as the average of records at two rainfall gauges located in the northeast and southern-most portions of the valley floor [*National Oceanographic and Atmospheric Administration (NOAA)*, 2012].

[22] 2. Streamflow for 1990–2011: Daily discharge data for the Scott River downstream of Scott Valley are available from the U.S. Geological Survey [*USGS*, 2012]. Streamflow data on ten tributaries, including the two main stem forks of the Scott River, at locations immediately upstream of the valley floor (i.e., upstream of the groundwater basin) have been collected at various times by local and state agencies. But no long-term records exist. Missing data on tributary inflows into the valley at the upgradient boundaries of the groundwater basin are estimated by performing a regression analysis of measured tributary flow against downstream flow, snowpack, and precipitation as independent variables (see supporting information).

[23] 3. Landuse: Digital land use survey maps for the year 2000 [*CDWR*, 2000] identify individual landuse parcels (polygons) and their landuse. The information was updated and corrected via interviews with landowners (Figure 1). Landuse is then aggregated into four major categories for purposes of computing the soil water budget: (1) Alfalfa/grain rotation in an 8 year cycle (each field is randomly assigned one of the 8 years in the cycle during which it goes into "grain" rotation), (2) pasture, (3) landuse with evapotranspiration but no irrigation (includes natural vegetation, natural high water meadow, misc. deciduous trees, trees), and (4) landuse with no evapotranspiration and no irrigation, but with potential recharge from precipitation via soil moisture storage (barren, commercial, dairy, extractive industry, municipal, industrial, paved, gravel mine tailings, etc).

[24] 4. Soil type: Digitally mapped soil type information is available from the U.S. Soil Survey Geographic (SSURGO) database [*Natural Resources Conservation Service (NRCS)*, 2012a, 2012b]. Soil type information includes water holding capacities at 0.9 m and 1.5 m depth. For the soil water budget, water holding capacity is computed as the average of these values assuming that average effective root-zone depth for alfalfa is approximately 1.22 m (4 ft) [*Luo et al*., 1995]. Here we use the same depth for grain and pasture. Each landuse polygon is associated with the soil type present at its centroid location.

[25] 5. Crop coefficients (k_c) and reference ET (ET_0): estimation methods of actual crop ET are primarily designed for

Table 1. Total Areas of Subwatersheds, Total Area for Various Irrigation Types, Total Area for Various Irrigation Water Sources, and Total Area of Landuse, in Square Kilometers[a]

Subwatersheds Name	Area (km^2)	Irrigation Type	Area (km^2)	Water Source	Area (km^2)	Landuse	Area (km^2)
Etna Creek	17	Non-irrigated	75	DRY	14	Water	1
French Creek	2	Flood	44	GW	67	Alfalfa/Grain	71
Kidder Creek	38	Sprinkler	51	MIX	16	Pasture	67
Mill Creek	9	Center Pivot	28	SUB	9	ET/No irrigation	57
Moffett Creek	10	Unknown	4	SW	31	No ET	7
Patterson Creek	16			None/unknown	67		
Scott River	84						
Scott River tailings	14						
Shackleford Creek	12						
Study area total	202	Total	202	Total	202	Total	202

[a]All values represent 2011 conditions. Note that not all areas in the alfalfa/grain and pasture category are irrigated.

irrigation scheduling purposes but are here applied to estimate daily varying actual crop ET (equations (4)–(6)). Daily reference ET is estimated from study area climate data [*Hargreaves and Samani*, 1982; *Snyder et al*., 2002]. Crop coefficients vary by crop, by stage of crop growth, and by cultural practices. For alfalfa, a crop coefficient of 0.95 was fitted to field data from the study area [*Hanson et al*., 2011b], since we did not simulate alfalfa cutting dates individually at each field. For grain (variable k_c) and pasture ($k_c = 0.9$), state agricultural extension recommendations were applied [*University of California Cooperative Extention (UCCE)*, 2012].

[26] 6. Irrigation type: The year 2000 landuse survey by CDWR [*CDWR*, 2000] identified the irrigation type associated with each landuse polygon. In the Scott Valley, flood, center pivot sprinkler, and wheel-line sprinkler irrigation are used almost exclusively. Over the past 25 years, significant conversion from wheel-line sprinkler (but also from flood irrigation) to center pivot sprinkler has occurred. The location (extent) and year of such irrigation type conversions are mapped to landuse polygons by reviewing 1990–2011 aerial photos. Total areas for 2011 are shown in Table 1.

[27] 7. Irrigation efficiency is assumed to be a function of irrigation type. It accounts for irrigation nonuniformity and deep percolation losses to below the root zone. Delivery and interception losses are not accounted for. Efficiencies are based on informal surveys of local growers and expertise of local agricultural consultants, although they do not account for unintended underirrigation or deficit irrigation: 90% for center pivot sprinkler, 75% for wheel-line sprinkler, and 70% for flood irrigation (University of California Cooperative Extension (UCCE), personal communication, 2011).

[28] 8. Water source for irrigation: Water source is identified for each landuse polygon by the year 2000 landuse survey [*CDWR*, 2000] and is updated through landowner survey. Water sources include groundwater, surface water, subirrigated (shallow groundwater table), mixed groundwater-surface water, and nonirrigated (dry land farming) (Table 1).

[29] 9. Surface water diversion allocation: Each landuse parcel is associated with one of nine subwatersheds corresponding to the various tributaries to the main stem Scott River (Table 1). Discharge on these tributaries defines available maximum diversion rates (see below).

[30] The soil water budget for each landuse polygon is performed using a storage routing approach with soil water inputs from precipitation and irrigation [e.g., *Neitsch et al*., 2011]. Adjusted daily precipitation (P_{adj}) is the portion of daily precipitation (P) that infiltrates into the soil and is available for daily evapotranspiration (ET) or recharge [*Allen et al*., 1998]:

$$P_{adj}(i) = P \quad \text{if } P(i) > 0.2^{*}\mathrm{ET}_0(i) \tag{1a}$$

$$P_{adj}(i) = 0 \quad \text{if } P(i) \le 0.2^{*}\mathrm{ET}_0(i) \tag{1b}$$

where ET_0 (i) is the daily reference evapotranspiration on day i, assumed uniform across the valley floor due to the size of the study area and its level topography. The storage routing mass balance for the 1.22 m thick root zone is then computed as:

$$\theta(i) = \max(0, \theta(i-1) + P_{adj}(i) + \mathrm{Irrig}(i) - \text{actual ET}(i) - \mathrm{Recharge}(i)) \tag{2}$$

$$\text{actual ET}(i) = \min\left(\mathrm{ET}(i),\ \theta\ (i-1) + P_{adj}(i) + \mathrm{Irrig}(i)\right) \tag{3}$$

$$\mathrm{Recharge}\ (i) = \max(0,\ \theta\ (i-1) + P_{adj}(i) + \mathrm{Irrig}(i) - \text{actual ET}(i) - \mathrm{WC4}(i)) \tag{4}$$

where $\theta(i)$ is water content at the end of day i, $P_{adj}(i)$ is precipitation on day i, Irrig(i) is irrigation on day i, ET(i) is evapotranspiration on day i, computed from potential ET as: $\mathrm{ET}(i) = \mathrm{ET}_0(i)^{*}k_c(i)$, $k_c(i)$ is crop coefficient, Recharge(i) is deep percolation to groundwater, to below the 1.22 m thick root zone, and WC4 is water holding capacity of the 1.22 m root zone.

[31] Runoff, particularly during the irrigation season, is considered negligible due to the low land surface gradient. The algorithm intrinsically exerts complete mass balance control on each landuse polygon:

$$P_{adj}(i) + \mathrm{Irrig}(i) - \text{actual ET}(i) - \mathrm{Recharge}(i) = \theta(i) - \theta(i-1). \tag{5}$$

[32] Furthermore, we can compute the amount of water deficit relative to optimal growing conditions as follows:

$$\mathrm{Deficiency}(i) = \mathrm{ET}(i) - \text{actual ET}(i). \tag{6}$$

[33] The source of irrigation water, Irrig(i), depends on the water source and landuse specified for an individual landuse polygon. For pasture, irrigation water is most often

exclusively supplied from surface water. Alfalfa/grain landuse polygons are most often irrigated from groundwater. Based on information from stakeholders, alfalfa/grain fields with a surface water source are treated as if equipped for a mixed source.

[34] For mixed sources of irrigation water, the decision process that leads to a landuse polygon switching from surface water irrigation to groundwater irrigation is simulated based on the available surface water supply: if the total surface water irrigation demand within a subwatershed, in a given month, exceeds stream discharge, groundwater is used to make up the landuse polygon-specific difference between surface water available and the irrigation demand. The available surface water is distributed to all polygons designated for use of surface water at equal water depth (water volume proportional to polygon size).

3. Irrigation Scheduling Simulation

[35] Surface water delivery and groundwater pumping rates are driven by daily precipitation and evapotranspiration. Urban and domestic pumping are small in comparison and are here neglected. Irrigation water demand is calculated following FAO guidelines [*Allen et al*., 1998]. The approach computes irrigation timing and demand as a function of climate, soil, crop type, irrigation type, and water source.

3.1. Alfalfa/Grain and Pasture

[36] Alfalfa irrigation in polygon k starts on the first day i after 24 March 24, on which the soil water content has dried to less than 45% of field capacity (*ibid*., Table 22):

$$\theta(i) < (1 - 0.55)^{*}\mathrm{WC4}(k). \tag{7}$$

[37] 25 March is the earliest reported irrigation date. The last alfalfa irrigation application in Scott Valley typically occurs before 5 September. For the water budget computations, irrigations are assumed to occur daily through 5 September based on perfect farmer foresight of crop water demand.

[38] For grain, the first irrigation on a field k is determined exactly as for alfalfa but the reported earliest starting date is 15 March. The last day of continuous irrigation on grain is assumed to be 10 July, after which the grain crop is harvested.

[39] For pasture, the Scott Valley irrigation season is typically from 15 April to 15 October (184 days). Simulated irrigation is applied daily based on ET demand and irrigation efficiency. However, on pasture that is surface water irrigated (which represents most pasture), no irrigation occurs once surface water supplies become unavailable. For each polygon k and for each day i, the daily irrigation amount is calculated as:

$$\mathrm{Irrig}_k(i) = (\mathrm{Ieff}_k)^{-1^{*}}\left(\mathrm{Max}\left(0,\ \left(\mathrm{ET}_k(i) - P_{\mathrm{adj}}(i)\right)\right)\right. \tag{8}$$

where Ieff_k is the irrigation efficiency in polygon k. We assume that there is no contribution to plant evapotranspiration from groundwater. To the degree that groundwater irrigated areas are subject to direct groundwater uptake by crops, the uptake is implicitly accounted for in the net stress estimated with this approach. It is the difference between estimated groundwater pumping and recharge from polygon k.

3.2. Evapotranspiration (ET) Losses Without Irrigation

[40] The main assumption is that, at all times:

$$\mathrm{Irrig}(i) = 0. \tag{9}$$

[41] In this category, ET computed from the soil water budget model does not include direct ET from groundwater (e.g., wetlands, riparian vegetation).

[42] In the first step, we use the soil water budget model to compute daily ET (on day i):

$$\mathrm{ET}(i) = k_c{}^{*}\mathrm{ET}_0(i) = 0.6^{*}\mathrm{ET}_0(i) \quad \text{subject to:} \quad \mathrm{ET}(i) \le \theta(i-1) + P_{\mathrm{adj}}(i). \tag{10}$$

[43] This latter constraint distinguishes this category from an irrigated crop.

3.3. No Irrigation/No ET Category

[44] Landuse categories of this type do not receive irrigation, and they also are not subject to evaporation or evapotranspiration from plants:

$$\mathrm{Irrig}(i) = 0 \text{ at all times} \tag{11a}$$

$$\mathrm{ET}(i) = 0 \text{ at all times.} \tag{11b}$$

[45] Given the flat topography of the valley floor, runoff is here considered negligible and recharge is equal to the adjusted precipitation:

$$\mathrm{Recharge}(i) = P_{\mathrm{adj}}(i). \tag{12}$$

4. The Analytical Solution for Stream Depletion

[46] Following *Jenkins* [1968], *Wallace et al*. [1990], and *Bredehoeft* [2011], we simplify the groundwater system and assume a semi-infinite, homogeneous and isotropic aquifer, with transmissivity constant in time and space; recharge to the aquifer is not considered prior to the time of interest, hence the water table is horizontal; the stream is considered to fully penetrate the aquifer; wells also fully penetrate the aquifer; and constant rate pumping starts at time $t = 0$.

[47] Under those assumptions, stream depletion due to pumping is given by *Jenkins* [1968]:

$$\frac{q}{Q} = \mathrm{erfc}\left(\frac{t_a}{4t}\right)^{1/2} \qquad t < t_p \tag{13}$$

where: $t_a = \frac{a^2 S}{T}$ is the Stream Depletion Factor (SDF) defined by *Jenkins* [1968] and used by *Bredehoeft* [2011]; q is the change in rate of streamflow caused by the well pumping; Q is the rate of pumping; a is the distance of the well from the stream; S is the aquifer storativity and a value of 0.12 is used for the (unconfined) Scott Valley

system; T is the aquifer transmissivity; t is time since pumping began; and t_p is the duration of pumping.

[48] The stream depletion after pumping stops at $t = t_p$ is calculated following *Wallace et al*. [1990]:

$$q = Q\left(erfc\left(\frac{t_a}{4t}\right)^{\frac{1}{2}} - erfc\left(\frac{t_a}{4(t-t_p)}\right)^{\frac{1}{2}}\right) \quad t_p \le t < \infty. \tag{14}$$

[49] The rate of stream depletion due to nonsteady, annual cyclical pumping is calculated using (equation (15)) and the principle of superposition. As shown by *Wallace et al*. [1990], for constant t_p and t_d, the stream depletion corresponds to:

$$q = \sum_{i=0}^{N-1}\delta(t - t_d i)\left(Q\ erfc\left(\frac{t_a}{4(t-t_d i)}\right)^{\frac{1}{2}}\right) - \sum_{i=0}^{N-1}\delta(t - t_p - t_d i)\left(Q\ erfc\left(\frac{t_a}{4(t-t_p-t_d i)}\right)^{\frac{1}{2}}\right) \quad 0 \le t < \infty \tag{15}$$

where δ is the unit step function which has a value of 1 when its argument is greater than zero and a value of zero when its argument is equal or less than zero; N is the number of time the pump is turned on; t_d is the interval at which the pattern repeats itself.

5. Coupling Soil Water Budget and Stream Depletion Model

[50] Analytical solutions for simplified stream-aquifer depletion evaluation were originally developed and used for investigations that were lacking today's computer resources. These analytical tools remain attractive, partly because of the computational efficiency and relative ease of implementation, typically with spreadsheets or simple computer programs. More importantly, they are powerful tools that provide fundamental, rigorous theoretical insight into the physical behavior of the groundwater-stream system, even if under highly simplified, hypothetical conditions [*Jenkins*, 1968; *Glover*, 1974; *Wallace et al*., 1990; *Hunt*, 2003; *Bredehoeft and Kendy*, 2008]. In a complex and often misunderstood management system such as the aquifer-stream system, these simplified approaches allow for quickly establishing major operational constraints imposed by basic system variables. Here coupling the water budget model with the analytical solution for stream depletion provides a framework (a) to estimate the magnitude of streamflow depletion and its sensitivity to key system parameters, (b) to implement a benchmark test against an existing numerical model, and (c) to develop management scenarios for discussion and analysis with stakeholders.

[51] The soil water budget model and the streamflow depletion model are coupled, first, by assigning the estimated pumping in each field to its nearest existing well. Active wells in Scott Valley are identified through a review of well drilling permits, GIS analysis, and partial, randomized on-the-ground verification. If multiple wells are located within one landuse polygon, the total pumping is evenly split between wells, while the pumping from a well that is serving multiple polygons is the sum of all daily water needs in the associated fields. Secondly, recharge from each polygon is similarly assigned to the nearest well, but as an injection rate (negative pumping rate). Then, 1990–2011 net daily groundwater pumping rates at each well are computed as the difference between daily groundwater pumping and groundwater recharge assigned to the well.

[52] The distance of each well to the stream is computed as the orthogonal distance from the well to the Scott River, not to the nearest tributary. Here streamflow in the main stem Scott River is the key concern (Figure 1). Transmissivity is obtained from *Mack* [1958] and *SSPA* [2012].

[53] Finally, the superposition principle (equation (15)) is applied to show the effect of transient, combined recharge and pumping on the total streamflow depletion rate along the integrated length of the Scott River within the Scott Valley. We apply each well's average, yearlong net pumping time series cyclically until a dynamic (cyclical) steady state is achieved in annual stream depletion rates. Convergence is considered to be achieved once all wells exhibit less than 1% change in relative depletion on all calendar days. Using the results of the final cyclical year, the 163 wells' computed daily stream depletion (or stream replenishment) rates are summed to obtain a time series of the net total daily stream depletion of the Scott River ("base scenario").

[54] We apply the tool to several additional scenarios to demonstrate the sensitivity of the solution to the SDF parameters, to compare the estimated streamflow impacts from changes in pumping and recharge stress with those obtained with a fully three-dimensional groundwater model, and to outline potential impacts of alternative groundwater management practices that affect timing and amount of additional recharge when additional surface flows are available and the distribution of groundwater pumping.

6. Results and Discussion

6.1. Soil Water Budget

[55] The water budget simulation provides daily soil water fluxes in water years 1991 through 2011, which are aggregated to monthly, yearly and long-term averages. Table 2 summarizes average annual fluxes, by landuse category. The total amount of annual recharge (groundwater system input) from the irrigated landscape is on the order of 46 $Mm^3\ y^{-1}$ (37 thousand acre-feet per year [TAF y^{-1}]). Groundwater pumping (groundwater system output) is about 25% larger, nearly 55 $Mm^3\ y^{-1}$ (44 TAF y^{-1}). Surrounding non-irrigated landuses, including dry land farming and riparian vegetation, contribute 26 $Mm^3\ y^{-1}$ (21 TAF y^{-1}) to basin recharge, mostly from winter precipitation, with 23 $Mm^3\ y^{-1}$ (18 TAF y^{-1}) of water uptake by natural vegetation and dry land crops (not including direct groundwater uptake). The ET demand from natural vegetation and dry land farming (274 mm) is provided through

Table 2. Average Annual Soil Water Fluxes, Water Years 1991–2011, for Irrigated Crops, for Dry Land Farming and Natural Vegetation Areas ("ET noIRR"), and for Areas With No Consumptive Water Use ("noET noIRR")[a]

	Crop ET	Actual ET	Irrigation	SW Irrigation	GW Pumping	Recharge	Deficiency	Area (ha)
mm y^{-1}								
Alfalfa	1068	1018	840	104	736	370	49	5,622
Grain	411	409	358	55	303	467	2	803
Pasture	1017	861	755	528	228	437	155	4820
ET noIRR	284	274				273	10	8240
noET noIRR						547		686
Mm y^{-1}								
Alfalfa	60.0	57.3	47.2	5.8	41.4	20.8	2.8	5622
Grain	3.3	3.3	2.9	0.4	2.4	3.8	0.0	803
Pasture	49.0	41.5	36.4	25.4	11.0	21.1	7.5	4820
ET noIRR	23.4	22.6				22.5	0.8	8240
noET noIRR						3.8		686

[a]"SW": surface water, "GW": groundwater. Deficiency refers to the difference in ET between optimal water supply ("Crop ET") and actual, limited water supply ("Actual ET").

spring precipitation with the dominant source coming from root zone water storage filled during the cold winter rainy season. The nominal deficit in natural vegetation is small, but for this category, recharge and deficit are highly sensitive to the selected k_c (0.6): if k_c values are chosen higher, the deficit is correspondingly higher (due to water availability being limited) with no simulated impact on groundwater; if k_c values are chosen lower, the simulated deficit decreases or disappears and additional groundwater recharge would occur, depending on the annual dynamics of the crop coefficient.

[56] Early spring groundwater levels in the basin do not experience a long-term declining or increasing trend indicating a balanced groundwater budget (Figure 2b). The net surplus of 17.1 Mm^3 y^{-1} (14 TAF y^{-1}) between recharge and pumping across the basin indicates a net inflow from the groundwater basin to the Scott River. However, the model does not account for annual direct recharge from the stream system to groundwater that is subsequently discharged back to the stream. Both, actual recharge from and groundwater discharge to the stream are likely larger, due to the complex interaction of the groundwater system with streams and tributaries that are not accounted for here. This includes hyporheic zone exchanges due to streambed topography and groundwater-surface water exchanges due to the larger scale streambed and water table variability [e.g., *Wondzell et al*., 2009; *Boano et al*., 2010].

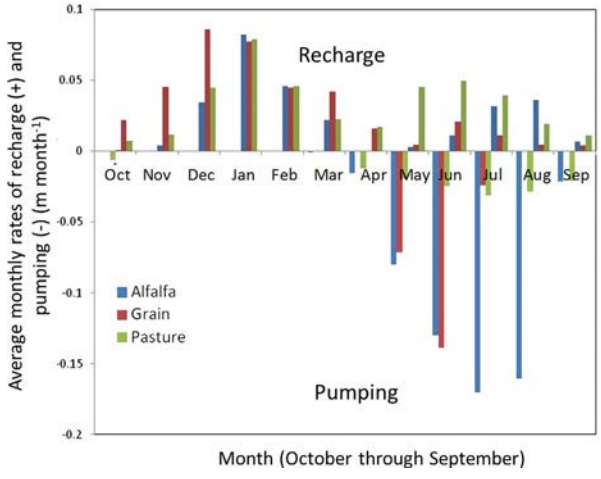

Figure 3. Simulated monthly rates of recharge and pumping (m month^{-1}) for each of the three main landuses as calculated with the water budget model.

[57] Irrigation amounts are highest in alfalfa, 840 mm y^{-1}, due to continuous availability of groundwater (736 mm y^{-1} of simulated groundwater pumping) (Table 2). Grains have an early and much shorter cropping season than alfalfa, with lower ET rates and, hence, lower irrigation (358 mm y^{-1}). Pasture, while irrigated much more generously when surface water supplies are available and with crop ET rates comparable to alfalfa (Figure 3), has a lower average annual irrigation rate (755 mm y^{-1}) than alfalfa. This is due to the surface water limitations on this predominantly surface water irrigated crop. Some pasture areas near the western margin of the valley are subject to direct groundwater uptake (not accounted for here).

[58] Average monthly recharge and pumping rates indicate strong seasonal variations. Most pumping occurs during the summer months. Most recharge occurs in the late winter and early spring (Figure 3). On pasture, significant recharge also occurs during the irrigation season due to widespread surface water flooding at rates that are significantly higher than crop water use (relatively lower irrigation efficiency). In August–September, streamflow available for flood irrigation decreases significantly, thus lowering recharge in pasture. Few pasture fields, often wheel-line sprinkler irrigated, switch to groundwater as a water source. Recharge in alfalfa is highest in July and August, when all fields are fully irrigated. Fields in grains (12.5% of the alfalfa/grain cropping area) are fallow after their harvest in July, which causes recharge and pumping in those areas to become nearly negligible after harvest. During the winter months, differences in the amount of recharge between the three landuses reflect varying levels of soil moisture depletion and slight differences in average soil characteristics across each landuse type, in particularly water holding capacity. Although very different in seasonal dynamics (Figure 3), annual average recharge in alfalfa/grain fields and pasture is not dissimilar (Figure 4b). Alfalfa has a simulated average recharge of 370 mm y^{-1},

Table 3. Total Amount of Simulated Irrigation Water Applied to Alfalfa, Grain and Pasture in a Typical Dry (2001) and Typical Wet Year (2003) in mm y^{-1}

	Dry Year		Wet Year	
	Ground Water Applied (mm y^{-1})	Surface Water Applied (mm y^{-1})	Ground Water Applied (mm y^{-1})	Surface Water Applied (mm y^{-1})
Alfalfa	862	50	723	83
Grain	419	29	397	55
Pasture	178	361	167	636
Total	701	326	596	573

about 20% lower than the average grain and pasture recharge of 467 and 437 mm y^{-1}, respectively (Table 3), but significant between-field variability exists due to varying soil water holding capacity.

[59] Few field data exist to confirm the soil water budget results. While simulated ET in alfalfa is consistent with *Hanson et al*. [2011a], the simulated average annual irrigation amounts for alfalfa (840 mm) and grain (358 mm) are found to be significantly higher than reported by growers in the study area: Preliminary field monitoring data for the 2012 irrigation season and interviews with growers on irrigation practices indicate that actual irrigation rates may be on the order of 500–600 mm in alfalfa and 150–200 mm in grain. Lower irrigation rates, when using groundwater for irrigation, may be due to overestimation of ET due to deficit irrigation, direct groundwater uptake by the crop, not accounted for in the model, or due to underestimating root zone depth and, hence, soil moisture storage capacity. Deficit irrigation has been found to lower ET by as much as 55 mm in Scott Valley and up to 200 mm elsewhere [*Hanson et al*., 2011b]. Lower ET would lower the net stress on groundwater. Direct groundwater uptake, where it occurs in groundwater irrigated areas, does not change the simulated net stress to the aquifer obtained from the soil water budget model unless it also affects crop ET. Doubling the water holding capacity (effectively assuming a thicker root zone) reduces simulated irrigation requirements by 3% in alfalfa and only 1% in grain, thus not explaining the discrepancy with observed irrigation rates. New field work was initiated among the study area stakeholders to obtain representative measurements of soil water dynamics, irrigation rates, evapotranspiration and the occurrence of deficit irrigation that can be used in the future to improve soil water budget simulations.

[60] Analysis of the spatial distribution of annual average values over the 21 year period for surface water irrigation, recharge, pumping, and pumping minus recharge (Figure 4) provides useful insight to evaluate the differences in irrigation amount and pumping based on landuse and water source. Some key observations include:

[61] 1. Highest recharge rates (Figure 4b) occur in polygons with pasture as landuse and with groundwater as water source due to relatively low irrigation efficiency and long irrigation season; also in the non-vegetated mine tailings at the southern end of the valley and in areas with very small water holding capacity;

[62] 2. Highest pumping rates occur in the few polygons with pasture as landuse and groundwater as water source

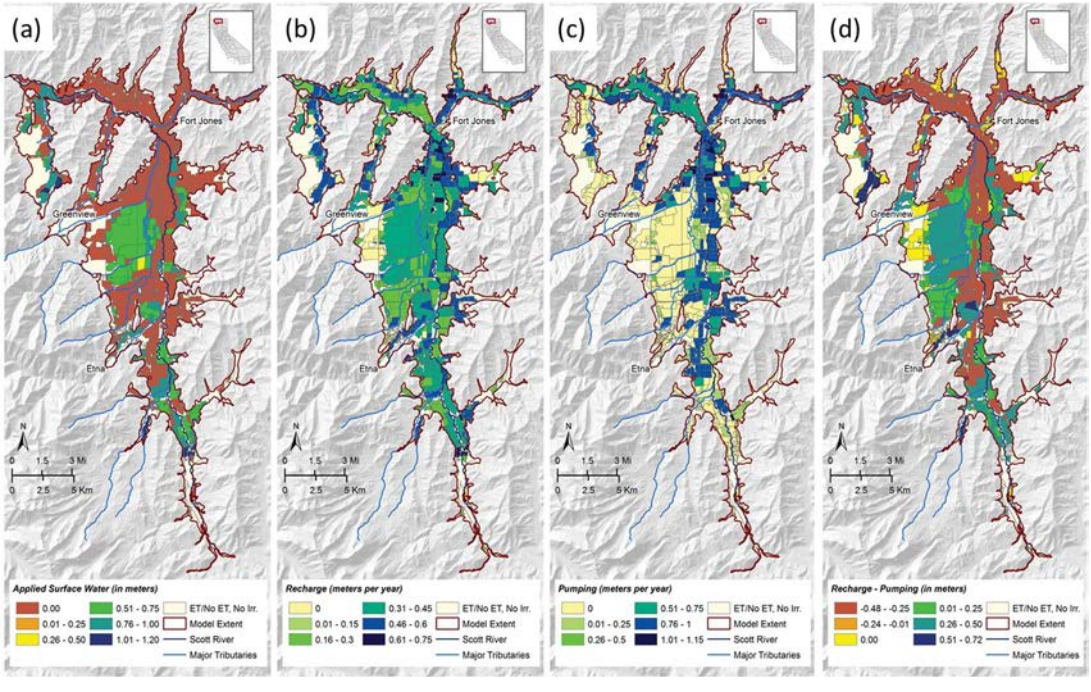

Figure 4. Water budget simulation results: (a) Average annual applied surface water rates (m y^{-1}) in irrigated crops between October 1990 and September 2011; (b) Average annual recharge (m y^{-1}) in irrigated areas between October 1990 and September 2011; (c) Average annual irrigation pumping rates (m y^{-1}) between October 1990 and September 2011; (d) Average annual difference between recharge (positive) and pumping (negative) (m y^{-1}) in irrigated areas between October 1990 and September 2011.

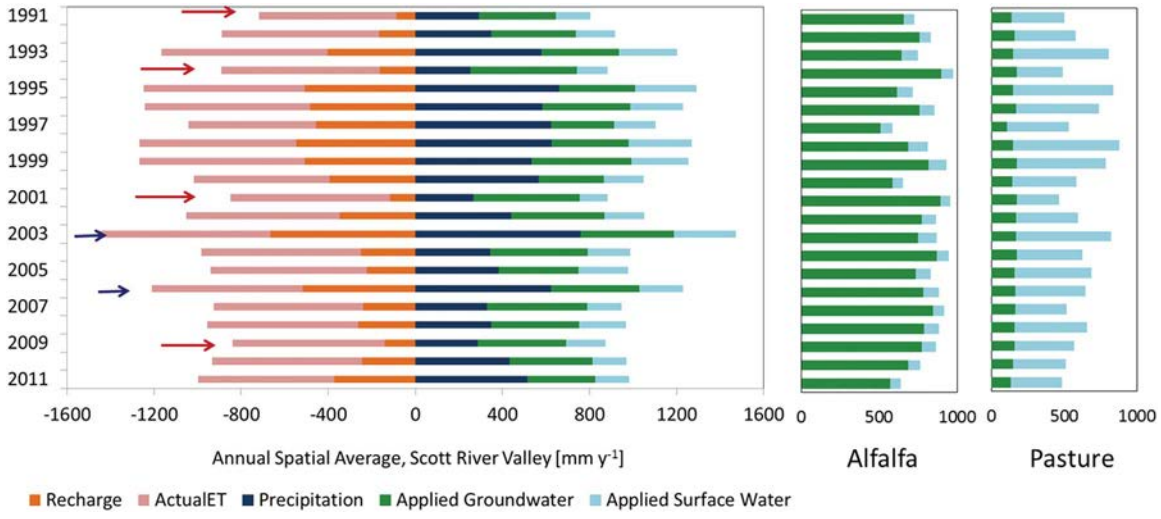

Figure 5. (a) Annual soil root zone water budget (mm y^{-1}), area-weighted average for the alfalfa/grain and pasture area in the Scott Valley. Input to the root zone shown as positive values (precipitation, applied groundwater and applied surface water). Outputs from the root zone are shown as negative values (actual ET and recharge). Annual applied surface water and annual applied groundwater (mm y^{-1}) for (b) alfalfa/grain and (c) pasture, area-weighted average over all alfalfa/grain landuse polygons in the project area. Critically dry years are highlighted in red and wet years are highlighted in blue.

(Figure 4c): this can be explained by the fact that pasture has the longest irrigation season. In polygons with groundwater as water source, the estimated irrigation rate is equal to the estimated pumping rate and it is not limited by (surface) water availability;

[63] 3. The lowest recharge rates occur in polygons that correspond to dry land farming or natural vegetation. They rely on precipitation as water source for plants, which are effective at extracting available moisture;

[64] 4. Since irrigation is driven by ET and irrigation efficiency, there is no water deficiency during the irrigation season. The water deficiency shown in Table 2 occurs mostly in the months immediately following the end of the irrigation season (September, October, and November) and prior to winter dormancy. In practice, much higher deficiencies may occur in wheel-line and center pivot sprinkler irrigated crops, as possibly indicated by preliminary data on field irrigation rates.

[65] Significant differences in water flows are found between dry years and wet years (Figure 5 and Table 3). Valley wide recharge to groundwater is significantly lower in dry years (as little as 100 mm y^{-1}) than in wet years (over 600 mm y^{-1}). Low recharge in dry years is mostly due to lack of streamflow from the surrounding watershed and, hence, lower amounts of applied surface water (Table 3). Dry year surface water irrigation is only 60% of wet year surface water irrigation. Changes in groundwater pumping due to dry year conditions are relatively small when compared to the large reductions in surface water irrigation, as is common in semiarid regions [*Ruud et al.*, 2004]. Dry years, therefore, significantly affect the agricultural productivity of the Scott Valley with most impact focused on pasture areas (Figure 5c).

[66] Simulated groundwater use in alfalfa, on average, is about 16% higher in dry years than in wet years. Higher groundwater use in dry years is driven mostly by higher evapotranspiration from alfalfa/grain landuses early in the growing season, demanding a higher irrigation amount. Less importantly here, higher groundwater use in dry years is also due to limited surface water availability on those fields equipped to switch from surface water to groundwater (Figure 5b). Groundwater irrigated pasture land is the exception (Figure 5c). The amount of applied groundwater, driven by spring precipitation, ET, and soil moisture availability, varies within a limited range throughout the 21 year period because there are no significant differences in the

Table 4. Summary of the Data on the Eight Wells Selected for the Analysis (for Location, See Figure 3)

SDF (d)	Polygon	HK (m/d)	Storage Coefficient	Aquifer Thickness (m)	Transmissivity (m^2/d)	Distance From the River (m)	Daily Pumping (m^3/d)
2.7	595	45	0.12	45.4	2042	215	1400
9.7	88	45	0.12	40.5	1821	385	2620
9.8	46	45	0.12	44.7	2013	405	4870
12	414	45	0.12	44.7	2013	446	2490
78	226	45	0.12	42.3	1905	1114	3180
133	103	45	0.12	39.6	1782	1407	7460
233	617	12	0.12	66.8	801	1248	5060
1503	1728	12	0.12	32.5	390	2211	2200

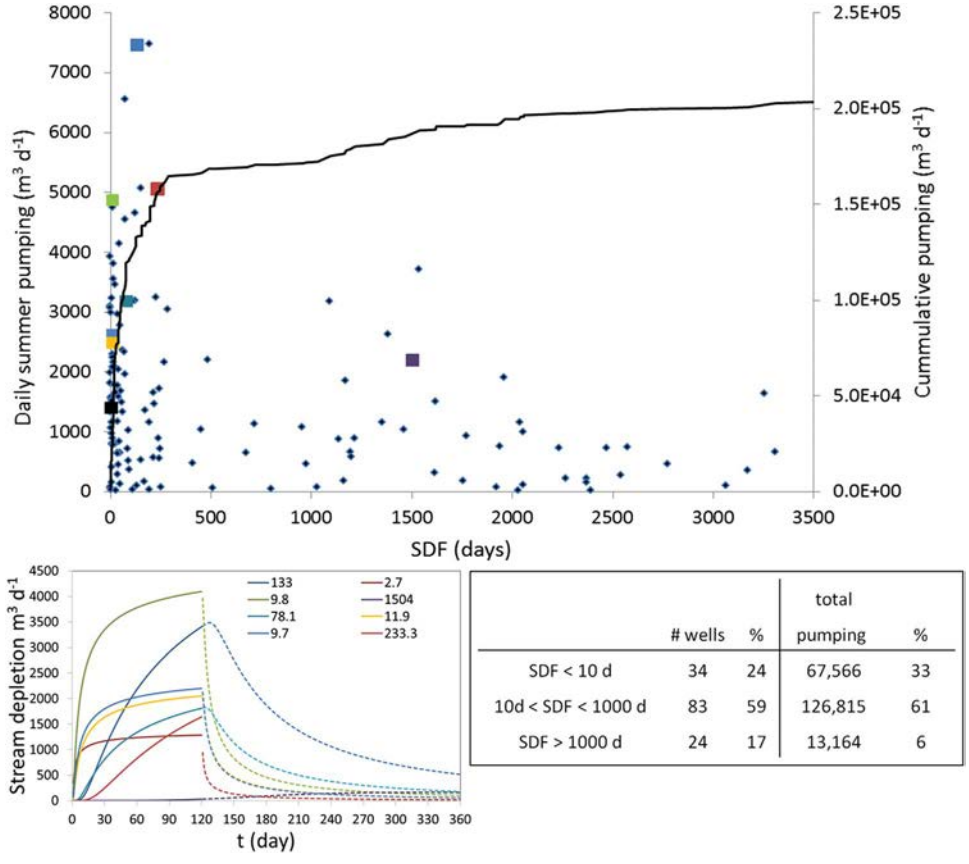

	# wells	%	total pumping	%
SDF < 10 d	34	24	67,566	33
10d < SDF < 1000 d	83	59	126,815	61
SDF > 1000 d	24	17	13,164	6

Figure 6. Daily cumulative summer pumping as a function of the stream depletion function (SDF, blue dots) for all 163 wells (Figure 1). For eight wells shown in larger colored squares, the graph on the lower left shows simulated stream depletion over 1 year, assuming 120 days of constant pumping and 240 days without pumping (in corresponding colors). Solid lines represent the pumping period and dashed line the subsequent period without pumping. The eight wells are labeled by their SDF (d) (also see Figure 1 for location).

length of the irrigation season between different years. Where the water source is groundwater, irrigation continues for the entire irrigation season, unaffected by surface water availability. This does not account for grower responses to climate, such as increasing/decreasing deficit irrigation.

6.2. Scott River Stream Depletion Dynamics

[67] The stream depletion factor, t_a [SDF; *Jenkins*, 1968] associated with each of the 163 wells identified (Figure 1) varies from less than 1 day to over 3600 days. High SDF values lead to slow stream depletion and vice versa. The SDF increases (stream depletion slows down) with increasing aquifer storage coefficient and distance. But the SDF decreases (stream depletion occurs more rapidly) with higher transmissivity between the well and the stream (equation (13)). Distance, varying over orders of magnitude from few meters to several kilometers is the key controlling variable for the variability of the SDF across Scott Valley. In contrast, the storage coefficient, here assumed constant, has been found to vary within a relatively narrow range throughout most of the valley (7–15%) [*Mack*, 1958]. Regional hydraulic conductivity varies by about half an order of magnitude between subareas, significantly influencing SDF. Hydraulic conductivity has been estimated from short-term pump tests to evaluate the specific capacity of wells, typically performed during well construction [*Mack*, 1958; *SSPA*, 2012]. Accuracy of these estimates may be limited, as they reflect local conditions in the immediate vicinity of the well, rather than effective conditions. However, total (integrated) stream depletion in the Scott River is less sensitive to random errors of local transmissivity estimates than to systematic under or overestimation of transmissivity across multiple wells, especially those with small SDF. This suggests that further field evaluation of hydraulic conductivity is needed, particularly near high capacity wells in close proximity to the river.

[68] Spatial distributions of crop type and the SDF values show some similarities: alfalfa/grain fields are concentrated in the vicinity of the Scott River, where well capacity is likely higher due to coarser and thicker sediments with higher aquifer transmissivity and with low SDF (Figure 6, equation (13)). Pasture fields are often located away from the Scott River in areas with higher SDF (Figure 1), and are irrigated with surface water from tributaries emanating off the surrounding canyons.

[69] Considering stream depletion due to average seasonal pumping at eight selected wells with a wide range of

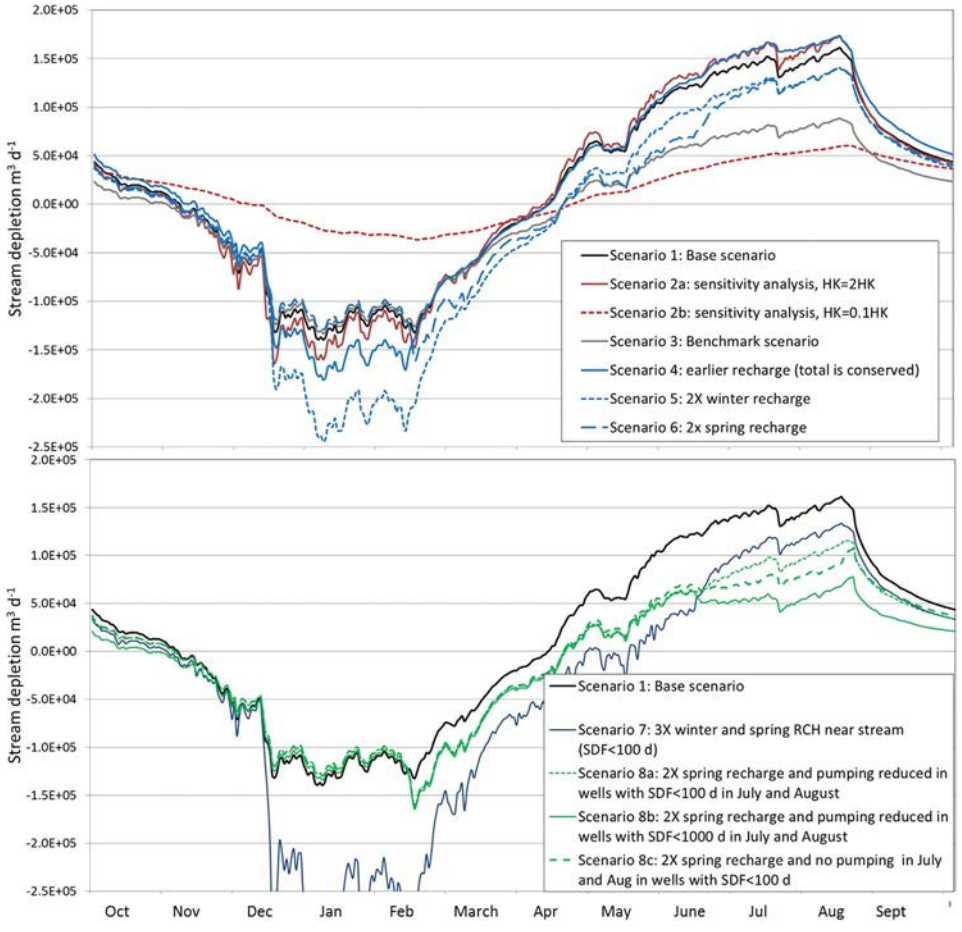

Figure 7. Simulated total daily stream depletion of the Scott River in response to 1991–2001 average daily varying net stress (pumping minus recharge), spatially distributed across the Scott Valley. Results represent a cyclical, dynamic equilibrium. Absolute stream depletion values are subject to significant uncertainty due to parameter uncertainty (compare Scenarios 1, 2a, 2b) and the simplicity of the conceptual approach, but relative changes in stream depletion over time and between management scenarios (Scenarios 3–8) provide guidance on the magnitude of stream depletion changes affected by managed changes in recharge and pumping. Note: 100,000 m^3 d^{-1} corresponds to approximately 40 cfs.

SDF values (Table 4) indicates that wells with very small SDF (<10), lead to measurable stream depletion within hours to few days after the onset of pumping. About half of the full depletion effect occurs within approximately one week. Within 2 months, the stream is affected at 90% of the full depletion rate (Figure 6). For SDFs on the order of 100, significant effects on stream depletion are observable within less than 1 month and increasing impacts occur throughout the 4 month pumping season. Only wells with SDF > 1000, have limited effect on stream depletion during the 4 month pumping season. Climate variability would therefore exacerbate stream depletion: dry years lead to more stream depletion during the later summer months due to reduced basin-wide spring and summer recharge (total runoff in the Scott River, e.g., in 2009, was less than 45% of average), while groundwater pumping to support crop irrigation remains unchanged or maybe even somewhat higher than in average or wet years due to increased crop ET.

[70] Wells with SDF of less than 10 days represent 24% of all wells, but 33% of the total pumping. This is consistent with the alluvial hydrogeology of the valley, which dictates that larger capacity wells are located closer to the river, where aquifer thickness is large and sediments are coarsest. For the same reason, wells with an SDF of over 1000 days represent less than one-fifth of all wells (17%) delivering merely one-twentieth (6%) of the total pumpage (Figure 6).

[71] Cyclical simulations based on average daily pumping rates converge to a dynamic steady state only after 20 years, due to the long-term effects of wells with high SDF on stream depletion. The CPU time for computing 20 years of stream depletion due to daily varying net pumping stresses across 163 wells and for performing the convolution is 470 s (0.13 h) on a PC with Intel(R) Core^{TM} i7–3520M CPU @ 2.90GHz and 64-bit operating system. In comparison, a fully integrated, three-dimensional numerical hydrological model with sufficient resolution to resolve individual landuse parcels requires about 8 h using monthly stresses for 21 years on the same platform.

[72] For the base scenario, the maximum total stream replenishment (negative depletion) in the study area occurs

from mid-December through mid-February, at approximately 125,000 m^3 d^{-1} (50 cfs), while the largest stream depletion occurs in August, at approximately 150,000 m^3 d^{-1} (60 cfs) (Figure 7). The latter represents slightly more than one-third of the simulated peak groundwater pumping rate, nearly 400,000 m^3 d^{-1} (160 cfs) in July.

[73] Summed over the entire year, the stream depletion model, which assumes an infinite aquifer, yields a small net annual stream depletion despite the water budget of the study area showing more recharge than pumping (Table 2). Due to the high streamflows during November through June (in excess of 250,000 m^3 d^{-1} [100 cfs]), stream depletion is here only of concern during the summer period. During that period, existing winter and spring recharge is not sufficient to offset summer groundwater pumping effects on stream depletion due to the large number of wells with SDF $\ll$ 1000 days and especially those with SDF $<$ 10 days.

[74] If the selected transmissivity values for the base scenario consistently underestimated actual aquifer transmissivity by a factor 2, actual stream depletion during the critical period in July and August would be about 9200 m^3 d^{-1} (3.8 cfs) more than estimated with the base scenario (Figure 7, Scenario 2a). Similarly, if actual transmissivity in the Scott Valley consistently were only half of the values assumed for the base scenario, actual stream depletion due to the same stresses would be 9200 m^3 d^{-1} (3.8 cfs) lower than in the base scenario (not shown). The transmissivity term in (13) is an effective transmissivity for the flow between a well and the stream. If the aquifer is heterogeneous or flow paths are constricted, especially near the stream, the lowest transmissivity values along the flow path between a well and a stream would dominate the effective value. If such factors reduced the effective field transmissivity between Scott River and wells to 10% of that assumed in the base scenario, actual stream depletion in July and August would be about 80,000 m^3 d^{-1} (33 cfs) less than in the simulated base scenario. This shows that estimated stream depletion is highly sensitive to actual hydraulic conductivity and flow configuration, especially near the stream.

[75] To understand the accuracy of predictions based on equation (15), *Sophocleous et al*. [1995] analyzed the predictive accuracy of the *Glover* [1954] stream-aquifer analytical solution with a numerical groundwater flow model. Across a range of aquifer conditions, assumptions in the analytical solution were tested, e.g., by removing the hydraulic equilibrium conditions. Generally, the analytical solution overestimated stream depletion suggesting that the analytical solution approach leads to a relatively conservative assessment in guiding decisions about water rights administration. A rank of the importance of the various assumptions involved in the derivation of the analytical solution was presented and the three most significant factors were: (1) streambed clogging, as quantified by streambed-aquifer hydraulic conductivity contrast, (2) degree of stream partial penetration, and (3) aquifer heterogeneity. Aquifer width, not considered by the SDF, has also been demonstrated to be important [*Miller et al*., 2007].

[76] Streambed clogging or low streambed hydraulic conductivities (relative to the aquifer) may be addressed by applying the method of additional seepage resistance [*Sophocleous et al*., 1995] to raise the SDF value. In our study area, it is unlikely to play an overriding role due to the absence of fine materials in the streambed and frequent scouring and redeposition of streambed materials during the high flow season. The effect of partial well penetration on stream depletion has also been shown to be small [ibid].

[77] The range of maximum stream depletion obtained from this sensitivity analysis (54,000–143,000 m^3 d^{-1} (22–55 cfs)) provides a coarse approximation of possible actual stream depletion in July and August given the pumping and recharge distribution simulated for the Scott Valley. This range would be proportionally lower, if actual ET, especially in alfalfa, will be shown to be lower in the Scott Valley than simulated here, due, e.g., to deficit irrigation.

[78] A benchmark test (Scenario 3) is used to perform an independent assessment of the order of accuracy provided by this simplified stream depletion analysis, when used to provide predictions of changes in stream depletion due to certain changes in pumping and recharge. For the benchmark test, results of the coupled water budget-stream depletion model are compared against a third-party fully 3-D, numerical, cyclical steady-state groundwater model that represents year 2000 conditions in groundwater pumping and recharge. The spatial distribution of pumping and recharge is qualitatively similar to that of our soil water budget model, but not identical [*SSPA*, 2012]. The numerical model simulates a partially penetrating streambed and its streambed hydraulic conductivity has been calibrated against measurements of well water levels. Aquifer hydraulic conductivities vary across the valley, but are of similar magnitude in both models (7–45 m d^{-1}). For the benchmark test, basin-wide net groundwater extraction (pumping minus recharge) is reduced by approximately equivalent amounts, 12.0 Mm^3 y^{-1} (13.5 cfs) in the numerical model, and 14 Mm^3 y^{-1} (15.7 cfs) in the analytical model. The resulting late summer reduction in streamflow (July–September) depletion reported for the numerical groundwater model is 39,000 m^3 d^{-1} (16 cfs). The corresponding reduction estimated with our simple analytical model is 50,000 m^3 d^{-1} (21 cfs). The analytical model results, while exceeding the numerical estimates by 25%, are sufficiently consistent with the numerical results to consider this tool useful for evaluating broad options for pumping and recharge that can guide preliminary planning for alternative groundwater management practices to evaluate.

6.3. Groundwater Management Scenarios

[79] With surface water storage not available at the scale required for agricultural water use in the basin, the groundwater basin is the *de facto* storage basin to hold water from winter and spring recharge for irrigation water use during the summer. As in other semiarid and arid basins, groundwater is a key local water management instrument to extend the cropping season beyond that possible without power pumps, especially in dry years.

[80] The water budget model indicates that there are broad opportunities to redistribute surface water available during the wetter periods of the year for irrigation water use during the dry season. Alternative management practices may include those affecting groundwater recharge, practices affecting groundwater pumping, or both. In the

past, changes in recharge have occurred due to changes in landuse, and due to changes in irrigation efficiency and methods in the Scott Valley. Given the soil water budget results, switching from mostly flood irrigation to wheel-line sprinkler irrigation between the 1950s and the 1970s had a significant impact on the timing and amount of recharge. It also incentivized the much increased use of groundwater since pumps were needed to pressurize wheel-line sprinklers and, later, center pivot sprinklers (introduced during the late 1990s and 2000s). *Van Kirk and Naman* [2008] suggested considering the difference in irrigation efficiency between flood irrigation and sprinkler irrigation.

[81] Management scenarios 4 to 7 highlight potential benefits to stream depletion during the critical summer months by managing groundwater recharge during seasons with high streamflow. Scenario 4 illustrates the effect of recharge timing, while keeping the total annual recharge amount the same as in the base scenario: recharge timing is moved from spring and early summer months to January–February, a difference that may occur naturally between individual years due to interannual climate variability. Having recharge occur earlier in the year, albeit at the same total amount, increases stream depletion in July and August by nearly 10% (by 15,000 m^3 d^{-1}, 6 cfs) over the base scenario (Figure 7). In contrast, hypothetically doubling the amount of (already high) recharge in January–February while keeping recharge during other months identical to that in the base scenario (Scenario 5) reduces July and August stream depletion by 16,000 m^3 d^{-1} (7 cfs) (Figure 7). Additional recharge in January and February would not significantly interfere with agronomic practices as crops are dormant, if aquifer storage capacity is available.

[82] Stronger reduction in streamflow depletion may be expected when increasing the amount of recharge closer to the period of high stress in July and August. Indeed, doubling recharge in March through June rather than in January and February (Scenario 6) substantially decreases stream depletion (relative to Scenario 5) during the months with additional recharge (by as much as 30,000 m^3 d^{-1}, 12 cfs), but 3–4 weeks after the additional recharge seizes, there are no observable differences between Scenarios 5 and 6 (Figure 7).

[83] Tripling the amount of recharge during the entire first half of the year, but only in areas near the Scott River (SDF $<$ 100 d, Figure 1), yields large stream replenishment (negative depletion) for most of the winter months and into May (Scenario 7), much longer than in the base scenario. Also, through much of July and August, stream depletion is much lower than in the base scenario and never reaches base scenario levels. Although additional recharge in this scenario occurs only near the Scott River and ends on July 1, stream depletion is consistently smaller (by 8000 m^3 d^{-1}, 4 cfs) in July and August when compared to Scenario 6. A significant delay in the onset of strong stream depletion could benefit other streamflow management scenarios that rely on the enhancement of instream flows: later onset of stream depletion would result in shorter periods where additional instream flow requirements are needed. Later spring recharge (April–June) could therefore provide a particularly important management tool to limit stream depletion during the critical period of July and August. Additional surface water could be obtained through acquisition of surface water rights from the valley margin (where a discontinuation of recharge during the summer months has no detrimental effect on Scott River flow), or by creating an external surface or subsurface storage capacity [*Schneider*, 2010].

[84] Groundwater management options may not only include additional recharge, but also altered groundwater pumping patterns. These scenarios are designed following the classification of SDF values by *Bredehoeft and Kendy* [2008]:

[85] 1. Wells with SDF $>$ 1000 d (17% of the wells, Figures 1 and 6, representing 6% of the total pumping) present the most interesting pool of wells for the design of mitigation strategies. Significant recharge occurring in the areas between the wells and the stream during the spring months is sufficient to offset potential long term, delayed stream depletion from pumping during the summer months.

[86] 2. Wells with 10 d $<$ SDF $<$ 1000 d (59% of the wells, Figures 1 and 6, representing 61% of the total pumping) represent the most uncertain situation. The pumping causes significant seasonal fluctuations. Different patterns of streamflow depletion can be produced depending on the SDF value, which is subject to uncertainty due to varying aquifer properties and boundary conditions not considered in the analytical model. For example, a combination of significant additional late spring and early summer recharge, switching from groundwater pumping to surface water irrigation or increasing already ongoing surface water irrigation, while streamflows are high, may significantly dampen effects of summer pumping from these wells. In the Scott Valley case, more detailed analysis using a numerical groundwater-surface water model and additional data collection will further guide specific future decision making.

[87] 3. Wells with SDF $<$ 10 d (24% of the wells, Figures 1 and 6, representing 33% of the total pumping) have quick impact on streamflows and produce large annual fluctuations in stream depletion. Pumping may be offset by additional streamflow, which would require additional surface water rights. Pumping may also be offset by groundwater transfers that replace groundwater pumping from wells with SDF $<$ 10 d with groundwater pumping from wells with SDF $\gg$ 100 d, at least during the most impacted season (July–August).

[88] Scenarios 8a–8c investigate potential benefits obtained by jointly managing groundwater recharge and groundwater pumping. Increased recharge during spring and early summer delays the onset of significant stream depletion, while the translocation of pumping away from the river during the sensitive summer period mutes the groundwater stresses that impact streamflow most immediately. A 50% reduction of July and August pumping in the wells closest to the river (SDF $<$ 100 d, Figure 1), and replenishment of that water by additional pumping (1.6 fold) outside that zone (Scenario 8a) would potentially yield reductions in July and August streamflow depletion of 42,000 m^3 d^{-1} (17 cfs). Expanding to a hypothetical 75% reduction of pumping in the zone with SDF $<$ 1000 d (Figure 1), yields additional July and August streamflow reductions of another 37,000 m^3 d^{-1} (16 cfs) when compared to Scenario 8a (Figure 7, Scenario 8b). Alternatively, an additional streamflow depletion of 12,000 m^3 d^{-1} (5 cfs), when compared to Scenario 8a, are obtained when

completely replacing groundwater pumping in the zone with SDF < 100 d and providing that irrigation water by transporting additional groundwater pumping from outside that zone to those fields (Scenario 8c). The latter two scenarios are hypothetical designs to estimate the magnitude of possible reductions in streamflow depletion. But Scenarios 8b and 8c would impose unachievable pumping requirements on outlying areas (3.5 fold and 2.3 fold pumping increases, respectively). Reductions in streamflow depletion achieved by these scenarios therefore reflect unrealistic goals.

[89] The scenario analysis indicates that both, recharge alone and the combination of recharge and selective changes in groundwater pumping patterns yield some reductions in streamflow depletion, which is here hypothesized to yield equivalently larger instream flows. The magnitude of the simulated reductions in streamflow depletion is significant. Potential streamflow increases are on the same order as current summer flow rates in the Scott River, which sometimes fall below 24,000 m^3 d^{-1} (10 cfs) suggesting that measurable gains in streamflow can be made. Stream temperature modeling indicates that a 50% increase of these low summer streamflows may substantially reduce the extent of Scott River reaches that are above 25°C, considered lethal for salmon habitat [*North Coast Regional Water Quality Control Board (NCRWQCB)*, 2005]. Flow increases also create opportunities for creating additional local habitat.

[90] Regulatory agencies have not defined numeric objectives regarding streamflow, largely because streamflow management to protect salmonid habitat via groundwater management remains an emerging research arena [*Malcolm et al*., 2012; *Milner et al*., 2012]. Salmonid ecosystem responses to streamflow are highly variable and confounded by other factors. Local investigations of flow impacts and solutions were identified as most promising [*Milner et al*., 2012]. In the case of managing the salmonid GDE in Scott Valley, regulators envision a broad range of measures and assessments across hydrologic and ecological disciplines [*NCRWQCB*, 2007].

[91] All scenarios are based on average monthly 1991–2011 recharge and pumping conditions. Other scenarios that could be considered with this tool may account for climate variability, the transient effects of consecutive dry or wet years, as have occurred in the recent past, and artificial aquifer recharge (AR) and aquifer storage and recovery (ASR) projects [*Nelson*, 2011; *Sophocleous*, 2012]. Scenarios may include sensitivity analysis to parameters in the soil water budget model. And the analytical stream depletion model can also be implemented as a fully transient, long-term impact analysis model.

[92] The scenarios presented here are purposefully designed to mimic relatively simple, extreme management cases. While not considered accurate and subject to significant uncertainty, such scenarios enable scientists and stakeholders to better understand the relationship between management outcome (the amount of reduction in stream depletion) and the associated magnitude of specific management changes needed to affect the outcome (change in pumping and recharge operations). Such scenarios may also enhance the interaction between stakeholders and scientists [*Margerum*, 2008]. For example, the scenario analysis has prompted stakeholders to identify large tracts of alfalfa that have suitable infrastructure to use a combination of in lieu recharge (switching from groundwater pumping to surface water irrigation) and increased recharge via lowering irrigation efficiencies, during spring months while streamflows are high. Stakeholders are further considering to reintroduce beaver dams as a way to increase recharge to groundwater in the immediate vicinity of the stream, while also creating potential salmonid habitat improvements.

[93] Other issues and limitations will need to be considered in the process: Implementation of programs to translocate summer pumping toward the valley margins would require further feasibility analysis with a hydraulic groundwater model to assess the limitations imposed, for example, by the aquifer geometry and heterogeneity, with often lower transmissivity near the valley margins. The scenarios also sketch out potential routes for an assessment of legal and political issues related to transferring groundwater across property boundaries, and applying surface water to increase groundwater recharge. The economic feasibility of such management strategies would further require an assessment of infrastructure needs and costs to install the required groundwater pumping capacity and distribution system.

[94] The approach presented here identifies important groundwater management options that warrant additional analyses including the design of useful scenarios to be simulated with a fully developed numerical groundwater-surface water model [*Sophocleous*, 1995; *Neupauer and Cronin*, 2010]. The approach must therefore be considered as only one of a broader range of tools that support monitoring and assessment programs and adaptive management of groundwater-dependent streamflows under complex conditions and at multiple scales. One potential option that warrants further research is the application of this computationally efficient methodology in automated multiobjective groundwater management optimization that considers various management constraints and uncertainties. Such an application would be particularly relevant because future groundwater management in systems like the study area typically consists of a portfolio of multiple management options that optimize for economic cost, political acceptability, and desired ecologic outcome within the hydrologic constraints of the basin.

7. Conclusion

[95] The modeling approach presented here, a combination of a spatiotemporally distributed soil water budget model and an analytical streamflow depletion model, represents a powerful, computationally efficient, while conceptually simple means to effectively integrate science into a social network watershed process driven by legal and policy decisions. The tool has been applied to the Scott Valley watershed in Northern California, a groundwater-dependent ecosystem that relies on sufficient groundwater discharge into the stream during July–September. The estimation of spatiotemporally distributed recharge and pumping stresses with the soil water budget model allowed us to develop and implement a range of groundwater management scenarios to broadly bracket options that can serve as catalyst to direct stakeholder discussions, and to

demonstrate the potential range of beneficial impacts from groundwater management on stream depletion. The scenarios provide significant insights into spatial and temporal scales of measures and potential venues needed to mitigate existing conflicts between stakeholders representing local farms and those representing downstream fisheries:

[96] 1. Increased groundwater storage of winter and spring streamflow, especially near the Scott River, may significantly decrease the impact of the pumping season on streamflow depletion during the critical summer period.

[97] 2. Groundwater pumping effects in August and July could be further mitigated by transferring groundwater pumping in the most sensitive areas to wells that are some distance away from the Scott River. This would require water trading and transport infrastructure. But the analysis also identified significant limitations on the amount of stream depletion reduction that can realistically be expected.

[98] 3. Addressing uncertainty about the effective hydraulic conductivity between the stream and the aquifer due to geologic heterogeneity, due to geomorphologic complexity, and the unknown complexity of the flow field between groundwater and the stream is critical to better quantify actual stream depletion impacts. We also found that the soil water budget significantly overestimates currently reported farm irrigation rates in center pivot and wheel-line sprinkler systems, possibly due to significant, but unreported deficit irrigation. Sensitivity analysis yields a measure of uncertainty. More importantly it provides direction for critical field measurement programs and the design of more complex hydrologic models for site-specific assessment and feasibility studies of specific recharge and pumping management projects.

[99] The approach has broad merit in the initial phases of a stakeholder driven process to address groundwater-stream interactions through groundwater management, to identify broad areas of potentially feasible projects, and to convey information on the scope of potential projects and expected outcomes. The approach may possibly also be applicable, e.g., for computationally demanding complex management systems optimization applications. Further research on such applications is warranted. The approach is not intended as a tool to provide accurate, quantitative answers for site-specific assessments. Some of its components, especially in the soil water budget, can be significantly improved (e.g., by addressing ditch and canal losses, potential winter runoff, deficit irrigation and reduced ET).

[100] **Acknowledgments.** This work was funded by California State Water Resources Control Board awards 09–084-110 and 11–189-110. We gratefully acknowledge helpful discussions with Sari Sommarstrom, Steve Orloff, Bryan McFadin, and the Scott Valley Groundwater Advisory Committee to the Siskiyou County Board of Supervisors. We also appreciate the very constructive comments provided by three anonymous reviewers and the editor, Selker. The views expressed here are solely those of the authors.

References

Allen, D. M., D. C. Mackie, and M. Wei (2004), Groundwater and climate change: A sensitivity analysis for the Grand Forks aquifer, southern British Columbia, Canada, *Hydrogeol. J.*, *12*, 270–290, doi:10.1007/s10040-003-0261-9.

Allen, R. G., L. S. Pereira, D. Raes, and M. Smith (1998), Crop evapotranspiration—Guidelines for computing water requirements, *FAO Irrig. and Drain. Pap. 56*, Food and Agric. Organ. of the U. N., Rome.

Bertrand, G., N. Goldscheider, J.-M. Globat, and D. Hunkeler (2012), Review: From multi-scale conceptualization to a classification system for inland groundwater-dependent ecosystems, *Hydrogeol. J.*, *20*, 5–25, doi:10.1007/s10040-011-0791-5.

Boano, F., C. Camporeale, and R. Revelli (2010), A linear model for the coupled surface-subsurface flow in a meandering stream, *Water Resour. Res.*, *46*, W07535, doi:10.1029/2009WR008317.

Bredehoeft, J. (2011), Hydrologic trade-offs in conjunctive use management, *Ground Water*, *49*, 468–475, doi:10.1111/j.1745-6584.2010.00762.x.

Bredehoeft, J., and E. Kendy (2008), Strategies for offsetting seasonal impacts of pumping on a nearby stream, *Ground Water*, *46*, 23–29, doi:10.1111/j.1745-6584.2007.00367.x.

Burt, O. R., M. Baker, and G. A. Helmers (2002), Statistical estimation of streamflow depletion from irrigation wells, *Water Resour. Res.*, *38*(12), 1296, doi:10.1029/2001WR000961.

Caissie, D. (2006), The thermal regime of rivers: A review, *Freshwater Biol.*, *51*, 1389–1406, doi:10.1111/j.1365-2427.2006.01597.x.

California Department of Water Resources (2000), Siskiyou County Land Use Survey 2000, Division of Planning and Local Assistance. [Available at: http://www.water.ca.gov/landwateruse/lusrvymain.cfm.]

California Department of Water Resources (CDWR) (2003), California's ground water, *Bull. 118*, 265 p., Calif. Dep. of Water Res., Sacramento, Calif.

California State Water Resources Control Board (CSWRCB) (1980), Scott River Adjudication in the Superior Court of Siskiyou County, no. 30662.

Chung, I.-M., N.-W. Kim, J. Lee, and M. Sophocleous (2010), Assessing distributed groundwater recharge rate using integrated surface water-groundwater modelling: Application to Mihocheon watershed, South Korea, *Hydrogeol. J.*, *18*, 1253–1264, doi:10.1007/s10040-010-0593-1.

Clean Water Act (1972), 33 U.S.C. §1251 et seq. [Available at http://epw.senate.gov/water.pdf.]

Döll, P., H. Hoffmann-Dobrev, F. T. Portmann, S. Siebert, A. Eicker, M. Rodell, G. Strassberg, and B. Scanlon (2012), Impact of water withdrawals from groundwater and surface water on continental water storage variations, *J. Geodyn.*, *59–60*, 143–156, doi:10.1016/j.jog.2011.05.001.

Drake, D., K. Tate, and H. Carlson (2000), Analysis shows climate-caused decreases in Scott River Fall Flows, *Calif. Agric.*, *54*(6), 46–49.

Faunt, C. C. (Ed.) (2009), Groundwater Availability of the Central Valley Aquifer, California, U.S. Geol. Surv. Prof. Pap., *1766*, 225 p.

Freeman, D. M. (2000), Wicked water problems: Sociology and local water organizations in addressing water resources policy, *J. Am. Water Res. Assoc.*, *36*, 483–491.

Gassman, P. W., M. R. Reyes, C. H. Green, and J. G. Arnold (2007), The soil and water assessment tool: Historical development, applications, and future research directions, *Trans. ASABE*, *50*(4), 1211–1250.

Gleeson, T., J. VanderSteen, M. A. Sophocleous, M. Tanikuchi, W. M. Alley, D. M. Allen, and Y. Zhou (2010), Groundwater sustainability strategies, *Nat. Geosci.*, *3*(6), 378–379, doi:10.1038/ngeo881.

Glover, R. E., and C. G. Balmer (1974), River depletion resulting from pumping a well near river, *Eos AGU Trans.*, *35*(3), 468.

Hanson, B., S. Orloff, K. Bali, B. Sanden, and D. Putnam (2011a), Evapotranspiration of fully-irrigated alfalfa in commercial fields, Proceedings, 2011 Conference of the California Chapter of the American Society of Agronomy, 1–2 Feb. 2011, Fresno, Calif.

Hanson, B., S. Orloff, K. Bali, B. Sanden, and D. Putnam (2011b), Midsummer deficit irrigation of alfalfa in commercial fields, Proceedings, 2011 Conference of the California Chapter of the American Society of Agronomy, 1–2 Feb. 2011, Fresno, Calif.

Hare, M., R. A. Letcher, and A. J. Jakeman (2003), Participatory natural resource management: A comparison of four case studies, *Integrated Assess.*, *4*(2), 62–72, doi:10.1076/iaij.4.2.62.16706.

Hargreaves, G. H., and Z. A. Samani (1982), Estimating potential evapotranspiration, *J. Irrig. Drain. Eng.*, *108*(3), 225–230.

Hart, J. (1996), *Storm Over Mono: The Mono Lake Battle and the California Water Future*, Univ. of Calif. Press, Berkeley. [Available at: http://ark.cdlib.org/ark:/13030/ft48700683/.].

Harter, T., and R. Hines (2008), *Scott Valley Community Groundwater Study Plan, Groundwater Cooperative Extension Program*, Univ. of Calif., Davis.

Harter, T., and L. Rollins (Eds.) (2008), *Watersheds, Groundwater, and Drinking Water: A Practical Guide*, 274 pp., Univ. of Calif. Agric. and Nat. Resour. Publ. 3497.

Howard, J., and M. Merrifield (2010), Mapping groundwater dependent ecosystems in California, *PLOS ONE*, *5*(6), e11249, doi:10.1371/journal.pone.0011249.

Hunt, B. (2003), Unsteady stream depletion when pumping from semiconfined aquifer, *J. Hydrol. Eng.*, *8*(1), 12–19, doi:10.1061/(ASCE)1084-0699(2003)8:1(12).

Jenkins, C. T. (1968), Computation of rate and volume of stream depletion by wells, *U.S. Geol. Surv. Tech. Water Resour. Invest., Book 4, Chap. D1*, 17 pp., U.S. Gov. Printing Office, Washington, D. C.

Jolly, I., D. Rassam, T. Pickett, M. Gilfedder, and M. Stenson (2010), Modelling Groundwater-Surface Water Interactions in the New Generation of River Systems Models for Australia, Groundwater 2010, 31 October–4 November 2010, Natl. Water Comm., Canberra.

Ker Rault, P. A., and P. J. Jeffrey (2008), Deconstructing public participation in the Water Framework Directive: Implementation and compliance with the letter or with the spirit of the law?, *Water Environ. J.*, *22*, 241–249, doi:10.1111/j.1747-6593.2008.00125.x.

Kollet, S. J., V. A. Zlotnik, and G. Ledder (2002), ''A Stream Depletion Field Experiment'' by Bruce Hunt, Julian Weir, and Bente Clausen, March–April 2001 issue, 39(2), 283–289, *Ground Water*, *40*, 448–449, doi:10.1111/j.1745-6584.2002.tb02523.x.

Kreuter, M., C. De Rosa, E. H. Howze, and G. T. Baldwin (2004), Understanding wicked problems: A key to advancing environmental health promotion, *Health Educ. Behav.*, *31*, 441–454.

Kustu, M. D., Y. Fan, and A. Robock (2010), Large-scale water cycle perturbation due to irrigation pumping in the US High Plains: A synthesis of observed streamflow changes, *J. Hydrol.*, *390*, 222–244, doi:10.1016/j.bbr.2011.03.031.

Lefkoff, L. J., and S. M. Gorelick (1990), Simulating physical processes and economic behavior in saline, irrigated agriculture: Model development, *Water Resour. Res.*, *26*(7), 1359–1369, doi:10.1029/WR026i007p01359.

Loheide, S. P., and S. M. Gorelick (2007), Riparian hydroecology: A coupled model of the observed interactions between groundwater flow and meadow vegetation patterning, *Water Resour. Res.*, *43*, W07414, doi:10.1029/2006WR005233.

Luo, Y., P. A. Meyerhoff, and R. S. Loomis (1995), Seasonal patterns and vertical distribution of fine roots of alfalfa (Medicago sativa L.), *Field Crops Res.*, *40*, 119–127, doi:10.1016/0378-4290(94)00090-Y.

Mack, S. (1958), Geology and ground-water features of Scott Valley Siskiyou County, California, *U.S. Geol. Surv. Water Supply Pap. 1462*, 98 pp.

Malcolm, I. A., C. N. Gibbins, C. Soulsby, D. Tetzlaff, and H. J. Moir (2012), The influence of hydrology and hydraulics on salmonids between spawning and emergence: Implications for the management of flows in regulated rivers, *Fish. Manage. Ecol.*, *19*, 464–474, doi:10.1111/j.1365-2400.2011.00836.x.

Margerum, R. D. (2008), Multi-stakeholder platforms for integrated water management. in *Ashgate Studies in Environmental Policy and Practice, Nat. Resour. Forum*, vol. *32*, edited by J. Warner, pp. 261–262, doi:10.1111/j.1477-8947.2008.00199.x.

Maxwell, R. M., and S. J. Kollet (2008), Interdependence of groundwater dynamics and land-energy feedbacks under climate change, *Nat. Geosci.*, *1*(10), 665–669, doi:10.1038/ngeo315.

Maxwell, R. M., F. K. Chow, and S. J. Kollet (2007), The groundwater-land-surface-atmosphere connection: Soil moisture effects on the atmospheric boundary layer in fully-coupled simulations, *Adv. Water Resour.*, *30*(12), doi:10.1016/j.advwatres.2007.05.018.

Miller, C. D., D. Dumford, M. R. Halstead, J. Altenhofen, and V. Flory (2007), Stream depletion in alluvial valleys using the SDF semianalytical model, *Ground Water*, *45*(4), 506–514, doi:10.1111/j.1745-6584.2007.00311.x.

Milner, N. J., I. G. Cowx, and K. F. Whelan (2012), Salmonids and flows: A perspective on the state of the science and its application, *Fish. Manage. Ecol.*, *19*, 445–450, doi:10.1111/fme.12016.

Moellenkamp, S., M. Lamers, C. Huesmann, S. Rotter, C. Pahl-Wostl, K. Speil, and W. Pohl (2010), Informal participatory platforms for adaptive management. Insights into niche-finding, collaborative design, and outcomes from a participatory process in the Rhine basin, *Ecol. Soc.*, *15*(4), 41. [Available at: http://www.ecologyandsociety.org/v ol15/iss4/art41/.]

National Oceanographic and Atmospheric Administration (NOAA) (2012), Precipitation Records for Stations CA043182 (Fort Jones) and CA041316 (Callahan). [Available at http://www.noaa.gov, last accessed 1 July 2012.]

Natural Resources Conservation Service (NRCS) (2012a), National Geospatial Management Center. [Available at: http://soildatamart.nrcs.usda.gov/, last accessed 1 July 2012.]

Natural Resources Conservation Service (2012b), Soil Survey Staff, United States Department of Agriculture, Soil Survey Geographic (SSURGO) Database for Siskiyou County, CA. [Available at: http://soildatamart.nrcs.usda.gov., last accessed 16 July 2011.]

Neitsch, S. L., J. G. Arnold, J. R. Kiniry, and J. R. Williams (2011), Soil and water assessment tool theoretical documentation version 2009, *Texas Water Resour. Inst. Tech. Rep. 409*, 618 p., College Station, Tex. [Available at http://swat.tamu.edu/documentation/, last accessed 1 June 2013.]

Nelson, R. L. (2011), Developments in groundwater management planning in California, *Water in the West Working Pap. 1*, Woods Inst. for the Environ., The Bill Lane Cent. for the Am. West, Stanford Univ.

Nelson, R. L. (2012), Assessing local planning to control groundwater depletion: California as a microcosm of global issues, *Water Resour. Res.*, *48*, W01502, doi:10.1029/2011WR010927.

Neupauer, R. M., and M. T. Cronin (2010), Adjoint model for the selevtion of groundwater wells locations to minimize stream depletion, paper presented at the Congress: World Environmental and Water Resources Congress, Challenge of changes, ASCE, Providence, R. I., 6–10 May.

North Coast Regional Water Quality Control Board (NCRWQCB) (2005), Chapter 4 of Staff Report for the Action Plan for the Scott River Watershed Sediment and Temperature TMDLs. [Available at: http://www.waterboards.ca.gov/northcoast/water_issues/programs/tmdls/scott_river/staff_report.shtml.]

North Coast Regional Water Quality Control Board (NCRWQCB) (2007), Scott River TMDL Implementation Workplan, 12 p. [Available at http://www.waterboards.ca.gov/northcoast/water_issues/programs/tmdl s/scott_river/070322/final_scott_tmdl_workplan.pdf.]

North Coast Regional Water Quality Control Board (NCRWQCB) (2011), Staff Report for the Action Plan for the Scott River Watershed Sediments and Temperature TMDLs, Santa Rosa, California.

Ostrom, E., J. Burger, C. Field, R. B. Norgaard, and D. Policansky (1999), Revisiting the commons: Local lessons, global challenges, *Science*, *284*, 278–282, doi:10.1126/science.284.5412.278.

Pulido-Velazquez, M., J. Andreu, A. Sahuquillo, and D. Pulido-Velazquez (2008), Hydro-economic river basin modelling: The application of a holistic surface-groundwater model to assess opportunity costs of water use in Spain, *Ecol. Econ.*, *66*, 51–65, doi:10.1016/j.ecolecon. 2007.12.016.

Reid, W. V., et al. (2010), Earth system science for global sustainability: Grand challenges, *Science 12*, 916–917, doi:10.1126/science.1196263.

Ruud, N., T. Harter, and A. Naugle (2004), Estimation of groundwater pumping as closure to the water balance of a semi-arid, irrigated agricultural basin, *J. Hydrol.*, *297*(1), 51–73, doi:10.1016/j.jhydrol.2004.04.014.

Schneider, J. (2010), Stream depletion and groundwater pumping: Part two: The timing of groundwater depletions, *Water Matters*, *5*, 1–4.

Schoups, G., C. L. Addams, J. L. Minjares, and S. M. Gorelick (2006), Reliable conjunctive use rules for sustainable irrigated agriculture and reservoir spill control, *Water Resour. Res.*, *42*, W12406, doi:10.1029/206WR005007.

Scibek, J., and D. M. Allen (2006), Modeled impacts of predicted climate change on recharge and groundwater levels, *Water Resour. Res.*, *42*, W11405, doi:10.1029/2005WR004742.

Siebert, S., J. Burke, J. M. Faures, K. Frenken, J. Hoogeveen, P. Döll, and F. T. Portmann (2010), Groundwater use for irrigation: A global inventory, *Hydrol. Earth Syst. Sci.*, *14*, 1863–1880, doi:10.5194/hess-14-1863-2010.

Singh, A. (2012), An overview of optimization modeling applications, *J. Hydrol.*, *466–467*, 167–182, doi:10.1016/j.jhydrol.2012.08.004.

Sophocleous, M. A. (2000), From safe yield to sustainable development of water resources, and the Kansas experience, *J. Hydrol.*, *235*(1–2), 27–43, doi:10.1016/S0022-1694(00)00263-8.

Sophocleous, M. A. (2002), Water resources sustainability and its application in Kansas, in Proceedings of the Arbor Day Farm Conference on Sustainability of Energy and Water through the 21st Century, 8–11 October, edited by L. C. Gerhard, P. P. Leahy, and V. J. Yannacone, Jr., pp. 115–124, KGS in Assoc. with AAPG and the AAPG Div. of Environ. Geosci.

Sophocleous, M. A. (2012), The Evolution of groundwater management paradigms in Kansas and possible new steps towards water sustainability, *J. Hydrol.*, *414–415*, 550–559, doi:10.1016/j.jhydrol.2011.11.002.

Sophocleous, M. A., A. Koussis, J. L. Martin and S. P. Perkins (1995), Evaluation of simplified stream-aquifer depletion models for water rights administration, *Ground Water*, *33*(4), 579–588.

Snyder, R. L., M. Orang, and S. Matyac (2002), A long-term water use planning model for California, *ISHS Acta Hortic.*, *584*, 115–121.

S.S. Papadopoulos & Associates (SSPA) (2012), Groundwater conditions in Scott Valley, report prepared for the Karuk Tribe, March.

Thompson, B. H. Jr., J. D. Leshy, R. H. Abrams and J. L. Sax (2006), *Legal Control of Water Resources: Cases and Materials*, 4th ed., 285 pp., West Book Publ.

UNESCO (2010), World Social Science Report—Knowledge Divides, 443 pp., UNESCO, Paris, France. [Available at http://unesdoc.unesco.org/images/0018/001883/188333e.pdf.]

United Nations World Water Development (2009), Report 3: ''Water in a Changing World'' and ''Facing the Challenges'', UNESCO, Paris, France. [Available at: http://www.unesco.org/new/en/natural-sciences/environment/water/wwap/ww dr/wwdr3–2009/downloads-wwdr3.]

University of California Cooperative Extention (UCCE) (2012), Using Reference Evapotranspiration (ET0) and Crop Coefficients to estimate Crop Evapotranspiration (Etc) for agronomic crops, grasses, and vegetable crops, Leaflet 21427. [Available at http://lawr.ucdavis.edu/irrigation/irrigation_leaflets/L21427.html, last accessed 1 July 2012.]

U.S. Geological Survey (USGS) (2012), Water-Data Report 2012 11519500 Scott River Near Fort Jones, CA, Klamath River Basin, *U.S. Geol. Surv. Water-Data Rep. WDR-US-2012, site 11519500*, 3 pp. [Available at http://wdr.water.usgs.gov/wy2012/pdfs/11519500.2012.pdf, last accessed 1 June 2013.]

Van Kirk, R. W., and S. W. Naman (2008), Relative effects of climate and water use on base-flow trends in the lower Klamath basin, *J. Am. Water Resour. Assoc.*, *44*(4), 1035–1052, doi:10.1111/j.1752-1688.2008. 00212.x.

Von Korff, Y., K. A. Daniell, S. Moellenkamp, P. Bots, and R. M. Bijlsma (2012), Implementing participatory water management: Recent advances in theory, practice, and evaluation, *Ecol. Soc.*, *17*(1), 30, doi:10.5751/ES-04733-170130.

Wada, Y., L. P. H. van Beek, C. M. van Kempen, J. W. T. M. Reckman, S. Vasak, and M. F. P. Bierkens (2010), Global depletion of groundwater resources, *Geophys. Res. Lett.*, *37*, L20402, doi:10.1029/2010GL044571.

Wada, Y., L. P. H. van Beek, and M. F. P. Bierkens (2012), Nonsustainable groundwater sustaining irrigation: A global assessment, *Water Resour. Res.*, *48*, W00L06, doi:10.1029/2011WR010562.

Wallace, R. B., Y. Darama, and M. D. Annable (1990), Stream depletion by cyclic pumping of wells, *Water Resour. Res.*, *26*(6), 1263–1270, doi:10.1029/WR026i006p01263.

Wen, F., and X. Chen (2006), Evaluation of the impact of groundwater irrigation on streamflow in Nebraska, *J. Hydrol.*, *327*, 603–617, doi:10.1016/j.jhydrol.2005.12.016.

Wondzell, S. M., J. LaNier, and R. Haggerty (2009), Evaluation of alternative groundwater flow models for simulating hyporheic exchange in a small mountain stream, *J. Hydrol.*, *364*, 142–151, doi:10.1016/j.jhydrol.2008.10.011.

Zume, J., and A. Tarhule (2008), Simulating the impacts of groundwater pumping on stream-aquifer dynamics in semiarid northwestern Oklahoma, USA, *Hydrogeol. J.*, *16*, 797–810, doi:10.1007/s10040-007-0268-8.

RESEARCH ARTICLE

Modeling guides groundwater management in a basin with river–aquifer interactions

A Scott Valley study shows gains in understanding seasonal dynamics of groundwater–surface water fluxes as model tools address more complex natural phenomena.

by Laura Foglia, Jakob Neumann, Douglas G. Tolley, Steve B. Orloff, Richard L. Snyder and Thomas Harter

Abstract

The Sustainable Groundwater Management Act (SGMA) of 2014 seeks to maintain groundwater discharge to streams to support environmental goals. In Scott Valley, in Siskiyou County, the Scott River and its tributaries are an important salmonid spawning habitat, and about 10% of average annual Scott River stream flow comes from groundwater. The local groundwater advisory committee is developing groundwater management alternatives that would increase summer and early fall stream flows. We developed a model to provide a framework to evaluate those alternatives. We first created a water budget for the Scott Valley groundwater basin and integrated the detailed, spatiotemporally distributed water budget results into a computer model of the basin that simultaneously accounted for groundwater flow, stream flow and landscape water fluxes. Different conceptual representations (using the MODFLOW RIV package and MODFLOW SFR package) of the stream–aquifer boundary provided significantly different results in the seasonal dynamics of groundwater–surface water fluxes. As groundwater sustainability agencies draw up plans to meet SGMA requirements, they must choose and test simulation tools carefully.

Management of California's water supplies serves diverse goals. Securing the needs of urban and agricultural water customers is a key goal. Meeting environmental health, ecosystem services and stream water quality goals has also been an integral part of many California water management systems. To meet this range of goals, groundwater, soil water and surface water will need to be managed conjunctively, management will likely become more tightly linked with land use and land resources planning and management, and modelling will play a key role in the development of successful and useful management plans.

The 2014 California Sustainable Groundwater Management Act (SGMA) and recent salt- and nitrate-related regulations to protect groundwater quality have put a focus on groundwater resources management, both quality and quantity, particularly in agricultural regions (Harter 2015). They mandate that local agencies pursue groundwater sustainability goals: avoiding long-term groundwater storage depletion, land subsidence,

Online: https://doi.org/10.3733/ca.2018a0011

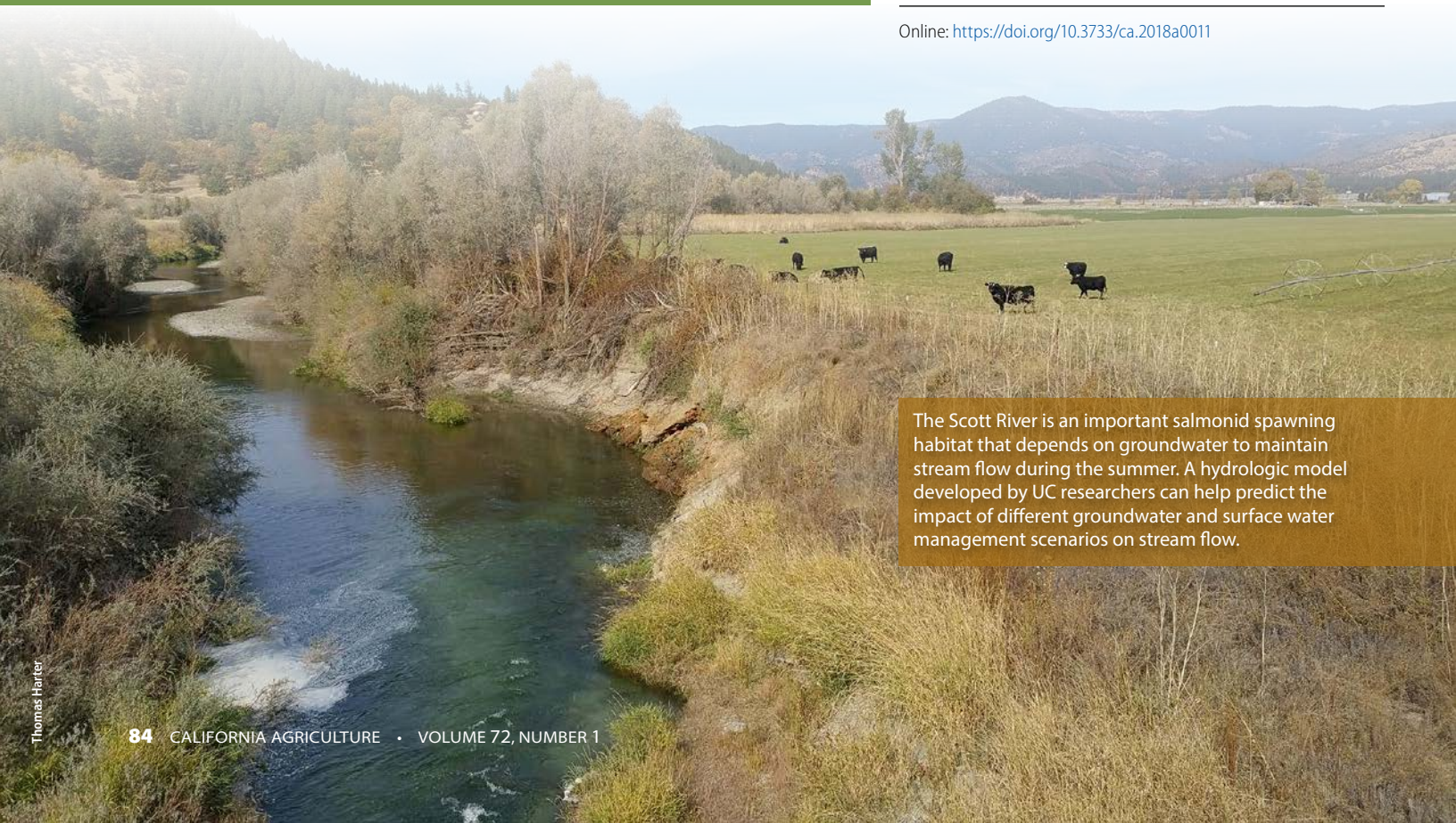

The Scott River is an important salmonid spawning habitat that depends on groundwater to maintain stream flow during the summer. A hydrologic model developed by UC researchers can help predict the impact of different groundwater and surface water management scenarios on stream flow.

Thomas Harter

seawater intrusion, groundwater management–related water quality degradation, and deterioration of groundwater–surface water interactions.

Particularly important under the SGMA regulations is the interaction between groundwater and surface water: how do groundwater management decisions — by individual landowners or by groundwater sustainability agencies (GSAs) — impact not only beneficial users, but also streams (Zume and Tarhule 2011) and groundwater-dependent ecosystems (GDEs) (Boulton and Hancock 2006; Hatton 1998). Prominent California examples of areas where groundwater–surface water interactions are already addressed include the Napa River in Napa County and the Scott River in Siskiyou County. Both feature important salmonid fish habitat and therefore temperature is a critical issue (Brown et al. 1994; Moyle and Israel 2005); and low or decreased late-summer stream flow over the last half-century has impacted the quantity and quality of fish habitat (Kim and Jain 2010; NCRWQCB 2005; Nehlsen et al. 1991). During drought, portions of these rivers may temporarily dry up. In intermontane Scott Valley, dry sections disconnect lower sections of the stream from tributaries in the headwaters. Summer stream temperatures in the Scott River are affected by groundwater discharge into the streambed and by riparian shading and were being addressed under the federal Clean Water Act (NCRWQCB 2005) before SGMA.

Some measurements can be collected in the field to evaluate groundwater–surface water interactions, but computer models are needed to fully understand groundwater basin flow dynamics and assess impacts to stream flow under future groundwater management scenarios. For example, computer models can show the response of integrated water systems to management decisions such as pumping and intentional recharge. They are expected to play a key role in the implementation of SGMA and regulatory efforts.

Various modeling approaches have been developed for groundwater–surface water interactions (Furman 2008; Harter and Seytoux 2013). These range from analytical or spreadsheet tools (Foglia, McNally, Harter 2013) and coupled or iteratively coupled numerical model codes for computer simulations, such as the MODFLOW river (RIV) package (Harbaugh et al. 2000) and the MODFLOW stream flow routing SFR1 package (Prudic et al. 2004) and SFR2 package (Harbaugh 2005; Niswonger and Prudic 2005), to fully coupled models such as ParFlow (Ashby and Falgout 1996; Kollet and Maxwell 2006) and Hydrogeosphere (Brunner and Simmons 2012).

Fully coupled models provide the physically and mathematically most consistent and complete integration of groundwater, surface water and soil water systems. But they are computationally more expensive and require more parameterization (data input) than iteratively coupled models. In coupled or iteratively coupled models, multiple models are coupled such that one model provides input to the other model and vice versa, sometimes iteratively. Full coupling may not always yield better results (Furman 2008). For some applications, statistical models or analytical tools, which are based on highly simplified concepts and therefore have the least data input requirements and are computationally much less demanding, may be appropriate.


Thomas Harter

Almost 70% of Scott Valley is used for agricultural production, with a nearly even split between alfalfa/grain and pasture.

In Scott Valley, groundwater–surface water interactions are analyzed as part of an action plan to meet temperature TMDL (Total Maximum Daily Load) requirements for the Scott River. Climate change and groundwater pumping for irrigation in the valley have impacted late-summer and early fall stream flows in the Scott River (Drake et al. 2000). The local groundwater advisory committee is developing potential groundwater management scenarios that would increase summer and early fall stream flows. To evaluate those scenarios, we explored three levels of conceptual complexity at which information can be obtained about groundwater–surface water interactions: a water budget approach, a groundwater model with a conceptually simplified stream model (RIV) and a fully coupled groundwater–surface water model (SFR).

Scott Valley study area

Our study area was Scott Valley in northern California. Almost 70% of the valley is used for agricultural production, with a nearly even split between alfalfa/grain and pasture.

Geography and climate

Scott Valley is an intermontane 220-square-kilometer agricultural groundwater basin at an elevation of 2,600 to 3,100 feet in Siskiyou County (fig. 1). The Scott River

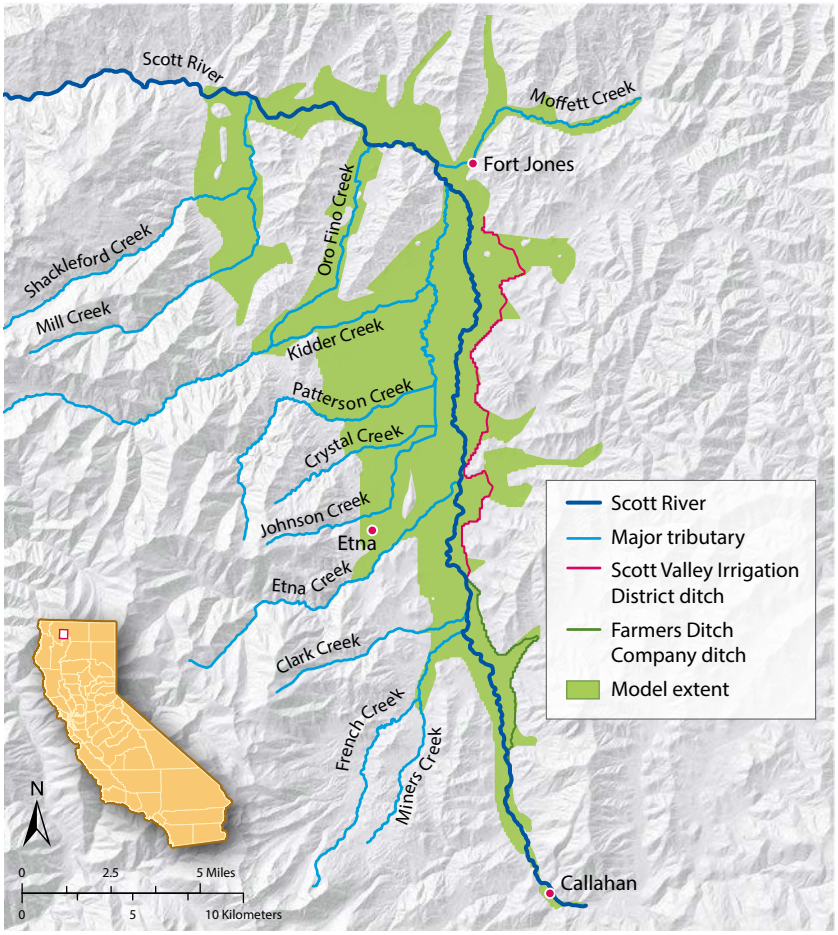

FIG. 1. The boundaries of the groundwater model study in Scott Valley, and its surface waters. The Scott River and its tributaries are an important salmonid spawning habitat, home to native populations of the threatened coho. Source: Model extent derived from Mack (1958) and Soil Survey Geographic Database (SSURGO) data. Projection: North American Datum 1983, UTM Zone 10.

flows from south to north along the east-central and northern portion of the valley. At the valley's northwest corner, the river descends into a gorge before joining the Klamath River several miles below Scott Valley. The Scott River watershed above Scott Valley extends into the surrounding Klamath Mountains to elevations of over 8,500 feet. The river and its tributaries are an important salmonid spawning habitat, home to native populations of the threatened *Oncorhynchus kisutch* (coho).

Scott Valley formed primarily due to movement along an eastward dipping normal fault, with unconsolidated, highly heterogeneous fluvial and alluvial fan deposits forming an alluvial groundwater basin (Mack 1958). Surrounding the valley, the geology is comprised of relatively impermeable bedrock composed of metamorphic and volcanic units, although fractures do yield some water in the form of springs at the margins of the valley and in surrounding upland areas.

Aquifer thickness may be as much as 400 feet in the wide central part of the valley (Mack 1958). However, there is no evidence of sufficiently coarse material to support agricultural groundwater pumping below 250 feet (Foglia, McNally, Harter 2013). The aquifer pinches out at the valley margin.

Climate in the valley is Mediterranean, with 89% of the nearly 500-millimeter average annual precipitation falling between October and April. Daily mean temperatures range from 70°F in July to 32°F in January. Precipitation depths in the surrounding mountains are much higher, and snowmelt is a major source for ephemeral tributaries feeding the Scott River and recharging into the aquifer. Snowmelt dominates Scott River flows through June. During the summer months, flows in the Scott River immediately below the montane valley (USGS gage 11519500 Ft. Jones) can drop to 4 cubic feet per second (cfs), while maximum flows during winter can reach 40,000 cfs. After snowpack storage has been depleted, the Scott River is dependent on discharge from the Scott Valley aquifer to support base flow. In dry years, sections of the Scott River overlying the valley floor become ephemeral.

Land use and irrigation

Land use was surveyed in 2000 (DWR 2000) and further refined using aerial photo analysis and on-the-ground verification through interviews with landowners. A total of 2,119 land use parcels overlie the Scott Valley groundwater basin (fig. 2): 710 parcels (17,400 acres) are alfalfa/grain (an 8-year rotation with, on average, 1 year of grain crop followed by 7 years of alfalfa), 541 parcels (16,600 acres) are pasture, 451 parcels (20,400 acres) belong to land use categories with significant evapotranspiration but no irrigation (e.g., cemeteries, lawns, natural vegetation) and 417 parcels (1,700 acres) represent land uses with no evapotranspiration or irrigation (e.g., residential areas, parking lots, roads, and — most significantly — historic mine tailings).

The year 2000 land use survey by DWR (DWR 2000) also identified the irrigation type associated with each land parcel. About 6,200 acres of cropland were identified as nonirrigated, dry or subirrigated. In Scott Valley, flood, center-pivot sprinkler and wheel-line sprinkler irrigation are used almost exclusively. Over the past 25 years, significant conversion from wheel-line sprinkler (but also from flood irrigation) to center-pivot sprinkler has occurred. For our study, we mapped the location (extent) and year of such irrigation-type conversions to land parcels by reviewing 1990 to 2011 aerial photos.

The beginning of the irrigation season is determined by soil moisture depletion but also by grower peer behavior. Earliest irrigation dates reported by local growers were March 15, March 24 and April 15 for grains, alfalfa and pasture, respectively. Growers irrigate based on soil moisture data, experience, peer behavior and established irrigation practices. The irrigation season typically ends on July 10, Sept. 1 and Oct. 15 for grain, alfalfa and pasture, respectively.

Water sources (identified for each land parcel by the DWR 2000 land use survey and updated through landowner survey) include groundwater, surface water, subirrigated (shallow groundwater table, not actually irrigated), mixed groundwater–surface water, and nonirrigated (dryland farming). Land parcels are

distributed across nine subwatersheds associated with the major tributaries and the main stem Scott River. Discharge on these streams into the Scott Valley defines available maximum diversion rates for surface water irrigations. Where surface water is the only source of irrigation, lack of surface water will terminate the irrigation season. Groundwater pumping for a land parcel is from nearby or on-site irrigation wells. Well locations and type for the study area were obtained from DWR well permit records (fig. 2).

Hydrogeology

Within the alluvial groundwater basin of the Scott Valley, Mack (1958) distinguished six subareas (fig. 3). In our work, we also included the mine tailings at the southern end of the alluvial basin, an important hydrogeologic area consisting almost exclusively of reworked boulders from mine dredging operations (Foglia, McNally, Harter 2013).

Aquifer pumping tests were performed to determine hydraulic properties in the main subarea of the valley, along the Scott River corridor. The tests showed that even within hydrogeologic subareas, hydraulic property values vary greatly. Estimates of hydraulic property values were also obtained from literature available for the region (DWR 2000; Mack 1958; SSPA 2012). The ratio of vertical hydraulic conductivity to horizontal hydraulic conductivity was estimated to be 1:10, a relatively high value representing relatively strong vertical connectivity of the coarser sediments.

The aquifer receives recharge from excess rainfall and irrigation but also from streams entering the basin on highly permeable alluvial fans. Groundwater discharge generally occurs through groundwater-dependent wetlands and riparian vegetation, pumping (primarily for irrigation) and discharge to streams, mostly along the valley thalweg.

Modeling tools

We developed the Scott Valley Integrated Hydrologic Model (SVIHM) to (1) provide a tool that integrates a diverse set of data and information within a consistent physical, hydrological framework; (2) estimate water budget components and their seasonal and interannual dynamics in the groundwater, stream and landscape–soil system; (3) better understand the relationship between land use, irrigation, groundwater pumping and stream flow; (4) provide a tool to predict potential impacts on stream flow from future groundwater and surface water management scenarios; and (5) provide an educational and decision-making tool for local stakeholders, regulators and policy- and decision-makers engaged in developing solutions to support and protect groundwater-dependent salmon habitat in the Scott Valley watershed.

For the simulation, we considered the period from October 1991 through September 2011, a period that includes the transformation of the Scott Valley landscape from predominantly sprinkler to significant center-pivot irrigation, a series of wet periods (1996 to 1999, 2006) and dry periods (1991, 2001, 2007 to 2009) and a series of years with potentially higher temperature. We developed several distinct model elements, representing the 1991 to 2011 period of the different hydrologic system components at varying levels of complexity that meet the modeling objectives. These were linked together into the SVIHM:

The upper watershed was represented by a statistical regression model to simulate incoming stream flows in the Scott River and its tributaries from the upper watershed to the valley, which are also used for irrigation. The Scott Valley landscape overlying the groundwater basin was represented by a tipping-bucket-type soil water budget model (SWBM) that simulates daily and monthly landscape-related water fluxes at the land parcel scale (see description above), including irrigation from diversions of surface water inflows to the valley and by groundwater pumping, evapotranspiration and groundwater recharge. Valley groundwater and surface water were simulated using a numerical model capable of simulating groundwater flow dynamics and the groundwater–surface water interface at sufficient detail to guide future data collection and simulate future water management scenarios.

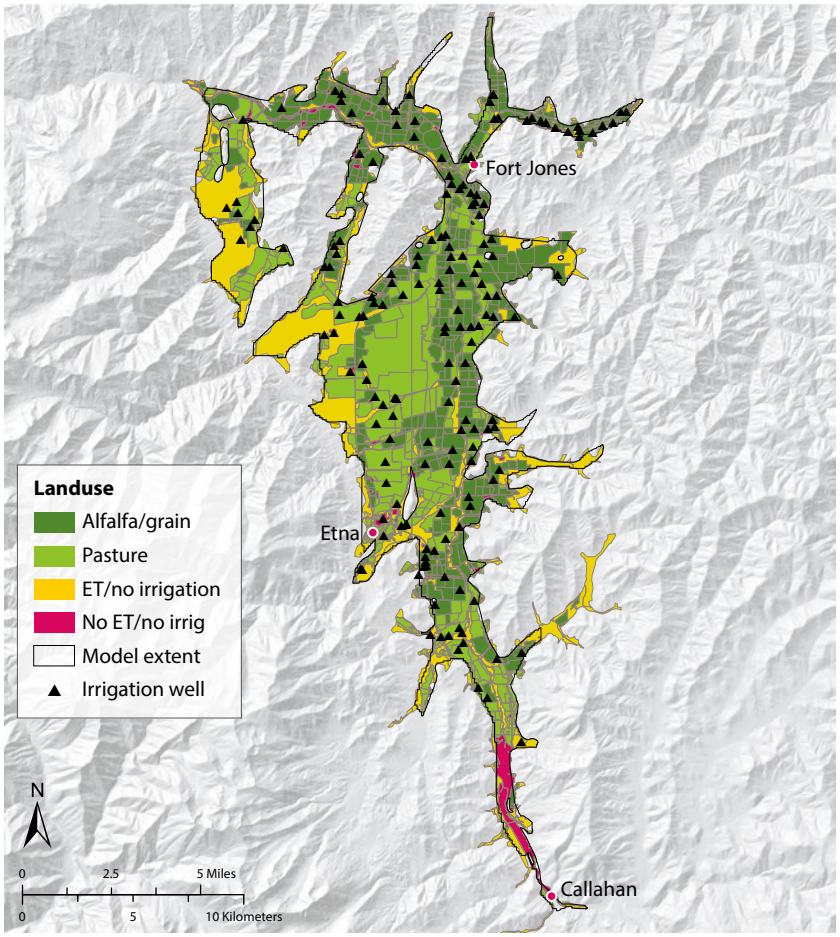

FIG. 2. Land use information and well locations in Scott Valley. ET/no irrigation reflects nonirrigated vegetation, e.g., lawns and riparian vegetation. No ET/no irrigation represents nonvegetated land surfaces including the mine tailings near Callahan. Well location information was obtained from well logs filed with the Department of Water Resources and verified in the field. Source: Model extent derived from Mack (1958) and SSURGO data. Land use polygon data source: DWR (2000). Revised to reflect 2011 land use patterns (GWAC, Groundwater Advisory Committee). Projection: North American Datum 1983, UTM Zone 10.

Upper watershed stream flows

Surface water inflows to Scott Valley from the upper watershed are an important source of irrigation water. During the summer, incoming low flows may limit or terminate surface water diversions for irrigation. This in turn affects groundwater pumping in some crop parcels equipped for dual irrigation (surface and groundwater). Quantitative estimates of surface water inflows are also an important input to simulation of stream flow dynamics (including tributaries) within the valley, where streams are in direct connection with groundwater (the groundwater–surface water interface).

Since only limited stream gauging data were available on inflowing streams, a stream flow regression model was developed (Foglia, McNally, Hall 2013). Several factors were considered in developing the regression model, including precipitation, precipitation history, snowpack, and stream flows at the valley outlet, where the USGS Ft. Jones gage has provided nearly continuous records since the early 1940s. Foglia, McNally, Hall (2013) showed that the latter was the most critical factor to predict available monthly total incoming stream flow measured near the valley margins.

Soil water budget model, SWBM

In California, no water rights permits are issued for groundwater pumping, and wells, including wells in the study area, are largely unmetered. The primary purpose of the soil water budget model (SWBM) was therefore to estimate spatially and temporally varying recharge and pumping across the groundwater basin. A second goal was to quantify crop evapotranspiration (crop ET) and irrigation water use from surface water and from groundwater, and to understand the role of soil water storage. Conceptually, the soil water budget model encompasses the managed and unmanaged landscape including its vegetation and soil root zone and also the managed components of the surface water system (diversions) and of the groundwater system (well pumping).

SWBM does not account for fluxes at the groundwater–stream interface (stream recharge, groundwater discharge to streams) or for evapotranspiration due to root water uptake directly from groundwater by nonirrigated crops or in natural landscapes with a shallow water table. These processes were instead accounted for by the groundwater–surface water models MODFLOW RIV or MODFLOW SFR.

SWBM provided daily estimates of groundwater pumping, groundwater recharge, and evapotranspiration from Oct. 1, 1991, to Sept. 30, 2011, for each of the 2,115 parcels delineated in the land use survey of Scott Valley. Storage routing and mass balance were calculated for each land parcel as

$$\theta_i = \max(0, \theta_{i-1} + Padj_i + AW_i + actualET_i - Recharge_i) \quad (1)$$

$$actualET_i = \min(ET_i, \theta_{i-1} + Padj_i + AW_i) \quad (2)$$

$$Recharge_i = \max(0, \theta_{i-1} + Padj_i + AW_i - actualET_i - WC4_i) \quad (3)$$

where θ_i is the water content at the end of day i; $Padj_i$ is the precipitation that infiltrates into the soil and is available for recharge or evapotranspiration on day i; AW_i is the applied water (irrigation) amount on day i; ET_i is the evapotranspiration on day i (computed as the product of the crop coefficient Kc and measured reference ET); $Recharge_i$ is deep percolation to the groundwater below the 1.22 meter (4 foot) deep root zone; and $WC4_i$ is the soil-dependent water holding capacity of the 1.22 meter (4 foot) root zone (Foglia, McNally, Harter 2013).

SWBM approximated growers' irrigation decisions in a simplified fashion: In the model, daily irrigation depths, AW_i, were controlled by crop evapotranspiration depth and effective precipitation, which in turn were computed from daily climate data, using appropriate crop coefficients:

$$AW_i = \frac{(actualET_i - Padj_i)}{\frac{AE}{100}}$$

where AE is the water application efficiency, which was assumed to be constant over the growing season. The AE values were based on published values (Canessa et al. 2011) adjusted for local conditions: 90% for center-pivot sprinkler, 75% for wheel-line sprinkler and 70% for flood irrigation. The model accounted for the strong relationship between crop evapotranspiration and irrigation, but it did not represent temporal details of the actual irrigation schedule or alfalfa cuttings, as these have negligible impact on variations in groundwater conditions. The model also did not account for delivery losses.

Within the alluvial groundwater basin of the Scott Valley, there are six subareas. In this work, the authors also included the mine tailings at the southern end of the alluvial basin, an important hydrogeologic area consisting almost exclusively of reworked boulders from mine dredging operations.

MODFLOW simulations

A water budget model accounts for water fluxes into and out of a groundwater basin, the associated landscape and streams, and it provides some insight into large-scale, regional groundwater–surface water interactions. But integrated groundwater–surface water computer models, such as the MODFLOW packages, are more useful to fully assess and understand groundwater–surface water dynamics that are also driven by human impacts (e.g., pumping).

We used the MODFLOW-2005 code to build the groundwater–surface water model element of SVIHM (Harbaugh 2005). MODFLOW-2005 is a computer-based groundwater–surface water model that simulates groundwater flows and surface water flows by representing the aquifer basin and overlying stream system through discretized blocks (much like the way pixels on a TV screen are a representation of a continuous image). Aquifer and stream properties were defined for each block, which allowed the model to not only take on the actual shape of a groundwater–surface water system but also to represent the internal variability in aquifer and streambed properties that best reflects that actual system.

At the core, the model code solved the equations governing groundwater flow and stream flow, one time step after another. The entire Scott Valley groundwater basin (fig. 1) was discretized into 50-meter-by-50-meter cells, and it was divided into two vertical layers to better capture vertical fluxes associated with groundwater–surface water interactions. Due to the basin geometry, the bottom layer is not laterally expanding as much as the top layer (see supporting information S1 online).

Figure 3 summarizes the boundary conditions used to develop the groundwater model. The model simulates groundwater–surface water interactions along the Scott River, along major tributary streams (Shackleford, Mill, Kidder, Oro Fino, Moffett, Patterson, Etna, Crystal, Johnson, Clark Miner's and French Creeks) and along two major irrigation ditches (Farmers Ditch Company and Scott Valley Irrigation District). These features were simulated using different combinations of the river, stream flow routing (SFR1) and drain (DRN) packages of MODFLOW.

In our study, we developed two versions of SVIHM to represent two levels of conceptual complexities in the simulation of the groundwater–surface water interface. Both used the same algorithm to determine groundwater–surface water exchanges based on water level differences between the stream and groundwater, and as a function of streambed hydraulic conductivity.

In SVIHM-RIV, using the MODFLOW RIV package (Harbaugh 2005), stream water levels were user assigned and might vary in time and space. The advantage of SVIHM-RIV is that it is computationally much less expensive (has a much lower simulation run time) than SVIHM-SFR, since it does not simulate the stream flow system. The computational efficiency is advantageous in model calibration. In Scott Valley, only sparse data were available on stream water levels. As an initial modeling design step, we chose a simple approximation of stream water levels using a constant, average stream depth uniform across the valley at all times.

In SVIHM-SFR, using the MODFLOW SFR package (Prudic et al. 2004), inflows from the upper watershed (obtained from the statistical model of watershed inflows), after irrigation diversions (obtained from SWBM), were physically routed by simulation through the valley's stream system. The simulation computed stream water level as a function of flow rate, stream slope, streambed morphology and stream roughness (Manning's equation). Detailed streambed morphology was available from two LIDAR surveys (SSPA 2012). With SFR, stream flow varied from stream cell to stream cell due to diversions, tributary inflows or groundwater–surface water exchanges. In this way, MODFLOW SFR tracked stream water depth variations in time and along the stream system. It could also estimate the timing and location of stream sections that fell dry.

The land parcel–based output results of SWBM — agricultural groundwater pumping, groundwater recharge and irrigation — were used as input to the MODFLOW RIV and MODFLOW SFR versions of

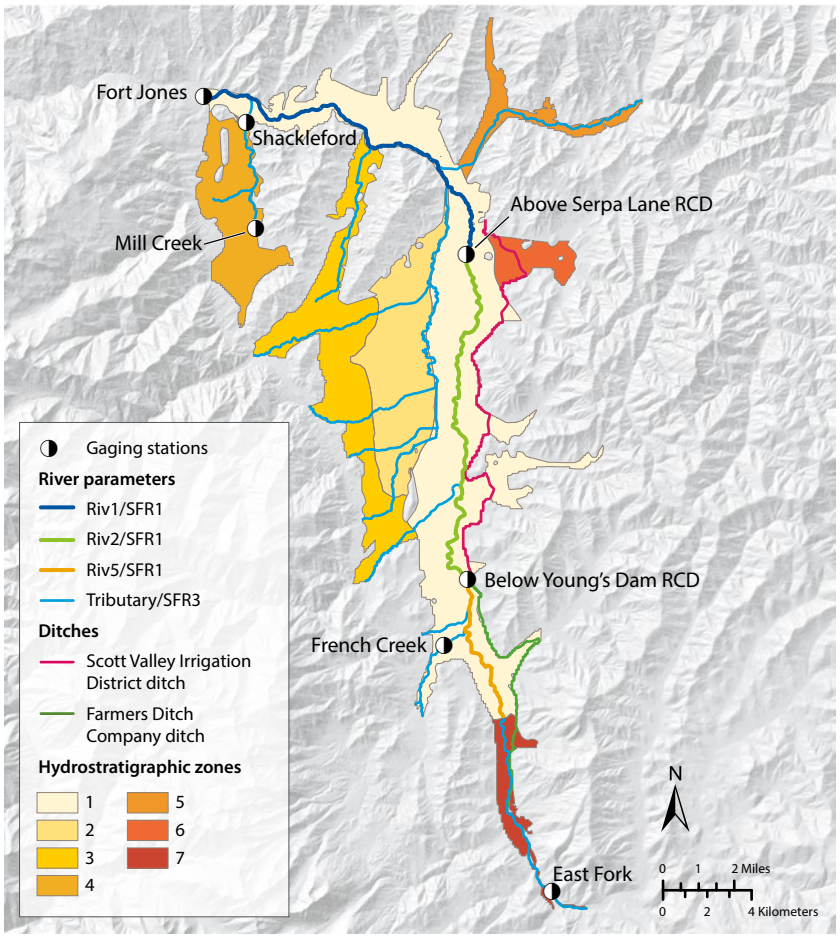

FIG. 3. Representation of the main characteristic of the modelled area, including boundary conditions, hydraulic conductivity and specific storage as defined by hydrostratigraphic zone, irrigation ditches, stream flow gaging stations and river segments (represented as Riv1, Riv2 and Riv5). Source: Model extent derived from Mack (1958) and Soil Survey Geographic Database (SSURGO) data. Projection: North American Datum 1983, UTM Zone 10.

SVIHM, which simulated the 21-year period using monthly variable boundary conditions (monthly stress periods). Recharge was applied to the top of the highest active cell in the model using the recharge (RCH) package. Evapotranspiration rates were calculated using SWBM for irrigated and for nonirrigated vegetated areas. In addition, in vegetated areas where irrigation water was not applied, additional evapotranspiration from shallow groundwater was calculated within MODFLOW using the evapotranspiration segments (ETS) package (Banta 2000).

Groundwater pumping rates for individual land parcels were assigned to the nearest irrigation well. The sum of groundwater pumping assigned in a given month to a well by SWBM was the input for the MODFLOW well (WEL) package. Surface water irrigations estimated by SWBM were subtracted from the incoming tributary stream flows prior to routing surface water through Scott Valley with MODFLOW. Hydraulic parameters and other relatively uncertain components of the conceptual model were separately evaluated with the numerical model using sensitivity analysis and calibration (Tolley et al., unpublished data).

For SVIHM-RIV, groundwater level measurements across the valley and the net gain or loss in stream flow for three stream reaches along the Scott River were used as calibration targets. For SVIHM-SFR, the same valleywide groundwater level measurements have been included, but flow discharges were calibrated against the time series in the four locations used in the SVIHM-RIV and in the Fort Jones station gaging station, since SVIHM-SFR tracks stream gains and losses for computing stream flows.

Soil water budget calibrated collaboratively

The results of the initial version of SWBM (Foglia, McNally, Harter 2013) were vetted with the Scott Valley Groundwater Advisory Committee, local growers and the UC Cooperative Extension (UCCE) farm advisor. The initial SWBM estimated an average applied irrigation on (mostly sprinkler-) irrigated alfalfa of about 33 inches per year. However, landowners in the valley reported irrigation equipment to be set up for only about 20 to 24 inches per year.

To understand the origin of the discrepancy between simulated and grower-reported irrigation depths, a manual sensitivity analysis was performed with SWBM. SWBM was implemented with varying parameter combinations to quantify the effect these parameters had on water budget results.

To account for the possibility of deficit irrigation and deep soil moisture depletion during the irrigation season, the irrigation model in SWBM (Foglia, McNally, Harter 2013) was modified: Under deficit irrigation, application efficiency is assumed to be 100%, evapotranspiration is assumed to be met by precipitation and applied water but also by soil moisture depletion, where applied water demand is computed from

$$AW_i = \frac{(actualET_i - Padj_i)}{1 + \frac{SMDF}{100}}$$

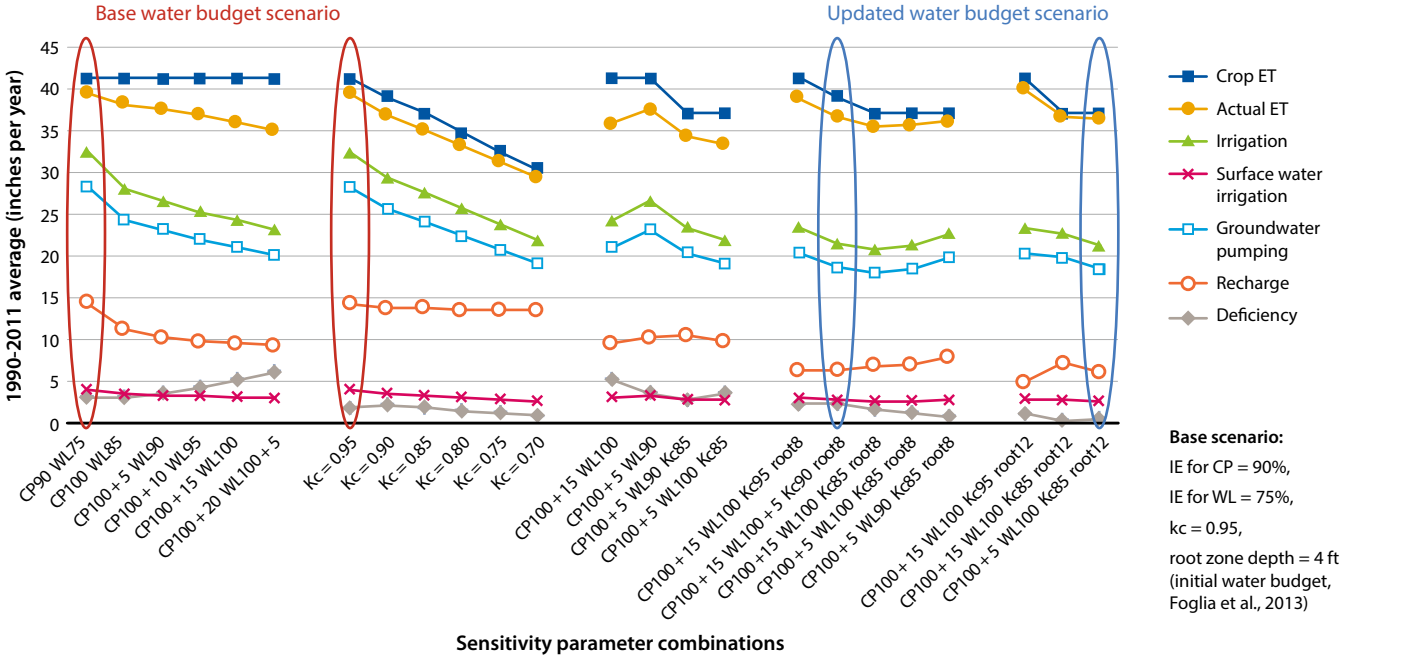

FIG. 4. Sensitivity of the simulated soil water fluxes to application efficiency, soil moisture depletion, root zone depth, and crop evapotranspiration (represented as crop coefficient Kc). For the soil water budget model sensitivity analysis, we adjusted root zone depth, from 4 feet (base value) to 8 feet (root8) and 12 feet (root12); alfalfa crop coefficient, from 0.95 (base value, Kc95) to 0.7; application efficiency for center-pivot from 90% (base value, CP90) to 100% + 20% SMDF (CP100 + 20), and for wheel-line from 75% (base value, WL75) to 100% + 5% SMDF (WL100 + 5); and (for deficit irrigation) the soil moisture depletion fraction (SMDF).

and *SMDF* is the soil moisture depletion fraction, defined as the ratio of soil moisture depletion to applied water during the irrigation season:

$$SMDF = \frac{\Sigma(\textit{soil moisture depletion}) \textit{ during the irrigation season}}{\Sigma(AW) \textit{ during the irrigation season}} \times 100\%$$

For the sensitivity analysis, root zone depth, alfalfa crop coefficient (Kc), application efficiency and (for deficit irrigation) SMDF were adjusted (fig. 4).

The scenarios offered several combinations of these parameters that resulted in irrigation amounts of 24 inches or less: Reducing the Kc value led to lower irrigation needs but conflicted with previously measured Kc values (0.95). Increasing application efficiency, increasing the soil moisture depletion fraction for deficit irrigation and increasing root zone depth all led to significant reductions in simulated irrigation without significantly affecting simulated evapotranspiration. It remained unclear which parameter option to choose.

A 3-year field research project was launched in cooperation with local growers to measure evapotranspiration, irrigation water applications and deep soil moisture profiles in eight alfalfa fields distributed across representative locations in Scott Valley. The study established a new, slightly lower Kc value of 0.9. For alfalfa, the soil water profile from 5 feet to 8 feet was found to generally decline in soil water content throughout the irrigation season. Thus, alfalfa was found to be effectively deficit irrigated, that is, the application efficiency was 100%. Experimental results better constrained input choices in SWBM. Using an 8-foot root zone for alfalfa, the new Kc = 0.9 value and soil moisture depletion fractions of 5% for wheel-line irrigation and 15% for center-pivot irrigation (on both alfalfa and grain), the total annual simulated irrigation depth on alfalfa, computed by the adjusted SWBM, averaged 22 inches per year instead of 33 inches per year, corresponding with measured irrigation rates (blue oval in fig. 4).

Aggregated water budget results from this calibrated SWBM provided some important insights into understanding the groundwater–surface water interface dynamics (table 1): The total amount of groundwater pumping (an output from the groundwater account) was equal to about two-thirds of the estimated total landscape recharge (an input to the groundwater account). Since long-term groundwater levels were balanced, the surplus in recharge relative to pumping, 14,000 acre-feet per year, was the net contribution of the landscape to base flow, that is, to the groundwater discharge to the Scott River.

A small portion of the 14,000 acre-feet per year may also contribute to evapotranspiration from groundwater (e.g., riparian vegetation). Note that actual net groundwater discharge to the Scott River is higher, as SWBM does not account for about 44,000 acre-feet per year of mountain-front recharge from tributaries and leakage to groundwater from irrigation ditches (a result obtained from the groundwater–surface water modeling, below). The total amount of net groundwater discharge to streams is only about one-tenth of the much larger Scott River total annual flow, most of which originates from the upper watershed. However, during the low flow period (July/August through September/October) the Scott River outflow from the basin is mostly groundwater dependent, particularly in dry years. Over that period, total stream outflow from the

TABLE 1. Aggregated average annual water budget model results over the 21-year simulation period by land use

	Crop ET*	Actual ET†	Irrigation‡	SW irrigation	GW pumping	Recharge	Area
	Inches per year						*Acres*
Alfalfa	39.2	36.8	21.5	2.8	18.7	6.3	13,893
Grain	16.1	16.1	10.3	1.6	8.7	10.6	1,985
Pasture	38.2	34.8	26.0	20.5	5.5	11.6	11,909
ET/no irrigation	14.0	11.0	0.0	0.0	0.0	10.8	20,383
No ET/no irrigation	0.0	0.0	0.0	0.0	0.0	21.6	1,695
	Acre-feet per year						*Acres*
Alfalfa	45,384	42,065	24,871	3,207	21,665	7,294	13,893
Grain	2,663	2,663	1,707	263	1,444	1,753	1,985
Pasture	37,910	34,536	25,791	20,351	5,440	11,512	11,909
ET/no irrigation	23,780	18,684	—	—	—	18,345	20,383
No ET/no irrigation	—	—	—	—	—	3,051	1,695

Note: All calculations assume that the water table is below the root zone.

* Annual evapotranspiration rate if optimal irrigation was applied year-round.

† May be less than crop evapotranspiration due to discontinued irrigation in late summer (lack of surface water) or fall (no irrigation is typically applied after August).

‡ Includes irrigation with surface water and irrigation with groundwater.

SW = surface water, GW = groundwater.

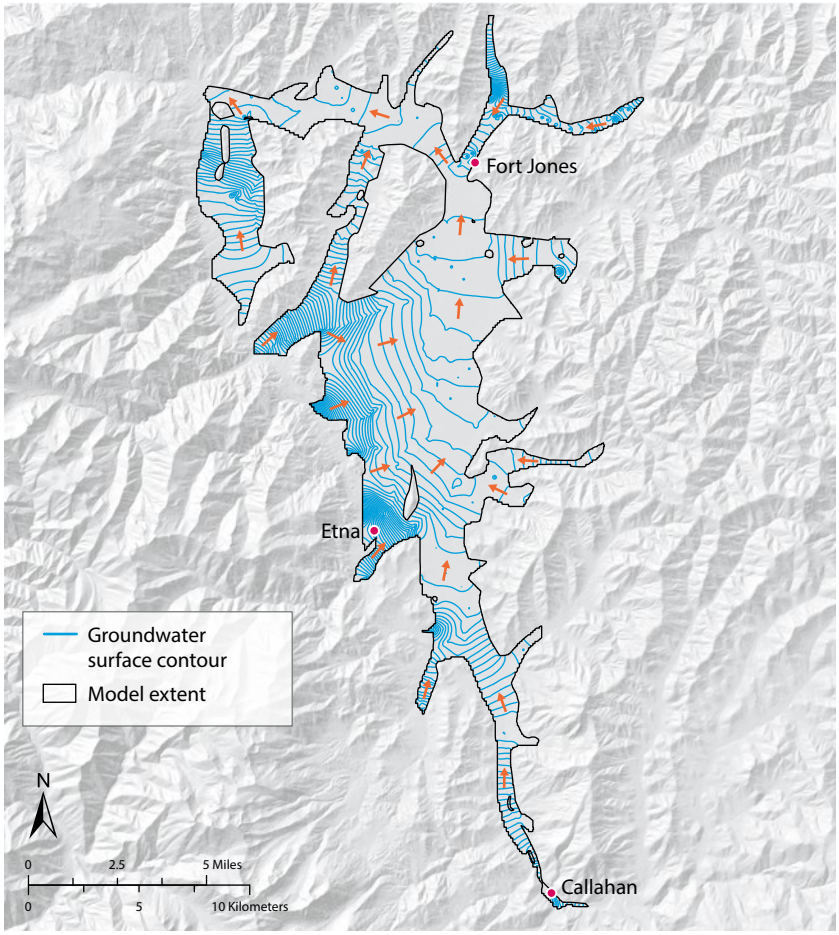

FIG. 5. Groundwater levels and flow direction in August 2001. This is one of the results from the groundwater–surface water model. Other output from the groundwater–surface water model included monthly water levels, groundwater flow directions and amounts, and groundwater–surface water exchanges for water years 1991 to 2011. Arrows indicate the flow direction but are not scaled to groundwater flow velocity. See supporting information S1 for comparison of simulated water levels and flow rates to measured water levels and flow rates. Source: Model extent derived from Mack (1958) and SSURGO data. Projection: North American Datum 1983, UTM Zone 10.

During the low flow period (July/August through September/October) the Scott River outflow from the basin is mostly groundwater dependent, particularly in dry years.

valley may amount to less than 10,000 acre-feet, and in exceptionally dry years (e.g., 2001, 2014, 2015) to less than 2,000 acre-feet. Relative to these flows, landscape recharge contribution to base flow was significant.

SWBM did not account for recharge contributions to groundwater from streams or for the dynamics of groundwater discharge to streams. SWBM also did not provide insight in how those may be affected by groundwater pumping and recharge or by intentional groundwater storage in the basin (a potential future project). For these additional analyses, SWBM must be coupled to a more complex groundwater–surface water model.

Importantly, SWBM was an important tool for outreach and education. That outreach led to initiation of the new field research, results from which improved model development. Refinement of SWBM was made possible through regular interactions between local stakeholders and growers on the groundwater advisory committee, the local UCCE farm advisor, the modeling team and the new field research. The collaboration on the SWBM increased the community's trust of the groundwater–surface water (MODFLOW) model component of SVIHM. (SWBM drives the pumping and recharge condition in the MODFLOW component, which in turn drives the dynamics at the groundwater–surface water interface.)

Water fluxes: RIV versus SFR representations

The groundwater–surface water model component of SVIHM, represented using both the RIV and SFR packages, simulated 21 years of groundwater and stream flow dynamics driven by monthly data of the statistically simulated stream inflows at each tributary from the upper watershed, by pumping in nearly 200 wells and by recharge from over 2,000 land parcels. Output included monthly water levels, groundwater flow directions and amounts, and groundwater–surface water exchanges at the 50-meter scale throughout Scott Valley for water years 1991 to 2011 (fig. 5).

Sensitivity analysis and calibration of the numerical MODFLOW-based groundwater–surface water simulation model were completed to assess model performances and to fine-tune model parameters (supporting information S1 and Tolley et al., unpublished data). These steps were taken to ensure that SVIHM's input and structure yielded simulation results that were consistent with 1991 to 2011 measured water level and long-term stream gauging information on the Scott River.

Groundwater budgets, including groundwater–surface water fluxes, will be one of the critical components evaluated and discussed by groundwater sustainability agencies. It's important to understand how to read the groundwater budget outputs from the conceptually very different RIV and SFR models and how the difference in the model can affect predictions of future scenarios.

SVIHM-RIV and SVIHM-SFR fundamentally differ in the representation of the elevation of the stream's water surface (stream state) — one user defined, one based on a streamflow model. In all other aspects, they are identical. The RIV representation, which lets the user specify stream stage (water level elevation) at each river cell, is an excellent option where water depth in the stream does not vary significantly in time or measurements are available about changes in stream stage at high spatial resolution and where these are not impacted or impacted in known ways under future scenarios of interest. Our very simplified RIV representation (constant, uniform stream water depth) was developed as a simplified conceptual approach to generate a first-order approximation of the groundwater–surface water interface, and we had no stream depth data.

In contrast, in the SFR representation, stream stage is simulated by a stream flow routing model that internally computes stream water levels while preserving water balance within the stream system dynamically. Stream stage at each grid cell is a function of stream flow into the cell, of physical characteristics of the stream available from detailed surveys and of groundwater–surface water fluxes at each grid cell. The SFR representation also accounts for the confluence of streams and for diversions to surface water users, which in turn affect local stream flow rates. When flow is insufficient to support stream flow, the streambed falls dry until either upstream inflow becomes available or groundwater begins to emerge into the streambed due to a higher water table. Given data available for Scott Valley and the dynamics of its stream system, MODFLOW SFR provided a physically more accurate, if computationally more expensive, model representation.

Aquifer water budgets for both the irrigation season (summer) and the nonirrigation season (winter) (fig. 6) showed that exchange of water between surface water and groundwater was about three times larger in SVIHM-RIV than SVIMH-SFR. All other boundary fluxes were identical due to both models having otherwise identical boundary conditions. In figure 6, the exchange between surface water and groundwater is represented in green and labeled "Stream". For all the terms in figure 6, the flow "in" represents the amount of water entering into the aquifer from various sources, while the flow "out" is the flow leaving the aquifer.

The difference between stream recharge (input to the water budget) and groundwater discharge (output from the budget), however, is the same in both models — a net groundwater discharge to the stream of 80 cfs (58,000 acre-feet per year), when averaged over the entire year. This is not coincidental: The net groundwater discharge of 58,000 acre-feet per year is independent from the groundwater–stream connectivity. It is instead entirely driven by the average annual difference between mountain-front recharge (determined by the upper watershed model), ditch losses to groundwater (user input based on measured data) and landscape recharge (SWBM result) on the one hand and groundwater pumping (SWBM result) and evapotranspiration losses from groundwater (MODFLOW result) on the other hand, none of which is a function of the choice of RIV or SFR package. The exception was the MODFLOW simulated evapotranspiration losses from groundwater near streams, which may be affected by the model choice (RIV or SFR).

With SVIHM-SFR, net groundwater discharge (fig. 6, difference between the Stream "in" and the Stream "out") was only slightly smaller over the summer months than over the winter months (about 60 cfs in both seasons). In contrast, with SVIHM-RIV, the net discharge to streams was about 50 cfs in summer but almost 140 cfs in winter. This large seasonal variation was driven by seasonal variations in groundwater storage that operate differently in the SVIHM-RIV model than in the SVIHM-SFR model: Groundwater storage during winter increased in SVIHM-RIV by just 40 cfs, or 15,000 acre-feet per 6 months, half the increase in SVIHM-SFR (80 cfs, or 29,000 acre-feet per 6 months), due to the larger winter net groundwater-to-stream discharge in SVIHM-RIV. By the same token, groundwater storage during summer decreased in SVIHM-RIV by just half of that in SVIHM-SFR due to the much lower net groundwater-to-stream discharge in SVIHM-RIV in summer.

The difference between the simulated fluxes was caused by differences in the stream stage between SVIHM-RIV and SVIHM-SFR. The SVIHM-SFR model relied on measured and estimated stream flow entering the valley, which in turn drove the local and seasonal dynamics of stream stage and the magnitude of groundwater–surface water interaction. Inflows to the valley are highly dynamic and vary strongly between winter and summer. The SVIHM-RIV model with its uniform, constant stream water depth that we chose did not sufficiently capture the spatial and temporal changes in stream flow dynamics. In this simplified representation, the stream became an artificial buffer to groundwater level changes. SVIHM-RIV added recharge from streams during the low flow periods when no exchange occurred in SVIHM-SFR simulations.

When using SVIHM-RIV, it would therefore be important that dry stream sections are properly characterized a priori for simulating future management projects. Also, even in flowing sections of the stream, characterization could be improved by providing

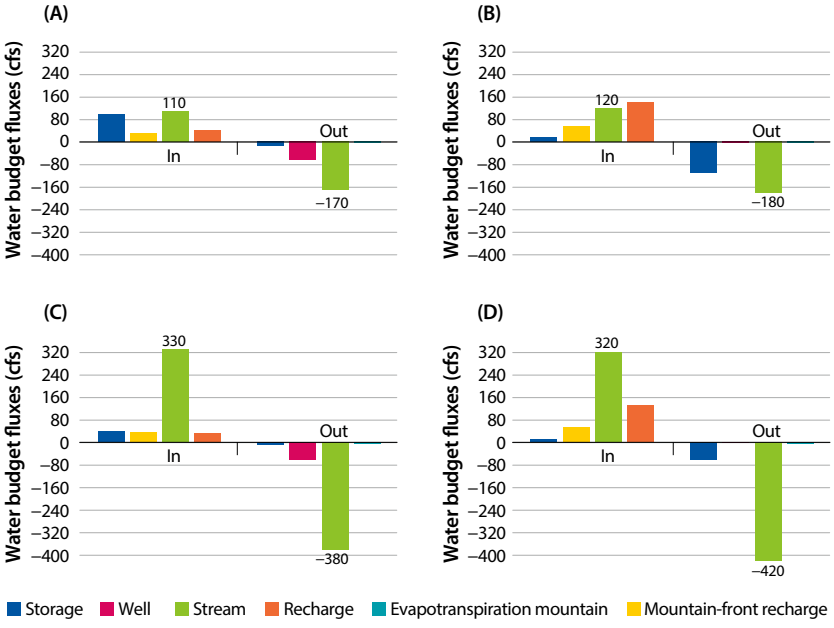

FIG. 6. Water budget results for various seasons and stream models. Markedly different groundwater–surface water fluxes were evident in the results of SFR and RIV models: (A) SFR during summer (the irrigation season, April to Sept), (B) SFR during winter (the nonirrigation season, October to March), (C) RIV during summer and (D) RIV during winter.

Scott Valley Irrigation District diversion and fish ladder. The river and its tributaries are an important salmonid spawning habitat, home to native populations of the threatened *Oncorhynchus kisutch* (coho).

spatially more detailed, seasonally varying water level depth within the stream network as part of the RIV representation. In Scott Valley, however, one of the future scenario modeling goals for which the model will be used is to predict the change in the timing and extent of dry stream sections in response to groundwater management actions. For that purpose, only the SVIHM-SFR approach can be used.

Our Scott Valley study suggests that knowledge of stream stage at high spatial and temporal detail is critical when representing the groundwater–surface water boundary with a RIV approach. More detailed calibration that has been carried out for the SVIHM-SFR model (Tolley et al., unpublished data) demonstrated that the presence of river reaches that become dry during a certain time in the summer was a critical observation to calibrate or validate SVIHM-SFR.

Models for SGMA implementation

Under California's new groundwater governance, groundwater sustainability agencies across the state have to consider the potential impact of new groundwater management measures on groundwater–surface water interaction and specifically on estimating the effect of groundwater management on surface water depletion. Only a groundwater model that also has some representation of streams can provide the spatially and temporally more detailed information on groundwater–surface water exchange that may be required when evaluating individual groundwater management projects and their impacts to stream flow.

As shown in our Scott Valley study, the choice of stream representation will depend on availability of data, data density in space, and data continuity in time for stream flow and stream stage. Depending on implementation, significantly different results may be obtained. The value of the model outcome will increase with better physical representation of the integrated hydrologic system, which in turn is driven by good data availability.

Integrated numerical modeling tools represent and link upper watersheds, the basin soil–landscape systems, the groundwater system and the basin surface water system. These tools will be useful to evaluate groundwater conditions (in SGMA referred to as sustainability indicators) and the benefits of management actions to address undesirable results. Some of these conditions, such as depletion of surface water by groundwater pumping, are otherwise difficult to measure from field data alone.

For the broader audience among groundwater agency stakeholder groups, the important take-away from our work is that numerical groundwater modeling tools are all based on the same mathematical representation of groundwater flow. But other elements of the hydrologic cycle to which a groundwater model must inevitably be linked — for example, the soil–landscape system, including the ways in which urban and agricultural water demands operate; the stream system; and the upper watershed system — are subject to more varied model representations. This variability affects the simulation of groundwater–surface water interface, pumping, recharge from various sources, and flows of surface water and groundwater at the basin boundaries.

Irrigation well in Scott Valley.

As we demonstrated, an integrated model is not only a platform for a unifying, scientifically defensible framework to connect spatially and temporally distributed data of many different kinds and to represent a range of groundwater (and surface water) sustainability indicators. It is also a tool to explore conceptual uncertainties and initiate additional research and data collection to improve representation of the driving elements of groundwater–surface water interactions and other drivers of groundwater dynamics. The integration of various model components also (1) allows representation of fluxes within the basin and between different basins, (2) allows evaluation of the sensitivity of the integrated model to different parameters and observations, (3) facilitates an estimate of the uncertainty in the results (Tolley et al., unpublished data) and (4) supports the design of future management scenarios (not yet implemented here).

Our Scott Valley study shows that models of various complexity (regression model, mass balance model, and numerical dynamic model) can be successfully integrated and provide a useful interface to communicate with and successfully engage stakeholders in developing groundwater sustainability plans. Our results demonstrate the importance for stakeholders to fully understand the conceptual implications of the different assumptions of model development and how these can impact water budgets and management of fluxes between basins. This understanding is fundamental for the successful development of groundwater sustainability plans as required by SGMA. CA

L. Foglia is Assistant Adjunct Professor, University of California Davis; J. Neumann is at Technical University Darmstadt, Germany; D.G. Tolley is Ph.D. Candidate, University of California Davis; S. Orloff was County Director and Farm Advisor, UCCE Siskiyou County; R.L. Snyder is UC Cooperative Extension Biometeorology Specialist in the Department of Land, Air and Water Resources at University of California Davis; and T. Harter is Professor, University of California Davis.

In memory of our co-author Steve Orloff and his many contributions to this work.

Funding for our research was provided by the California State Water Resources Control Board contracts 11-189-110 and 14-020-110. We would like to thank the Scott Valley Groundwater Advisory Committee, Sari Sommarstrom, and Bryan McFadin for many helpful discussions during the development of our modeling tools.

California Agriculture *thanks Guest Associate Editor Hoori Ajami for her work on this article.*

References

Ashby SF, Falgout RD. 1996. A parallel multigrid preconditioned conjugate gradient algorithm for groundwater flow simulations. Nucl Sci Eng 124:145–59. (Also available as LLNL Technical Report UCRL-JC-122359.)

Banta ER. 2000. MODFLOW-2000, the U.S. Geological Survey Modular Ground-Water Model - Documentation of Packages for Simulating Evapotranspiration with a Segmented Function (ETS1) and Drains with Return Flow (DRT1). U.S. Geological Survey Open-File Report 00-466. 127 p.

Boulton AJ, Hancock PJ. 2006. Rivers as groundwater-dependent ecosystems: A review of degrees of dependency, riverine processes and management implications, Aust J Bot 54:133–44.

Brown LR, Moyle PB, Yoshiyama RM. 1994. Historical decline and current status of Coho salmon (*Oncorhynchus kisutch*) in California. N Am J Fisheries Manage 14(2):237–61. doi:10.1577/1548-8675(1994)014<0237

Brunner P, Simmons CT. 2012. HydroGeoSphere: A fully integrated, physically based hydrological model. Ground Water 50:170–6. doi:10.1111/j.1745-6584.2011.00882.x

Canessa P, Green S, Zoldoske D. 2011. Agricultural Water Use in California: A 2011 Update. Staff Report, Center for Irrigation Technology, California State University, Fresno, CA. 80 p. www.waterboards.ca.gov/waterrights/water_issues/programs/hearings/cachuma/exbhts_2012feir/cachuma_feir_mu289.pdf

Drake D, Tate K, Carlson H. 2000. Analysis shows climate-caused decreases in Scott River fall flows. Calif Agr 54(6):46–9. https://doi.org/10.3733/ca.v054n06p46

[DWR] California Department of Water Resources. 2000. Siskiyou County Land Use Survey 2000, Division of Planning and Local Assistance. www.water.ca.gov/landwateruse/lusrvymain.cfm

Foglia L, McNally A, Hall C, et al. 2013. Scott Valley Integrated Hydrologic Model: Data Collection, Analysis, and Water Budget, Final Report, April 2013. UC Davis. http://groundwater.ucdavis.edu. 101 p.

Foglia L, McNally A, Harter T. 2013. Coupling a spatiotemporally distributed soil water budget with stream-depletion functions to inform stakeholder-driven management of groundwater-dependent ecosystems. Water Resour Res 49:7292–310. doi:10.1002/wrcr.20555

Furman A. 2008. Modeling coupled surface–subsurface flow processes: A review. Vadose Zone J 7(2):741. doi:10.2136/vzj2007.0065

Harbaugh AW. 2005. *MODFLOW-2005, The US Geological Survey Modular Ground-Water Model — the Ground-Water Flow Process*. US Geological Survey Techniques and Methods. 253 p.

Harbaugh A, Banta E, Hill M, McDonald M. 2000. *MODFLOW-2000, The US Geological Survey Modular Ground-Water Model – Users Guide to Modularization Concepts and the Ground-Water Flow Process*. US Geological Survey Open-File Report 00-92.

Harter T. 2015. California's agricultural regions gear up to actively manage groundwater use and protection. Calif Agr 69(3):193–201. https://doi.org/10.3733/ca.E.v069n03p193

Harter T, Morel-Seytoux H. 2013. *Peer Review of the IWFM, MODFLOW and HGS Model Codes: Potential for Water Management Applications in California's Central Valley and Other Irrigated Groundwater Basins*. California Water and Environmental Modeling Forum, Sacramento, August 2013. 121 p.

Hatton TJ. 1998. *The Basics of Recharge and Discharge, Part 4: Catchment Scale Recharge Modeling*. CSIRO: Commonwealth Scientific and Industrial Research Organization, Collingwood, Victoria, Australia.

Kim JS, Jain S. 2010. High-resolution streamflow trend analysis applicable to annual decision calendars: A western United States case study. Climatic Change 102(3):699–707. doi:10.1007/s10584-010-9933-3

Kollet SJ, Maxwell RM. 2006. Integrated surface-groundwater flow modeling: A free-surface overland flow boundary condition in a parallel groundwater flow model. Adv Water Res 29:945–58.

Mack S. 1958. Geology and Ground-Water Features of Scott Valley Siskiyou County, California. US Geological Survey Water-Supply Paper 1462. Washington DC.

Moyle PB, Israel JA. 2005. Untested assumptions: Effectiveness of screening diversions for conservation of fish populations. Fisheries 30(5):20–8. doi:10.1577/1548-8446(2005)30[20:UA]2.0.CO;2

NCRWQCB. 2005. Staff Report for the Action Plan for the Scott River Watershed Sediment and Temperature Total Maximum Daily Loads. www.waterboards.ca.gov/water_issues/programs/tmdl/records/region_1/2010/ref3872.pdf

Nehlsen W, Williams JE, Lichatowich JA. 1991. Pacific salmon at the crossroads: Stocks at risk from California, Oregon, Idaho, and Washington. Fisheries 16(2):4–21. doi:10.1577/1548-8446(1991)016<0004:PSATCS>2.0.CO;2

Niswonger RG, Prudic DE. 2005. Documentation of the Streamflow-Routing (SFR2) Package to Include Unsaturated Flow beneath Streams—A modification to SFR1. US Geological Survey Techniques and Methods 6-A13. 50 p.

Prudic DE, Konikow LF, Banta ER. 2004. A New Stream-Flow Routing (SFR1) Package to Simulate Stream-Aquifer Interaction with MODFLOW-2000. US Geological Survey Open-File Report 2004-1042. 95 p.

[SSPA] SS Papadopulos & Associates. 2012. Groundwater Conditions in Scott Valley. Report prepared for the Karuk Tribe, March 2012.

Zume JT, Tarhule AA. 2011. Modeling the response of an alluvial aquifer to anthropogenic and recharge stresses in the United States Southern Great Plains. J Earth Syst Sci 120(4):557–72.

Water Resources Research

RESEARCH ARTICLE
10.1029/2018WR024209

Key Points:
- Multiple sensitivity analyses varying initial parameters provide a frugal method to account for nonlinearity of integrated hydrologic models
- Calibration results from integrated hydrologic models of irrigated landscapes may be sensitive to parameters of the crop water demand system
- Weakly coupled integrated models are a viable and efficient approach for reproducing observed groundwater-surface water interactions

Supporting Information:
- Figure S1

Correspondence to:
T. Harter,
thharter@ucdavis.edu

Citation:
Tolley D., Foglia, L., & Harter, T. (2019). Sensitivity analysis and calibration of an integrated hydrologic model in an irrigated agricultural basin with a groundwater-dependent ecosystem. *Water Resources Research*, *55*. https://doi.org/10.1029/2018WR024209

Received 2 OCT 2018
Accepted 19 JUN 2019
Accepted article online 27 JUN 2019

Sensitivity Analysis and Calibration of an Integrated Hydrologic Model in an Irrigated Agricultural Basin With a Groundwater-Dependent Ecosystem

D. Tolley[1], **L. Foglia**[1], **and T. Harter**[1]

[1]Department of Land, Air, and Water Resources, University of California, Davis, CA, USA

Abstract While sensitivity analysis and calibration are common practice in integrated hydrologic modeling, little work has been done to understand how the design of the sensitivity analysis and calibration affects the simulation outcome in these often highly nonlinear models. This is especially true for irrigated agricultural basins with a strong connection between land use, groundwater, and surface water. Using a range rather than a single set of initial parameter values, multiple sensitivity analyses, calibrations, and linearity tests were performed using UCODE_2014 on the Scott Valley Integrated Hydrologic Model. Calibration results show that parameters related to crop demand and applied irrigation water are most sensitive. Influence statistics show that low streamflow observations provide the most information during model calibration, indicating preference should be given to these observations during model development, sensitivity analysis, and calibration. Importantly, due to the nonlinearity of the integrated model, significant differences are found in results when initial parameter values are sampled from within their respective expected ranges. Estimates for some parameters varied up to an order of magnitude between calibrations, while all produced similar final objective function values, groundwater elevations, and stream flow. Confidence intervals for individual sensitivity analyses and calibration runs only spanned a fraction of the ensemble estimated parameter range across multiple runs. Our work suggests that a calibration design with multiple sensitivity analyses and calibrations of integrated hydrologic models, each using one of several widely varying sets of initial values, provides a frugal approach to identify parameters across the global parameter space.

1. Introduction

Groundwater and surface water resources are increasingly being stressed due to changes in population, land use, management practices, and climate (Van Roosmalen et al., 2009; Hanson et al., 2012; Taylor et al., 2012; Kløve et al., 2014; Dettinger et al., 2015). In order to gain insight and understanding of system behavior and complex feedbacks inherent between groundwater, the landscape, and surface water, numerical models that approximate physical flow processes are typically used. Although interactions between groundwater and surface water and between groundwater and the irrigated landscape have been known since the inception of numerical modeling, these systems have traditionally been handled separately with little to no connection between them. This was primarily due to computational limitations and different response times and spatial scales between surface and subsurface routed water (Prudic, 1989; Brunner et al., 2010; Unland et al., 2013; Singh, 2014).

A variety of models have been developed in the last two decades that simulate the flux of water between the surface and subsurface to varying degrees. These include (1) analytical or spreadsheet models (S. S. Papadopulos and Associates, Inc, 2000; Manghi et al., 2012; Foglia, McNally, & Harter, 2013; Lane et al., 2015), (2) iteratively coupled models like the Integrated Water Flow Model (IWFM; California Department of Water Resources, 2016a, 2016b), MODFLOW (Harbaugh, 2005) with the stream package (STR; Prudic, 1989), streamflow routing (SFR) package (Prudic et al., 2004), and/or farm process package (FMP2; Schmid et al., 2000; Schmid & Hanson, 2005), MODFLOW One-Water Hydrologic Model (MF-OWHM; Hanson, Boyce, et al., 2014), and GSFLOW (Markstrom et al., 2008), and (3) fully coupled models such as ParFlow (Ashby & Falgout, 1996; Kollet & Maxwell, 2006) and Hydrogeosphere (Therrien & Sudicky, 1996; Brunner & Simmons, 2012). Iteratively coupled models solve multiple systems of equations (e.g., saturated flow, unsaturated flow, and surface flow) at each time step and iteratively pass fluxes between these systems until

convergence is achieved. Fully coupled models assemble the entire system into a single system of equations. This is computationally much more expensive and generally requires a greater degree of parameterization than simpler iteratively coupled models. Superiority of full coupling over iterative coupling is largely application dependent, since full coupling may lead to numerical difficulties resulting from the different nature of the equations used to describe flow (Furman, 2008). Effective water management requires an accurate but also efficient method to represent the hydrologic system with sufficient detail, including appropriate coupling of subsystems, to answer specific questions, yet simple enough to reflect data availability, economic cost, and serve stakeholder needs (La Vigna et al., 2016).

In areas with Mediterranean climate (wet winters and dry summers) and dominated by irrigated agriculture, the connection between groundwater and surface water is highly pronounced due to significant alteration and seasonality of the water resources availability and use in the landscape. Application of surface water for irrigation generally increases groundwater recharge in the spring and early summer (Roark & Healy, 1998; McMahon et al., 2003). Groundwater pumping for irrigation and urban water use can result in streamflow depletion (Chen & Yin, 2001; Barlow & Leake, 2012) and adversely impact groundwater-dependent ecosystems by decreasing flows and increasing temperatures in critical fish habitat (Stark et al., 1994).

Rates of groundwater extraction and recharge in irrigated agricultural areas often lack historic data and are not commonly measured even though they are significant portions of a basin's water budget (Ruud et al., 2004; Yin et al., 2011). Where metering data are not available, groundwater pumping is usually estimated as the difference between crop water demands and applied surface water and precipitation (Ramireddygari et al., 2000; Pokhrel et al., 2015; California Department of Water Resources, 2016a). Groundwater recharge is estimated by closure of the water balance and may include consideration of vadose zone flux constraints (Ruud et al., 2004; De Silva & Rushton, 2007). These estimates are sometimes made a priori and used as boundary conditions for numerical groundwater-surface-water models. Some integrated hydrologic models allow for a dynamic calculation of groundwater pumping for irrigation and recharge, as they include an iterative coupling between a crop water demand model and a hydrologic model within a time step. This is available in software such as MODFLOW with FMP2, MF-OWHM, and IWFM. Coupling the crop water, vadose zone, groundwater, and streamflow models allows shallow groundwater to influence crop water demands, which can ultimately affect groundwater pumping, recharge, and evapotranspiration (ET) rates in the model. Irrigated agriculture accounts for about 45% of consumptive water use in the United States and about 78% in western states like California (Dieter et al., 2018). Despite this large proportion of consumptive water use and due to lack of regulatory pressures, there are few studies focusing on sensitivity analysis and calibration of integrated groundwater-surface-water models in agricultural areas when compared, for example, to the large body of literature on groundwater contaminant models (Miller & Pinder, 2004; Jousma et al., 2012; Singh, 2014) developed primarily for regularly compliance. Regional integrated models of California's Central Valley have been developed by James M. Montomery Consulting Engineers (1990), Faunt et al. (2009), and Brush and Dogrul (2013). Basin-scale models are available for the Pajaro Valley near Santa Cruz, CA (Hanson, Schmid, et al., 2014), and Butte Basin near Chico, CA (CDM, 2008), among others.

As for groundwater models developed at contaminant sites, sensitivity analysis and calibration are an essential part of integrated hydrologic model development (Hill & Tiedeman, 2007). However, unlike many contaminant site groundwater flow (and transport) models, integrated hydrologic models include numerous nonlinear cross dependencies between model subsystems (e.g., stream-aquifer flux is a function of the head difference, but heads in the stream and aquifer are also a function of stream-aquifer flux). When multiple sources of nonlinearity are present in a model, their effects are compounded (Cooley, 2004). Also, in significant departure from the site modeling practice, basin models typically use both, larger horizontal cell dimensions (on the order of 10^3 m) and coarser time steps (days and months). Perhaps because of the longer-standing, dominant groundwater modeling practice for contaminant sites, integrated hydrologic model development has mostly utilized the same calibration tools (Huntington & Niswonger, 2012; Hanson, Schmid, et al., 2014).

When applied to nonlinear models, however, these tools may be problematic, leading to nonglobal minima in parameter estimation and to ill-defined uncertainty predictions (Hill & Tiedeman, 2007). Clark and Kavetski (2010) and Kavetski and Clark (2010) have shown that hydrologic model nonlinearities make sensitivity analyses and calibration more difficult. New statistical tools in sensitivity analysis and calibration to address some of these difficulties have been developed and demonstrated (e.g., Foglia et al., 2009;

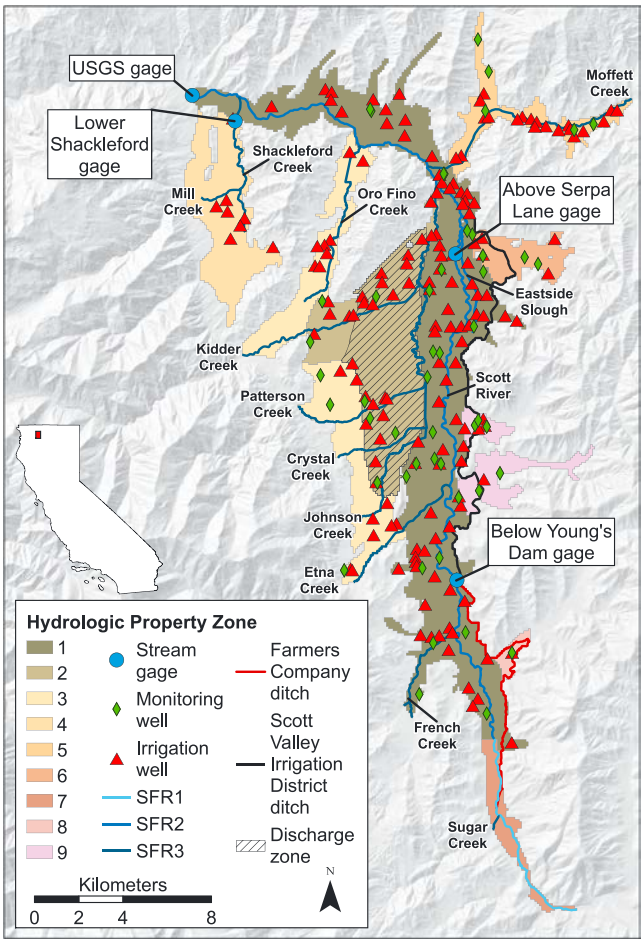

Figure 1. Map of Scott Valley showing model domain, major hydrologic features, irrigation wells, and monitoring wells used in the model. Aquifer properties were distributed among nine zones and streambed properties were distributed to tailings reaches (SFR1), nontailings Scott River (SFR2), and tributaries (SFR3). USGS = U.S. Geological Survey; SFR = streamflow routing.

Rakovec et al., 2014). The work shows the need to not only select from alternative parameters but also evaluate alternative model structures, including alternative structures for designing sensitivity analysis and calibration (Clark et al., 2008; Mendoza et al., 2015; Borgonovo et al., 2017). Using frugal methods to overcome potential computational inefficiencies in such a complex model development process has been shown to be a necessary and potentially successful alternative for integrated hydrologic models (Hill et al., 2016).

This paper contributes to the small but increasing collection of integrated hydrologic models developed to support management of irrigated agricultural groundwater basins with groundwater-dependent ecosystems in interconnected streams (e.g., Faunt et al., 2009; Brush & Dogrul, 2013; Hanson, Schmid, et al., 2014; Phillips et al., 2015; Hanson et al., 2018). Specifically, this paper investigates two related questions: What is the relative importance of and uncertainty about a diversity of parameters across the physical submodels in these systems? And how does the design of the sensitivity analysis and calibration affect the assessment of parameter importance and uncertainty?

The Scott Valley Integrated Hydrologic Model (SVIHM) consists of a soil water budget model (SWBM) weakly coupled to a groundwater-surface-water model. UCODE_2014, a universal inverse modeling software suite, was used to perform sensitivity analyses and calibrate the model, yielding information about parameter importance and uncertainty. In a frugal approach to test the sensitivity analysis and calibration design, we focus on examining the influence of the initial parameter values. Varying initial parameter values across a physically realistic range would potentially provide a conceptually simple and computationally efficient alternative for evaluating highly nonlinear integrated hydrologic models as a best practice approach when using such models to inform water management and policy decisions.

2. Study Area

The Scott Valley (Figure 1) in Northern California was chosen as a type case for an agricultural groundwater basin with Mediterranean climate and a groundwater-dependent ecosystem. Part of the larger Klamath Basin watershed that straddles the California-Oregon border, the Scott River watershed drains 2,100 km^2 and provides key spawning habitat for native anadromous fish species, including *Oncorhynchus tschawytscha* (Chinook salmon) and the threatened *Oncorhynchus kisutch* (coho salmon) (NCRWQCB, 2005). A large portion of the Scott River has been mapped as medium to high ranking on a groundwater-dependent ecosystem index by Howard and Merrifield (2010), indicating a high degree of connectivity between groundwater and surface water.

The montane valley, at over 800 m above mean sea level, is approximately 200 km^2 and formed during the Pleistocene by extension along a steep normal fault that dips to the east and strikes to the northwest (Mack, 1958). The surrounding uplands are part of the Klamath Mountains province, a sequence of accreted terranes and granitic intrusions associated with subduction of the Farallon plate beneath the North American plate (Irwin, 1990). Valley floor aquifer sediments are highly heterogeneous fluvial and alluvial deposits composed of gravels, sands, silts, and clays. Thickness reaches a maximum of more than 120 m (390 ft) in the central portion of the valley between Etna and Greenview and thins toward the valley margins. However, below 76 m (250 ft) the aquifer is not productive (Foglia, McNally, Hall, et al., 2013). Groundwater levels show interannual variation depending on the water year type but do not indicate long-term overdraft in the basin (University of California at Davis, 2016).

Climate in the area is Mediterranean with cold, wet winters and warm, dry summers. Mean annual precipitation on the valley floor is about 500 mm and accumulates predominantly during the winter and early

spring months (October–May). The mountains surrounding the valley receive higher precipitation rates due to their elevation. Mean temperature for January and July are 0 °C (32 °F) and 21 °C (70 °F), respectively. Mean annual runoff from Scott Valley, measured at the U.S. Geological Survey (USGS) stream gage (11519500) located in the Scott River Canyon just below the valley, is 543×10^6 m^3 (U.S. Geological Survey, 2015). Winter and spring flows (December–May) average about 28.3 m^3/s (1,000 ft^3/s) but have peaked at 1,120 m^3/s (39,500 ft^3/s). Mean summer streamflow is about 0.85 m^3/s (30 ft^3/s) but commonly drops below 0.57 m^3/s (20 ft^3/s) in the late summer and early fall. Maintaining sufficient instream flow during this critical low flow period is a key policy driver for water management in Scott Valley.

Land use in the valley is predominantly agricultural. There is a nearly even split between alfalfa hay/grain and pasture, which together account for 136 km^2 (68%) of land use (California Department of Water Resources, 2000). Both surface water and groundwater are used as sources of irrigation water. Reliance on groundwater increased following the 1976–1977 drought with the widespread introduction of pressurized wheel line sprinkler systems and eventually center pivots to replace flood irrigation, although all three irrigation methods are still used in the valley (Van Kirk & Naman, 2008). The growing season typically lasts from mid-April to mid-September but varies depending on the year. The southern, narrow upstream portion of the valley has been heavily modified by dredging operations that left behind tailings 6 m (20 ft) high, forming a zone of highly permeable open-framework gravels. The main stream channel was straightened in many parts of the valley by the Army Corps of Engineers in the early 1930s for flood control purposes (U.S. Department of War, 1938), which has resulted in channel incision at some locations.

The Scott River flows from south to north through the valley, fed by 10 major tributaries (Figure 1). Two large irrigation diversions, Farmer's Ditch and the Scott Valley Irrigation District (SVID) Ditch, have their point of diversion located near river km 87 and 74, respectively. These two ditches are primarily active from April to July and run along the east side of the valley. In the north central area of the valley is a drainage slough ("eastside slough") that collects agricultural tailwater for discharge back into the Scott River. Several other minor irrigation ditches exist on most tributaries in the valley.

3. Methods

3.1. SVIHM Overview

The SVIHM simulates hydrologic conditions in the Scott Valley from 1 October 1990 to 30 September 2011 by integrating three different models representing four subsystems: the upper watershed, and the alluvial basin landscape water, groundwater, and surface water. A statistical model is used to estimate tributary inflows at the valley margins when upper watershed flow data are unavailable ("streamflow regression model"; Foglia, McNally, Hall, et al., 2013). A land use/crop-soil water budget model ("soil water budget model") simulates agricultural practices in the valley to estimate hydrologic fluxes at the individual field scale using a tipping bucket approach (Foglia, McNally, Hall, et al., 2013), including determination of recharge and agricultural pumping rates. A finite difference groundwater-surface-water model simulates spatial and temporal groundwater and surface water conditions in the valley overlying the alluvial basin ("MODFLOW model"). The SVIHM is weakly coupled in that fluxes are passed from the SWBM to the MODFLOW model, but there are no direct feedbacks from the MODFLOW model to the SWBM.

Workflow for SVIHM involves running the streamflow regression model to generate average monthly streamflows at the valley margins. This is a preprocessing step as we assume no feedback from the valley to the upper watershed, and therefore, estimated values do not change unless the regression is modified. In a typical SVIHM run the SWBM is called which writes the necessary MODFLOW input files for streamflow, recharge, pumping, and ET. The MODFLOW model is then called, which calculates groundwater heads and streamflow in the valley. Flow into tile drains (see section 3.4) is extracted from the MODFLOW output, and the SWBM and MODFLOW model are run once more to route flows from tile drains to the surface water system. A summary of input data, key parameters, and model outputs is available in the supporting information. The SWBM takes about 10 min to run, and the MODFLOW model takes less than 2 hr using a desktop computer with Intel® Core™ i7-4770 @3.4-GHz processors with 16 GB of RAM for a total run time of typically less than 4 hr. Tighter integration of the landscape, groundwater, and stream subsystems is available in some software (e.g., IWFM or OWHM) but was not considered necessary for this study and avoided due to run time concerns.

3.2. Streamflow Regression Model

Upper watershed stream inflow data are available for limited and differing time periods for most tributaries as either daily mean flow values or monthly volumes (see the supporting information for date ranges and data available for each tributary). The streamflow regression model is used to fill in data gaps for tributary inflows to the valley, which are used as model boundary conditions. Data from all tributary gages are regressed against the USGS gaging station, where continuous daily streamflow data are available. When tributary flow data are available, measured values are used as model inputs. When tributary inflow data are unavailable, monthly streamflow is estimated using the regression model. Two of the tributaries, Johnson Creek and Crystal Creek, do not have any streamflow observations and therefore could not be included in the regression. Inflows for these two tributaries are calculated by scaling the estimated values for nearby Patterson Creek using the ratio of the subwatershed areas (Foglia, McNally, Hall, et al., 2013).

3.3. SWBM

The purpose of the SWBM is to estimate the unknown rates of groundwater pumping and recharge using a mass balance approach that incorporates local agricultural management practices (Foglia, McNally, Hall, et al., 2013). Fluxes of water in the shallow vadose zone are simulated on a daily basis using a tipping bucket style approach for 2041 fields identified from the California Department of Water Resources land use survey (California Department of Water Resources, 2000). Field areas vary from 5.2E3 to 6.6E6 m^2 (1.3 to 1,600 acres), with a median area of 6.9E4 m^2 (17 acres). The daily water budget for each field is calculated according to

$$\theta_k = \max\left(0, \theta_{k-1} + P_k + \mathrm{AW}_k - \mathrm{ET}_k - R_k\right) \tag{1}$$

$$\mathrm{AW}_k = \begin{cases} \max\left(0, \frac{\mathrm{ET}_k - P_k}{\mathrm{AE}}\right) & \text{when } AE < 100\% \\ \max\left(0, \frac{\mathrm{ET}_k - P_k}{1+\mathrm{SMDF}}\right) & \text{when } AE = 100\% \end{cases} \tag{2}$$

$$\mathrm{SMDF} = \frac{\sum \text{ soil moisture depletion}}{\sum \text{ AW}} \text{ (during irrigation season)} \tag{3}$$

$$R_k = \max(0, \theta_{k-1} + P_k + \mathrm{AW}_k - \mathrm{ET}_k - \theta_{\max}) \tag{4}$$

$$\mathrm{ET}_k = \mathrm{ET}_{0,k} * K_c \tag{5}$$

$$P_k = \begin{cases} 0 & \text{when } P_k \le 0.2 * \mathrm{ET}_0 \\ P_k & \text{when } P_k > 0.2 * \mathrm{ET}_0 \end{cases} \tag{6}$$

where θ is available soil moisture, $\theta_{\max}$ is the soil field capacity, P is effective precipitation, AW is applied water, ET is actual evapotranspiration, ET_0 is the reference evapotranspiration, K_c is the crop coefficient, R is recharge, AE is application (irrigation) efficiency, SMDF is the soil moisture depletion factor, and the subscript k denotes the day. The SWBM takes into account land use, irrigation method, water source, and soil storage properties for each field. Irrigation demand (equation (2)) for each field is driven by daily reference ET (ET_0) in excess of daily effective precipitation (P_k), land use crop coefficient (K_c), and soil moisture depletion factor (SMDF) specific to the land use and irrigation type. The SMDF allows for actual ET to exceed applied water to account for deficit irrigation, for contributions from deep soil moisture below the depth of the simulated soil zone (Foglia, McNally, Hall, et al., 2013), or for other generic sources of water (Dogrul et al., 2018). For fields with access to groundwater, pumping is assigned to the nearest well. Groundwater is assumed to be available at all times as there have been no reports of wells going dry in the valley, even during the 2012–2015 drought. Runoff from fields is considered to be negligible. Soil moisture in excess of field capacity at the end of each day is assumed to recharge groundwater. Daily values of pumping and recharge are converted to monthly average rates to match the stress period of the MODFLOW model.

3.4. Groundwater-Surface-Water Model

Groundwater fluxes, heads, groundwater-surface-water exchange, and streamflow are simulated with MODFLOW and the SFR package using monthly stress periods and daily time steps. The domain consists of 440

rows, 210 columns, and two layers with 100-m (328 ft) lateral resolution ranging from 0 to 61 m (0–200 ft) thick. A combination of remotely sensed elevation data using a digital elevation model and light detection and ranging (LiDAR) with horizontal resolutions of 10 and 1 m, respectively, is averaged within each model cell to determine ground surface elevation. LiDAR data from the valley has a 2σ relative accuracy of 4 cm (Watershed Sciences, 2010) and covers more than 90% of the model domain. Bedrock surrounding and outcropping within the valley is assumed to be impermeable relative to the valley sediments. Hydraulic conductivity and storage properties for the valley aquifer are spatially distributed between nine hydrogeologic zones (Figure 1), similar to those proposed by Mack (1958). The model simulates unconfined flow with variable storage and transmissivity using the Newton formulation of MODFLOW (MODFLOW-NWT; Niswonger et al., 2011) to allow for rewetting of cells that go dry during the simulation, especially along the valley margin. Newton solver variables are set to default values corresponding to the "COMPLEX" option defined in the user manual, as "SIMPLE" and "MODERATE" result in shorter run times but unsatisfactory numerical errors.

Groundwater pumping is simulated at 164 agricultural wells (Figure 1) located in the second layer using the well (WEL) package (Harbaugh, 2005). The wells and their locations were identified through well logs, stakeholder feedback, aerial photography, and field surveys when possible. Due to the low population density of the valley, domestic pumping is not included in the model as it is a small portion of total groundwater extractions (Mack, 1958). The default value of 0.05 for PHIRAMP in the WEL package is used for reducing pumping rates in cells when there was not enough water to satisfy the applied pumping rate. The weak coupling between the SWBM and MODFLOW can result in a mass balance error between the two submodels, as the SWBM is not aware of pumping reductions that happen within MODFLOW. Pumping reductions range from 0% to 7.6% on a monthly basis, with a mean of 3.7%, so it is not considered to be a significant limitation of SVIHM at this time.

Seepage from the SVID and Farmers Company ditches (Figure 1) have been determined using field seepage experiments. They are represented using injection wells with rates of 1.8×10^{-2} m^3/s per km (1.0 ft^3/s per mile) and 8.8×10^{-3} m^3/s per km (0.5 ft^3/s per mile), respectively (Echols, 1991; S. S. Papadopulos and Associates, Inc, 2012). Water is diverted from the stream using "ghost" SFR segments at the respective points of diversion at the same rate it is injected via the WEL package in order to conserve mass. Ditches in the valley are generally active from April to July and primarily used for stock watering and limited irrigation (S. Sommarstrom, personal communication, June 21st, 2017). As most of the flow is needed to generate sufficient head for water to reach the end of the ditches (P. Harris, personal communication, June 21st, 2017), diversions from the Scott River into ditches are greater than the ditch seepage rate supplied to the WEL package to account for evaporation losses and stockwater use. These consumptive losses are assumed to be 5.7E−2 m^3/s for each ditch, or 12.5% and 25% of the Farmers Company ditch and SVID ditch diversion rates, respectively. Mountain front recharge (MFR), used here to describe the diffuse portion of recharge to adjacent basins from surrounding mountains (Wilson & Guan, 2013), was simulated only along the western model boundary using injection wells placed in the first layer. Rates and spatial distribution of MFR segments were estimated by S. S. Papadopulos and Associates, Inc. (2012) using a water balance approach. No MFR occurs along the eastern valley boundary as these mountain ranges are lower and in the rain shadow of the western ranges of the watershed.

The SFR package was used to simulate the surface water system (Figure 1) and its interactions with groundwater. Bed elevations for each SFR node were extracted from the elevation data sets using the nearest thalweg data point to the stream node. Inflows for each tributary and the main stem of the Scott River are specified at the model boundaries for each stress period using the streamflow regression model described above. Surface water used by SWBM is subtracted from the inflow estimated by the streamflow regression model at the model boundary, as most diversions from tributaries occur near or upstream of the model boundary. The stream channel is assumed to be rectangular with flow calculated using Mannings equation. Stream properties (e.g., bed conductivity and roughness) were assigned using one of three groups: (1) tailings reaches, (2) nontailings Scott River, and (3) tributaries (Figure 1).

Drains were placed at the land surface within the Discharge Zone shown in Figure 1. This area is known to have a water table very near or at the land surface (Mack, 1958), resulting in lateral fluxes of water between fields that SWBM does not account for. Water intercepted by these drains is routed into a nearby stream segment, approximating overland flow. In the Discharge Zone, crop water demands are met primarily through

subsurface irrigation (direct uptake from groundwater). A tight integration of landscape/crop-soil water and groundwater subsystems would be most suitable in this zone. Here, a work-around was applied: Fields with subirrigation were not irrigated in SWBM, resulting in "dry" soils and underestimation of crop ET. To compensate, the MODFLOW ET package was employed instead to simulate ET from these fields, using an extinction depth of 0.5 m. The applied ET rate for these fields is equal to the average potential ET rate for the specific stress period and crop, scaled by the fraction of time per month when the field was "dry" (and therefore ET was not occurring) in SWBM. For example, a field within the Discharge Zone that had 0 m/day of ET in SWBM simulation for 5 days in July because available soil moisture dropped to 0 m^3 would be simulated in MODFLOW with an applied ET rate equal to the average potential ET rate for that month multiplied by 0.16 (5 of 31 days). This ensures that ET is neither double counted between SWBM and MODFLOW, nor significantly underestimated, given the water table depth.

3.5. Sensitivity Analysis and Calibration

Sensitivity analysis and calibration of SVIHM was performed using the universal inverse modeling software suite UCODE_2014 (Poeter & Hill, 1998; Poeter et al., 2014), which compares observed and simulated values to create an objective function given by

$$\phi = \sum_{i=1}^{ND} \left(y_i - y_i'\right) w_i^{1/2} \tag{7}$$

where ϕ is the objective function value, y_i is the observed value, y_i' is the simulated value, w_i is the observation weight, and ND is the number of observations. Given the nonlinear structure of SVIHM, global methods for sensitivity analysis and calibration would provide the most rigorous approach. However, this is impractical due to the large number of model runs required and the long ($\gg$1 hr) single-run CPU time for SVIHM. Gradient-based perturbation methods are more efficient, but computed parameter sensitivities can vary as a function of the starting values (Hill & Tiedeman, 2007). As an alternative design for the sensitivity analysis and to account for model nonlinearity, multiple forward difference sensitivity analyses using different starting parameter combinations (referred to as parameter sets 1–5) were performed. This is similar to the distributed evaluation of local sensitivity analysis methodology proposed by Rakovec et al. (2014) and the use of multiple sensitivity indices (e.g., variance based and local sensitivity) by Borgonovo et al. (2017), although less rigorous to preserve computational efficiency. Starting values for the different sensitivity runs (Table 1) were selected either from a previous model calibration using the river package (RIV; Harbaugh, 2005; Foglia et al., 2018) or from within an expected range based on professional judgment. Parameters were log-transformed and increased by 1% from their starting values for all sensitivity analyses.

Measured groundwater elevations at 55 wells (Figure 1) accounted for 2,197 observations (47% of total). The majority of these were collected monthly beginning in 2006 as part of the voluntary Scott Valley Community Groundwater Monitoring Program. Weights for groundwater head observations were set to the inverse of the measurement error variance (Hill & Tiedeman, 2007) given by

$$w_i = \frac{1}{\sigma_i^2} \tag{8}$$

where σ_i^2 is the measurement error variance and assumed to be 1.0 m^2 for all head observations. This accounts for measurement errors in both well reference point elevation and depth to water.

Streamflow data at four gage locations (Figure 1) were also included as calibration targets in the objective function and separated into three categories: (1) below 2.44×10^5 m^3/s (100 ft^3/s; 68% flow exceedance probability), (2) between 2.44×10^5 and 2.44×10^6 m^3/s (100–1,000 cfs), and (3) greater than 2.44×10^6 m^3/s (1,000 cfs; 22% flow exceedance probability). These reflect low, medium, and high streamflow rates for the Scott River, respectively. A total of 2485 streamflow observations, consisting of 1,385 at the USGS Fort Jones gage, 500 at the Lower Shackleford Creek gage, 300 at the Above Serpa Lane (AS) gage, and 300 at the Below Young's Dam (BY) gage, was randomly selected from data available during the model simulation period so the total number of streamflow observations was similar to the number of groundwater head observations. Streamflow observation weights were determined using the equation

$$w_i = \frac{1}{\left(y_i * CV_i\right)^2}, \tag{9}$$

Table 1
Parameters Adjusted During Sensitivity Analysis With Initial Starting Values

Parameter	Description	Initial value				
		Parameter Set 1	Parameter Set 2	Parameter Set 3	Parameter Set 4	Parameter Set 5
Kx1		100	20	60	200	250
Kx2		11	60	2	100	100
Kx3		100	80	100	50	100
Kx4	Hydraulic	20	2	50	10	30
Kx5	conductivity	10	1	80	10	25
Kx6	(m/day)	30	200	70	10	50
Kx7		1,000	500	50	1,000	500
Kx8		30	90	5	10	10
Kx9		60	2	100	10	20
Kvar1		100	10	50	20	71
Kvar2		100	10	50	50	73
Kvar3		100	10	50	100	92
Kvar4	Vertical	100	10	50	80	95
Kvar5	anisotropy	100	10	50	40	10
Kvar6	(—)	100	10	50	30	77
Kvar7		1	1	1	10	55
Kvar8		100	10	50	60	94
Kvar9		100	10	50	50	46
Sy1		0.1	0.15	0.05	0.1	0.12
Sy2		0.15	0.05	0.12	0.07	0.08
Sy3		0.15	0.2	0.1	0.1	0.11
Sy4	Specific	0.1	0.12	0.11	0.1	0.1
Sy5	yield	0.15	0.15	0.1	0.1	0.13
Sy6	(—)	0.15	0.08	0.1	0.1	0.09
Sy7		0.3	0.25	0.15	0.3	0.25
Sy8		0.15	0.11	0.06	0.1	0.05
Sy9		0.15	0.12	0.15	0.1	0.07
Ss1		1.00E−05	5.00E−04	2.00E−04	6.40E−05	1.50E−05
Ss2		1.00E−05	5.00E−04	2.00E−04	5.90E−05	9.00E−05
Ss3		1.00E−05	5.00E−04	2.00E−04	2.70E−05	2.60E−04
Ss4	Specific	1.00E−05	5.00E−04	2.00E−04	8.30E−05	3.10E−04
Ss5	Storage	1.00E−05	5.00E−04	2.00E−04	1.30E−05	8.00E−05
Ss6	(1/m)	1.00E−05	5.00E−04	2.00E−04	2.00E−05	2.00E−05
Ss7		1.00E−05	5.00E−04	2.00E−04	6.50E−05	7.00E−05
Ss8		1.00E−05	5.00E−04	2.00E−04	2.90E−04	3.00E−04
Ss9		1.00E−05	5.00E−04	2.00E−04	8.00E−04	1.00E−05
Wel5		2.34E+02	2.34E+03	1.17E+04	2.34E+03	8.19E+02
Wel6		6.30E+03	1.05E+04	5.25E+02	1.05E+04	2.10E+03
Wel7	Mountain front	1.20E+04	8.60E+02	2.58E+04	1.72E+03	5.16E+03
Wel8	recharge	2.24E+04	8.94E+03	2.98E+03	1.12E+04	2.98E+04
Wel9	(m^3/day)	2.00E+03	2.00E+04	4.00E+04	6.00E+03	4.00E+03
Wel10		3.86E+03	1.93E+04	3.86E+02	9.65E+02	2.90E+03
Wel11		2.43E+03	2.70E+02	2.70E+01	1.89E+03	3.24E+03

Table 1 *(continued)*

Parameter	Description	Initial value				
		Parameter Set 1	Parameter Set 2	Parameter Set 3	Parameter Set 4	Parameter Set 5
Wel20	Ditch seepage	1.45E+04	2.42E+04	6.44E+03	1.61E+04	2.42E+04
Wel21	(m^3/day)	7.02E+04	4.68E+04	1.17E+04	2.34E+04	7.02E+04
BedK1	Streambed	10	0.1	10	10	10
BedK2	conductivity	10	0.1	10	5	10
BedK3	(m/day)	10	0.1	10	15	10
Rough1	Streambed	0.035	0.03	0.04	0.035	0.035
Rough2	Roughness	0.035	0.03	0.04	0.035	0.035
Rough3	($d/m^{1/3}$)	0.035	0.03	0.04	0.035	0.035
RD_Mult		1	0.9	1.1	1	1.2
SMDF_Flood	SWBM	0.7	0.75	0.55	0.7	0.55
SMDF_WL_LU25	parameters	1.05	1.09	1.01	1.09	1.1
SMDF_CP_LU25	(—)	1.1	1.15	1.01	1.15	1.1
SMDF_WL_LU2		0.85	0.81	0.99	0.81	0.95
SMDF_CP_LU2		0.95	0.91	0.91	0.95	0.99
Kc_alfalfa_mult		1	1.04	0.96	1	1.05
Kc_grain_mult		1	0.96	1	1.05	0.98
Kc_pasture_mult		1	1	0.96	1.04	0.95
Kc_noirr		0.6	0.7	0.79	0.65	0.65

Note. Sensitivity analysis was performed using a 1% forward difference perturbation. Note that the reported soil moisture depletion factor (SMDF) is the sum of the application efficiency (AE) and SMDF but is reported as a single value for convenience.

where CV_i is the coefficient of variation. The low, medium, and high streamflow categories were assigned coefficients of variation equal to 10%, 20%, and 40%, respectively. Low flows at the non-USGS gages were the only exception as they included observations at or very near 0, and weights approach infinity when observation values approach 0 using the coefficient of variation weighting method. The median weight of the USGS low flow observations, equal to 1×10^{-8} d^2/m^2, was assigned to the low flow category for the non-USGS gages to prevent weights from becoming too large and dominating the objective function.

Physical hydrologic properties or fluxes were represented by 61 parameters (Table 1) contained within SWBM and MODFLOW portions of SVIHM. These include seasonal crop coefficient multipliers (e.g., Kc_Alfalfa_Mult) and aquifer parameters for each zone such as hydraulic conductivity (e.g., Kx1) and storage (e.g., Sy1 and Ss1). Specific cuttings of alfalfa were not represented using a variable crop coefficient as cutting times vary across the valley due to distributed ownership, management practices, and climate conditions. Instead, crop coefficients for alfalfa and pasture were set to seasonal averages of 0.9 during the growing season and zero otherwise. A variable K_c was used for grain due to growers having similar management practices and ranged from 0 to 1.15 with an average of 0.62 over the 4-month growing period. Effective root zone depth was assumed to be 2.44 m (8 ft) for alfalfa and 1.22 m (4 ft) for grain and pasture (Weaver, 1926), adjusted by the use of a single root zone depth multiplier (RD_Mult). Each of the five simulated combinations of land use (alfalfa/grain, A/G; pasture, P) and irrigation (flood; wheel line sprinkler, WL; center pivot sprinkler, CP) was assigned specific AE and SMDF values (Table 1). Channel roughness and bed conductivity (Figure 1) parameters were distributed among the three stream segment classifications (see section 3.4). Seepage fluxes from MFR and ditches were also included as parameters. Recharge and groundwater pumping were not explicitly included as calibration parameters because they are accounted for with SWBM parameters. SWBM parameterization also affects surface water inflows to the simulated stream network via simulated surface water diversions from streams at the model boundary. In contrast, daily total precipitation across the valley was considered to have relatively small measurement error and was not considered in the sensitivity analysis.

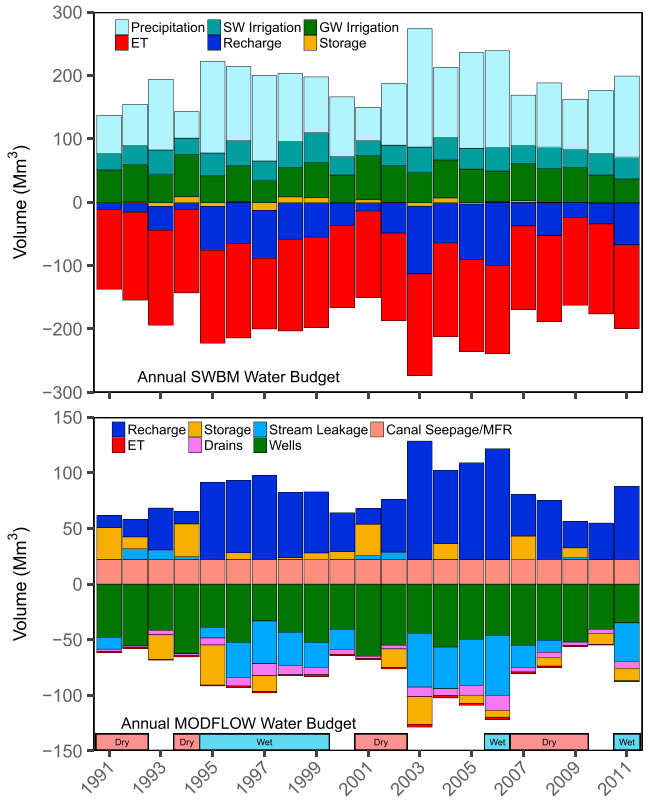

Figure 2. Annual water budgets for SWBM (top) and MODFLOW (bottom) portions of Scott Valley Integrated Hydrologic Model. Values are water year totals, with colors along the bottom of the lower plot indicating dry (red) and wet (blue) years. Positive and negative storage values correspond with decreases and increases in storage, respectively. ET = evapotranspiration; SW = surface water; GW = groundwater; SWBM = soil water budget model; MFR = mountain front recharge.

Composite scaled sensitivity (CSS), a measure of the importance of observations as a whole to a single parameter, is calculated for each parameter from the sensitivity analyses according to

$$\mathrm{CSS}_j = \left[\frac{\sum_{i=1}^{\mathrm{ND}} \left[\left(\frac{\partial y_i'}{\partial b_j} \right) b_j w_i^{1/2} \right]^2 \Big|_{\mathbf{b}}}{\mathrm{ND}} \right]^{1/2} \tag{10}$$

where CSS_j is the composite scaled sensitivity of the jth parameter and b is the vector of parameters. These values were normalized in order to compare between sensitivity analyses using

$$\mathrm{CSS}_{j,s,\mathrm{norm}} = \frac{\mathrm{CSS}_{j,s}}{\max\left[\mathbf{CSS}_s\right]} \tag{11}$$

where $\mathrm{CSS}_{j,s}$ is the composite scaled sensitivity of the jth parameter for set s (1–5 in the study) and CSS_s is the array of CSS values for parameter j. Calibration parameters were selected by ranking the CSS values for each parameter set and identifying parameters that consistently showed the greatest sensitivity across all five sensitivity analyses. Multiple calibrations (Runs 1–5) were then performed, again with different starting values for adjustable parameters to test for model uniqueness. Values of fixed parameters (i.e., those excluded from the calibration process) were selected from the first sensitivity analysis parameter set (Table 1). Adjustable parameters were modified by UCODE_2014 in an attempt to minimize the objective function and therefore provide the best match between observed and simulated values. Convergence was met when either parameter values did not vary by more than 1% (TolPar = 0.01), or the objective function did not change by more than 1% for three consecutive iterations (TolSOSC = 0.01). Nonlinearity of SVIHM was evaluated using the modified Beale's measure (Cooley & Naff, 1990) calculated by the program MODEL_LINEARITY, available in the UCODE_2014 distribution (https://igwmc.mines.edu/ucode/).

The influence that observations exerted during the calibration process were evaluated using the DFBETAS and Cook's D statistics. The DFBETAS statistic provides information about the influence of an observation on each calibration parameter, with more influential observations having greater absolute values. Cook's D measures how influential an observation is on the entire parameter set by calculating how much regression estimates would change if the observation was omitted. Like DFBETAS, greater values indicate greater influence. Both statistics have critical values for defining when observations are considered influential. For DFBETAS and Cook's D this is equal to $4/(\mathrm{ND} + \mathrm{NPR})$ and $2/(\mathrm{ND} + \mathrm{NPR})^{1/2}$, respectively, where ND is the number of observations and NPR is the number of prior information equations (Yager, 1998; Hill & Tiedeman, 2007). Prior information equations were not used in this version of SVIHM.

3.6. Streamflow Matching

Comparison of simulated streamflow to observed values at gages was done both graphically and using a modified version of the Nash-Sutcliffe model efficiency coefficient (NSE; Nash & Sutcliffe, 1970)

$$\mathrm{NSE} = 1 - \frac{\sum_{i=1}^{n} \left(\log\left[y_i - \log y_i'\right] \right)^2}{\sum_{i=1}^{n} \left(\log\left[y_i - \log \bar{y}_i\right] \right)^2}, \tag{12}$$

where n is the number of streamflow observations for the gage. A NSE of 1.0 indicates the model perfectly matches observations, while a value of 0.0 means the model is no more accurate than predicting the mean value. Streamflow data were log-transformed because they span nearly 4 orders of magnitude in the Scott Valley and large variance can produce high NSE values even if model fit is relatively poor (Jain & Sudheer, 2008). Therefore, NSE values presented in this paper are conservative.

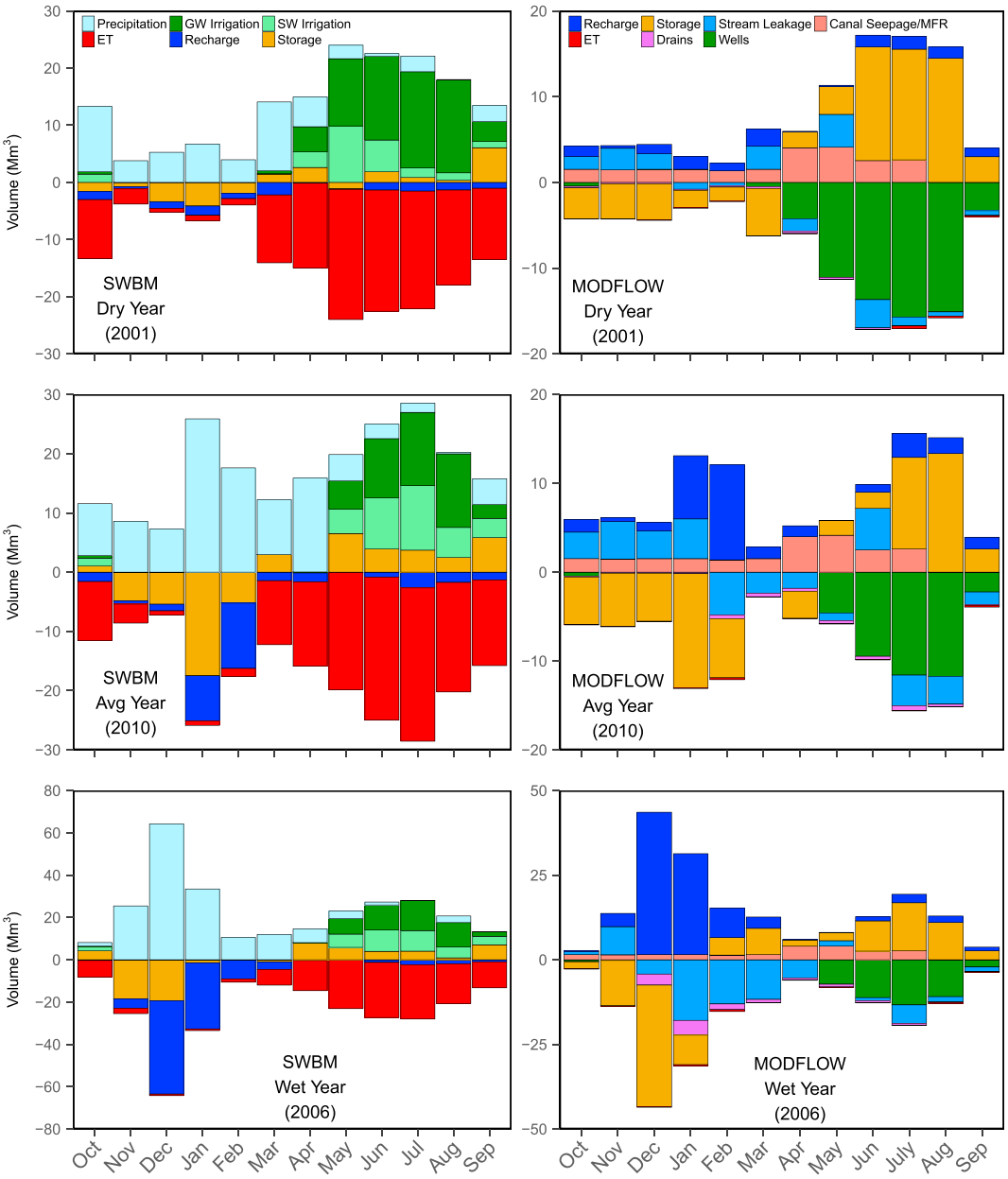

Figure 3. Monthly water budgets for SWBM (left column) and MODFLOW (right column) portions of SVIHM for dry (top row), average (middle row), and wet (bottom row) years. Positive and negative storage values correspond with decreases and increases in storage, respectively. Colors along the bottom of the plot indicate dry/critical (red) and wet (blue) water year types according to the Sacramento Valley water year hydrologic classification. ET = evapotranspiration; GW = groundwater; SW = surface water; SWBM = soil water budget model; MFR = mountain front recharge.

3.7. Qualitative Model Validation

To validate the usefulness of SVIHM for informing water management decisions related to the critical late summer period when stream connectivity is most compromised, a model validation was performed to test SVIHM's capability to predict late summer dry reaches. Data obtained from the U.S. Department of Agriculture's National Agriculture Imagery Program (NAIP) in combination with direct observations by landowners and resource professionals were used to map dry/disconnected stream reaches in the Scott Valley. Imagery and direct observations from August 2005 and 2014, representing average and dry water year conditions in the Scott Valley, respectively, were digitized using ArcGIS. Water year 2014 was used as a proxy for water year 2001 in the model since NAIP data only extend back to 2003 and SVIHM terminates in 2011. Both

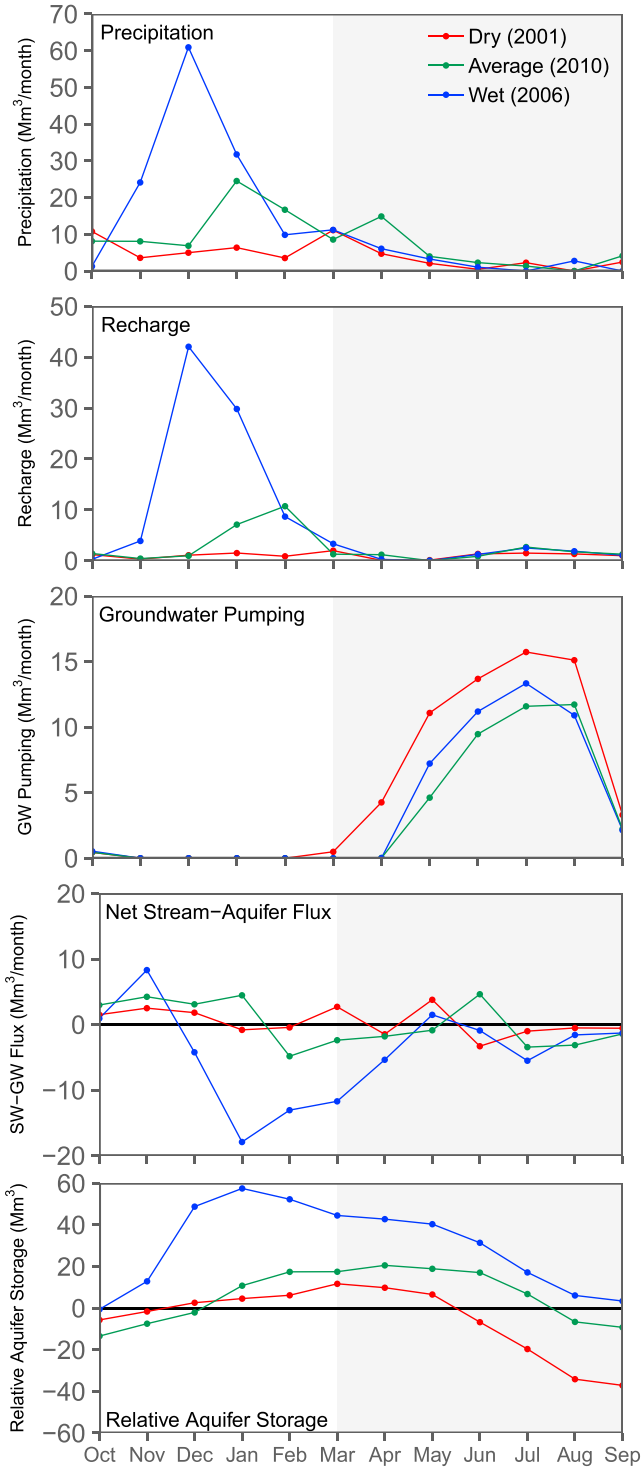

Figure 4. Monthly fluxes of selected basin water budget components for dry (2001), average (2010), and wet (2006) years. Negative values for net stream-aquifer flux correspond with groundwater discharge to surface water. Relative aquifer storage is the cumulative change in groundwater storage from initial conditions. Gray shaded area indicates growing season. GW = groundwater; SW = surface water.

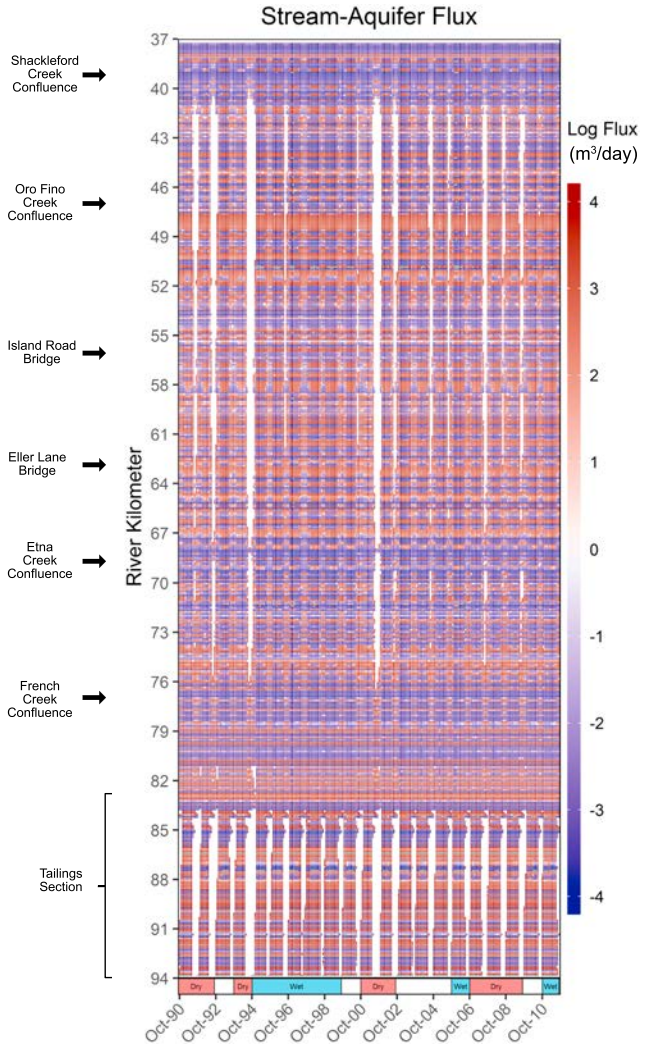

Figure 5. Spatiotemporal heat map of fluxes between groundwater and surface water for the Scott River with geographic locations noted. Fluxes are highly spatially variable, despite relatively homogeneous parameterization of the stream. White areas indicate dry reaches. Colors along the bottom of the plot indicate dry/critical (red) and wet (blue) water year types according to the Sacramento Valley water year hydrologic classification. The absolute value is the magnitude of the flux, while the sign indicates flux direction: Red and blue indicate losing and gaining reaches, respectively.

years show similarities in timing and magnitudes of streamflow. Reaches were assigned one of four categories: dry/disconnected, flowing, questionable, and no data. These mapped sections were compared with streamflow values produced by SVIHM at the end of the corresponding month. Modeled stream reaches with flows less than 2.8×10^{-2} m^3/s (1 ft^3/s) were considered dry/disconnected, whereas all other reaches were considered flowing.

NAIP imagery is taken during the growing season but generally before field observations were collected, typically at the seasonally lowest streamflow in late August or September. Where only NAIP imagery is available, the data may therefore be biased toward wetter conditions than would have been observed later in the year. However, it was considered to be a useful data set for qualitative model validation.

4. Results

4.1. Water Budget and Groundwater-Surface-Water Interactions

In order to provide context for the sensitivity analysis and calibration results, we first present model results from one of the calibrated parameter sets. Run 4 was chosen because it had the lowest objective function value. Annual water budgets were computed separately for the soil landscape (SWBM) and groundwater (MODFLOW) systems (Figure 2). Landscape inflows consist of precipitation and irrigation, while outflows are to ET and groundwater recharge. Groundwater inflows include landscape recharge and stream recharge. Groundwater outflows include pumping, drains, discharge to streams, and ET within the discharge zone and along the riparian corridor. Precipitation varies considerably from year to year, ranging from 22.5 cm (8.9 inches) to 98.1 cm (38.6 inches). Applied irrigation from groundwater and surface water in the valley also varies interannually from 31.7 cm (12.5 inches) to 50.4 cm (19.8 inches). Groundwater pumping accounts for about 50% of irrigation water in wet years but nearly 75% in dry years. Evapotranspiration has small interannual variability and is the largest flux out of the soil zone due to the dominant presence of agriculture in the valley. Given that interannual soil moisture storage changes are small (0.2% to 15% relative to field capacity), interannual fluctuations in recharge therefore follow those of precipitation, with which it is highly correlated ($R^2 = 0.89$). Monthly and annual water budgets are available in the supporting information.

At the basin scale, landscape recharge is the largest inflow to the aquifer on an annual basis. In the current version of the model, canal seepage and MFR are constant and constitute the second largest inflow to the aquifer. Dry years show reductions in groundwater storage. At the valley scale, groundwater is a net contributor to streamflow in all but the driest years. In those years, streams are net contributors to the groundwater budget but only after significant depletion of groundwater storage in the preceding year (Figure 2). Groundwater pumping and discharge to the stream are the two largest annual outflows from the aquifer and show large variations, with 50% more groundwater pumping in dry years than wet years. Drains in the Discharge Zone account for approximately 4% of the annual aquifer outflow during dry years and nearly 15% during wet years. A small volume of water is removed from the aquifer directly via ET due to shallow water table conditions in the Discharge Zone (Figure 1, see section 3.4). Annual change in aquifer storage is highly variable and largely dependent on water year type.

Monthly water budgets for dry (2001), average (2010), and wet (2006) water type years (State Water Resources Control Board, 1999; Deas, 2006) demonstrate significant intra-annual, seasonal variations that drive the system (Figure 3). Generally, recharge is high and both, soil and groundwater storage increase during the

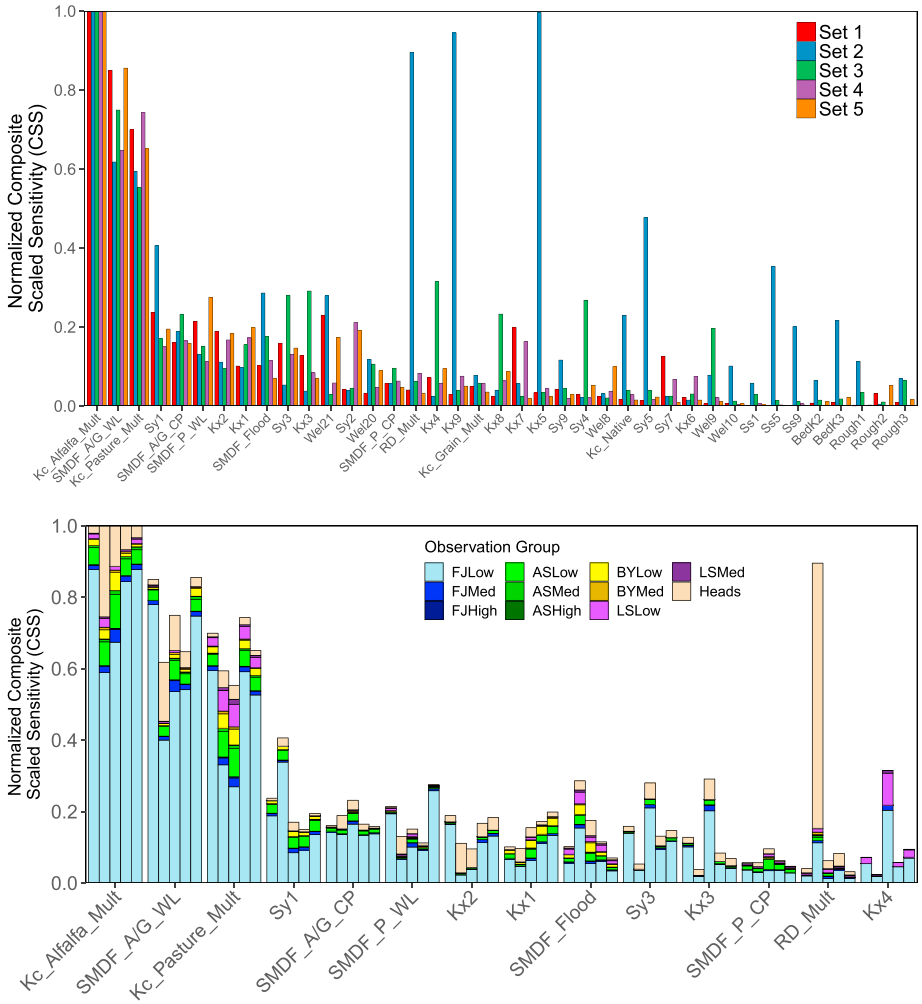

Figure 6. Normalized composite scaled sensitivities (CSS) for each parameter set (top) and the 14 most sensitive parameters in Scott Valley Integrated Hydrologic Model (bottom). Parameters with a value less than 5% for all sensitivity runs have been excluded for plotting purposes in the top graph. Colors represent either the parameter set (top) or the contribution of different observation groups to parameter sensitivity (bottom). Low streamflow observations, particularly those at the U.S. Geological Survey gage, are the most sensitive to changes in model parameter values.

winter months. Storage decrease, groundwater pumping, surface water irrigation, and high ET dominate from spring to early fall, leading to the lowest aquifer storage each year by late summer, although some recharge may again occur during the irrigation season (Figure 4).

While the general patterns persist, timing and magnitude of some fluxes contribute to significant differences in seasonal patterns between water year types. In a dry year, winter precipitation is lacking, soil moisture is not refilled, and pumping starts at the beginning of the growing season in March, whereas it is delayed until May during an average and wet year. Groundwater pumping is similar between most year types during the summer months, but dry years cause significant spring abstractions of groundwater, while summer recharge from irrigation return water is lower (Figures 3 and 4). In a wet year, cloud cover and precipitation days during the growing season can significantly reduce ET (Figure 3). Seasonal aquifer storage trends are very similar between a wet and a dry water year types, with similar reduction in storage between March and September. But with a dry winter, aquifer storage is significantly more depleted in March when compared to a wet year. In an average year, winter storage increases are not as large as in a wet year, while summer depletion is not as significant as in a dry year. Hence, an average year type tends to see the least groundwater storage change between March and October (Figure 4).

Table 2
Initial and Final Values for Five Calibration Runs

	Adjustable parameter values										
	Calibration Run 1		Calibration Run 2		Calibration Run 3		Calibration Run 4		Calibration Run 5		Calibration
Parameter	Initial	Final	Initial	Final	Initial	Final	Initial	Final	Initial	Final	Bounds
Kx1	100	40	20	26	60	74	200	194	250	46	10^{-7}–10^{3}
Kx2	11	4	60	4	2	6	100	7	100	9	10^{-7}–10^{3}
Kx3	100	56	80	116	100	9	50	10	100	7	10^{-7}–10^{3}
Kx4	20	24	2	25	50	24	10	16	30	23	10^{-7}–10^{3}
Sy1	0.1	0.09	0.15	0.08	0.05	0.13	0.1	0.13	0.12	0.09	0.01–0.35
Sy3	0.15	0.03	0.2	0.06	0.1	0.04	0.1	0.05	0.11	0.04	0.01–0.35
RD_Mult	1	2	0.9	1.7	1.1	1.9	1	1.4	1.2	1.2	0.5–2
SMDF_Flood	0.7	0.67	0.75	0.74	0.55	0.8	0.7	0.72	0.55	0.68	0.5–0.8
SMDF_A/G_WL	1.05	1.02	1.09	1.04	1.01	1.05	1.14	1	1.03	1.17	1–1.2
SMDF_A/G_CP	1.1	1.11	1.15	1.01	1.01	1	1.15	1.16	1.1	1.13	1–1.2
SMDF_P_WL	0.85	1	0.81	0.8	0.99	0.99	0.9	0.85	0.95	1	0.8–1
SMDF_P_CP	0.95	0.9	0.91	0.85	0.91	0.91	0.95	0.87	0.99	1	0.8–1
Kc_Alfalfa_Mult	1	0.97	1.04	1.05	0.96	1.05	1	1.05	1.05	1.01	0.95–1.05
Kc_Pasture_Mult	1	1.05	1	1.01	0.96	0.98	1.04	1.05	0.95	1.02	0.95–1.05
Objective function value		9.33E+04		9.57E+04		9.08E+04		8.90E+04		9.66E+04	

Note. The only differences between the five runs was the starting value of the adjustable parameters. Note that the reported soil moisture depletion factor (SMDF) is the sum of the application efficiency and SMDF but is reported as a single value for convenience.

Simulated stream-aquifer fluxes are highly variable along the stream profile (Figure 5). Exchange fluxes between groundwater and the stream vary from tens to thousands of cubic meters per day. Gaining stream reaches alter with losing stream reaches at a rate of typically 200 to about 1,000 m.

The lower 10 km of the Scott River (river km 37–47) is mostly gaining reaches interspersed with small segments of losing reaches. The same general pattern is observed for the 17 km (river km 67–84) of the Scott River below the Tailings section. In contrast, the 20-km-long midsection of the river, from just downstream of the confluence with Etna Creek to the confluence with Oro Fino Creek (river km 47–67), and much the Tailings section in the uppermost 10 km of the Scott River (river km 84–94) are dominated by losing reaches.

In contrast to the high variability of groundwater-surface water fluxes along the stream profile, local fluxes remain relatively constant over the 21-year simulation period. Some seasonal variations are observed in the simulation, involving either a slight upstream or downstream translocation of a gaining/losing reach transition (Figure 5). Transitions are often consistent between seasons, year after year, regardless of water year type. Some reaches show seasonal expansion/contraction patterns or reaches, with a longer area recharging the aquifer during the winter and spring months and longer sections of groundwater discharging to the stream in the summer and fall. Reaches consistently showing either gains or losses during the entire simulation period each accounted for about 25% of the length of the Scott River (Figures 5 and 10).

4.2. Sensitivity Analysis

CSS showed considerable variation across the parameter sets (Figure 6). The alfalfa crop coefficient multiplier (Kc_Alfalfa_Mult) was the most sensitive, having the highest value for each parameter set tested. The soil moisture depletion factor for wheel line irrigation of alfalfa and grain (SMDF_A/G_WL) and the pasture crop coefficient (Kc_Pasture_Mult) also showed a large degree of sensitivity for all runs. Aside from these three parameters, ordering of CSS values between sets was highly variable. Twenty-two parameters did not show sensitivity within 5% of Kc_Alfalfa_Mult (normalized CSS < 0.05) for any of the runs. A few parameters (e.g., Kx5, Kx9, and Kc_Native) showed relatively high sensitivity for a single run but were insensitive for other combinations of parameters.

Low streamflow at the USGS gage was the most sensitive observation group to changes in parameter values (Figure 6), followed by low flow observations at the other gages and then by groundwater heads. Medium and high streamflow observation groups did not show large sensitivities to parameter perturbations. Using

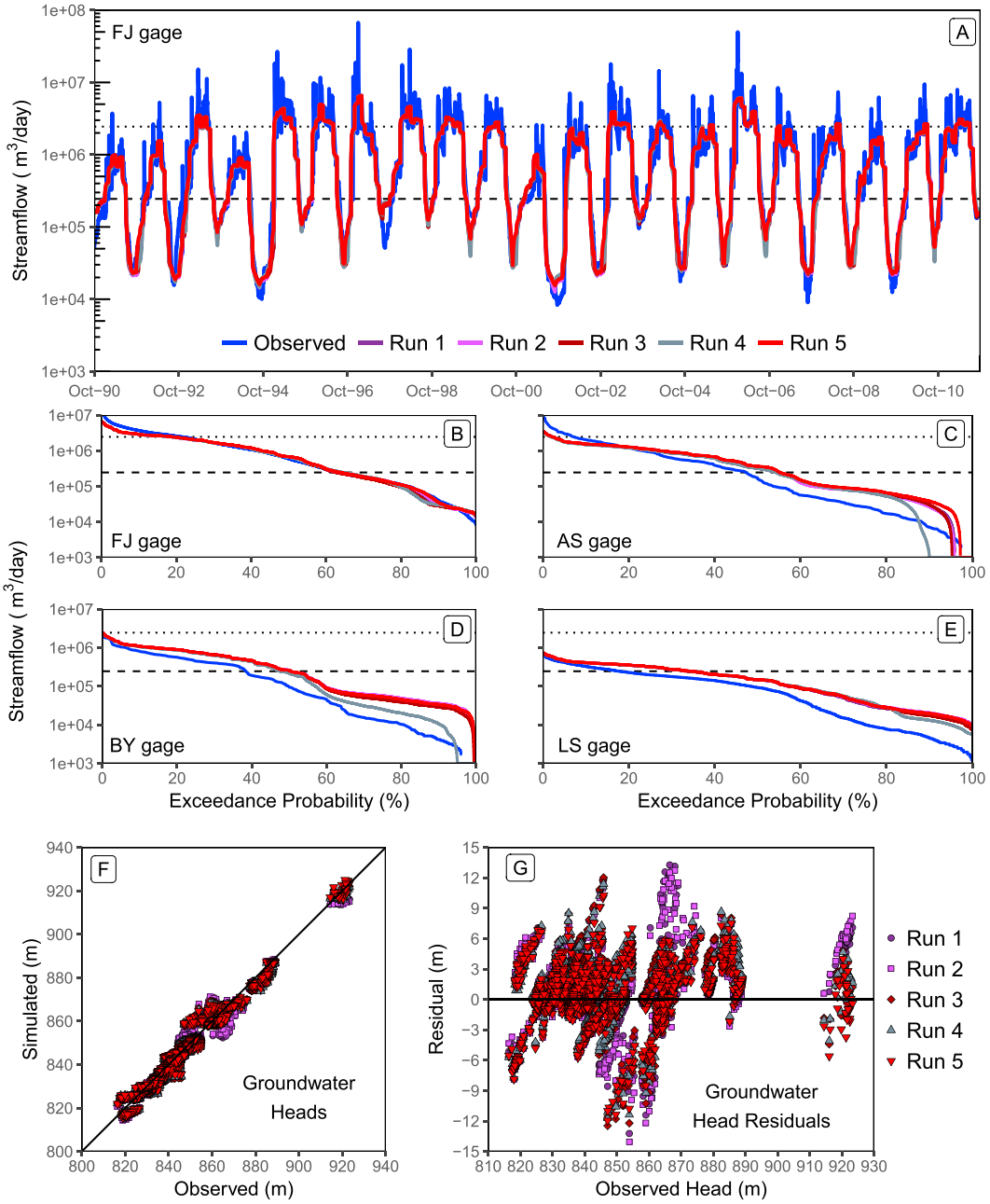

Figure 7. (a) Observed and simulated values of streamflow at the U.S. Geological Survey FJ gage using optimized values from all five calibration runs. (b–e) Observed and simulated streamflow exceedance probabilities at the four gaging stations in the valley. (f and g) Observed and simulated groundwater heads and head residuals for the five calibrations. Low, medium, and high flow categories are below the dashed line, between the dashed and dotted line, and above the dotted line, respectively. FJ = Fort Jones; AS = Above Serpa Lane; BY = Below Young's Dam; LS = Lower Shackleford Creek.

the same weight for all three stream flow categories (CV = 10%) does not affect the much larger sensitivity of the low streamflow observation group when compared to the medium or high streamflow observation groups (not shown).

Parameter correlation coefficients exceeding 0.95, the general threshold at which parameters become nonuniquely estimable (Hill & Tiedeman, 2007), were only observed in two of the parameter sets. A negative correlation was found between specific storage and specific yield for hydraulic property Zones 6 and 8 in Parameter Set 2, which is expected given their relation to storativity. In Parameter Set 4 there was a strong

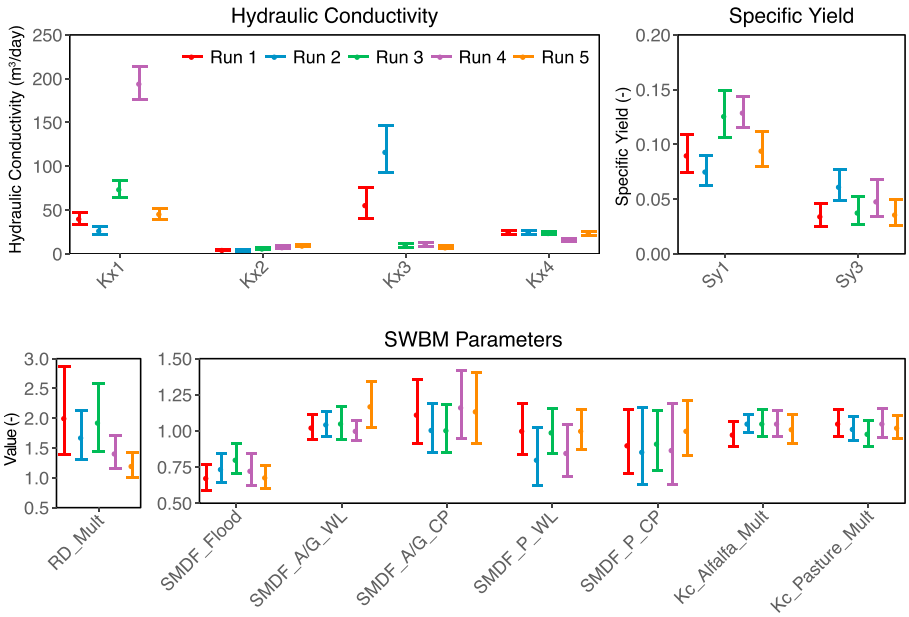

Figure 8. Optimized parameter values for the five calibration runs. Error bars show 95% linear confidence intervals calculated by UCODE_2014. SWBM = soil water budget model.

negative correlation between Wel5 and Wel7, two parameters that control MFR along the eastern boundary of the southern portion of the valley. While correlated, the parameters themselves were found to have low CSS values indicating that they were not suitable for calibration. None of the parameters selected for the calibration were correlated, suggesting that unique calibration estimates may be obtained.

4.3. Calibration

Based on information obtained from the sensitivity analyses, 14 parameters (Table 2) were selected for calibration. Streamflow and groundwater heads simulated by all five calibrated models show very good agreement with observed values (Figure 7). Both interannual and intra-annual streamflow variations are captured at all gage locations, with log-transformed NSEs ranging from 0.61 to 0.91 at all gages for the five calibration runs. Streamflow values are consistently underpredicted at the USGS gage during the winter and spring months when high flow events typically have a time scale much shorter than the monthly stress period. Low flows simulated at gages other than the USGS gage tend to be overestimated during the summer and fall (Figure 7). Simulated groundwater heads show a very strong correlation ($R^2 \geq 0.98$) with observed values, having root-mean-square errors between 2.28 and 2.78 m. Residuals less than or equal to 1, 2, and 3 m accounted for approximately 50%, 70%, and 80% of head observations, respectively.

All five of the calibration runs converged because the objective function did not change more than 1% for three consecutive iterations (TolSOSC convergence). Final objective function values varied between about 1% and 8% difference of each other (Table 2). Although the objective function reached a similar value for all runs, estimates of several parameters varied significantly between calibrations (Figure 8). The largest variations were observed in Kx1, Kx3, and Sy1, which ranged over an order of magnitude for hydraulic conductivity and varied up to 50% for specific yield. Parameters contained within SWBM showed similar variations across runs but with much less variability due to tighter imposed constraints. None of the parameters were calibrated to unreasonable values, with only a few limited by upper or lower calibration bounds.

Linear 95% confidence intervals estimated by UCODE_2014 are relatively narrow for the MODFLOW parameters when compared to the range of estimated values across all five calibration runs. For example, the largest confidence interval for Kx1 was observed in Calibration Run 4 and spanned 38 m/day. This is only 22% of the range in estimated values across all five calibration runs. Conversely, individual linear confidence intervals for SWBM parameters compared to the range in ensemble estimated parameter values are much greater, ranging from 52% to 386%. These linear confidence intervals may not reflect the true parameter

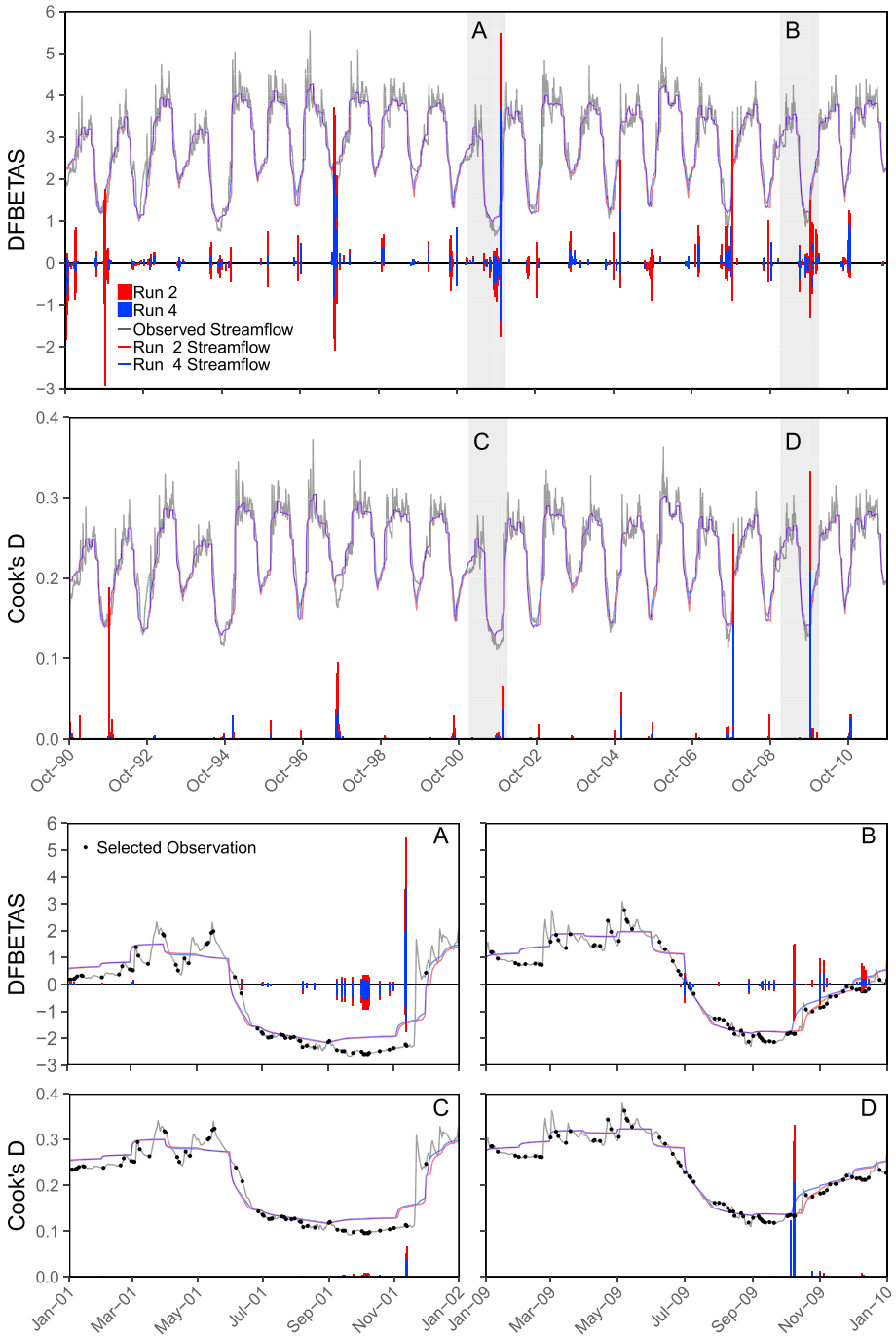

Figure 9. Influence statistics DFBETAS (top row) and Cook's D (bottom row) for streamflow observations at the U.S. Geological Survey gage. Lines show observed (gray) and simulated (red and blue) streamflow values that have been log-transformed and scaled to fit the DFBETAS and Cook's D axes to provide timing context. DFBETAS values are only differentiated by calibration run and not by parameter for plotting purposes. The most influential observations generally occur during or immediately following the lowest streamflow period of the year.

confidence intervals, as the modified Beale's measure ranged from 1.6 to 2.9 times the upper critical value and indicates a highly nonlinear model.

Values of DFBETAS and Cook's D (Figure 9) show that timing of the most influential observations occurs during or immediately following the lowest period of streamflow during the year. Although the seasonal timing of influential observations between the two statistics is similar, the most influential observations

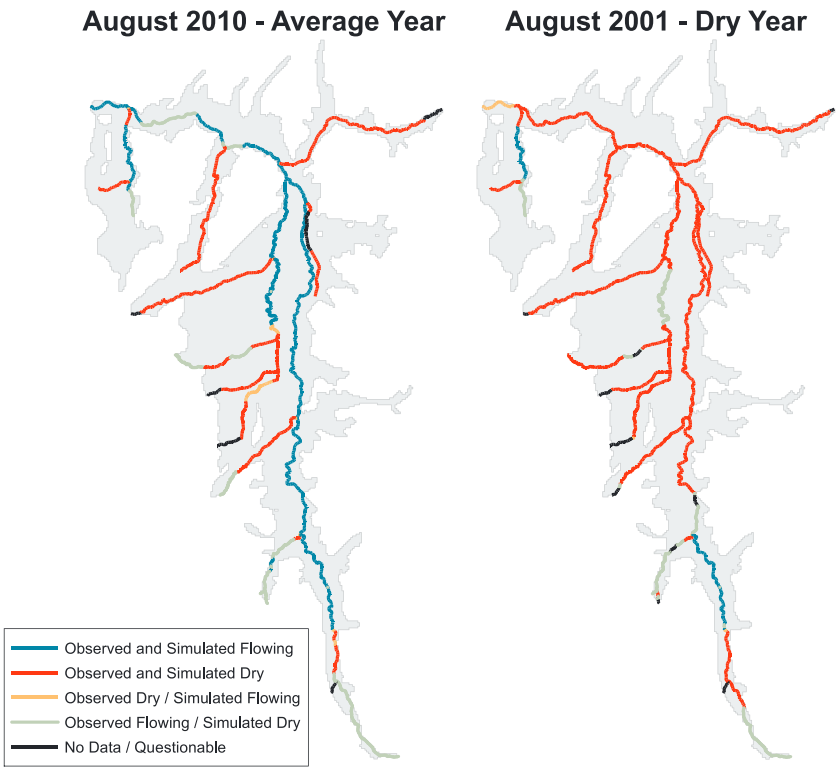

Figure 10. Observed and simulated stream status from Calibration Run 4 at all locations for the month of August in an average and dry water year. Simulated streamflow status shows strong agreement with observed values, indicating the model provides a good representation of streamflow spatially in addition to temporally at the streamflow calibration points (Figure 8).

for the two are located in different years highlighted by the shaded regions in Figure 9. The percentage of observations exceeding critical values ranged from about 15% to 18% for DFBETAS and 6% to 7% for Cook's D. Streamflows accounted for about 64–79% of the observations exceeding critical values, which were predominantly (>90%) low streamflow observations.

4.4. Model Validation

Qualitative streamflow observations of dry and flowing reaches for August in an average (2010) and dry (2001) year were matched by simulated conditions along 81% and 87% of the total stream length, respectively (Figure 10). This binary, spatially continuous information was not included during the calibration process and provides an independent check of model performance. Nearly the entire length of the main stem Scott River and most of the tributaries are accurately predicted for flowing and dry conditions. Some reaches, such as French Creek and portions of the tailings section, Patterson Creek, Big Slough, and Shackleford Creek, appear to have flows that are underpredicted by the model for both water year types (Figure 10). The qualitative, binary validation information suggests SVIHM not only is an excellent prediction tool for flow hydrographs at few existing stream gages but also performs well in predicting the spatial distribution of dry stream sections, the most critical low streamflow predictor for water managers.

5. Discussion

The water budget produced by the model shows the highly dynamic nature of the Scott Valley both seasonally and interannually. This is especially true for groundwater pumping and net groundwater-surface-water fluxes. While we typically associate wet years with less groundwater pumping in agricultural areas (Faunt et al., 2009), this is not always the case. Annual volume of precipitation is important from an overall water budget perspective, but precipitation amounts during the early spring, when the rainy season may overlap with the growing season, influence groundwater pumping rates. For example, 2006 had approximately 50% more total precipitation but also 12% more pumping compared with 2010 (Figure 4). This is because more

precipitation in 2010 fell during the growing season and helped satisfy crop ET demand, thereby reducing the amount of irrigation. Similar instances of this occurrence have been shown in Ruud et al. (2004) and Faunt et al. (2009).

Net fluxes between groundwater and surface water in the first half of the growing season appear to be largely controlled by precipitation and timing of runoff entering the valley from the upper watershed, while the second half is controlled by aquifer storage and groundwater pumping. Seasonal decrease in relative aquifer storage (i.e., cumulative change of groundwater storage relative to the first stress period) over the growing season (March–October) are similar in wet and dry years (Figure 4) due to the Mediterranean climate. In wet years, large gains in storage during the winter contribute to groundwater pumping and increased baseflow during the late summer. In dry years, initial groundwater storage is less and then reduced further by groundwater pumping. In the example average water year type shown, summer pumping affects groundwater storage but recovery begins already in late summer due to early arrival of storms in October (Figure 4). Similar patterns of storage change are observed in other Mediterranean, irrigated groundwater basins (Fleckenstein et al., 2004; CDM, 2008; Brush & Dogrul, 2013).

For highly nonlinear models like SVIHM, sensitivity analysis results show that CSS values and therefore the ranking of parameters by CSS vary as a function of the parameter starting value (Figure 6, top). Since selection of calibration parameters is done by CSS ranking, choice of calibration parameters varies, sometimes drastically, between sensitivity analyses. Simultaneously considering the CSS rankings from multiple sensitivity analyses provides additional information that overcomes the dependency of the (local) sensitivity analysis on the starting values. The very different parameter ranking that appeared in only one of the five sensitivity analyses (Parameter Set 2, Figure 6, top) was considered an outlier. In their more rigorous sensitivity analysis using distributed evaluation of local sensitivity analysis, Rakovec et al. (2014) found that model parameters (including those identified to be most sensitive generally) were insensitive for about 20% of the tested combinations. Here we see the reverse, with parameters that are insensitive in other runs showing greater sensitivity.

The seemingly anomalous sensitivity results for Parameter Set 2 are likely a consequence of overestimation of groundwater heads for one well in Zone 9 and two wells in Zone 5. Although the initial hydraulic conductivity for these zones in Parameter Set 2 is still relatively high at 1–2 m/day (Table 1), they are the lowest of the ensemble. The final calibration values indicate highly conductive aquifer sediments in these zones. The reason for increased sensitivity of some parameters in set three (e.g., Kx3, Kx4, Sy3, and Sy4) is not clear, as there does not appear to be a strong relationship between observations in zones three and four and their initial parameter values.

The most sensitive parameters in SVIHM are crop coefficients for alfalfa and pasture, which control water demand (ET), and the SMDF for alfalfa/grain fields, which affects how much irrigation water is applied and therefore recharge rates for that land use type. At first this appears to be counterintuitive since these parameters are contained in SWBM and subsequently filtered through the MODFLOW model. However, local differences between recharge and pumping (net extraction values) in SVIHM are highly dependent on these parameters. Head distributions resulting from groundwater pumping cannot fully explain this, as head observations generally contribute less than 20% to the CSS values. Instead, a likely driver for this sensitivity to net extraction is streamflow depletion due to groundwater pumping as low flows are proportionally most affected and those observations show the greatest contribution to CSS values. This suggests that groundwater-surface-water models in agricultural areas that fix typically unmeasured pumping rates or adjust them uniformly instead of estimating them based on spatially distributed crop demands and irrigation efficiencies (or SMDF if deficit irrigating) are missing important parameters that significantly influence calibration results. Uncertainty estimates of predicted outcomes obtained from models that do not include the most sensitive model parameters are not likely to span the true range of possible outcomes.

Seasonal average crop coefficient values for alfalfa estimated during model calibration range from 0.88 to 0.95, similar to previously published values of 0.94 for the Scott Valley (Hanson et al., 2011). The SMDF factors for alfalfa also agree with preliminary results from recent research in the Scott Valley that show alfalfa is deficit irrigated in large part due to cutting schedules (S. Orloff, personal communication, July 14th 2017) and irrigation events do not provide enough water to fully satisfy demand. Instead, storage within the effective root zone is continuously depleted as the growing season progresses. This shuts off groundwater recharge under those fields during the growing season. It is not clear whether such deficit irrigation in alfalfa

is common elsewhere. When present, not accounting for deep soil moisture depletion during the growing season would overestimate recharge from alfalfa fields (Luthin & Bianchi, 1954; Orloff & Hanson, 2000; Sanden et al., 2003).

Results from the various calibration runs indicate the model is generally converging to two locations in parameter space. Runs 1, 2, and 5 show lower values for Kx1 and Sy1 compared to those of Runs 3 and 4 (Figure 8). A heuristic explanation for this may be found by considering that the calibration is trying to match low streamflow values during the late summer: If storage near the Scott River (Zone 1) is low, then the hydraulic conductivity must be low as well to keep heads in the aquifer high enough in the late summer to provide a positive gradient to the stream. If heads in the aquifer drop too low streamflow is underestimated. Likewise, if storage near the river increases then the discharge per unit gradient between the aquifer and the stream increases. To compensate, near-stream hydraulic conductivity must increase to reduce the gradient between the aquifer and the stream; otherwise, low streamflow will be overestimated. This correlation between storage and hydraulic conductivity was not observed during the sensitivity analyses, possibly due to the lack of higher-order observations used to define the objective function. This may provide some insight for integrated groundwater-surface-water models in areas where knowledge of aquifer properties is limited and/or higher-order observations are not readily available.

Seasonality of fluxes between groundwater and surface water is driven by high winter and spring flows that recharge the aquifer, which in turn sustain baseflow during the summer and fall. The model produces a large amount of spatial heterogeneity in fluxes between groundwater and surface water for the Scott River, despite reaches having nearly homogenous hydraulic and cross-sectional (conductance) parameterization. Instead, the large spatial heterogeneity is due to undulations in the longitudinal streambed profile: Streambed elevations in the model were assigned using observed thalweg elevations obtained from high-resolution LiDAR and digital elevation model data and are the only stream parameters that have significant spatial variation. Even in a predominantly flat agricultural area like the Scott Valley, the profile of streambed elevations is not uniformly sloping. At the 100-m resolution of the model grid, significant nonuniformity in streambed elevations reflects typical variations in stream geomorphology. This leads to highly variable groundwater-surface water interactions, such as those seen in models that take into account geologic heterogeneity (Fleckenstein et al., 2006) or streambed geomorphic factors at multiple scales (Cardenas, 2009; Stonedahl et al., 2012). Assigned streambed elevations therefore exert a large control on interactions between groundwater and surface water in numerical models.

Influential observations were consistently representing periods of low streamflow. The low sensitivity of the model to medium and high streamflow observations stems from their origin: Medium and high streamflows are largely controlled by specified inflow to the SFR package and not by aquifer properties. During high streamflow, upper watershed streamflow input determines streamflow out of the Scott Valley at the downgradient boundary. It is orders of magnitude larger than baseflow and therefore provides little to no information about aquifer properties. During periods when baseflow dominates (summer and fall), streamflow provides significant information about aquifer flow and storage properties since flow in the stream predominantly reflects groundwater contributions. By extension, low flows also provide information about SWBM parameters that affect groundwater contributions during this time (e.g., crop coefficient and SMDF).

The ensemble calibration results show nonunique parameter estimations when calibration runs start at different locations in the parameter space. This occurred even though the inverse problem is well posed for SVIHM as the number of observations far exceed the number of parameters and no significant correlations were found between calibration parameters. Simulated streamflow and groundwater heads are similar across calibration runs despite some parameter values varying up to an order of magnitude.

Uncertainty estimates from an individual calibration run are lacking as they do not span the entire parameter space over which similar heads and streamflow are produced. Linear confidence intervals are often the only feasible measure of parameter uncertainty for models with significantly long run times as nonlinear analysis methods such as Markov chain Monte Carlo require far too many runs to be of practical use. The minimum number of model runs for a combined sensitivity analysis and calibration in this study was 202, which took a total of 5.8 days to complete when parallelized using five processors. A Markov chain Monte Carlo analysis, assuming (conservatively) a minimum of 1×10^4 nonparallelizable model runs that take 2 hr each, would require 2.3 years. Our results suggest that integrated hydrologic models need to be rigorously evaluated as much as feasibly possible for nonlinear behavior and sensitivity relationships to more

accurately capture sensitivities and resulting uncertainties in parameter estimation and predicted values. This is particularly important in basin-scale simulation models that will ultimately be used to inform decision makers and establish uncertainty ranges as part of project risk analyses and sustainability compliance. The results presented here do not provide a conclusive, rigorous evaluation of sensitivity, such as those provided in other methods (Rakovec et al., 2014; Borgonovo et al., 2017), due to long model runs times. Instead, running a limited number of sensitivity analyses and calibrations using a wide range of starting values provides a frugal heuristic method to capture some key uncertainties associated with nonlinearity inherent in basin-scale integrated groundwater-surface-water models.

6. Conclusions

Agricultural demands and groundwater-surface water conditions for the Scott Valley were simulated over 21 years by weakly coupling a streamflow regression model, a soil-water budget model, and a groundwater-surface-water model. The soil-water budget model operates at the field scale, providing high spatial resolution of groundwater recharge and pumping across the model domain. Coupling the groundwater-surface-water model with the soil-water budget model provided a simple, efficient, and transparent method of estimating groundwater pumping and recharge, two of the biggest forcings for agricultural groundwater basins. Multiple sensitivity analyses show that the most sensitive model parameters are those that control pumping and recharge, which are typically unmeasured and therefore often only available by employing estimation methods. Our work suggests it is important to embed the pumping and recharge estimation model into the sensitivity and calibration process for a a posteriori estimation rather than using values estimated a priori. This provides a quantitative measure of parameter importance across submodels and a more realistic representation of spatially distributed groundwater pumping and recharge across the agricultural landscape. Streamflow observations, particularly during the driest times of the year, provide the most information about model parameters. We did not include higher-order observations (e.g., drawdowns and streamflow differences) in this analysis, but their contributions and if/how they alter the parameter rankings should be explored in future work.

Performing multiple (local) sensitivity analyses and calibrations of this nonlinear integrated model was essential to develop a more comprehensive, quantitative understanding of model parameter importance and uncertainty. As complexity, and likely nonlinearity, of hydrologic models increases, sensitivity analyses and model calibrations must explore more of the parameter space by using multiple sets of initial parameters to gain a better understanding of which model parameters are sensitive overall as opposed to sensitive within a particular area of the parameter space. Calibration of the Scott Valley Integrated Hydrologic Model generally converges to two different areas in parameter space, with both producing results that show good agreement with observations. The use of multiple parallel calibrations revealed greater uncertainty in some model parameters that a single calibration could not detect. Optimized parameter values indicate that groundwater recharge from alfalfa fields is negligible during the growing season due to deficit irrigation. Linear 95% confidence intervals of parameter values calculated within each calibration run are generally very different than the range in estimated parameter values obtained across the five calibrations. Further research into parameter and prediction uncertainty of these weakly coupled, highly nonlinear models may utilize more rigorous nonlinear methods to more precisely define parameter uncertainty.

The Scott Valley Integrated Hydrologic Model shows that a weakly coupled, computationally efficient model can be successfully employed in lieu of an iteratively or fully coupled integrated model to simulate highly dynamic groundwater-surface-water interactions in an agricultural watershed. Computational efficiency and the ability to adjust model structure is an important consideration when developing models to meet the needs of various water managers and stakeholders. The model needs to be complex enough to capture salient hydrologic processes yet usable, modifiable, and capable of having its results communicated to and understood by a broad audience. California is an example of where models like this are likely to see expanded use, as integrated groundwater basin modeling and stakeholder outreach is an important component of the Sustainable Groundwater Management Act regulation that is currently being implemented.

Notation

θ Available soil water

θ_{max} Field capacity

P	Precipitation
ET	Evapotranspiration
ET_0	Reference evapotranspiration
AW	Applied water
R	Recharge
AE	Application efficiency (irrigation efficiency)
SMDF	Soil moisture depletion factor
K_c	Crop coefficient
$_k$	Subscript denoting the day
ϕ	Objective function value
y_i	Observed value
yi'	Simulated value
w_i	Observation weight
i	Observation number
ND	Total number of observations
σ_i^2	Observation error variance
CV_i	Coefficient of variation for streamflow observation
$\overline{y}_i$	Mean of observations
n	Number of observed-simulated data pairs
b_j	jth parameter
b	vector containing initial parameter values
$CSS_{j,s}$	Composite scaled sensitivity of the jth parameter for parameter set s
$\mathbf{CSS_s}$	Array of CSS values for parameter j

Acknowledgments
This research was funded through the California North Coast Regional Water Quality Control Board (SWRCB Agreement 14-020-110). We would like to thank Jim Morris, Sari Sommarstrom, Preston Harris, Erich Yokel, and the Scott Valley groundwater advisory committee. We would also like to thank the reviewers who provided very helpful comments and greatly improved the quality of the manuscript. A link to the SVIHM GitHub repository, which contains all of the model files and postprocessing scripts, can be found in the supporting information. This paper is dedicated to the memory of our wonderful friend, colleague, and researcher, Steve Orloff.

References

Ashby, S. F., & Falgout, R. D. (1996). A Parallel Multigrid Preconditioned Conjugate Gradient Algorithm for Groundwater Flow Simulations. *Nuclear Science and Engineering*, *124*(1), 145–159.

Barlow, P. M., & Leake, S. A. (2012). Streamflow depletion by wells—Understanding and managing the effects of groundwater pumping on streamflow. U.S. Geological Survey Circular 1376.

Borgonovo, E., Lu, X., Plischke, E., Rakovec, O., & Hill, M. C. (2017). Making the most out of a hydrological model data set: Sensitivity analyses to open the model black-box. *Water Resources Research*, *53*, 7933–7950. https://doi.org/10.1002/2017WR020767

Brunner, P., & Simmons, C. T. (2012). HydroGeoSphere: A fully integrated, physically based hydrological model. *Ground Water*, *50*(2), 170–176. https://doi.org/10.1111/j.1745-6584.2011.00882.x

Brunner, P., Simmons, C. T., Cook, P. G., & Therrien, R. (2010). Modeling surface water-groundwater interaction with MODFLOW: Some considerations. *Ground Water*, *48*(2), 174–180. https://doi.org/10.1111/j.1745-6584.2009.00644.x

Brush, C. F., Dogrul, E. C., & Kadir, T. N. (2013). *Development and calibration of the California Central Valley groundwater-surface water simulation model (C2VSim), version 3.02-CG*. California Department of Water Resources: Bay-Delta Office.

California Department of Water Resources (2000). 2000 Siskiyou County land use survey data.

California Department of Water Resources (2016a). *Integrated Water Flow Model: IWFM-2015, Theoretical documentation*. California Department of Water Resources: Bay-Delta Office.

California Department of Water Resources (2016b). *IWFM demand calculator: IDC-2015, Theoretical documentation and user's manual*. California Department of Water Resources: Bay-Delta Office.

Cardenas, M. B. (2009). Stream-aquifer interactions and hyporheic exchange in gaining and losing sinuous streams. *Water Resources Research*, *45*, W06429. https://doi.org/10.1029/2008WR007651

CDM (2008). Butte Basin Groundwater Model Update (Phase II Report, Technical Report).

Chen, X., & Yin, Y. (2001). Streamflow depletion: Modeling of reduced baseflow and induced stream infiltration from seasonally pumped wells. *Journal of the American Water Resources Association*, *37*(1), 185–195. https://doi.org/10.1111/j.1752-1688.2001.tb05485.x

Clark, M. P., & Kavetski, D. (2010). Ancient numerical daemons of conceptual hydrological modeling: 1. Fidelity and efficiency of time stepping schemes. *Water Resources Research*, *46*, W10510. https://doi.org/10.1029/2009WR008894

Clark, M. P., Slater, A. G., Rupp, D. E., Woods, R. A., Vrugt, J. A., Gupta, H. V., et al. (2008). Framework for Understanding Structural Errors (FUSE): A modular framework to diagnose differences between hydrological models. *Water Resources Research*, *44*, W00B02. https://doi.org/10.1029/2007WR006735

Cooley, R. L. (2004). *A theory for modeling ground-water flow in heterogeneous media*, U.S. Geological Survey Professional Paper 1679 (pp. 56). https://doi.org/10.3133/pp1679

Cooley, R. L., & Naff, R. L. (1990). Regression modeling of ground-water flow, *Techniques of water-resources investigations of the United States Geological Survey, Book 3, Chapter B4* (pp. 241).

De Silva, C. S., & Rushton, K. R. (2007). Groundwater recharge estimation using improved soil moisture balance methodology for a tropical climate with distinct dry seasons. *Hydrological Sciences Journal*, *52*(5), 1051–1067. https://doi.org/10.1623/hysj.52.5.1051

Deas, M. L. (2006). Water supply indices: Year types for the Scott River Basin (Technical Report), 29 pages, Watercourse Engineering: Davis, CA.

Dettinger, M. D., Udall, B., & Georgakakos, A. (2015). Western water and climate change. *Ecological Applications*, *25*(1), 2069–2093. https://doi.org/10.1890/15-0938.1

Dieter, C., Maupin, M., Caldwell, R., Harris, M., Ivahnenko, T., Lovelace, J., et al. (2018). *Estimated use of water in the United States in 2015* (pp. 1441). U.S. Geological Survey Circular. https://doi.org/10.3133/cir1441

Dogrul, E. C., Kadir, T. N., & Brush, C. H. (2018). *IWFM demand calculator, IDC-2015, Revision 68, theoretical documentation and user's manual* (pp. 325). California Department of Water Resources: Bay-Delta Office. https://doi.org/10.3133/cir1441

Echols, K. G. (1991). Scott River flow augmentation study (Technical report): California Department of Water Resources.

Faunt, C. C., Hanson, R. T., Belitz, K., Schmid, W., Predmore, S. P., Rewis, D. L., & McPherson, K. (2009). *Groundwater availability of the Central Valley Aquifer California* (pp. 246): U.S. Geological Survey Professional Paper 1766.

Fleckenstein, J., Anderson, M., Fogg, G., & Mount, J. (2004). Managing surface water-groundwater to restore fall flows in the Cosumnes River. *Journal of Water Resources Planning and Management*, *130*(4), 301–310. https://doi.org/10.1061/(ASCE)0733-9496(2004)130:4(301)

Fleckenstein, J., Niswonger, R. G., & Fogg, G. E. (2006). River-aquifer interactions, geologic heterogeneity, and low-flow management. *Ground Water*, *44*(6), 837–852. https://doi.org/10.1111/j.1745-6584.2006.00190.x

Foglia, L., Hill, M. C., Mehl, S. W., & Burlando, P. (2009). Sensitivity analysis, calibration, and testing of a distributed hydrological model using error-based weighting and one objective function. *Water Resources Research*, *45*, W06427. https://doi.org/10.1029/2008WR007255

Foglia, L., McNally, A., Hall, C., Ledesma, L., & Hines, R. (2013). Scott Valley Integrated Hydrologic Model: Data collection, analysis, and water budget (Technical report). Davis: University of California.

Foglia, L., McNally, A., & Harter, T. (2013). Coupling a spatiotemporally distributed soil water budget with stream-depletion functions to inform stakeholder-driven management of groundwater-dependent ecosystems. *Water Resources Research*, *49*, 7292–7310. https://doi.org/10.1002/wrcr.20555

Foglia, L., Neumann, J., Tolley, D. G., Orloff, S. B., Snyder, R. L., & Harter, T. (2018). Modeling guides groundwater management in a basin with river-aquifer interactions. *California Agriculture*, *72*(1), 84–95. https://doi.org/10.3733/ca.2018a0011

Furman, A. (2008). Modeling coupled surface-subsurface flow processes: A review. *Vadose Zone Journal*, *7*(2), 741–756. https://doi.org/10.2136/vzj2007.0065

Hanson, R. T., Boyce, S. E., Schmid, W., Hughes, J. D., Mehl, S. M., Leake, S. A., et al. (2014). One-Water Hydrologic Flow Model (MODFLOW-OWHM), U.S. Geological Survey Techniques and Methods 6-A51.

Hanson, R. T., Flint, L. E., Flint, A. L., Dettinger, M. D., Faunt, C. C., Cayan, D., & Schmid, W. (2012). A method for physically based model analysis of conjunctive use in response to potential climate changes. *Water Resources Research*, *48*, W00L08. https://doi.org/10.3133/sir20145111

Hanson, B., Orloff, S., & Putnam, D. (2011). Drought irrigation strategies for Alfalfa. *Agricultural and Natural Resources (University of California)*, *8448*, 1–10.

Hanson, R. T., Ritchie, A. B., Boyce, S. E., Galanter, A. E., Ferguson, I. A., Flint, L. E., & Henson, W. R. (2018). Rio Grande transboundary integrated hydrologic model and water-availability analysis. New Mexico and Texas, United States, and Northern Chihuahua, Mexico: U.S. Geological Survey Open-File Report 2018-1091.

Hanson, R., Schmid, W., Faunt, C. C., Lear, J., & Lockwood, B. (2014). Integrated hydrologic model of Pajaro Valley, Santa Cruz and Monterey Counties, California. *U.S. Geological Survey Scientific Investigations Report*, 2014–5111. https://doi.org/10.3133/sir20145111

Harbaugh, A. W. (2005). MODFLOW-2005, The U.S. Geological Survey modular ground-water model—The ground-water flow process: U.S. Geological Survey Techniques and Methods 6-A51.

Hill, M. C., & Tiedeman, C. R. (2007). *Effective groundwater model calibration: With analysis of data, sensitivities, predictions, and uncertainty*. Hoboken, NJ: John Wiley & Sons, Inc.

Hill, M. C., Kavetski, D., Clark, M., Ye, M., Arabi, M., Lu, D., et al. (2016). Practical use of computationally frugal model analysis methods. *Groundwater*, *54*(2), 159–170. https://doi.org/10.1111/gwat.12330

Howard, J., & Merrifield, M. (2010). Mapping groundwater dependent ecosystems in California. *PLoS ONE*, *5*(6), e11249. https://doi.org/10.1371/journal.pone.0011249

Huntington, J. L., & Niswonger, R. (2012). Role of surface-water and groundwater interactions on projected summertime streamflow in snow dominated regions: An integrated modeling approach. *Water Resources Research*, *48*, W11524. https://doi.org/10.1029/2012WR012319

Irwin, W. P. (1990). The San Andreas Fault System, California: U.S. Geological Survey Professional Paper 1515.

Jain, S., & Sudheer, K. (2008). Fitting of hydrologic models: A close look at the Nash-Sutcliffe index. *Journal of Hydrologic Engineering*, *10*(13), 981–986. https://doi.org/10.1061/(ASCE)1084-0699(2008)13:10(981)

James M. Montgomery Consulting Engineers (1990). Central Valley ground-surface water model, Central Valley, California (Technical Report).

Jousma, G., Bear, J., & Haimes, Y. Y. (2012). *Groundwater contamination: Use of models in decision-making, Proceedings of the International Conference on Groundwater Contamination, Amsterdam, The Netherlands, 26–29 October 1987 Organized by the International ground water modeling center (IGWMC)*. Indianapolis - Delft: Springer Science and Business Media.

Kavetski, D., & Clark, M. P. (2010). Ancient numerical daemons of conceptual hydrological modeling: 2. Impact of time stepping schemes on model analysis and prediction. *Water Resources Research*, *46*, W10511. https://doi.org/10.1029/2009WR008896

Kløve, B., Ala-Aho, P., Bertrand, G., Gurdak, J. J., Kupfersberger, H., Kværner, J., et al. (2014). Climate change impacts on groundwater and dependent ecosystems. *Journal of Hydrology*, *518*, 250–266. https://doi.org/10.1016/j.jhydrol.2013.06.037

Kollet, S. J., & Maxwell, R. M. (2006). Integrated surface-groundwater flow modeling: A free-surface overland flow boundary condition in a parallel groundwater flow model. *Advances in Water Resources*, *29*(7), 945–958. https://doi.org/10.1016/j.advwatres.2005.08.006

La Vigna, F., Hill, M. C., Rossetto, R., & Mazza, R. (2016). Parameterization, sensitivity analysis, and inversion: An investigation using groundwater modeling of the surface-mined Tivoli-Guidonia basin (Metropolitan City of Rome, Italy). *Hydrogeology Journal*, *24*(6), 1423–1441. https://doi.org/10.1007/s10040-016-1393-z

Lane, B. A., Sandoval-Solis, S., & Porse, E. C. (2015). Environmental flows in a human-dominated system: Integrated water management strategies for the Rio Grande/Bravo Basin. *River Research and Applications*, *31*. https://doi.org/10.1002/rra.2804

Luthin, J. N., & Bianchi, W. (1954). Alfalfa and water table levels. *California Agriculture*, *8*(5), 4–5.

Mack, S. (1958). Geology and ground-water features of Scott Valley, Siskiyou County, California, U.S.: Geological Survey water-supply paper 1462.

Manghi, F., Mortazavi, B., Crother, C., & Hamdi, M. R. (2012). Estimating regional groundwater recharge using a hydrological budget method. *Water Resources Management*, *23*(12), 2475–2489. https://doi.org/10.1007/s11269-008-9391-0

Markstrom, S. L., Niswonger, R. G., Regan, R. S., Prudic, D. E., & Barlow, P. M. (2008). SFLOW-coupled ground-water and surface water flow model based on the integration of the Precipitation-Runoff Modeling System (PRMS) and the Modular Ground-Water Flow Model (MODFLOW-2005): U.S. Geological Survey, Techniques and Methods 6-D1.

McMahon, P., Dennehy, K., Michel, R., Sophocleous, M., Ellett, K., & Hurlbut, D. B. (2003). Water movement through thick unsaturated zones overlying the Central High Planes Aquifer, Southwestern Kansas, 2000-2001. U.S. Geological Survey Water-Resources Investigations Report 03-4171.

Mendoza, P. A., Clark, M. P., Barlage, M., Rajagopalan, B., Samaniego, L., Abramowitz, G., & Gupta, H. (2015). Are we unnecessarily constraining the agility of complex process-based models? (*1*). https://doi.org/10.1002/2014WR015820

Miller, C. T., & Pinder, G. F. (2004). *Computational methods in water resources: Volume 2: Proceedings of the XVth International Conference on Computational Methods in Water Resources (CMWR XV)*. Chapel Hill, USA: NC.

NCRWQCB (2005). *Staff report for the action plan for the Scott River watershed sediment and temperature total maximum daily loads*. Santa Rosa, CA: North Coast Regional Water Quality Control Board.

Nash, J. E., & Sutcliffe, J. V. (1970). River flow forecasting through conceptual models Part 1—A discussion of principles. *Journal of Hydrology*, *10*, 282–290. https://doi.org/10.1016/0022-1694(70)90255-6

Niswonger, R. G., Panday, S., & Ibaraki, M. (2011). MODFLOW-NWT, A Newton formulation for MODFLOW-2005, U.S. Geological Survey Techniques and Methods 6—A37.

Orloff, S. B., & Hanson, B. (2000). Monitoring alfalfa water use with soil moisture sensors. In *proceedings of the 30th California Alfalfa Symposium*.

Phillips, S. P., ewis, D. L., & Traum, J. A. (2015). Hydrologic model of the Modesto Region, California, 1960–2004, U.S. Geological Survey Scientific Investigations Report.

Poeter, E. P., & Hill, M. C. (1998). Documentation of UCODE, A computer code for universal inverse modeling, U.S. Geological Survey Water-Resources Investigations Report 98-4080, 457–462.

Poeter, E. P., Hill, M. C., Lu, D., & Tiedeman, C. R. (2014). *UCODE_2014 , with new capabilities to define parameters unique to predictions, calculate weights using simulated values, estimate parameters with SVD, evaluate uncertainty with MCMC, and more, Integrated Groundwater Modeling Center*. IGWMC: Colorado School of Mines.

Pokhrel, Y. N., Koirala S., Yeh, P. J. F., Hanasaki, N., Longuevergne, L., Kanae, S., & Oki, T. (2015). Incorporation of groundwater pumping in a global Land Surface Model with the representation of human impacts. *Water Resources Research*, *51*, 78–96. https://doi.org/10.1002/2014WR015602

Prudic, D. (1989). Documentation of a computer program to simulate stream-aquifer relations using a modular, finite-difference ground-water flow model, U.S. Geological Survey Open-File Report 88-729.

Prudic, D. E., Konikow, L. F., & Banta, E. R. (2004). A new streamflow-routing (SFR1) package to simulate stream-aquifer interaction with MODFLOW-2000: U.S. Geological Survey Open-File Report 2004-1042, 104 pages.

Rakovec, O., Hill, M. C., Clark, M. P., Weerts, A. H., Teuling, A. J., & Uijlenhoet, R. (2014). Distributed Evaluation of Local Sensitivity Analysis (DELSA), with application to hydrologic models. *Water Resources Research*, *50*, 409–426. https://doi.org/10.1002/2013WR014063

Ramireddygari, S. R., Sophocleous, M. A., Koelliker, J. K., Perkins, S. P., & Govindaraju, R. S. (2000). Development and application of a comprehensive simulation model to evaluate impacts of watershed structures and irrigation water use on streamflow and groundwater: The case of Wet Walnut Creek Watershed, Kansas, USA. *Journal of Hydrology*, *236*, 223–246. https://doi.org/10.1016/S0022-1694(00)00295-X

Roark, M., & Healy, D. F. (1998). Quantification of deep percolation from two flood irrigated alfalfa fields, Roswell basin, New Mexico: U.S. Geological Survey Water-Resources Investigations Report 98-4096, 39 pages.

Ruud, N., Harter, T., & Naugle, A. (2004). Estimation of groundwater pumping as closure to the water balance of a semi-arid, irrigated agricultural basin. *Journal of Hydrology*, *297*, 51–73. https://doi.org/10.1016/j.jhydrol.2004.04.014

S. S. Papadopulos and Associates, Inc. (2000). Middle Rio Grande Water Supply Study (Technical Report), p. 338.

S. S. Papadopulos and Associates, Inc. (2012). Groundwater conditions in Scott Valley, California (Technical Report), p. 130.

SWRCB (1999). Water Right Decision 1641, California State Water Resources Control Board, Californa Environmental Protection Agency, 207 pages.

Sanden, B., Poole, G., & Hanson, B. (2003). Soil moisture monitoring in alfalfa: Does it pay?. In *Proceedings of the 33rd California Alfalfa Symposium*.

Schmid, W., & Hanson, R. (2005). The Farm Process Version 2 (FMP2) for MODFLOW-2005: Modifications and upgrades to FMP1, U.S. Geological Survey Techniques and Methods 6-A-32. p. 116.

Schmid, W., Hanson, R., Maddock, T. I., & Leake, S. A. (2000). User Guide for the Farm Process (FMP1) for the U .S. Geological Survey's modular three-dimensional finite-difference ground-water flow model, MODFLOW-2000 U.S. Geological Survey Techniques and Methods 6-A17. p. 140.

Singh, A. (2014). Groundwater resources management through the applications of simulation modeling: A review. *Science of the Total Environment*, *414–423*. https://doi.org/10.1016/j.scitotenv.2014.05.048

Stark, J. R., Armstrong, D. S., & Zwilling, D. R. (1994). Stream-aquifer interactions in the Straight River area, Becker and Hubbard Counties, Minnesota (*U.S. Geological Survey Water-Resources Investigation Report 94-4009*). p. 92.

Stonedahl, S. H., Harvey, J. W., Detty, J., Aubeneau, A., & Packman, A. I. (2012). Physical controls and predictability of stream hyporheic flow evaluated with a multiscale model. *Water Resources Research*, *48*, W10513. https://doi.org/10.1029/2011WR011582

Taylor, R. G., Scanlon, B., Döll, P., Rodell, M., van Beek, R., Wada, Y., et al. (2012). Ground water and climate change. *Nature Climate Change*, *3*, 1–9. https://doi.org/10.1038/NCLIMATE1744

Therrien, R., & Sudicky, E. A. (1996). Three-dimensional analysis of variably-saturated flow and solute transport in discretely-fractured porous media. *Journal of Contaminant Hydrology*, *23*(95), 1–44. https://doi.org/10.1016/0169-7722(95)00088-7

U.S. Department of War (1938). Report of the Chief of Engineers, U.S. Army (Technical Report): U.S. Army Corps of Engineers.

University of California at Davis (2016). Scott Valley, Siskiyou County, California: Voluntary Private Well Water Monitoring Program, Spring 2006 - January 2016 (PowerPoint Slides). retrieved from http://groundwater.ucdavis.edu/Research/ScottValley/

Unland, N. P., Cartwright, I., Andersen, M. S., Rau, G. C., Reed, J., Gilfedder, B. S., et al. (2013). Investigating the spatio-temporal variability in groundwater and surface water interactions: A multi-technique approach. *Hydrology and Earth System Sciences*, *17*(9), 3437–3453. https://doi.org/10.5194/hess-17-3437-2013

U.S. Geological Survey (2015). National Water Information System data available on the World Wide Web (USGS Water Data for the Nation). accessed [October 11, 2015], at URL [http://waterdata.usgs.gov/nwis/], U.S. Geological Survey.

Van Kirk, R. W, & Naman, S. W. (2008). Erratum to Van Kirk and Naman (2008). Relative effects of climate and water use on base-flow trends in the Lower Klamath Basin. *Journal of the American Water Resources Association*, *44*(4), 1053–1054. https://doi.org/10.1111/j.1752-1688.2008.00235.x

Van Roosmalen, L., Sonnenborg, T. O., & Jensen, K. H. (2009). Impact of climate and land use change on the hydrology of a large-scale agricultural catchment. *Water Resources Research*, *45*, W00A15. https://doi.org/10.1029/2007WR006760

Watershed Sciences (2010). LiDAR remote sensing data collection, Scott Valley, California (*Technical Report*). Submitted to Tetra Tech on November 11th, 2010, 28 pages.

Weaver, J. E. (1926). *Root development of field crops* (pp. 167). New York, NY: McGraw-Hill.

Wilson, J. L., & Guan, H. (2013). Mountain-block hydrology and mountain-front recharge. In J. Hogan, F. Phillips, & B. Scanlon (Eds.), *Groundwater recharge in a desert environment: The southwestern United States* (pp. 113–137). Washington, DC: American Geophysical Union.

Yager, R. M. (1998). Detecting influential observations in nonlinear regression modeling of groundwater flow. *Water Resources Research*, *34*(7), 1623–1633.

Yin, L., Hu, G., Huang, J., Wen, D., Dong, J., Wang, X., & Li, H. (2011). Groundwater-recharge estimation in the Ordos Plateau, China: Comparison of methods. *Hydrogeology Journal*, *19*(8), 563–157. https://doi.org/10.1007/s10040-011-0777-3

Data Gap Assessment

INTRODUCTION

Multiple datasets were utilized during development of this GSP to characterize current and historical Basin conditions. Monitoring networks were designed to support the evaluation of Basin conditions throughout GSP implementation, particularly with respect to the six sustainability indicators. The representative monitoring points (RMPs) in these monitoring networks are sites at which quantitative values for minimum or maximum thresholds, measurable objectives, and interim milestones are defined. New RMPs will be considered for the 5-years update based on the suggested expanded monitoring network. Data gaps that were identified throughout the GSP development process can be categorized into:

I. Data gaps in information used to characterize current and historical basin conditions.
II. Data gaps in monitoring networks developed to evaluate future Basin conditions which will be used in reporting and tracking Basin sustainability.
III. Additional data or information valuable for measuring progress towards the Basin's sustainability goal. This information has been identified as information that may be useful but has not been confirmed as a data gap,

These data gaps were identified based on spatial coverage of data, period for which data are available, frequency of data collection and representativeness of Basin conditions. An overview of data gaps in the first category is provided in Chapter 2, as part of the characterization of past and current Basin conditions, and the data gaps in the second and third categories are in Chapter 3 as part of descriptions of the monitoring networks. This appendix details the identification of data gaps and uncertainties in each of the categories and the associated strategies for addressing them. The process of data gap identification, and development of strategies to fill data gaps is illustrated in Figure 1 below, sourced from the Monitoring Networks and Identification of Data Gaps Best Management Practice (BMP), provided by DWR (2016).

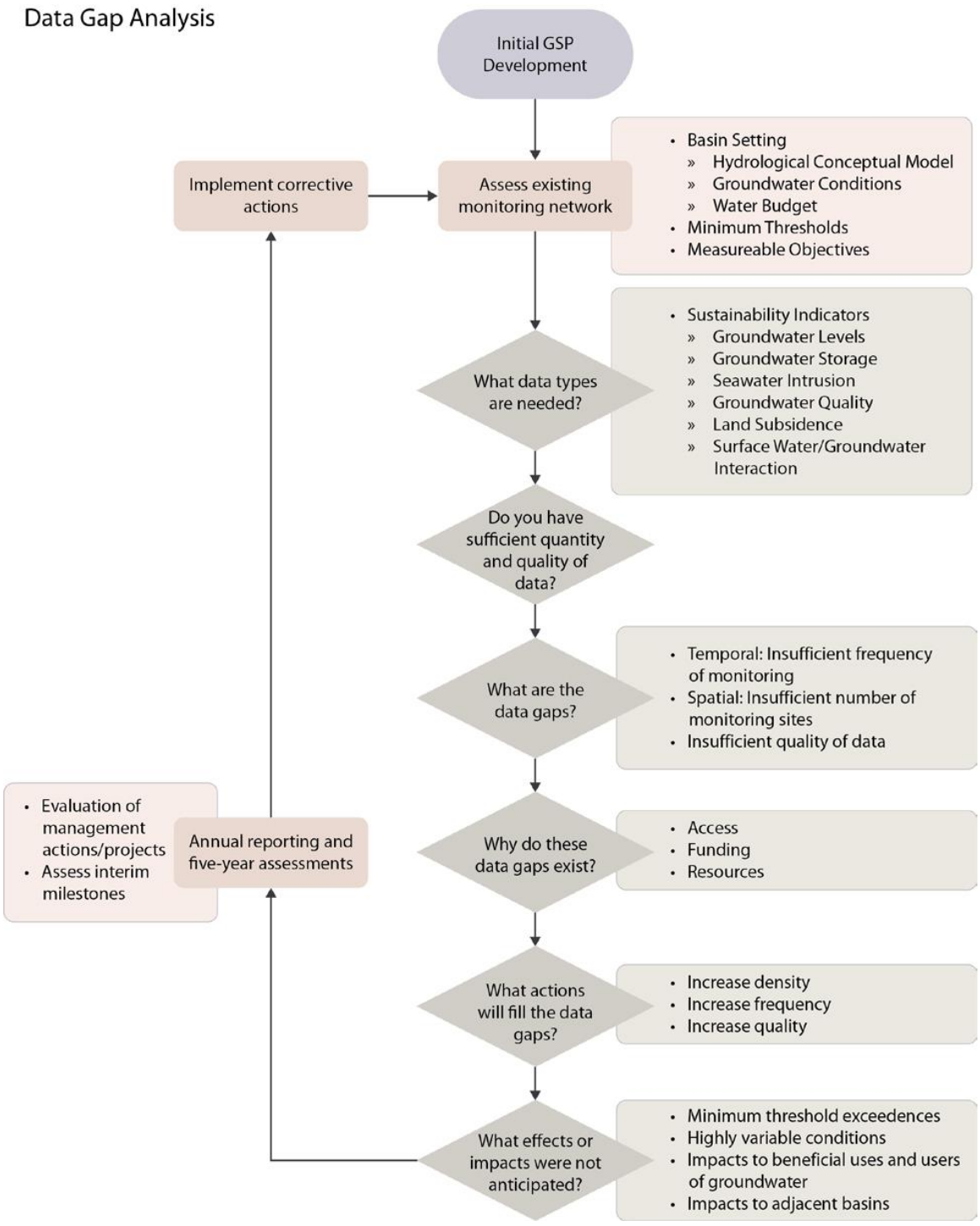

Figure 1: Data Gap Analysis Flowchart (DWR 2016)

I. DATA GAPS IN EXISTING INFORMATION USED FOR BASIN CHARACTERIZATION

Definition of the hydrogeological conceptual model (HCM) is a key requirement for understanding the Basin setting and characterizing existing and historical Basin conditions. An accurate assessment of the physical setting and processes that control groundwater occurrence in the Basin and is foundational to development of the sustainable management criteria and monitoring networks in Chapter 3 and identification of projects and management actions in Chapter 4.

Identification of data gaps and uncertainty within the HCM is a requirement per 23 CCR 354.14 (b)(5) and is important to inform locations and types of additional monitoring to reduce these gaps and uncertainties.

Identification of Data Gaps

The HCM is detailed in Chapter 2 of this GSP. Data gaps and uncertainties were identified throughout development of the HCM and are briefly discussed in Chapter 2 under applicable subsections. A discussion of the components of the HCM for which key datasets were used, associated data gaps, and uncertainties is provided below.

Climate

Long-term records are available from National Oceanic and Atmospheric Administration (NOAA) weather stations in and around Scott Valley. A list of the applicable NOAA weather stations used in development of the climate component of the HCM can be found in Section 2.2.1.2. Data from these stations were used to evaluate historical and current precipitation and evaluate spatial and temporal (seasonal and long-term) trends in precipitation. Maximum and minimum air temperatures from 1936 to 2020 were obtained from the Fort Jones Ranger Station (USC00043182), and reference evapotranspiration (ET) from 2015 to 2019 is calculated at CIMIS Station 225, near Fort Jones. Temperature and ET data was used to evaluate short and long-term trends in the Basin. Snow measurement data is available in multiple stations in the Scott River Watershed through the California Data Exchange Center (CDEC). A full list of these stations is included in Section 2.2.1.2.

Current and historical climate data is readily available for Scott River watershed (Watershed) and has sufficient spatial coverage, frequency of measurement and length of record to evaluate current and historical conditions and identify trends. Based on an initial assessment of the data, a rainfall gradient is suspected but not confirmed in the Watershed. The presence of a rainfall gradient is an uncertainty in this section of the HCM.

Rainfall data collected from rain gauges in additional locations (such as those where continuous groundwater monitoring sensors have been deployed) could be used to confirm the presence of a rainfall gradient.

Geology

The primary sources of information used in development of the geology section of the HCM are the California Geologic Survey digitized geologic map (Charles W. Jennings, with modifications by Carlos Gutierrez, William Bryant and Wills 2010), and the foundational geologic report (Mack 1958). The presence and/or extent of confining or semi-confining layers has been identified as a data gap in this section.

Soils

A 1983 soil survey of central Siskiyou County (USDA 1983) was the primary source used for development of this component of the HCM. Additionally, soil properties as they relate to groundwater recharge were characterized through the Soil Agricultural Banking Index (SAGBI) ratings for the soil series in the Scott Valley area can be viewed on a web application (app), developed by the California Soil Resource Lab at the University of California at Davis and University of California Agriculture and Natural Resources (UC Davis Soil Resource Lab and University of California Agriculture and Natural Resources 2019).

No data gaps were identified in the development of this section.

Hydrology

The hydrology and natural flow regime in Scott Valley have been discussed in detail in previous reports (i.e., SRWC 2005). Streamflow data is primarily available from the Fort Jones USGS stream gauge (11519500). This flow data is used to evaluate the long-term streamflow record (available dating back to the 1940s), trends in streamflow with water year types, and evaluate seasonal and long-term streamflow trends. As detailed in Section 2.2.1.6, shorter streamflow records are available for numerous tributaries in the Basin but long term, consistent records are not available.

Streamflow records on the tributaries were identified as a data gap, both for long-term records and for current conditions. A streamflow gauge on the mainstem of Scot River was also identified as a useful monitoring tool. Additionally, while the magnitude of flows on the tributaries to Scott River is recognized to be strongly correlated to flows at the Fort Jones gauge (Foglia et al., 2013, Deas and Tanaka, 2005), this relationship has not been well-defined. Quantifying impacts to streamflow in the tributaries with changes in flow rates at the Fort Jones gauge is therefore difficult. This relationship, particularly flow rates at which stream disconnection occurs, is important in defining ecological implications,

particularly for anadromous fish, which rely on flows in the tributaries for several life stages, as discussed in Section 2.2.1.8.

In summary, new streamgauges in the tributaries and along the mainstem of the Scott river would be helpful to fill this data gap (see Figure 2).

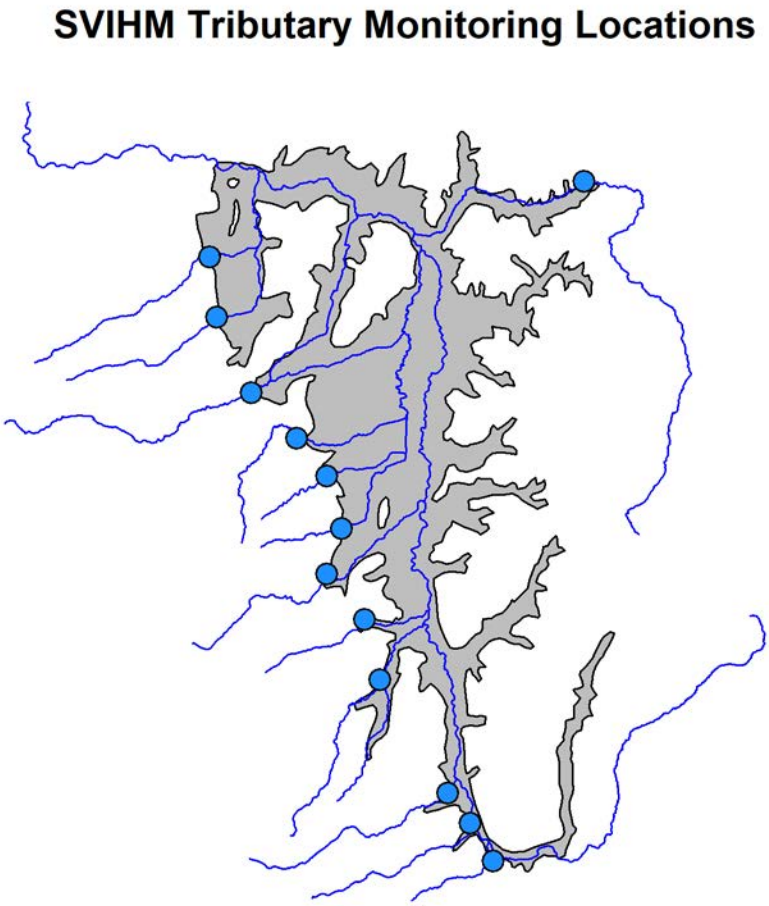

Figure 2. Ideally, tributary monitoring locations could geolocated in the vicinity of the inflows into the SVIHM model domain, as shown above.

Identification of Interconnected Surface Water Systems

While interconnected surface water systems were identified in Section 2.1.1.7, there are uncertainties in this identification. A continuous saturated zone between the stream and

aquifer is assumed for all locations that were identified as interconnected surface waters, as no locations are known to be separated from the water table by thick unsaturated zones, but this has not been physically confirmed.

New streamgauges and new monitoring wells with continuous data collection, combined with seepage runs will provide stronger support to the conclusion presented in this GSP.

Identification of Groundwater Dependent Ecosystems

Data from the National Wetlands Inventory, The Nature Conservancy, and other sources (as detailed in Section 2.2.1.8) was used to identify groundwater dependent ecosystems (GDEs) in the Basin. While the results of the initial GDE inventory were evaluated by the Surface Water Ad Hoc Committee, physical verification has not been completed. There is therefore some uncertainty between riparian and non-riparian GDEs that were mapped and the existence and extent of these GDEs on the ground.

Ground truthing of the identified GDEs will help to verify the GDE identification and mapping that has been completed so far. Collaboration with CDFW, and/or other agencies with expertise in identifying, evaluating, and monitoring GDEs will support GDE consideration throughout the implementation of this GSP. Satellite images evaluated twice per year would provide information on the health of GDEs over time and would be critical to fully understand their seasonal cycles.

Groundwater Dependent Ecosystems Health and Habitat Requirements

Several species of fish are prioritized for management in the Basin. CDFW's juvenile salmonid outmigrant monitoring program tracks coho and Chinook salmon populations returning to the Basin. Additionally, juvenile salmonid outmigrant monitoring provides data on another critical life cycle stage of fish in the Basin. Within the groundwater dependent ecosystem discussion in Chapter 2, there are some data gaps in habitat requirements. For example, while there are return numbers for coho and Chinook salmon, there is less data available for steelhead as migration occurs largely outside of the time that the Scott River Fish County Facility is operational (Knechtle 2021). While juvenile outmigrant monitoring does exist, flow requirements for juvenile salmonids are not clearly known.

The GSA will continue to use monitoring data from existing programs and will coordinate with agencies that conduct this monitoring to gain a better understanding of flow requirements for all life stages for these species of anadromous fish.

Current and Historical Groundwater Conditions

Groundwater Elevation Data

A total of 85 wells with groundwater elevation data are available in the Basin. Groundwater elevation data is sourced primarily from the California Statewide Groundwater Elevation Monitoring Program (CASGEM), Quartz Valley Indian

Reservation (QVIR) and the Scott Valley Community Groundwater Measuring Program. Well data is available dating back to the 1960s and wells have adequate spatial coverage of the Basin, measurement frequency and period of record. CASGEM, QVIR and Scott Valley Community Groundwater Measuring Program wells are measured at a frequency of bi-annually, with the exception of the Scott Valley Community Groundwater Measuring Program which is measured monthly. These frequencies are sufficient to enable determination of seasonal, short-term, and long-term trends. With implementation of new Projects and Management Actions, pressure transducers with continuous record of water level and temperature have been considered essential. For the NFWF Scott Recharge Project (see Chapter 4 and Appendix 4-B) five transects with continuous groundwater data on existing groundwater wells are already being installed (5 wells are already collecting data). Other continuous data have been funded through a Bureau of Reclamation SmartWater grant and currently 10 wells had instruments installed in 2021.

A summary of the wells with groundwater elevation data, and additional available information is shown in **Error! Reference source not found.**. Continuous groundwater monitoring locations are shown in Figure 3.

Table 1: Wells with groundwater elevation data in the Scott River Valley Basin

Wells	Groundwater Basin
Wells with coordinates (including data from WCRs referenced to nearest PLSS section)	295
Wells with screen depth information	62
Wells with coordinates and recent[1] water level data	74
Wells with pumping data	None

[1] Recent is here used to refer to data from the past ten years.

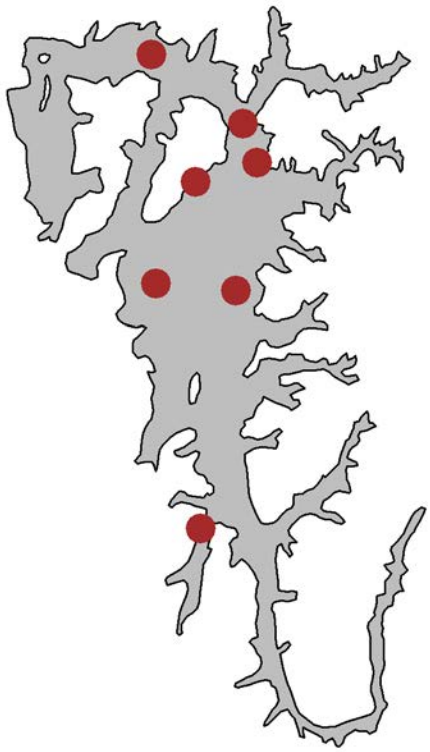

Figure 3. Continuous groundwater monitoring locations (as of September 2021).

Estimate of Groundwater Storage

Groundwater storage data is available from the foundational geological report (Mack 1958) and specific yield and storativity were estimated using the Scott Valley Integrated Hydrologic Model (SVIHM). No data gaps have been identified for this section, however continuous groundwater level data would be useful for evaluation of changes in groundwater storage.

Groundwater Extraction Data

No pumping monitoring program currently exists in the Basin and this data is not available for any of the wells with groundwater elevation data. Although this is estimated using the SVIHM, reported groundwater extraction data has been identified as a data gap.

Surface Water Diversion Data – stock water

Surface water diversions for irrigation are estimated using SVIHM. However, surface water diversion data for watering livestock is not explicitly modeled in SVIHM, and has been identified as a data gap.

Groundwater Quality

Groundwater quality data was obtained from several sources including the California Groundwater Ambient Monitoring and Assessment (GAMA) Program Database, the USEP Storage and Retrieval Data Warehouse (STORET), GeoTracker GAMA and data from QVIR groundwater quality monitoring. As detailed in Appendix 2-B, available water quality data were compared to regulatory standards and mapped. Constituents of concern were identified through visual analysis of recent data (within the past 30 years) of the generated maps and timeseries for each constituent (available in appendix 2-B). As seen on these maps, and noted in Section 2.2.2.3, there are multiple data gaps in the groundwater quality information used to develop the HCM. Spatially, groundwater quality data is frequently concentrated near Fort Jones and Etna and coverage in other areas of the Basin is missing for multiple constituents. Additionally, most of the groundwater quality data used in the assessment did not have a long record with consistent measurements, or measurements with a frequency that would be sufficient for determination of historical trends in groundwater quality. Further data gap discussion and the strategy for filling these data gaps is discussed under the groundwater quality monitoring network associated with Chapter 3, below.

Additional water quality monitoring data is being collected by the North Coast Water Quality Control Board and this data will be utilized by the GSA in future reporting.

Land Subsidence Conditions

Land subsidence data is entirely sourced from the TRE Altamira Interferometric Synthetic Aperture Radar (InSAR) dataset which provides estimates of vertical displacement from January 2015 to June 2015. No data gaps were noted in this section.

Water Budget

The water budget is dependent on monitoring data inputs. For data gaps in the water budget see previous sections on climate and hydrology (i.e., tributary) data gaps.

DATA GAPS MONITORING NETWORKS

Requirements

Multiple data gap requirements are relevant to the definition of monitoring networks for sustainability indicators. Per 23 CCR 354.38 ("Assessment and Improvement of Monitoring Network"):

(a) Each Agency shall review the monitoring network and include an evaluation in the Plan and each five-year assessment, including a determination of uncertainty and whether there are data gaps that could affect the ability of the Plan to achieve the sustainability goal for the basin.
(b) Each Agency shall identify data gaps wherever the basin does not contain a sufficient number of monitoring sites, does not monitor sites at a sufficient frequency, or utilizes monitoring sites that are unreliable, including those that do not satisfy minimum standards of the monitoring network adopted by the Agency
(c) If the monitoring network contains data gaps, the plan shall include a description of the following:
    a. The location and reason for data gaps in the monitoring network
    b. Local issues and circumstances that prevent monitoring
(d) Each Agency shall describe steps that will be taken to fill the data gaps before the next five-year assessment, including the location and purpose of newly added or installed monitoring sites.

The following discussion summarized the identified data gaps, description, and strategy to fill the identified data gaps.

Groundwater Level and Storage Monitoring Network

Though not identified as a data gap, continuous groundwater level and temperature data would be useful for the groundwater level and storage monitoring network (as discussed above).

Groundwater Quality Monitoring Network

Requirements

Requirements for the monitoring network for the degraded water quality sustainability indicator are outlined in 23 CCR 354.34 (c)(4): Degraded Water Quality. Collect sufficient spatial and temporal data from each applicable principal aquifer to determine groundwater quality trends for water quality indicators, as determined by the Agency, to address known water quality issues.

Data Gaps

Data gaps in the groundwater quality monitoring network were identified due to inadequate spatial coverage, monitoring frequency, and/or lack of representativeness of Basin conditions and activities. The three sites with existing and ongoing groundwater quality monitoring are public supply wells and are therefore concentrated near population, or seasonal population, centers near Fort Jones and Kidder Creek Orchard Camp, leaving much of the Basin without representative monitoring data. The location of these data gaps is shown on the map of the existing groundwater quality monitoring locations (see Figure 2 in Chapter 3). The south, central and northernmost parts of the Basin are not covered

under the current monitoring network. These data gaps are due to the limited number of wells that conduct current and ongoing monitoring for the identified constituents of concern, all public supply wells. The wells in the existing groundwater quality network also have a temporal data gap with a frequency of measurement annually or greater, corresponding to the public water supply system sampling frequency. No local issues or circumstances are expected to prevent monitoring. As discussed in Section 3.3.3, the groundwater quality monitoring network will be expanded with a minimum addition of five wells within the first five years of plan implementation to address this data gap. Candidate wells have been identified for inclusion in this expansion including wells used by dairy operators to report groundwater data to NCRWQCB, domestic wells, QVIR wells, and wells included in the monitoring network for groundwater levels.

Depletions of Interconnected Surface Water Monitoring Network

Requirements

The requirements for the depletion of interconnected surface water monitoring network, as part of § 354.34. Monitoring Network, are detailed below:

(A) Flow conditions including surface water discharge, surface water head, and baseflow contribution.

(B) Identifying the approximate date and location where ephemeral or intermittent flowing streams and rivers cease to flow, if applicable.

(C) Temporal change in conditions due to variations in stream discharge and regional groundwater extraction.

(D) Other factors that may be necessary to identify adverse impacts on beneficial uses of the surface water.

(E) Changes in gradient between river and groundwater system

Data Gaps

While the Scott Valley Integrated Hydrologic Model (SVIHM) is the primary tool for estimating depletions of interconnected surface water, monitoring is necessary for inputs and calibration of the model. As a result, data gaps in the hydrology and climate sections of the Basin setting are also relevant here. Data gaps were identified for physical monitoring to be used in combination with the SVIHM. Wells near the mainstem of Scott River, to be used in observation of long-term trends in the hydraulic gradient between the aquifer and stream were identified as a data gap for the monitoring network associated with the depletions of interconnected surface water sustainability indicator. No local issues or circumstances are anticipated to prevent this monitoring. To fill this data gap, additional wells are planned to be added within the first five years of implementation.

ADDITIONAL DATA OR INFORMATION VALUABLE FOR MEASURING PROGRESS TOWARDS THE BASINS SUSTAINABILITY GOAL

Additional data has been identified that may be valuable to evaluations of progress towards the Basin's sustainability goal. This is primarily additional monitoring information that may be useful to identify adverse impacts on biological uses of surface water, in addition to existing biological monitoring in the Basin.

These include evaluation of streamflow depletion impacts on juvenile salmonids and use of satellite imagery for monitoring riparian and non-riparian vegetation. The GSA may consult other entities or specialists, as feasible, to determine the value of this data.

DATA GAP PRIORITIZATION

The identified data gaps are prioritized for actions to be taken to resolve them. Data gaps are categorized into "high", "medium", and "low" prioritization statuses based on the value to understanding basin setting or in comparison to the defined SMCs to evaluate Basin sustainability. Filling data gaps can be achieved through increasing monitoring frequency, addition of monitoring sites to increase spatial distribution and density of the monitoring network or adding or developing new monitoring programs or tools. Summaries of the data gaps discussed in this appendix, associated prioritizations, and strategies to fill the data gap are shown in Table 2.

New monitoring in the Basin includes collection of isotope data, water quality data and five transects with continuous groundwater data for the NFWF Scott Recharge Project (see Chapter 4 and Appendix 4-B). This information will be used to help fill the identified data gaps and supplement data collected through existing monitoring programs. Additionally, a minimum of eight continuous groundwater and temperature and eight soil moisture sensors has been funded by the Bureau of Reclamation. This additional monitoring will also help to fill data gaps.

Table 2: Data gap prioritization

Priority	Data Gap Summary	Strategy to Fill Data Gap
High	Groundwater quality monitoring network	Planned expansion of groundwater quality monitoring network in the first five years. Additional expansion will be evaluated at the five-year update.
High	Depletions of interconnected surface water monitoring network	Planned addition of continuous groundwater level and temperature measurement near the river to determine the gradient between the aquifer and stream and for use in calibration of SVIHM.
High	Continuous groundwater level monitoring network	Planned addition of these measurements through implementation of PMAs

Medium	Groundwater extraction data	
Medium	Identification and evaluation of Groundwater-Dependent Ecosystems	Using satellite imagery to confirm location and extent of GDEs and evaluate twice per year to assess GDE health over time.
Medium	Groundwater Dependent Ecosystems Health and Habitat Requirements	Collaborating with an agency and/or personnel with expertise in requirements for anadromous fish identified as high priority for management in the Basin.
Low	Additional precipitation data to confirm presence of rainfall gradient.	No strategy has been defined yet to fill this data gap.

REFERENCES

California Department of Water Resources (2016). BMP 2: Best Management Practices for the Sustainable Management of Groundwater Monitoring Networks and Identification of Data Gaps, December 2016. https://water.ca.gov/-/media/DWR-Website/WebPages/Programs/Groundwater-Management/Sustainable-Groundwater-Management/BestManagement-Practices-and-Guidance-Documents/Files/BMP-2-Monitoring-Networks-andIdentification-of-Data-Gaps_ay_19.pdf

Knechtle, M., & Giudice, D. (2021). *2020 Scott River Salmon Studies, Final Report*. California Department of Fish and Wildlife.

Appendix 3-B Monitoring Protocols for Data Collection

Monitoring Protocols

This appendix provides the monitoring protocols for data collection used in the monitoring networks described in Chapter 3.

Groundwater Levels

Groundwater level data collection may be conducted remotely via telemetry equipment or with an in-person field crew. The following section provides a brief summary of monitoring protocols for groundwater level collection. Establishment of these protocols will ensure that data collected for groundwater quality are accurate, representative, reproducible, and contain all required information. All groundwater level data collection in support of this GSP is required to follow these established protocols for consistency throughout the Basin and over time. These monitoring protocols will be updated as necessary and will be re-evaluated every five years.

All groundwater elevation measurements are referenced to a consistent elevation datum, known as the Reference Point (RP). For monitoring wells, the RP consists of a mark on the top of the well casing. For most production wells, the RP is the top of the well's concrete pedestal. The elevation of the (RP) of each well is surveyed to the National Geodetic Vertical Datum of 1929 (NGVD 29). The elevation of the RP is accurate to at least 0.5 ft (15.2 cm), and most well RPs are accurate to 0.1 ft (3 cm) or less.

Groundwater level measurements are taken to the nearest 0.01 ft (0.3 cm) relative to the RP using procedures appropriate for the measuring device. Equipment is operated and maintained in accordance with manufacturer's instructions, and all measurements are in consistent units of feet, tenths of feet, and hundredths of feet.

Groundwater elevation is calculated using the following equation:

GWE = RPE - DTW

where:

GWE = groundwater elevation

RPE = reference point elevation

DTW = depth to water

In cases where the official RPE is a concrete pedestal but the hand soundings are referenced off the top of a sounding tube, the measured DTW is adjusted by subtracting the sounding tube offset from the top of the pedestal.

All groundwater level measurements must include a record of the date, well identifier, time (in 24-hour military format), RPE, DTW, GWE, and comments regarding factors

which may influence the recorded measurement, such as nearby production wells pumping, weather, flooding, or well condition.

Manual Groundwater Level Measurement

Groundwater level data collected by an in-person field crew will follow the following general protocols.

- Prior to sample collection, all sampling equipment and the sampling port must be cleaned.

- Manual groundwater level measurements are made with electronic sounders or steel tape. Electronic sounders consist of a long, graduated wire equipped with a weighted electric sensor. When the sensor is lowered into water, a circuit is completed and an audible beep is produced, at which point the sampler will record the depth to water. Some production wells may have lubricating oil floating on the top of the water column, in which case electric sounders will be ineffective. In this circumstance, steel tape may be used. Steel tape instruments consist of simple graduated lines where the end of the line is chalked to indicate depth to water without interference from floating oil.

- All equipment is used following manufacturer specifications for procedure and maintenance.

- Measurements must be taken in wells that have not been subject to recent pumping. At least two hours of recovery must be allowed before a hand sounding is taken.

- For each well, multiple measurements are collected to ensure the well has reached equilibrium such that no significant changes in groundwater level are observed.

- Equipment is sanitized between well locations to prevent contamination and maintain the accuracy of concurrent groundwater quality sampling.

Data Logger Groundwater Level Measurement

Telemetry equipment and data loggers can be installed at individual wells to record continuous water level data, which is then remotely collected via satellite to a central database and accessed on the Water Level Portal in a web browser.

Installation and use of data loggers must abide by the following protocols:

- Prior to installation the sampler uses an electronic sounder or steel tape to measure and calculate the current groundwater level in order to properly install and calibrate the transducer. This is done following the protocols listed above.

- All data logger installations follow manufacturer specifications for installation, calibration, data logging intervals, battery life, and anticipated life expectancy.

- Data loggers are set to record only measured groundwater level to conserve data capacity; groundwater elevation is calculated after data are downloaded.

- In any log or recorded datasheet, the well ID, transducer ID, transducer range, transducer accuracy, and cable serial number are recorded.

- The sampler notes whether the pressure transducer uses a vented or non-vented cable for barometric compensation. If non-vented units are used, data are properly corrected for natural barometric pressure changes.

- All data logger cables are secured to the well head with a well dock or other reliable method. This cable is marked at the elevation of the reference point to allow estimates of future cable slippage.

- Data logger data are periodically checked against hand-measured groundwater levels to monitor electronic drift, highlight cable movement, and ensure the data logger is operating correctly. This check occurs at least annually, typically during routine site visits.

For wells not connected to a supervisory control and data acquisition (SCADA) system, transducer data are downloaded as necessary to ensure no data are overwritten or lost. Data are entered into the data management system as soon as possible after download. After the transducer data are successfully downloaded and stored, the data are deleted or overwritten to ensure adequate data logger memory.

Sample collection will follow the USGS
(USGS 2015) and
(Rice et al., 2012), as applicable, in addition to the general sampling protocols listed below.

The following section provides a brief summary of monitoring protocols for sample collection and testing for groundwater quality. Establishment of these protocols will ensure that data collected for groundwater quality are accurate, representative, reproducible, and contain all required information. All sample collection and testing for water quality in support of this GSP are required to follow the established protocols for consistency throughout the Basin and over time. All testing of groundwater quality samples will be conducted by laboratories with certification under the California Environmental Laboratory Accreditation Program (ELAP). These monitoring protocols will be updated as necessary and will be re-evaluated every five years.

Wells used for sampling are required to have a distinct identifier, which must be located on the well housing or casing. This identifier will also be included on the sample label to ensure traceability.

Event Preparation:

- Before the sampling event, coordination with any laboratory that will be used for sample analysis is required. Coordination must include scheduling laboratory time for sample testing, and a review of the applicable sample holding times and preservation requirements that must be conducted before the sampling event.

- Sample labels must include the sample ID, well ID, sample date and time, personnel responsible for sample collection, any preservative in the sample container, the analyte to be analyzed, and the analytical method to be used. Sample containers may be labelled prior to, or during, the sampling event.

Sample Collection and Analysis:

- Sample collection must occur at, or close to, the wellhead for wells with dedicated pumps and may not be collected after any treatment, from tanks, or after the water has travelled through long pipes. Prior to sample collection, the sample collector should clean all sampling equipment and the sampling port must be cleaned. The sample equipment must also be cleaned with any change at each new sample location or well.

- Sample collection in wells with low-flow or passive sampling equipment must follow protoco
Puls and Barcelona, 1996) and USGS Fact Sheet 088-00 (USGS, 2000), respectively. Prior to sample collection in wells without low-flow or passive